Weakening mechanisms in reactivated crustal-scale faults: the Dover Fault Shear Zone, Newfoundland

ISABEL ROSE ASHMAN

Weakening mechanisms in reactivated crustal-scale faults: the Dover Fault Shear Zone, Newfoundland

Isabel Rose Ashman

Department of Earth Sciences

Durham University

2018

This thesis was submitted to the University of Durham in full fulfilment of the requirements for the degree of Master of Science by Research.

Weakening mechanisms in reactivated crustal-scale faults: the Dover Fault Shear Zone, Newfoundland

Isabel Rose Ashman

Crustal-scale faults have been argued to represent relative and absolute zones of weakness in comparison to the intact continental crust due to their preferential reactivation and accumulation of strain. In order to understand the long term deformation behaviour of crustal-scale faults, it is important to study how deformation processes in the mid-crustal frictional-viscous transition zone (FVTZ) can alter the frictional strength of the crust. Exhumed fault rocks from the Dover Fault Shear Zone (DFSZ) record evidence of long-term weakening mechanisms. The DFSZ in north-eastern Newfoundland represents a major Appalachian terrane boundary that separates highly metamorphosed gneisses in the Gander Zone from deformed volcanics in the Avalon Zone.

Analysis of field data, hand specimens and microstructures revealed a series of progressively lower temperature, overprinting deformation phases in increasingly narrower, localised shear zones. The fault rocks show increasing strain towards the boundary as grain size reduces, fabric intensifies and folds tighten and become progressively curvilinear. Evidence of fluid influx during deformation includes microstructures that are indicative of fluid assisted diffusive mass transfer (DMT) and a high degree of phyllonitization of the fault rocks.

Increasing strain and structural overprinting towards the centre of the shear zone is indicative of strain weakening and the later brittle faulting that has reactivated the DFZ is evidence of this long term weakening. The most important weakening mechanisms to have affected the DFSZ arose from the syn-tectonic influx of fluids, including both hydrous fluids and magmas, as this led to production of phyllosilicates in reaction softening, the development of interconnected weak layers and thermal perturbations in the fault zone. These processes produced a highly localised network of shear zones whose frictional strengths were permanently reduced, thus impacting the long-term strength and behaviour of the fault in the upper crust.

Contents

Declaration and Copyright

I declare that this thesis which is presented for the degree of Master of Science by Research at Durham University is a result of my own original research, except where acknowledgement is made in the text. This thesis has not been previously submitted to the University of Durham or any other institution.

Isabel Ashman

September 2018

Acknowledgements

First and foremost, a sincere thanks to Bob Holdsworth and Jonny Imber for their advice, expertise and enthusiasm about my research. Despite your hectic schedules, you always made time to answer my questions and share your experience and for that I am truly grateful.

My endless gratitude goes to the Charles Waites Scholarship, as without the funding I would never have been able to become a postgraduate student or pursue my life-long goal of gaining a PhD.

Thanks go to Tom Uttley for being a kind and patient GIS wizard. Kit Hardman has my thanks for teaching me how not to break the expensive microscope. And thank you both for helping me decipher Bob's handwriting!

Chris Saville, Dave Selby and Jonny have my thanks for introducing me to demonstrating and the surprising revelation that I love teaching.

Thank you Emma Ownsworth for reminding me it's ok to relax and eat cake. Also thank you for tolerating all of my enthusing about cycling.

Thank you Laura Scott for always being willing to discuss and moan about microstructures.

Bay 1 (Lena, Katharine and Eloise) thank you for all of our fun and distracting chats.

A great big thank you goes to all of my friends in the earth sciences department for making me laugh and for always being kind and appreciative of my baking. I will miss you all!

As always, the deepest love and gratitude goes to my family for inspiring and encouraging me to be my best self.

1 Chapter 1: Introduction

1.1 Scientific Premise

Crustal-scale fault zones represent large mechanical anisotropies in the continental lithosphere and can create important variations in lateral strength. These fault zones commonly incorporate complex fault rock assemblages that record multi-phase deformation histories. Fault reactivation occurs when geologically separable displacement events (>1 Myr intervals) are repeatedly localised into pre-existing structures in favour of generating new structures (Holdsworth et al., 1997, 2001). The preferential accumulation of strain in reactivated crustal-scale faults on timescales of tens to hundreds of millions of years has been taken as evidence of their relative weakness compared to the adjacent country rock (Rutter et al., 2001; Wallis et al., 2013).

In addition to an inferred relative weakness, it has been argued that reactivated crustal-scale faults are weak in an absolute sense (Watterson, 1975; Imber et al., 1997; Holdsworth, 2004; Holdsworth et al., 2011). Geophysical data suggest that currently active crustal-scale fault zones, such as the San Andreas, have anomalously low frictional strength (μ) values ($\mu<0.3$, in some cases as low as 0.1, e.g. Sibson, 1980; Collettini et al., 2009) compared to the values expected from mechanical experiments (μ = 0.6-0.7, e.g. Byerlee, 1978; Niemeijer et al., 2010). Heat-flow measurements indicate that slip in the San Andreas fault zone is not generating the frictional heat expected from experimentally derived frictional values (Lachenbruch and Sass, 1980; Williams et al., 2004). In addition, the almost fault orthogonal orientation of the maximum principal stress to the San Andreas fault trace indicates that the resolved shear stress is very low across the fault (Zoback et al., 1987; Rutter et al., 2001). As well as geological evidence of crustal-scale fault weakness, geodetic data also indicates that there must be lateral variations in the viscosity of the crust. Variations in viscosity are required to explain how, within the earthquake cycle, there is pre-seismic strain localisation and post-seismic transient displacement on the active fault (Yamasaki et al., 2014). Yamasaki et al. (2014) argue that localised weak zones in the crust beneath active faults are needed to explain these phenomena, as opposed to models of constant crustal viscosity.

Continental crustal-scale faults have such complex histories, geometries and assemblages because the continental crust exhibits strong rheological layering as a result of changing conditions with depth. Rheology here refers to the study of flow and deformation of matter concerning the relation between stress and strain rate (Burgmann and Dresen, 2008). Rock rheology varies as a function of mineralogy, fluid content and chemistry, mineral grain size, melt fraction, temperature, pressure and differential stress conditions (Burgmann and Dresen, 2008). As temperature and pressure increase with depth, the mechanisms of deformation are therefore going to differ between the upper and lower crust.

Sibson (1977) introduced the first conceptual model concerning a major fault zone that cuts through the rheologically layered crust and linked the deformation regimes to the resultant fault rocks (see Figure 1.1.a). Although the model has been somewhat revised since then (e.g. Sibson, 1994; Bos and Spiers, 2002), the principle components of the model remain. In the upper crust (<5km depth), the continental crust is in a state of frictional equilibrium and the strength of the crust is limited by the strength of active faults (Townend and Zoback, 2000). Deformation of the upper crust occurs through elastic-frictional brittle behaviour with increasing frictional strength with depth due to a dependence on pressure (Sibson, 1977; Burgmann and Dresen, 2008). Fault rocks that form in the upper crust include fault gouges, breccias and cataclasites (Sibson, 1977). In contrast, the lower crust (>10-15km depth) deforms through plastic or viscous deformation mechanisms such as intracrystalline plasticity and diffusional creep (Herring, 1950; Sibson, 1977; Passchier and Trouw, 2005). Fault rocks in the mylonitic to gneissic series are produced by viscous deformation in the lower crust (Sibson, 1977). These deformation mechanisms are temperature-dependent and so the crust decreases in strength with increasing depth and temperature. At depths between these deformation regimes is a region termed the frictional-viscous transition zone (FVTZ) across which there is a change from pressure-dependent to thermally activated deformation mechanisms (Sibson, 1977; Burgmann and Dresen, 2008). The FVTZ occurs over the temperature range of 300-450°C (Fossen and Cavalcante, 2017) and so generally corresponds to depths of 10-15km, although the depth of the transition can be affected by fluid influx, grain size refinement, metamorphic reactions and changes in geothermal gradient (Imber et al., 1997; Stewart et al., 2000; Holdsworth et al., 2001; Wallis et al., 2013) . In addition to varying deformation styles with

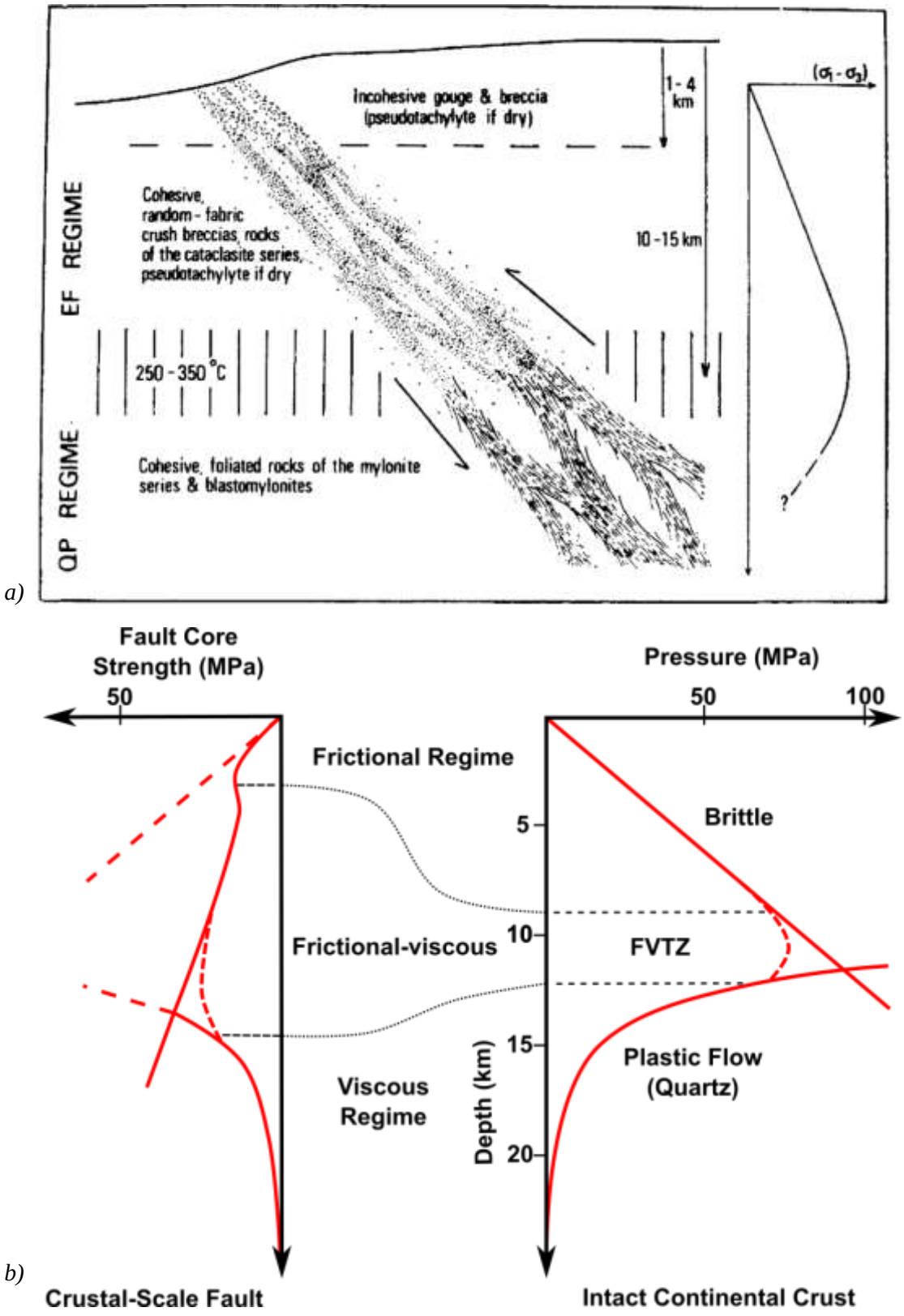

Figure 1.1: a) Sibson's (1977) conceptual model of a crustal-scale fault zone showing the different deformational regimes and resultant rock types. EF – elastic-frictional, QP – quasi-plastic. b) depth versus strength graphs for the intact continental crust (right) and a crustal-scale fault zone (left) (adapted from Holdsworth, 2004). The fault core strength graph shows that the greatest degree of weakening in the fault can occur in the FVTZ.

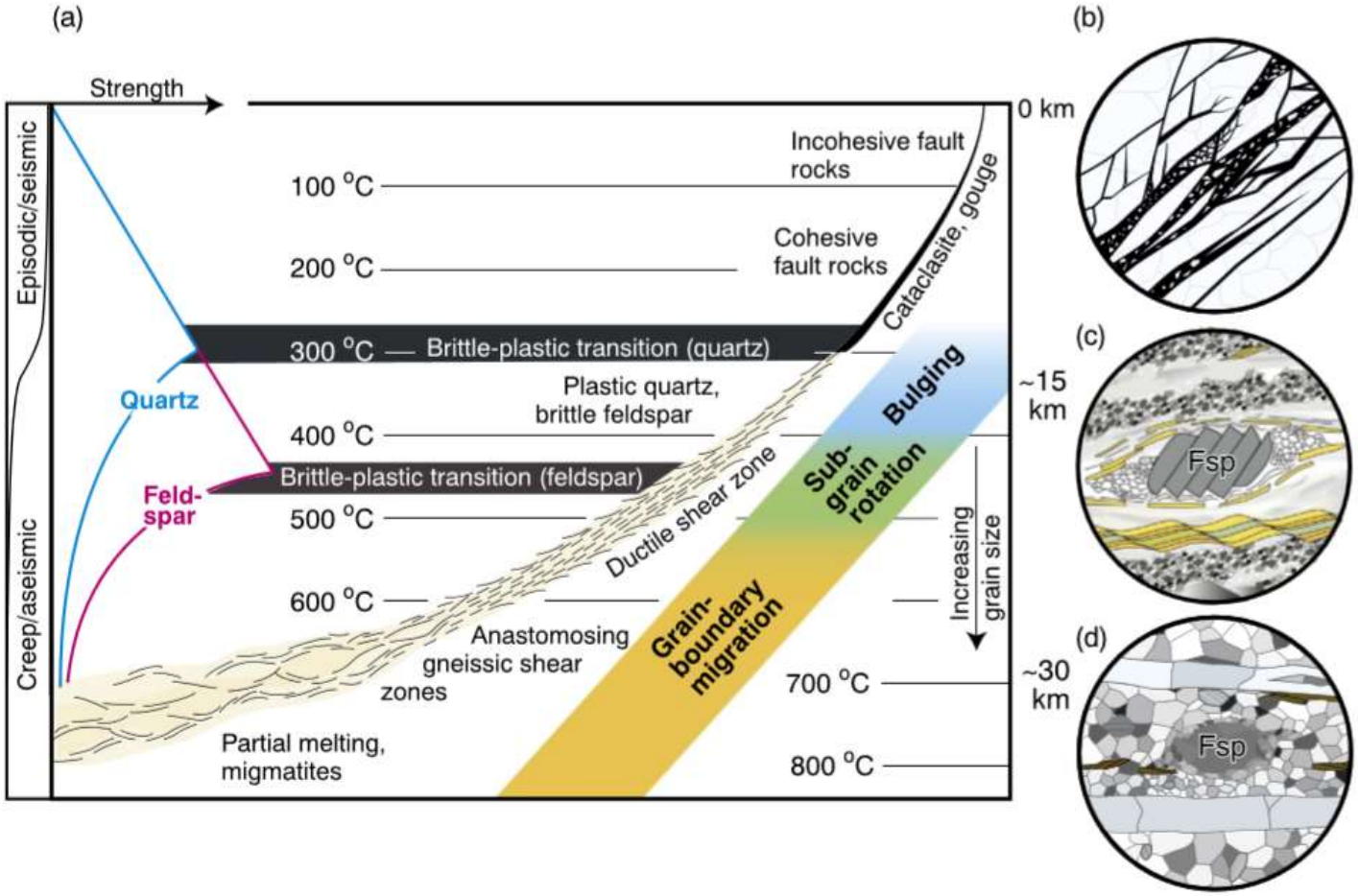

Figure 1.2: a) A simplified depth-strength profile indicating vertical variations in temperatures, fault rocks, shear zone textures and recrystallization mechanisms (Fossen and Cavalcante, 2017). b-d) Cartoons of microstructures characteristic of three different regimes within the shear zone: b) brittle fracturing and cataclastic textures in the upper, brittle crust; c) brittle-plastic textures with recrystallization of quartz contrasting with brittle deformation of feldspar in the brittle-viscous transition zone; d) high temperature plastic deformation with recrystallization of both quartz and feldspar in the lower crust (Fossen and Cavalcante, 2017).

depth, the continental crust also shows significant lateral variations in the accommodation of strain. The plate tectonic model states that the majority of crustal-scale deformation should be concentrated into narrow belts at plate boundaries (Storti et al., 2003). Similarly, in models in which the crust is the strongest portion of the lithosphere (e.g. Crème Brûlée model of Burov and Watts, 2006), it is predicted that crustal deformation will be accommodated on a small number of laterally extensive and narrow faults that penetrate the entire crust and show high slip rates (Wallis et al., 2013). These models are supported by the observation that intraplate crust away from major fault zones is generally strong (Townend and Zoback, 2000). Faults in the crust are thought to prevent pore pressures from exceeding hydrostatic conditions at depth so that the crust can sustain high differential stresses (Townend and Zoback, 2000). Observations of continental-scale deformation shows that large regional faults and shear zones accommodate most of the strain in the lithosphere and that these structures are long lived with active histories on the scale of 10^3 to 10^7 years (Handy and Brun, 2004). This concentration of deformation in major crustal fault zones is thought to result from the relative weakness of the fault zones compared to the intact continental crust (see Figure 1.1.b).

This relative and absolute weakness of crustal-scale faults has implications for the deformation of the continental crust as a whole. As continental lithosphere is not generally subducted, successive phases of deformation create a long-lived template of geometrically linked fault- and shear- zones with complex displacements, internal strains and overprinting relationships (Holdsworth et al., 1997). As deformation will preferentially localise into areas of weakness, reactivated crustal-scale faults influence the architecture and location of orogenic belts, fault-controlled sedimentary basins and continental rifts (Holdsworth et al., 1997, 2001). It is therefore important to understand the processes involved in reactivation as they will affect continental deformation and, as a result, the siting of subsurface fluid flow, economic resources and seismic hazards. Fault zones can act as either conduits or barriers to fluid flow and they often act as a control on the location and size of economic deposits of precipitated minerals, hydrocarbon reservoirs and aquifers (Watterson, 1975; Sibson, 1994; Rutter et al., 2001).

Studies of crustal-scale faults at shallow crustal depths in the brittle deformation regime (<5km, see Figure 1.2) have identified a variety of transient dynamic weakening mechanisms (e.g. Di Toro et al., 2011) and longer term weakness due to the presence of anomalously low-friction clay-gouges (e.g. Niemeijer et al., 2010; Rutter et al., 2001) However, this fails to address why there are long periods of inactivity between reactivation events and the consistent, preferential reactivation of the same long-lived structures in many settings. Transient weakening mechanisms, such as elevated pore fluid pressures or friction-induced melting, occur on timescales that are relatively small in geological time (~10^{-1} to 10^{2} yrs) when the timescales of fault reactivation can span hundreds of millions of years (10^{8} yrs) (Holdsworth, 2004).

It has therefore been proposed that long-term fault weakening originates due to processes that occur in the mid-crustal, load-bearing FVTZ (5-15km depth, see Figure 1.1) (Sibson, 1977; Handy et al., 1999; Holdsworth, 2004). Deformation and metamorphic processes in the FVTZ are known to rework fault rock mineralogy and microstructure as strain accumulates, which can result in permanent weakening of the fault rocks (Wintsch et al., 1995; Rutter et al., 2001). The effects of deformation weakening processes are at their most prominent in the FVTZ of crustal-scale faults as it represents the strongest and therefore load-bearing region of the crust (see Figure 1.1.b). These changes begin at the grain-scale but their effects can be transmitted to much larger scales due to the geometric interconnectivity of foliated fault rocks and mid-crustal fault networks (Imber et al., 1997; Holdsworth, 2004; Niemeijer et al., 2010).

Multiple deformation processes are often active within a fault zone that together can lead to long term weakening in the mid-crust; examples include reaction softening (White and Knipe, 1978; Wintsch et al., 1995), grain size reduction (De Bresser et al., 1998, 2001), fabric softening (White et al., 1980; Handy, 1990; Imber et al., 1997) and shear heating (Hutton et al., 1990; Leloup et al., 1999; Lee et al., 2018). As a result of these changes to mineralogy and fabric in the core of mid-crustal faults, strains are progressively localised into interconnected narrow shear zones with low-strain material preserved in elongate lenses or wall rocks (Rutter et al., 2001; Collettini et al., 2009). This configuration is mechanically very stable, can accommodate considerable strain and has been observed in many natural mid-crustal fault zones (e.g. Imber et al., 1997; Rutter et al.,

2001; Jefferies et al., 2006). Established fault rocks with low frictional strength within the fault zone impact processes associated with fault movement in the upper brittle crust that can affect fault strength, such as shear heating and metamorphism (Wallis et al., 2013).

At present, it is not possible to observe active weakening mechanisms in the mid-crust through either drilling or high resolution geophysical surveying due to the depth of the brittle-viscous transition zone and the low resolution of geophysical survey data (Holdsworth et al., 2011). Consequently, it is necessary to study ancient exhumed fault zone cores that preserve fault rocks from depths within the brittle-viscous transition zone in order to understand mid-crustal deformation processes (Imber et al., 1997; Stewart et al., 2000; Jefferies et al., 2006; Wallis et al., 2013). Observations of the preserved deformation fabrics and microstructures of fault rocks can then be related to experimental or modelled results of weakening mechanisms to infer absolute fault weakness through the reduction of frictional strength (e.g. Wallis et al., 2013).

A prime example of an ancient mid-crustal fault zone that has experienced multiple reactivation episodes is the Dover Fault Shear Zone (DFSZ) in north-eastern Newfoundland. Fault rocks within the DFSZ record several distinct deformation regimes that relate to episodic accretionary orogenic phases in the Palaeozoic that occurred during exhumation of the current level of exposure through the brittle-viscous transition zone at depth (Pollock et al., 2012; Kellett et al., 2016). The DFSZ therefore offers the opportunity to study the products of mid-crustal deformation processes that are well preserved and easy to access. Additionally, the DFSZ can act as an ancient analogue for modern crustal-scale faults, such as the San Andreas fault, without the need to image the present day mid-crust.

1.2 Aims of the Project

This thesis will use the example of the Dover Fault Shear Zone (DFSZ) in Newfoundland in order to study microstructural evidence of the processes active in the mid-crust that may lead to significant long-term fault weakening. The first specific aim of this research is to document the microstructural development of fault rocks associated with the DFSZ. Microstructural analysis will be used to document changes in mineralogy, fabric and intensity of overprinting with the purpose

of integrating microstructural observations and field data into a comprehensive structural history for the DFSZ.

Secondly, this research aims to determine the distribution and nature of fluid related changes in mineralogy in DFSZ fault rocks and to assess how this may affect long-term fault strength. Fluid influx into mid-crustal fault zones has been identified as important for initiating and enhancing long-term weakening processes (Collettini et al., 2009; Niemeijer et al., 2010). By studying the microstructures of the DFSZ, this research aims to test the extent to which the influx of chemically-active fluids into a fault zone can cause the proposed weakening.

1.3 Hypothesis

The case study of the DFSZ fault rock assemblage will be used to test the hypothesis that:

Mid-crustal deformation processes lead to the development of weak phyllosilicate-rich fault rocks that impact fault strength throughout the crust.

The DFSZ has been chosen as the case study for this thesis because it constitutes a complex fault rock assemblage recording a multi-phase deformation history as a result of repeated episodes of strike-slip/transpression and exhumation (Holdsworth, 1994; Kellett et al., 2016). In addition, this study of the DFSZ is supported by the vast volume of research that has been undertaken into the wider regional setting of the Appalachian orogeny (Hibbard and Waldron, 2009; Pollock et al., 2012; van Staal et al., 2009). Previous fieldwork has also identified pervasive alteration and phyllonitisation of the fault rocks in the DFSZ, thus indicating that fluid influx into the fault zone may have affected long-term fault strength (Holdsworth, 1991).

If the primary hypothesis of this research is assumed to apply to the DFSZ, it is possible to predict several trends in the fault rock assemblage that developed due to fault zone weakening during mid-crustal deformation. Strain would be expected to progressively localise into weakened, narrow shear zones with intense overprinting of fabrics in these high strain shear zones. In a retrograde exhumation sequence, the expected overprinting relationship would show earlier, broader anastomosing, viscous shear zones that have been reworked by later, localised brittle fault networks (Rutter et al., 2001). Lee et al. (2018) have suggested that this strain localisation in the mid- to

upper crust could originate from organisation of partial melt in syn-melt forming shear zones in the lower crust. If this applies to the Gander-Avalon boundary, which experienced syn-tectonic influx of granitic melts into the shear zone, there may be evidence that the presence of melt in the shear zone acts as a control on the localisation of deformation (Lee et al., 2018; Schofield and D'Lemos, 2000).

Also, as fluid influx should lead to a greater degree of weakening, it is expected that regions with greater amounts of alteration will have accommodated the most strain. In studies of other reactivated crustal-scale faults (e.g. Imber et al., 1997; Stewart et al., 2000; Jefferies et al., 2006), cataclasis and fracturing in the deeper regions of the brittle regime have been proposed as grainsize reduction mechanisms that influence the influx of fluids into the fault zone. Fractures can also provide a migration pathway for fluids into the active fault zone. In addition, the grainsize reduction resulting from cataclasis promotes the activity of grainsize-sensitive deformation mechanisms, such as diffusive mass transfer (DMT) (Jefferies et al., 2006; Niemeijer et al., 2010). The DFSZ fault rocks should therefore display a greater degree of alteration, accommodated strain and evidence of DMT deformation in more pervasively fractured regions.

1.4 Research Methods:

This research will focus on the use of microstructures in thin section to infer the deformation mechanisms active during the evolution of the DFSZ fault rocks. Observations of both the rock fabrics and mineral assemblages will be used to infer the deformation regimes and histories preserved in the samples. As thin sections represent a single snapshot of one rock within a fault zone, the microstructural observations will be integrated with hand specimen observations, structural data and field observations in order to understand how the grain-scale weakening processes might transfer to larger scales.

The field data described in sections 5.1 and 5.3 are derived from fieldwork conducted by Robert Holdsworth in the field seasons of 1990-93 as new field data collection was beyond the scope of this research. The analysis of the structural data, thin sections and hand specimens was completed by the author but the descriptions of field relationships in sections 5.1 and 5.3 are derived from

field notebooks and therefore the work is attributed to Prof. Holdsworth. The field data are included in Chapter 5 to provide a more complete view of the structure and character of the DFSZ.

2 Chapter 2: Deformation, weakening and fluids: a review

This chapter will summarise the scientific models and processes that form the basis of this research, including a review of theories on the mechanisms of grain-scale deformation. In addition, this chapter will outline the current scientific understanding on the processes of deformation weakening and the role of phyllosilicates and fluids in crustal-scale faults.

2.1 Deformation at the grain-scale

As the majority of this thesis concerns deformation at the grain-scale, the different deformation mechanisms and their resultant microstructures will be introduced briefly in this section. Deformation mechanisms here mean processes on one scale, such as at the individual grain scale, that accommodate an imposed deformation from a larger scale, for example on the local to regional scale (Blenkinsop, 2000). There are three main categories of deformation mechanism including:

- Cataclasis and brittle deformation – deformation by microfracturing, frictional sliding and rotation of particles with no permanent crystal lattice distortion (Knipe, 1989; Passchier and Trouw, 2005);
- Crystal plasticity – deformation by the movement of defects in a lattice with permanent lattice distortion (Knipe, 1989; Hirth and Tullis, 1992);
- Diffusive mass transfer (DMT) – deformation by solid-state or fluid-assisted diffusion or the movement of lattice defects, ions, atoms or molecules in response to gradients of chemical potential (Knipe, 1989; Blenkinsop, 2000).

More than one deformation mechanism may operate within a single mineral or grain aggregate and their operation is mainly determined by the temperature, stress, strain rate, pore fluids, mineralogy and the texture (especially grain size) of the deforming rock. In homogeneous systems with multiple active deformation mechanisms, the mechanism with the lowest strain rate determines the total composite strain rate and is therefore the rate limiting process (Blenkinsop, 2000). The changing conditions with depth in the crust, as discussed in section 1.1, also causes a corresponding change in the dominant deformation mechanism. Hence, cataclasis and brittle fracturing dominates at low temperatures in the upper crust whereas intracrystalline crystal plasticity and DMT

deformation processes are thermally activated and so dominates in the lower crust (Sibson, 1977; Blenkinsop, 2000; Burgmann and Dresen, 2008).

Brittle fracturing and cataclasis operate through the breaking and rotation of grains and involves the creation of new surfaces, loss of cohesion and frictional sliding (Knipe, 1989). Brittle fracturing can be recognised in thin section by microstructures such as microcracks, microfaults and cataclastic shear bands. Crystal plasticity involves the movement of defects through the crystal lattice to increase internal strain in dislocation glide and the migration of vacancies to dislocation lines to reduce internal strain in dislocation climb (Hirth and Tullis, 1992; Passchier and Trouw, 2005). At lower temperatures (e.g. $T < 0.3\ T_{Melting}$), the microstructures used to recognise crystal plasticity include undulose extinction patterns, microkinks, deformation lamellae and twins and a preferred crystallographic orientation (CPO) of the grains. Recovery occurs at higher temperatures and is an intracrystalline deformation mechanism that minimises the free energy within a grain produced by dislocation glide (Passchier and Trouw, 2005). Microstructures formed by the process of recovery include deformation bands and subgrains within an individual grain (Passchier and Trouw, 2005). Dynamic recrystallisation is the nucleation and growth of new strain-free grains through the movement of grain boundaries or sub-grain rotation (Hirth and Tullis, 1992; Passchier and Trouw, 2005). The mechanism of dynamic recrystallisation is strongly temperature-dependent so that with increasing temperature the recrystallisation mechanism changes from bulging grain boundary migration (BLG) to subgrain rotation (SGR) then to rapid grain boundary migration (GBM) (White et al., 1980; Hirth and Tullis, 1992; Blenkinsop, 2000; Passchier and Trouw, 2005). Dynamic recrystallisation, the textures of which are shown in Figure 2.1, decreases the internal free energy of a strained grain. The grain boundary of the higher strain grain is displaced to the lower strain grain, thus causing the lower strain grain to grow (Hirth and Tullis, 1992; Passchier and Trouw, 2005).

As opposed to the process of dynamic recrystallisation reducing internal free energy, grain boundaries can also be considered as planar defects in the crystal lattice that associate with high levels of internal free energy (Passchier and Trouw, 2005). By reducing the total surface area of grain boundaries, the free energy levels are reduced in turn. Grain boundary area reduction

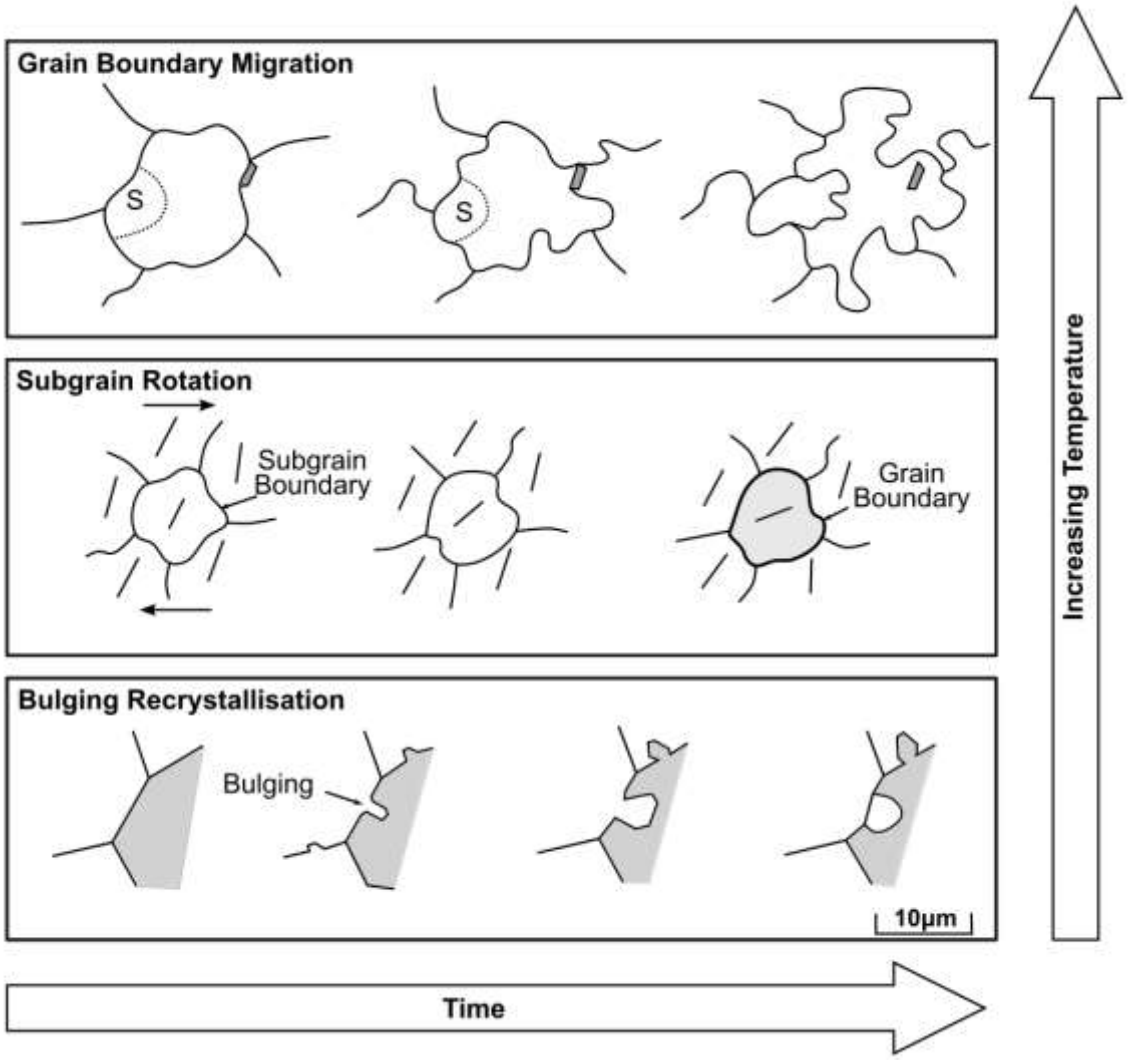

Figure 2.1: schematic diagram taken from Passchier & Trouw (2005) to show the processes of dynamic recrystallisation and their characteristic textures. Bulging recrystallisation is the lowest temperature recrystallisation mechanism, in which the boundary of the grain with the lowest density of dislocations bulges into the higher dislocation density grain. Subgrain rotation recrystallisation occurs in response to the migration of dislocations into subgrain walls to cause new high angle grain boundaries to form. At high temperatures, grain boundaries become highly mobile and sweep through the material to remove dislocations and subgrains in grain boundary migration.

(GBAR) can be recognised by straight grain boundaries, large grains and ~120° triple junctions of grain boundaries. In intracrystalline deformation, there is continuous competition between processes that cause distortion of the crystal lattice, such as dislocation glide, and the processes that reduce the dislocation density, including recovery and recrystallization (Passchier and Trouw, 2005).

DMT can occur in the solid state, but below amphibolite grade conditions DMT predominantly occurs via solution as solid-state diffusion operates too slowly to accommodate significant strain (Blenkinsop, 2000). DMT using an intergranular fluid film – typically water – is termed pressure solution. In DMT, material is removed from sites of high stress and is transported along a chemical potential gradient to be deposited at sites of low stress (Passchier and Trouw, 2005). The operation of DMT is recognised from microstructures that show a systematic relation to surfaces that may have been under higher normal stress, such as strain caps, mica beards and microstylolites (Blenkinsop, 2000). Strain cap microstructures are strongly foliated domains enriched in micas or less soluble minerals around opposite surfaces of relatively rigid objects, such as feldspar porphyroclasts (Blenkinsop, 2000). Strain caps form through dissolution of more soluble phases, such as quartz, around the rigid porphyroclast whereas overgrowths or pressure shadows form through secondary mineral growth (Blenkinsop, 2000). Pressure shadows, or specifically mica beards, are domains of secondary mineral growth in a strong shape fabric that forms in the low pressure areas around an object in a direction that is perpendicular to the maximum applied stress (Blenkinsop, 2000). Microstylolites are discontinuities with offset or wave-like shapes that may truncate grains and thin section-scale fabrics (Blenkinsop, 2000). The concentration of less soluble minerals, such as micas and opaque oxide phases, in strain caps, stylolites and cleavage domains suggests that these structures form by the removal of the more soluble matrix due to grain contact-controlled concentrations of normal stress (Blenkinsop, 2000).

An additional deformation mechanism has been proposed to operate in the FVTZ in the mid-crust that is especially prevalent in phyllosilicate-rich fault cores in the presence of a chemically active fluid. Frictional-viscous flow involves frictional sliding that is accommodated by pressure solution through the removal of asperities, as shown by Figure 2.2

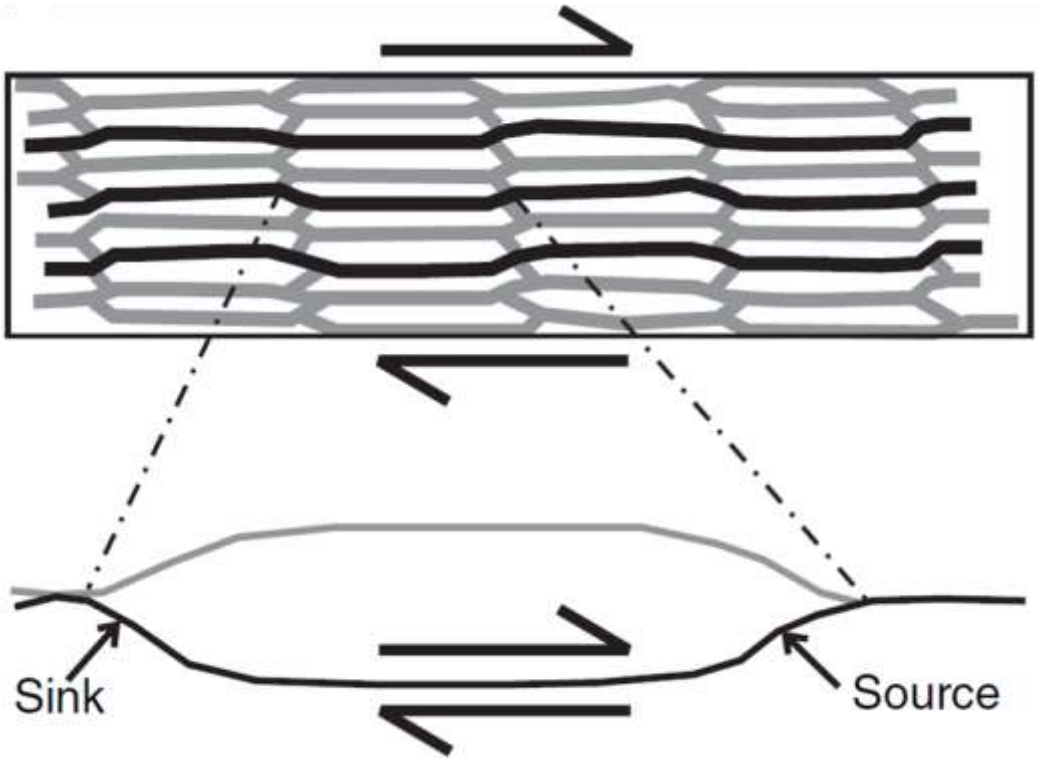

Figure 2.2: a microphysical model depicting frictional-viscous flow in phyllosilicate-rich fault rocks (Bos and Spiers, 2002; Imber et al., 2008). Slip on active, wavy phyllosilicate foliae (thick black lines, grey lines are inactive foliae) gives rise to incompatibilities at the leading edges of porphyroclasts (uncoloured polygons). Pressure solution removes material from the sources to accommodate the slip and the material diffuses to sink sites, namely at the trailing edges of the porphyroclasts (Bos and Spiers, 2002; Imber et al., 2008).

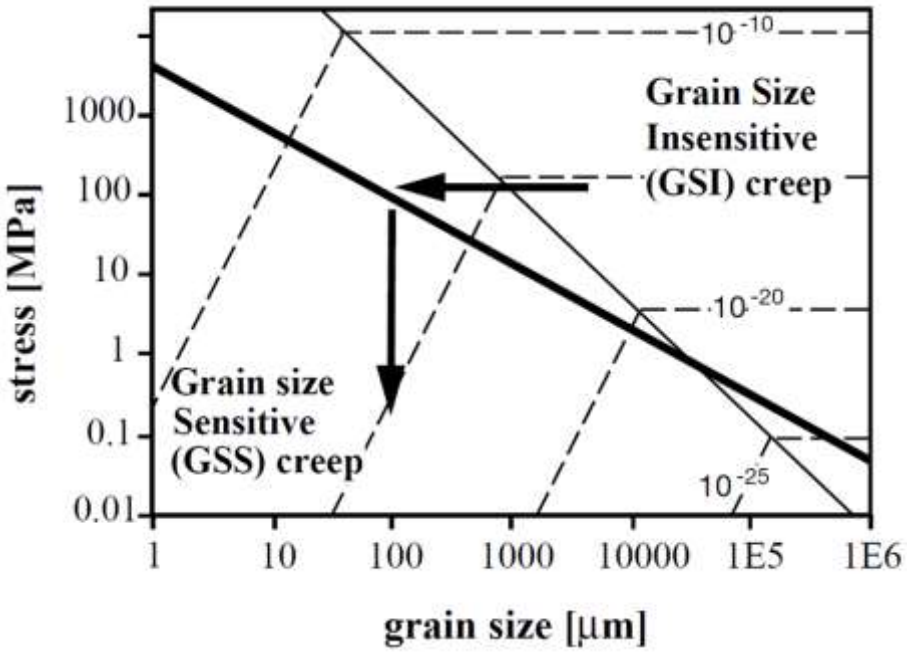

Figure 2.3: Empirical stress versus recrystallized grain size relative for the example mineral olivine extrapolated into a deformation mechanism map drawn for 600°C (De Bresser et al., 2001). The strain rate contours show the rheological weakening resulting from the switch in deformation mechanism due to grain size reduction.

(Bos and Spiers, 2002; Imber et al., 2008). This multi-mechanism deformation behaviour is dependent on both normal stress and the strain rate and it has been shown to generate highly foliated, apparently mylonitic fabrics (Bos and Spiers, 2002; Imber et al., 2008).

2.2 Deformation Weakening

Geological structures on any scale, from microcracks to crustal-scale faults, reflect the rheology of the rock, its constituent phases and its thermal and kinematic history (Handy and Brun, 2004). This is clear in crustal-scale faults because as strain accumulates, deformational and metamorphic processes change the fault rock mineralogy and microstructure (Rutter et al., 2001). In this manner, deformation weakening processes lead to changes in the rheological behaviour and mechanical strength of the fault rocks. If the grain-scale weakening processes are effectively transferred up to larger scales through the natural interconnectivity of shear zones, then the entire crustal-scale fault can be weakened (Imber et al., 1997; Holdsworth, 2004).

Although the focus here is on permanent weakening processes in the mid-crust, there are potential impacts on transient weakening mechanisms in the upper, frictional crust such as the processes of frictional melting and thermal fluid pressurisation (Rutter et al., 2001; Wallis et al., 2013). Weakening impacts the frictional strength (μ) of a fault in the upper crust so that a weak fault might experience limited frictional heating and it may inhibit seismic slip of the fault plane (Rutter et al., 2001). In theory, a weakened structure has an increased probability of reactivation, even at low stresses and in unfavourable orientations to the stress field.

2.2.1 Grain Size Reduction

The reduction in grain size through processes such as dynamic recrystallization, metamorphic reactions and cataclasis can lead to major rheological weakening and associated strain localisation (White et al., 1980; De Bresser et al., 2001; Rutter et al., 2001; Handy and Brun, 2004). A reduction in grain size brings about a switch from grain-size-insensitive dislocation creep deformation to grain-size-sensitive diffusion creep, as shown in Figure 2.3 (De Bresser et al., 2001). Hence as grain size decreases in a fault rock, the reduced stress at which diffusion creep operates compared with the stress required for dislocation creep induces a drop in the fault rocks solid state viscosity (De Bresser et al., 2001). De Bresser et al. (1998, 2001) showed that, under

consistent deformation conditions, aggregates deforming by dynamic recrystallisation generally evolve towards a balance between processes that reduce grain-size and cause grain-growth. Hence, deforming aggregates may deform by steady-state flow and would therefore only accommodate minor weakening. Other processes that reduce aggregate grain size, such as cataclasis, or a restriction on grain growth is required for major weakening due to grain size reduction in shear zones (De Bresser et al., 1998, 2001).

2.2.2 Fault Rock Fabric

The most stable microstructure in a fault rock is that which dissipates the least amount of strain energy per unit time and per unit volume of rock (Handy, 1990). Prior to shearing, rock strength is generally determined by strong minerals in a load bearing framework (LBF) microstructure, as shown in Figure 2.4.a (Handy, 1990; Handy et al., 1999). Due to the action of brittle fracturing, DMT, dynamic recrystallization and metamorphic reactions during shearing, fault rock microstructures generally evolve into interconnected weak layer (IWL) fabrics (Handy, 1990). An IWL refers to interconnected layers of an aligned weak phase with easy slip orientations, such as phyllosilicates, that surround boudins or clasts of a stronger phase in a discrete foliation fabric (Handy, 1990; Rutter et al., 2001). On a larger (metre to kilometre) scale, IWL can also refer to the similar structure of weakened shear zones surrounding lenses of low-strain protolith, as shown in Figure 2.4.b (Imber et al., 1997). An IWL is required in order to transmit the weakening processes at the grain scale to the larger fault or shear zone as the IWL fabrics at all scales can preferentially accommodate strain over the stronger, intact boudins or clasts (Imber et al., 1997). Rock deformation experiments have shown that the low frictional strength that results from slip on an IWL network of weak phases (μ = 0.2-0.45 compared to 0.6-0.8) allows the overall fault strength to be controlled by the weak mineral phases (Shea and Kronenberg, 1993; Collettini et al., 2009). Even at small proportions (10-20%) of the total rock volume, weak phases in an interconnected network can significantly reduce fault strength due to slip on their aligned basal planes (Niemeijer et al., 2010).

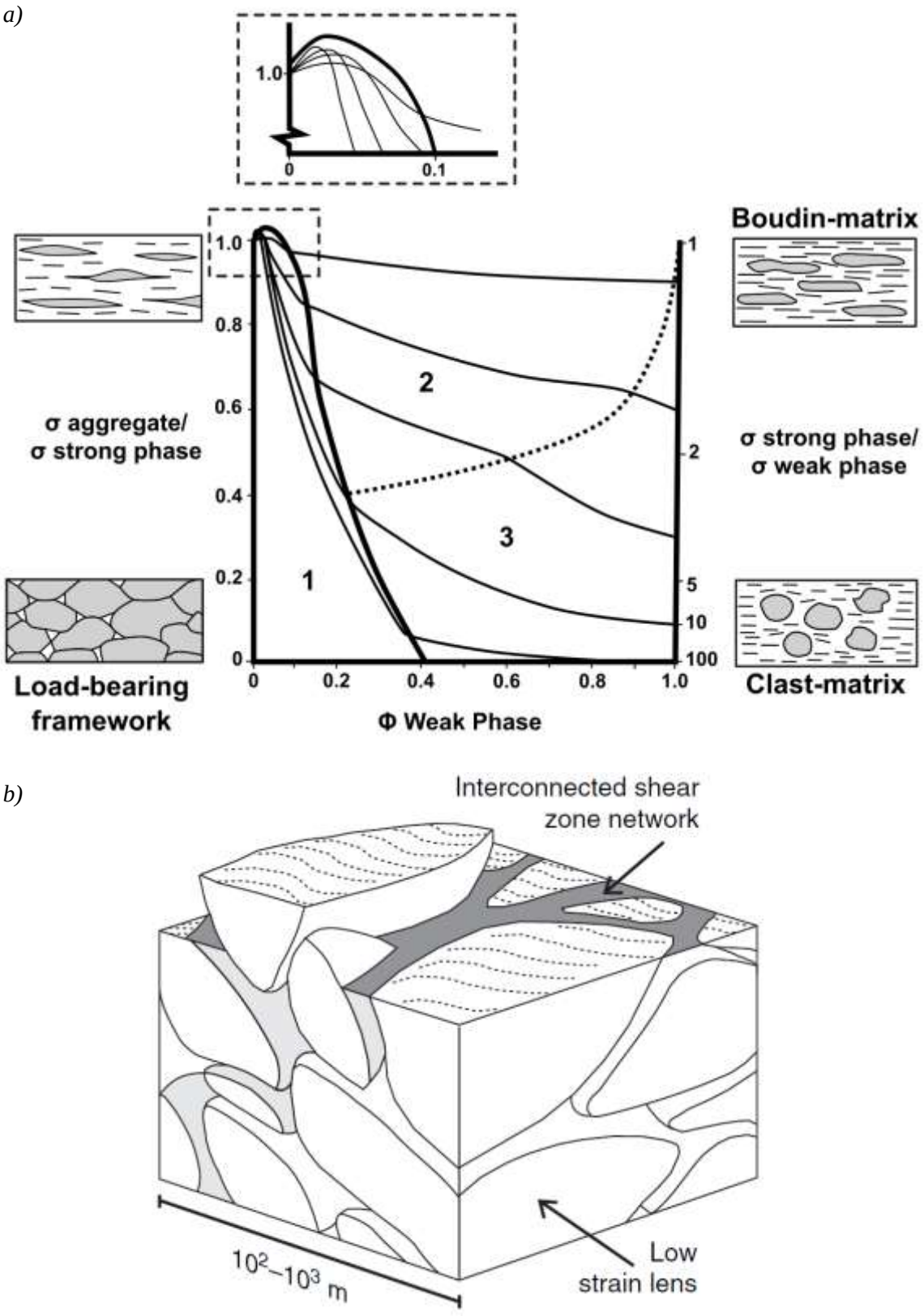

Figure 2.4: a) Hypothetical graph of normalised aggregate strength (left axis) or relative strength of the strong to weak phase (right axis) versus volume proportion of weak phase (horizontal axis) for a two-phase aggregate (adapted from Handy, 1990). Domain 1 relates to framework-supported rheologies and domains 2 (boudin-matrix) and 3 (clast-matrix) refer to matrix-controlled rheologies. b) a schematic diagram showing a crustal-scale interconnected weak layer (Imber et al., 2008).

2.2.3 Fluid Influx and Chemical Alterations

Field studies of exhumed mid-crustal faults (e.g. Imber et al., 1997; Jefferies et al., 2006) suggest that the processes of weakening are most effective in fault cores that have experienced a large influx of H_2O or CO_2-rich fluid during shearing (Storti et al., 2003). An intruding fluid will react with mineral phases in the fault zone because the fluid will change its temperature, pressure and density on infiltration into the fault (Wintsch et al., 1995). The fluid is therefore not in equilibrium with the fault rock minerals, thus leading to chemical alterations. Common reactions in the presence of an H_2O-rich fluid include the replacement of feldspars and amphiboles with chlorite, biotite and other phyllosilicates at temperatures above 200°C (Wintsch et al., 1995). In addition, metamorphic reactions during deformation at elevated temperatures and pressures can lead to the formation of weak minerals in small, strain-free grains, fluid release in dehydration reactions and changes in stress concentration due to volume changes (White et al., 1980; White and Knipe, 1978).

The syn-tectonic alteration of strong phases, such as feldspar phases, to fine grained aggregates of weak hydrous minerals, such as sericite, can trigger the collapse of a LBF to an IWL microstructure (Imber et al., 2008).The production of phyllosilicates through hydrous alteration reactions can have a profound impact on the frictional strength of a fault. Whilst other silicate minerals deform by fracturing or frictional sliding in the upper to mid-crust, phyllosilicates can also deform by dislocation glide throughout the entire crust (Wintsch et al., 1995). As phyllosilicates are highly anisotropic minerals, when phyllosilicate grains are aligned at high contiguities slip can occur at very low stresses (<10MPa) along their basal [001] plane (Wintsch et al., 1995; Niemeijer and Spiers, 2005). When the phyllosilicates are aligned in an IWL, the fault rock strength may approach a lower limit defined by the glide strength of single crystals (Wintsch et al., 1995). Consequently, as the volume, degree of alignment and contiguity of phyllosilicates in a fault rock increases due to hydration alteration reactions, the bulk strength of the rock decreases (Shea and Kronenberg, 1993; Imber et al., 1997).

The influx of water into an active mid-crustal fault zone can also affect the operation of different deformation mechanisms that operate at lower stress conditions than in dry conditions. Water-

deficient conditions during deformation hinder grain boundary diffusion, which is a process that in turn enables increased grain boundary mobility (Mancktelow and Pennacchioni, 2004). Grain boundary diffusion is influenced by the volume and composition of the free-fluid phase so that, in dry samples, grain boundary mobility is very low and the dominant recrystallization methods instead utilise intracrystalline plasticity and rotational mechanisms (Mancktelow and Pennacchioni, 2004). Fluids that are available within a fault zone during deformation also promote the operation of DMT, especially as at conditions below amphibolite grade solid-state DMT can only accommodate significant strains by using a fluid as the transport medium (Blenkinsop, 2000). DMT and other fluid-assisted deformation mechanisms are able to operate at lower stresses than other frictional or viscous mechanisms, thus leading to fault weakening.

2.2.4 Frictional-Viscous Flow

The multi-mechanism deformation regime of frictional-viscous flow can significantly reduce the strength of crustal-scale faults with respect to Byerlee's frictional model (Byerlee, 1978; Imber et al., 2008). Through the action of pressure solution, asperities that would inhibit frictional slip are removed and frictional-viscous deformation can be accommodated at relatively low stresses (<20MPa) (Imber et al., 2008). This mechanism results in weakening of 50-70% of a crustal-scale fault in the FVTZ as compared to a two-mechanism crustal strength profile (Bos and Spiers, 2002; Jefferies et al., 2006a; Imber et al., 2008).

2.2.5 Thermal Perturbations and Magma Emplacement

Crustal-scale faults and shear zones often associate with potentially high volumes of syn-tectonic magma emplacement and in-situ partial melting (e.g. Hutton et al., 1990; Holdsworth, 1994; D'Lemos et al., 1997). The presence of magmatic melts in a fault zone is known to weaken the crust even at small melt fractions due to the increased temperatures and magma-overpressure in the shear zone (D'Lemos et al., 1997; Lee et al., 2018). A slight temperature increase would lead to higher strain rates, which would lead to a feedback on fault strength (Leloup et al., 1999). Syn-melt and post-crystallisation strain partitioning into zones of maximum anisotropy within the magmas and plutons form permanent weak structures that are often reactivated with progressive deformation (D'Lemos et al., 1997; Lee et al., 2018).

It is thought that the most fundamental processes of fault weakening in crustal-scale faults are interconnected weak layer development, reaction softening and those processes arising from syn-tectonic fluid influx (Storti et al., 2003; Holdsworth, 2004; Wallis et al., 2013). If a fault continues to be active during exhumation, a sequence of overprinting, progressively lower temperature fault rocks may form that record information on deformation and weakening processes across a range of crustal depths (Holdsworth et al., 1997; Wallis et al., 2013).

3 Chapter 3: Geological Background of Newfoundland Case Study

This study focuses on the tectonic boundary that separates the Gander and Avalon Zones in Newfoundland, which formed as part of the Appalachian orogeny. The Dover Fault Shear Zone (DFSZ) is a long lived, crustal-scale fault system with a multiphase deformation history. Studies of the deep structure of Newfoundland have shown that the inboard Gander Zone and the outboard Avalon Zone are associated with different deep crustal blocks (Marillier et al., 1989; D'Lemos et al., 1997). These neighbouring crustal blocks are separated by the near-vertical DFSZ and offshore deep seismic profiles indicate that the Moho is offset by the DFSZ (Marillier et al., 1989; D'Lemos et al., 1997; Kellett et al., 2016). The modern expression of the Gander-Avalon tectonic boundary is the brittle Dover Fault that was likely active after the termination of the Appalachian orogeny (Waldron et al., 2015; Kellett et al., 2016). This chapter aims to outline the history of the DFSZ as it is currently known and to introduce the country rocks in the Gander and Avalon Zones that represent the protoliths of the fault rocks in the DFSZ.

3.1 Regional Setting and the Appalachian Orogeny

The area of interest in this study lies within the eastern Appalachian orogenic belt in Atlantic Canada, shown in Figure 3.1. The Canadian Appalachians developed as a result of a series of episodic accretionary orogens relating to the Paleozoic closure of the Iapetus and Rheic oceans (Hibbard and Waldron, 2009; van Staal et al., 2009; Pollock et al., 2012). In each subsequent accretionary episode, there was an eastwards migration (in the modern configuration) of the subduction zone and the associated focus of magmatism, deformation and metamorphism (van Staal et al., 2009; Pollock et al., 2012). The termination of this series of orogenic events occurred in the Variscan-Alleghenian-Ouachita orogeny related to the final amalgamation of the supercontinent Pangaea (Pollock et al., 2012).

Located in the northeast of this major orogenic belt, the island of Newfoundland is composed of a series of tectonic terranes, shown in Figure 3.2, which can be divided into Laurentian, Iapetan and peri-Gondwanan realms according to their affinities prior to the Appalachian orogeny (Hibbard and Waldron, 2009). In the west of the island, the Humber Zone represents the ancient

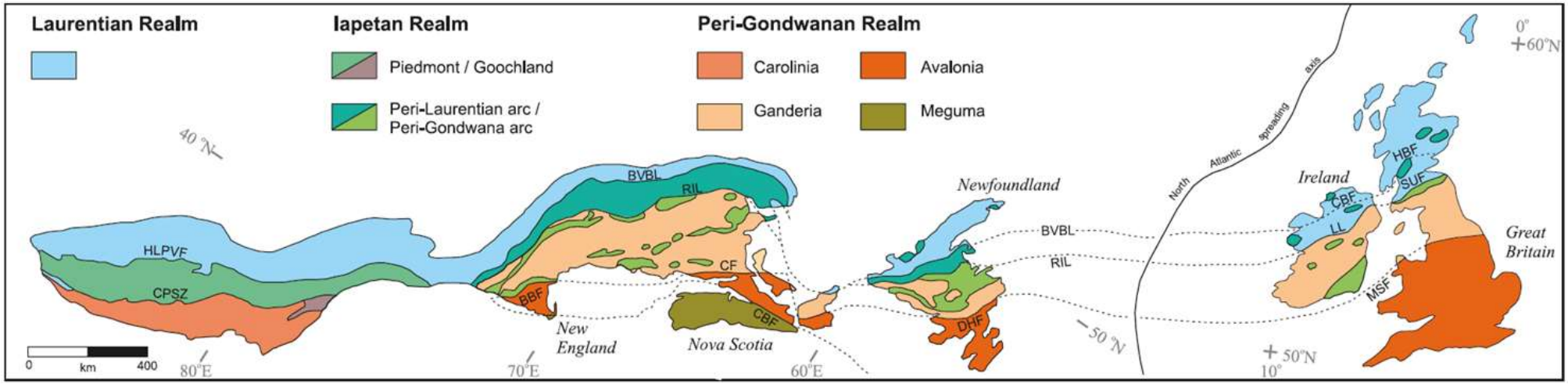

a)

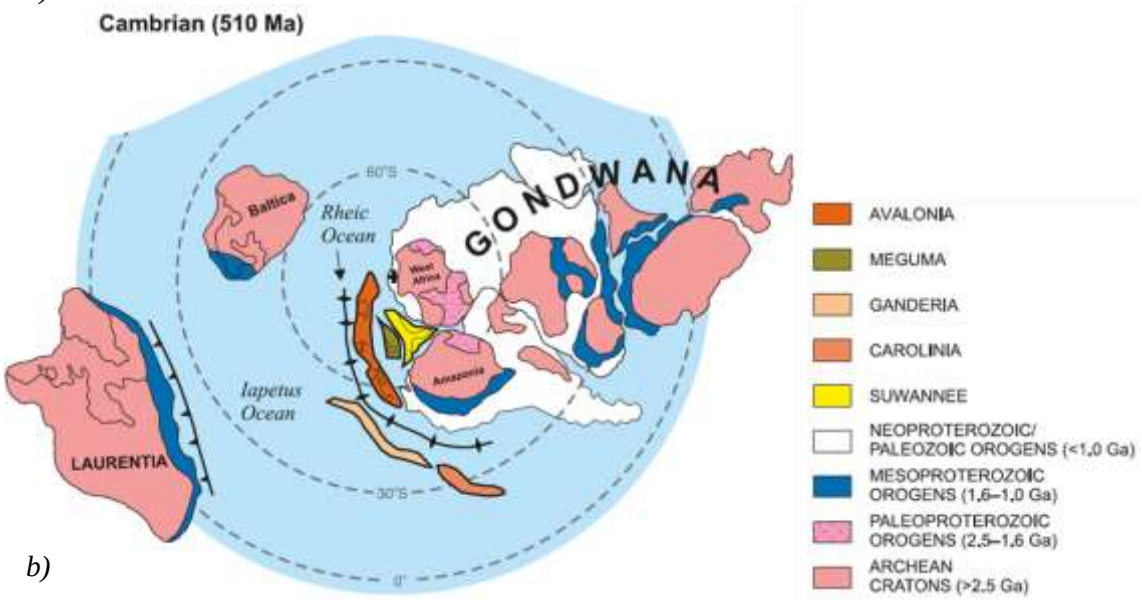

b)

Figure 3.1: a) a schematic map showing the regional setting of the Appalachian orogen with the constituent Laurentian, Iapetan and Per—Gondwanan realms (Pollock et al., 2012). b) a paleogeographic reconstruction proposed by Pollock et al. (2012)for the Appalachian terranes in the Cambrian. Avalonia and Ganderia are positioned at high southern latitudes proximal to the margin of Gondwana at the onset of closure in the Iapetus Ocean.

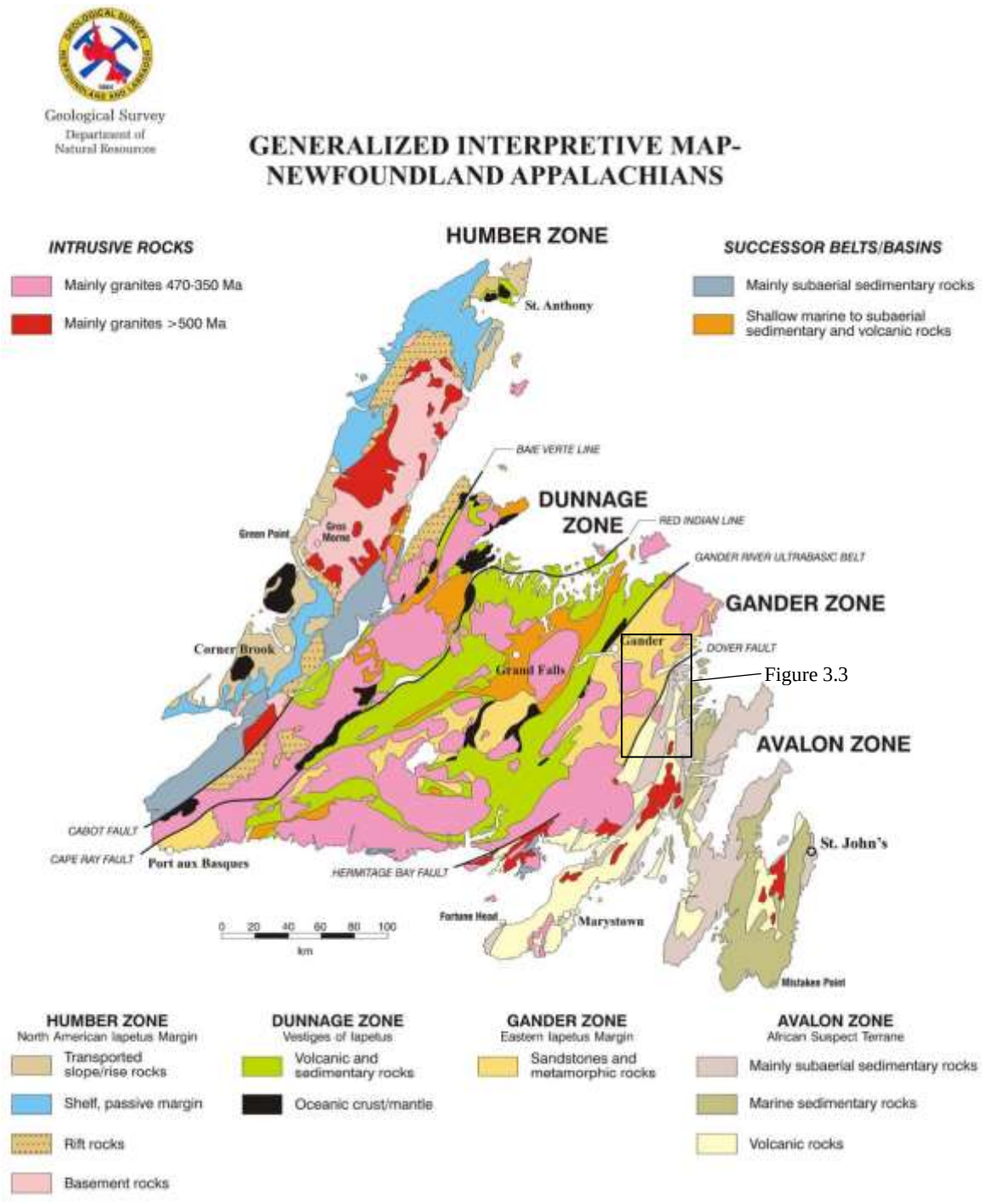

Figure 3.2: Generalised Interpretive Map – Newfoundland Appalachians (Hayes and Williams, 2004). Box indicates study area shown in Figure 3.3.

margin of Laurentia whereas the Dunnage Zone is interpreted as an ancient oceanic-arc assemblage that forms part of the Iapetan realm (Soper et al., 1992; van Staal et al., 2009). The tectonic terranes that are pertinent to this research include Ganderia and Avalonia of the peri- Gondwanan realm, meaningthat they are thought to be both microcontinents that were proximal to the Gondwanan margin prior to closure of the Iapetus (see Figure 3.1). The larger Ganderia and Avalonia microcontinents correspond to the Gander and Avalon Zones in central and eastern Newfoundland.

Ganderia comprises a distinct succession of Lower Cambrian to Tremadoc clastic sedimentary rocks and Mid Cambrian arc-back-arc systems that are built on a basement of Neoproterozoic volcanic and plutonic rocks (Pollock et al., 2012; Waldron et al., 2015). Palaeogeographic reconstructions of the Appalachian orogeny assign a source region proximal to the Amazonian craton for Ganderia and constrain the rifting of Ganderia from Gondwana to the Mid Cambrian (513-505 Ma) as shown in Figure 3.1.b (van Staal et al., 2009; Pollock et al., 2012). Avalonia comprises a characteristic suite of Neoproterozoic subduction-related plutonic and volcanic rocks that are overlain by a Cambrian – Early Ordovician platformal sedimentary succession (van Staal et al., 2009; Pollock et al., 2012; Waldron et al., 2015). Similarly to Ganderia, Avalonia is assigned a source proximal to the Amazonian craton in Gondwana (see Figure 3.1.b) but the rifting of this microcontinent is believed to have occurred in the Early Ordovician (Pollock et al., 2012).

Accretion of the Ganderia and Avalonia microcontinents to the margin of Laurentia gave rise to two episodes of the Appalachian orogeny: the Salinic and Acadian orogenies respectively. Ganderia docked in a two-stage orogeny from 450-421 Ma with an early collision between Laurentia and the active leading edge of Ganderia followed by the closure of the Tetagouche-Exploits basin that marked the final stage of the Salinic orogeny (van Staal et al., 2009; Pollock et al., 2012). The Acadian orogeny is interpreted to have occurred in the period 421-390 Ma and marks the final docking of the two terranes (van Staal et al., 2009; Pollock et al., 2012; van Staal and Barr, 2012; Kellett et al., 2016).

3.2 The Geology of the Gander Zone

The Gander Zone forms a linear belt in the centre and east of Newfoundland that is characterised by variable deformation and metamorphism of a series of metasediments and intrusive phases

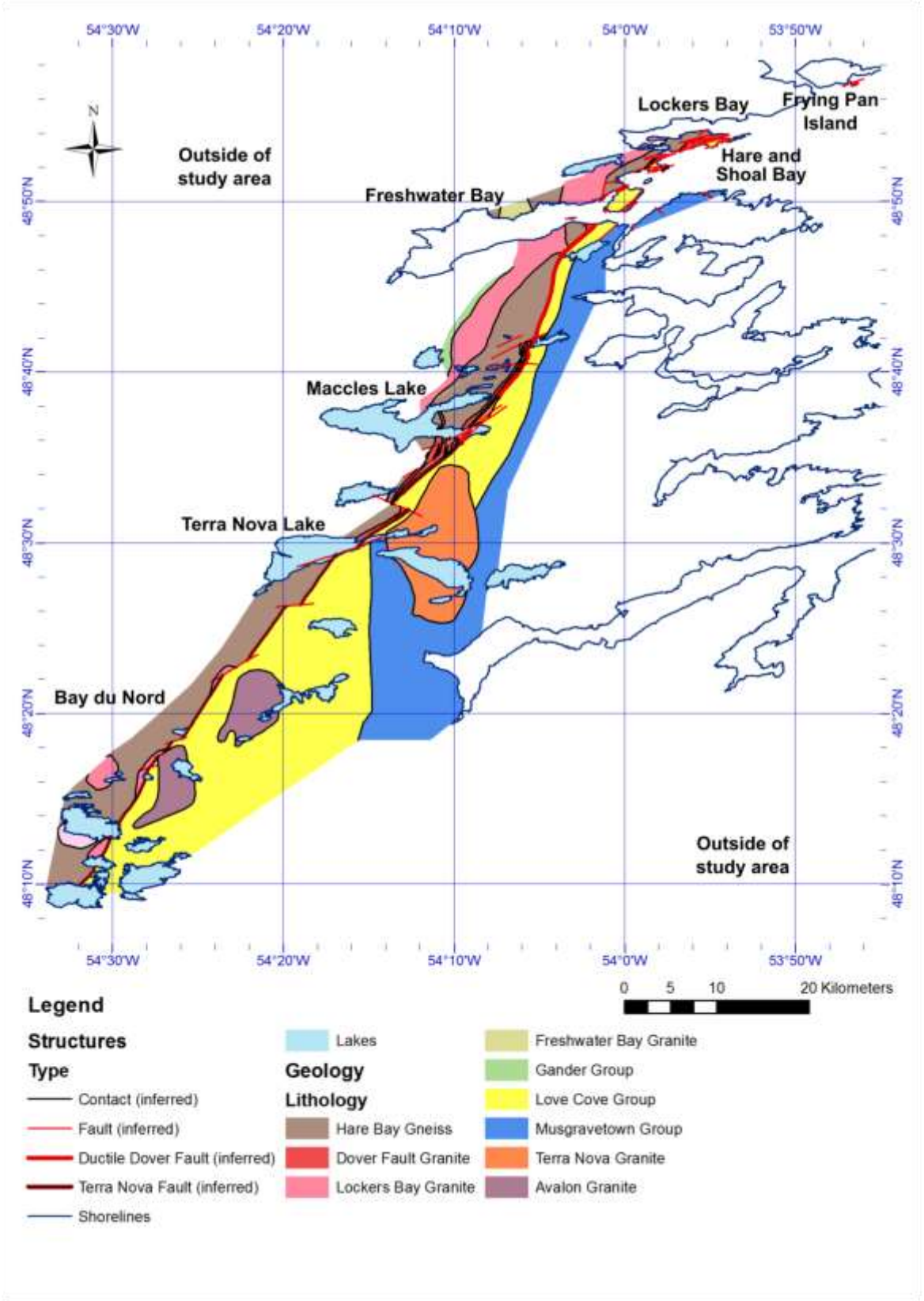

Figure 3.3: Geological map of lithologies and structures derived from field work by Holdsworth (1990-92) in the case study area in northeastern Newfoundland from the Bay du Nord wilderness reserve in the south to Lockers Bay in the north (see also Holdsworth, 1994).

(Holdsworth, 1994; King, 1997). Multiple phases of deformation are recorded in the Gander Zone that both precede and are associated with the development of the DFSZ. Throughout the Gander Zone, metamorphic grade and structural complexity progressively increase towards the DFSZ and Avalon Zone in the east (Holdsworth, 1991; Kellett et al., 2016). There are several shear zones present further to the west of the Gander Zone that are thought to be coeval with the DFSZ, including the Wing Pond Shear Zone and the Cape Freels Granite Shear Zone (O'Neill, 1991; Holdsworth et al., 1993; Jones et al., 2006) Granite bodies form a curvilinear belt with a focus at the Gander-Avalon boundary and, in the Gander Zone, several plutons display evidence of syntectonic emplacement (Holdsworth, 1994; Kellett et al., 2014).

2.2.1 The Gander Group

To the west of the DFSZ, the metasedimentary rocks of the Gander Group preserve structures and lithologies that have undergone less intense deformation and metamorphism than those that have been wholly reworked in the vicinity of the DFSZ. The Gander Group has been subdivided into two formations: the lower Jonathan's Pond Formation and the overlying Indian Bay Big Pond Formation (Kennedy and McGonigal, 1972; O'Neill, 1991; Holdsworth, 1994). The Jonathan's Pond Formation is formed of continentally derived quartz-rich clastic rocks and the Indian Bay Big Pond Formation contains sandstones, pelites and substantial volcanic detritus (Kennedy and McGonigal, 1972; Blackwood, 1977; O'Neill, 1991; Holdsworth, 1994)..

3.2.1 The Hare Bay Gneiss

First identified as a distinct unit by Blackwood (1977), the Hare Bay Gneiss (HBG) occurs in discontinuous northeast-trending belts in the Gander Zone that parallel the DFSZ, as shown in Figure 3.3. A gradational contact, usually on the order of several tens of metres wide, with the metasediments of the Gander Group to the west has been taken to indicate that both the Gander Group and HBG formed from the same lithological succession but underwent different degrees of deformation and metamorphism (Holdsworth, 1994; Langille, 2012).

The highly deformed and metamorphosed HBG consist predominantly of orthogneisses ranging in composition from granitic to tonalitic with locally abundant granitic intrusions (Langille, 2012). Minor lithological units of the HBG include tonalite, paragneiss, pegmatite, mafic intrusions and

quartz veins (Holdsworth, 1994; Langille, 2012). The metasedimentary units of the HBG contain migmatized semi-pelite, psammite and pelite (Holdsworth, 1991). All of these rock types are so closely intermingled across centimetre to metre-scales that they are commonly impractical to separate when represented on a map. Localised migmatites within the HBG indicate partial melting with varying degrees of metamorphic segregation, melt segregation and disaggregation of restite (Holdsworth, 1991; King, 1997). The migmatites range from relatively coherent stromatic migmatites to thoroughly mobilized schlieren-rich xenolithic granites (Holdsworth, 1991, 1994). Granites and orthogneisses from the HBG have peraluminous compositions and have been dated using U-Pb in zircon to give an age range from 510 ± 4 Ma to 387 ± 2 Ma, indicating an extended period of magmatism over 120 million years at the Gander-Avalon boundary (Langille, 2012).

3.2.2 Intrusive Rocks in the Gander Zone

Intrusive rocks are especially common in the east of the Gander Zone with many of the earliest intrusions wholly restricted to the HBG (see Figure 3.4). A series of irregular to anastomosing networks of fine, pinkish-grey aplogranites are the relative oldest intrusive phase as they are crosscut by all subsequent intrusive phases (Holdsworth, 1991). Subsequently, alkali-feldspar-megacrystic granites and dioritic to granitic-mixed-sheeted complexes were emplaced in the Silurian as a group of foliated elongate plutons that parallel the regional foliation in the HBG (Holdsworth, 1994; King, 1997). The sheeted complexes range in composition from dioritic to granitic, suggesting an evolution of the intruded magma from an intermediate to a more silicic composition. The Cape Freels Granite and Dover Fault Granite are examples of foliated-biotite-megacrystic granites that are located wholly within the HBG. All of these granites show steeply dipping, NE striking foliations and many, including the Cape Freels Granite, contain evidence of deformation in the magmatic state (Holdsworth, 1991; Holdsworth et al., 1993; King, 1997). Emplacement of these megacrystic granites is therefore taken to have occurred coeval with metamorphism and deformation of the Gander – Avalon boundary (Holdsworth, 1991).

In contrast, Devonian alkali-feldspar-megacrystic granites, such as the Deadmans Bay (390 ± 4 Ma, U-Pb zircon dating) and Newport Granites (385 Ma) shown in Figure 3.4, are unfoliated and are discordant to structures in the country rocks (King, 1997; Kellett et al., 2014). In addition, younger

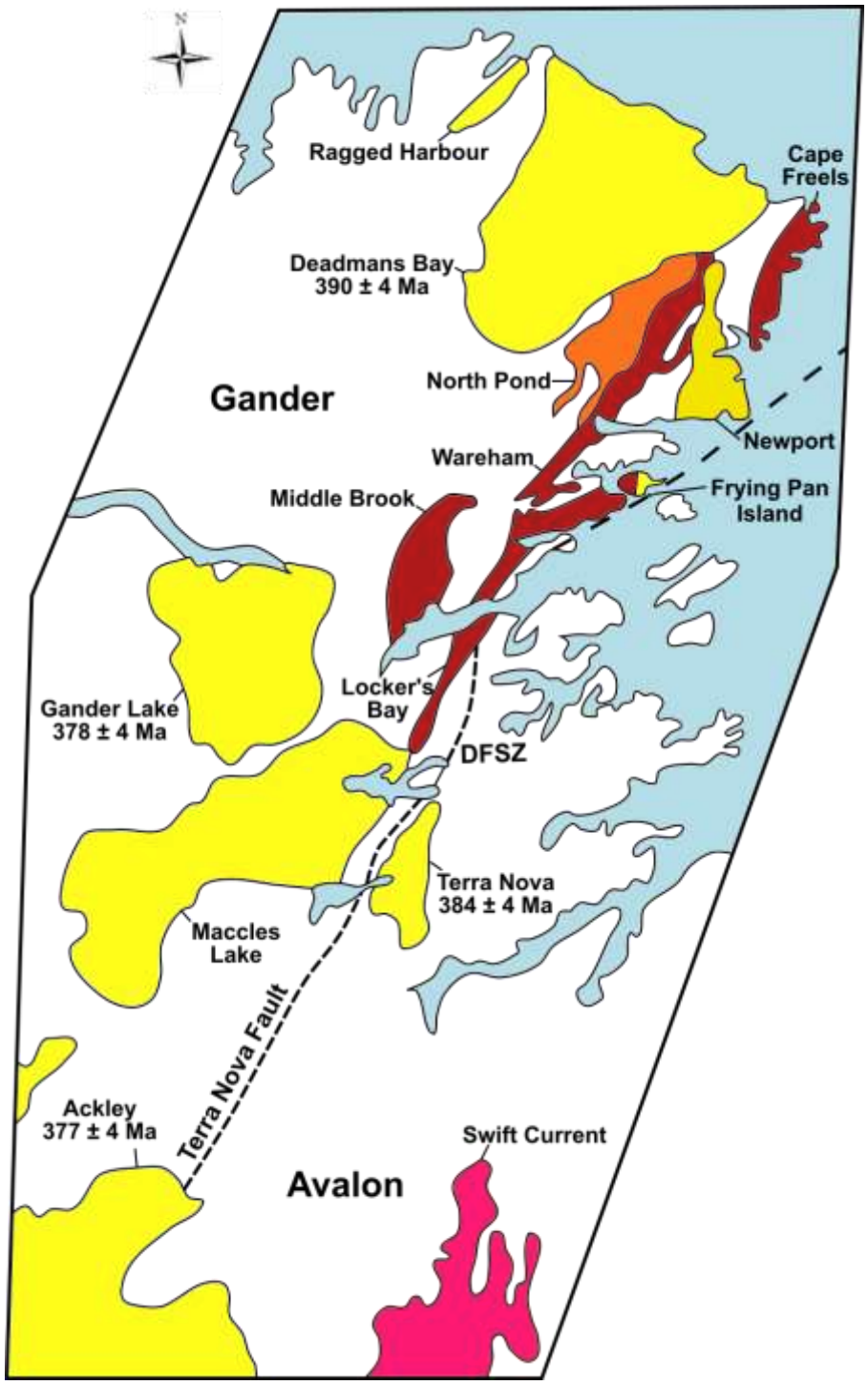

Figure 3.4: a schematic map of the major granitic plutons in both the Gander and Avalon zones of northeast Newfoundland (adapted from Holdsworth, 1994). Only a few plutons have been dated and few have accurate ages derived from U-Pb zircon dating, those provided are taken from Kellett et al. (2014, 2016). Pink – Precambrian intrusions, Red – Silurian intrusions, Orange – Silurian-Devonian boundary intrusions, Yellow – Devonian intrusions.

Gander Zone plutons display the development of contact aureoles and associated mineralisation, which is indicative of shallower crustal emplacement than the Silurian intrusions (King, 1997; Schofield and D'Lemos, 1998; Kellett et al., 2014, 2016). This too is consistent with progressive exhumation of the Gander-Avalon boundary through the Silurian to the Devonian.

3.3 The Geology of the Avalon Zone

The Avalon Zone has its own distinct lithostratigraphy thus showing that prior to the Silurian the geological history is markedly different to that of the Gander Zone. During the Late Precambrian (635-560Ma), the Avalon terrane experienced complex bimodal volcanism, comagmatic plutonism and sedimentation in fault bounded basins (O'Brien et al., 1983; Krogh et al., 1988; Holdsworth, 1994). The lithostratigraphic units in the Avalon Zone form a series of linear belts that trend north to NNE, as shown in Figure 3.2 and 3.3, and the regional metamorphic grade increases towards the DFSZ in the west, mirroring the Gander Zone. Most of the lithological contacts in the Avalon Zone are faults, which complicates relating the ages of the different lithostratigraphic units. Only those units that occur closest to the DFSZ are described here.

3.3.1 The Musgravetown Group

The Musgravetown Group (MSG) forms a linear lithostratigraphic belt of sedimentary and meta-sedimentary rocks in the Avalon Zone to the east of the Love Cove Group outcrop, as shown in Figure 3.3. Two main subdivisions of the MSG as suggested by Jenness (1963) are the lower Rocky Harbour Formation and the conformably overlying Crown Hill Formation. A monotonous series of planar-, trough-, and ripple-drift cross-bedded yellow sandstones form the bulk of the Rocky Harbour Formation along with minor conglomerates and volcanics (O'Brien and Holdsworth, 1992). In the lower Crown Hill Formation, the succession includes bright red sandstones, siltstones and shales whereas the upper succession contains pale green to purple pebbly sandstones with evidence of soft sediment deformation (O'Brien and Holdsworth, 1992). Within the MSG, the sedimentary rocks generally young to the west and towards the very top of the succession are several interbedded volcanic layers in close vicinity to the western belt of volcanic rocks that contact the DFSZ (O'Brien and Holdsworth, 1992). This has been taken as evidence that

the volcanic rocks are coeval or younger than the MSG (O'Brien and Holdsworth, 1992; Holdsworth, 1994).

3.3.2 The Love Cove Group

The westernmost lithostratigraphic belt of the Avalon Zone is the volcanic Love Cove Group (Jenness, 1963; Holdsworth, 1994). Dating using zircon U-Pb techniques has constrained the age of the Love Cove Group (LCG) to 590Ma (Dallmeyer et al., 1981; Holdsworth, 1994) and the compositions range from rhyolite to dacite, with rarer andesitic and basaltic units (O'Brien and Holdsworth, 1992). Bounded to the west by the brittle Dover Fault, the lithologies of the LCG include acid-intermediate crystal tuffs, lithic tuffs, breccias, agglomerates and rhyolite flows (Holdsworth, 1991). The units become progressively more deformed in a non-systematic trend towards the west so that in the southeast the LCG has a weak fracture cleavage, whereas at the boundary with the DFSZ the rocks show a mylonitic foliation (Holdsworth and O'Brien, 1993). Within the DFSZ, the lithologies become progressively more deformed and retrogressively altered so that the LCG becomes intensely folded, cleaved and phyllonitic (O'Brien and Holdsworth, 1992).

3.3.3 Intrusive Rocks in the Avalon Zone

Avalonian granites generally show two major compositions: coarse-grained to porphyritic pink-granites and fine- to medium-grained biotite granites (Holdsworth and O'Brien, 1993). The granitic plutons often trend north-south subparallel to the regional banding in the LCG. Many of the Avalon Zone granites, such as the Terra Nova Granite (U-Pb zircon 384 ± 4 Ma) display magmatic to solid state fabrics and show increasing amounts of deformation and retrogression towards the DFSZ (Holdsworth and O'Brien, 1993; Kellett et al., 2014). This suggests that they predate the formation of the fault zone (Holdsworth and O'Brien, 1993). In contrast, the post-tectonic Ackley Granite, dated using U-Pb in zircon at 377 ± 4 Ma (Kellett et al., 2016) straddles the DFSZ across both the Gander and Avalon Zones to 'stitch' together the different terranes (see Figure 3.4). The Ackley Granite's crystallisation age has therefore often been used to constrain a minimum age for displacement along the Gander-Avalon boundary.

3.4 Structural Geology of the Gander-Avalon Boundary

Prior to the Appalachian Orogeny in Newfoundland, there is no evidence of a shared deformational history between the Gander and Avalon Zones (Pollock et al., 2012; van Staal and Barr, 2012). In the Gander Zone, a total of six phases of deformation were identified by King (1997) that correlate to the sequence of accretionary orogens identified in Newfoundland. Mid-Ordovician accretion of the Dunnage Zone is thought to relate to D1 and D2 structures, as represented by flat lying sheath folds and broad upright to overturned folds (Holdsworth, 1994; King, 1997). These phases of deformation are absent in the Avalon Zone, thus indicating that the terrane had not yet been accreted. A localised, retrogressive shear fabric in the west of the Gander Zone was identified as D4 by King (1997) but it is not associated with the DFSZ.

After the Silurian, both the Gander and Avalon Zones contain evidence of three deformation phases that can be correlated across the terrane boundary. Described by both Holdsworth (1991, 1994) and King (1997), these deformation phases have been termed the Early Ductile, Late Ductile and Late Brittle phases or the regional D3, D5 and D6 phases respectively.

3.4.1 Early Ductile (D3) Deformation

Evidence of an Early Ductile phase of deformation is shown by a 20km wide, amphibolite grade shear zone in the Gander Zone and a narrower, 2km wide greenschist facies shear zone in the Avalon Zone (Holdsworth, 1991). The D3 phase of deformation is associated with peak regional metamorphic conditions, mobilization of migmatites in the HBG and the formation of ductile structures described in Chapter 5 (Holdsworth, 1994; King, 1997). D3 structures east of the GRUB line in the Gander Zone (see Figure 3.2) are generally thought to have formed in the final collision-related phases of the Salinic orogeny (Holdsworth, 1994; van Staal et al., 2009). There is some controversy, however, on which orogenic episode lead to the formation of the D3 phase as several authors have assigned the D3 phase in the DFSZ and the coeval Wing Pond Shear Zone to the Acadian orogeny (Kellett et al., 2016; Willner et al., 2017).Dating of the widespread syntectonic intrusions, especially in the HBG, which are usually taken to associate with D3 has constrained the timing of peak metamorphism to 430-422 Ma (Langille, 2012; Kellett et al., 2016).

3.4.2 Late Ductile (D5) Deformation

The D5 phase is generally correlated with the Acadian transpressional accretion of Avalonia to Ganderia during the formation of the DFSZ (Holdsworth, 1994; King, 1997; Kellett et al., 2016). Reactivation of the previously sinistral transpressive shear zone (D3) in the late Silurian to Early Devonian led to the formation of the dextral, ductile DFSZ (Holdsworth, 1994; Soper et al., 1992b). Shear zones on either side of the Gander-Avalon boundary show retrograde greenschist facies metamorphism and $^{40}Ar/^{39}Ar$ dating of muscovite mica in the Gander Zone indicates that the latest dextral slip on the DFSZ occurred at 385.9 ± 1.7 Ma, thus providing a constraint on the timing of D5 metamorphism. Dextral displacements were concentrated along the DFSZ during the D5 phase but this was accompanied by several coeval sinistral shear zones in the Gander Zone, such as the Cape Freels Granite Shear Zone (Holdsworth et al., 1993).

3.4.3 Late Brittle (D6) Deformation

Overprinting all earlier structures, D6 reactivated the previously ductile DFSZ to produce the brittle, strike-slip Dover Fault observed at the present day and is the youngest phase of deformation recorded along the Gander-Avalon boundary (King, 1997; Waldron et al., 2015). Faults assigned to the D6 phase crosscut all other structures and lithologies (Holdsworth, 1991). In southern Newfoundland, the Hermitage Bay Fault represents the continuation of the boundary between the Gander and Avalon Zones. The Hermitage Bay fault is thought to have formed coeval with activity on the brittle Dover Fault (Hibbard and Waldron, 2009). K-Ar dating of illite in the Hermitage Bay fault gouges at 351 ± 7 Ma is taken as a maximum age for the latest brittle movements along the faults. As the Dover and Hermitage Bay Faults are believed to be coeval, this date indicates that brittle deformation in northeast Newfoundland extended at least into the Carboniferous (Hibbard and Waldron, 2009; Kellett et al., 2016). The brittle faults are highly localised into pre-existing ductile shear zones in both of the tectonic zones (Holdsworth, 1994). In the Gander Zone, rotating fault blocks have produced complex second order fault arrays involving conjugate shearing (Holdsworth, 1991). In addition, minor faults that are slightly removed from the major regional faults appear to form in conjugate sets with sinistral and dextral offsets (Holdsworth, 1991). These

minor faults have been interpreted to accommodate shortening in a NW-SE trend at a high angle to the Gander-Avalon boundary by allowing extension along their strike (D'Lemos et al., 1997).

To conclude, the DFSZ represents a major terrane boundary in the Appalachian orogeny that has undergone multiple deformation phases in association with the closure of the Iapetan and Rheic oceans. Consequently, the rocks in the eastern Gander Zone and western Avalon Zone record multiphase histories of deformation, metamorphism and magmatism. This repeated reactivation of the DFSZ from the Silurian to the Carboniferous makes it an ideal case study location for research into deformation weakening on crustal-scale faults.

4 Chapter 4: Methodology

This chapter aims to introduce all of the datasets available for the research and to summarise the methods used for data collection. In order to understand the nature of deformation weakening in the DFSZ, the approach used aims to identify the fault rock fabrics, metamorphic grades and deformation mechanisms that are preserved in the available samples. It will also justify the choice of data and methods that were used out of all available data and the measures that were taken to standardise data collection to ensure the repeatability of the research method.

4.1 Available Data

Fieldwork in Newfoundland along the Gander-Avalon boundary was beyond the scope of this project, due to time and budget constraints. However, fieldwork conducted in the field seasons of 1990-93 by R. Holdsworth in northeast Newfoundland provided a substantial volume of data and specimens for study, including 9 notebooks covering 16 study areas, 44 aerial photo field slips and 197 thin sections with associated hand specimens. This original fieldwork covered an area encompassing most of Bonavista Bay with data collection from Cape Freels in the north-east to the Bay du Nord Wilderness Reserve in the south-east of Newfoundland. As this covers a total area of 8,000 km^2, it would not be feasible to study the entire region so only six areas were chosen for study here, as shown in Figure 4.1.

The areas chosen during the present study are those that are in close proximity to or straddling the Gander-Avalon boundary. In addition, areas of study were required to have good exposure, favourable sample coverage and all original data resources still available. The six main areas chosen for study are shown in Figure 4.1 and they range from the Bay du Nord region just north of the Ackley Granite to Lockers Bay near the town of Dover. Frying Pan Island in Bonavista Bay is the seventh and smallest area chosen for study. These locales cover the full onshore extent of the brittle Dover Fault and also include the main exposures of the wider shear zones that represent the Gander-Avalon boundary. In the descriptions of the field relationships and microstructural analysis, these areas are considered separately as they are detached spatially and display individual characteristics, such as unique intrusion histories.

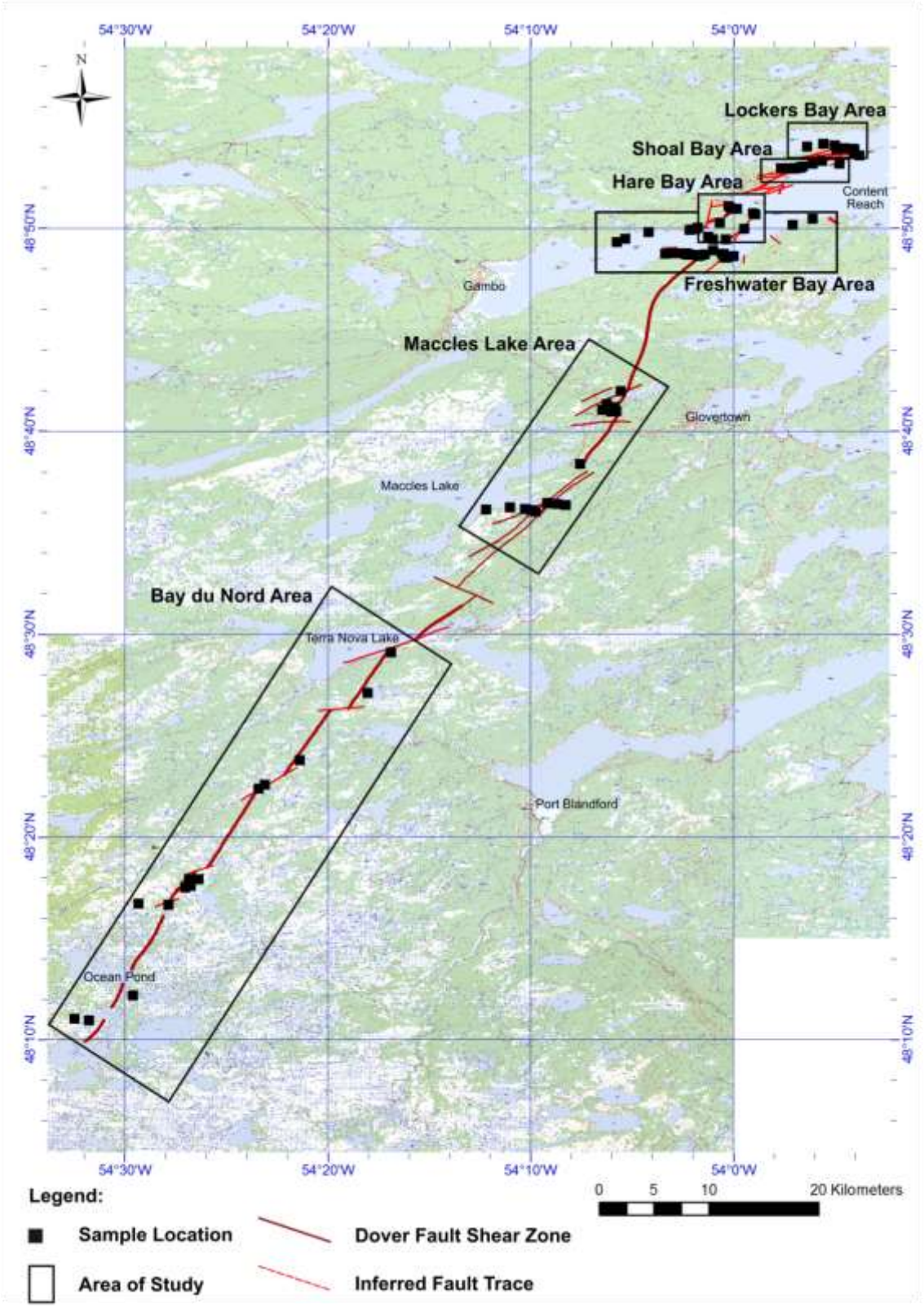

Figure 4.1: A map of the case study area in northeast Newfoundland showing the locations of the samples collected by Holdsworth (1990-92). The six areas chosen for analysis were chosen for their proximity to the DFSZ, good levels of exposure and good spatial coverage of samples.

The data sets available for use in this study include the original field notebooks, shown in Figure 4.2.a, that include structural measurements, lithological descriptions and interpretations for each area. Additional aerial photos and interpretive maps provided location data on sample collection that were used to generate maps such as that shown in Figure 4.1. The fieldwork conducted by R. Holdsworth resulted in the publication of a series of reports and papers in association with the Department of Energy and Mines in Newfoundland, which are used as an additional resource in this research. For the microstructural analysis, the total dataset numbered 117 thin sections with corresponding hand specimens.

4.2 Field Data Analysis

For analysis on the regional to local scale, geological maps were generated using ArcGIS software using both the aerial photos and interpretive maps provided for the study areas (see Figure 4.2.b). These maps were used to supply context for the thin section samples in the wider DFSZ and to identify trends in lithologies, structures and shear zone extent. To supplement this, structural measurements were extracted from the original field notebooks (see Figure 4.2.a) and input into Stereonet 10 software for visualisation and analysis of structural trends. The data were subdivided by region and by structure type so as to compare the orientations of potentially overprinting structures. Finally, the field relationships between lithologies and structures have been described using the information provided in the field notebooks, published material and field photographs (see Figure 4.2).

4.3 Microstructural Analysis

The analysis of the thin sections was limited to optical microscopic descriptions due to the high volume of samples and the limited time frame of a year for this research. The thin sections were all cut parallel to the mineral lineation and normal to the foliation of the hand specimens and all sections have cover slips. This orientation of thin section provides the most information as a non-coaxial deformation history in a sample creates fabrics with a monoclinic shape. By cutting the sample parallel to the stretching lineation and perpendicular to the foliation, the true angle between the foliation planes and the most asymmetric shape of porphyroclasts and sheath folds are revealed, as were any other kinematic information needed to determine sense of shear (see Figure 4.3).

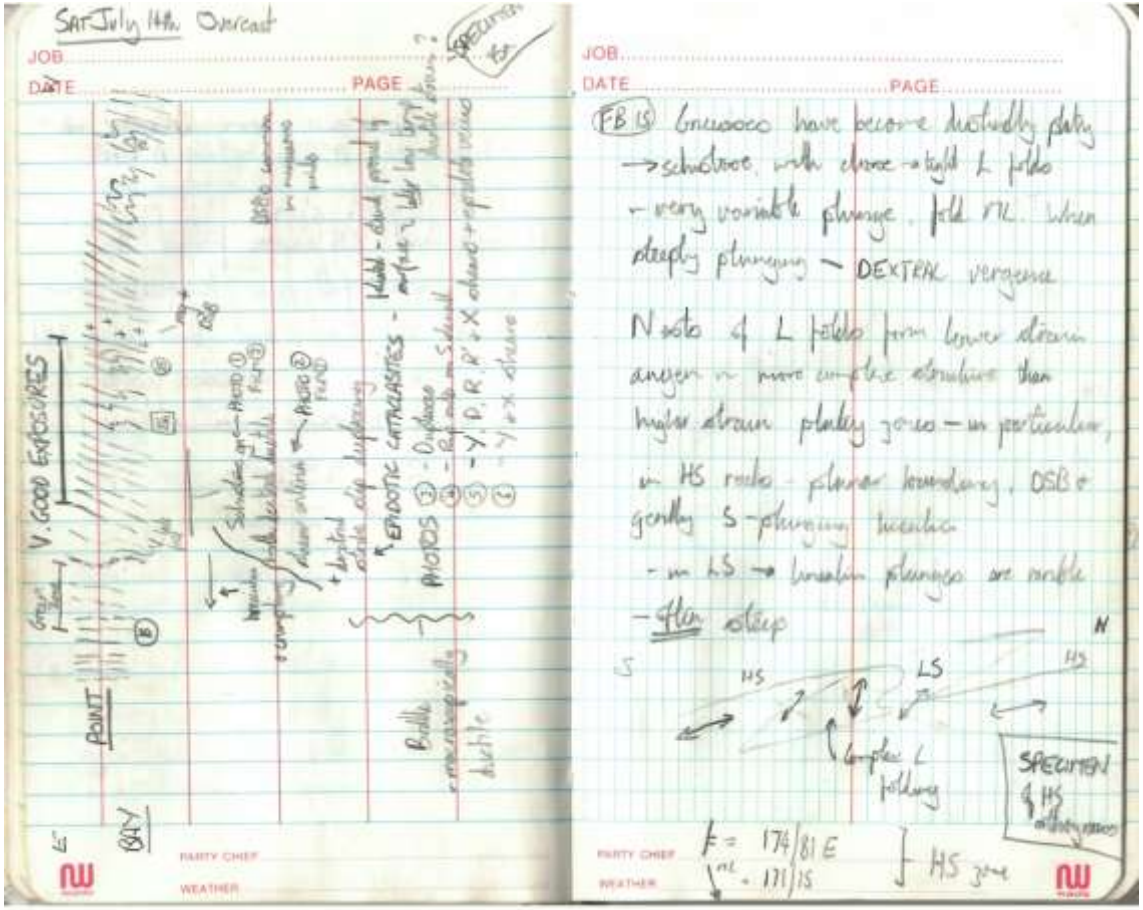

a)

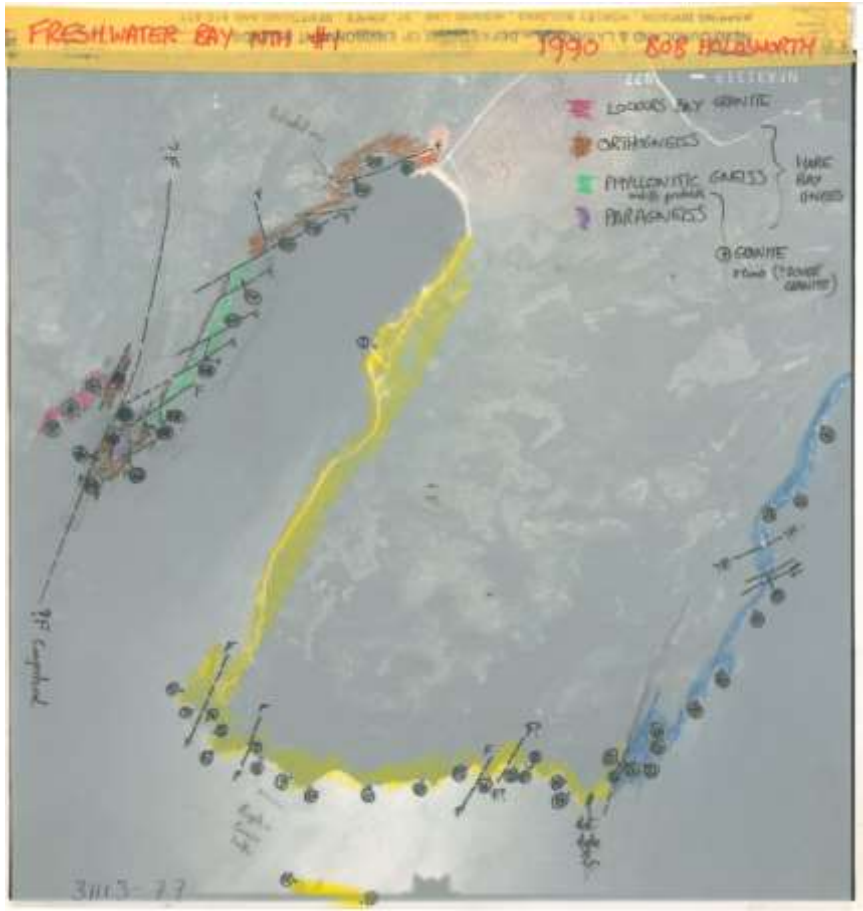

b)

Figure 4.2: a) example pages from a field notebook by R. Holdsworth from the Freshwater Bay study area. b) example aerial photo field slip by R. Holdsworth from the Hare Bay and Freshwater Bay areas with the localities, lithologies and structures marked on a transparent overlay.

In order to ensure consistent data collection during analysis, a standard table was used to describe all of the samples (see Table 4.1). The data collected from the thin sections included descriptions of the mineralogy, grain sizes, fabrics, shear sense indicators, recrystallization or cataclastic textures and any overprinting relationships. During microstructural analysis, the classification of recrystallization textures used the regimes defined by Hirth & Tullis (1992) and Passchier & Trouw (2005). The different regimes, recognised by their distinctive microstructures, are produced by the dominance of particular dynamic recrystallization mechanisms (Hirth and Tullis, 1992; Smith et al., 2007). These regimes are described in Table 4.2 and the characteristic textures are shown in Figure 4.3. In addition, the contrast in microstructures between quartz and feldspar were used in order to estimate the temperatures and metamorphic grades experienced by the samples. K-feldspar and plagioclase require higher temperatures for dynamic recrystallization than quartz and therefore feldspars often display brittle behaviour at temperatures that produce plastic structures in quartz (Passchier and Trouw, 2005; Smith et al., 2007). Consequently, the contrasting deformation styles between quartz and feldspars, in addition to the samples mineralogy, can be used to estimate the temperature conditions during deformation, as detailed in Table 4.3. Shear sense in the thin sections was identified using reliable markers such as stair stepping of wings or mantles on porphyroclasts, offset of markers by micro-faults and the form of S-C fabrics (see Figure 4.3). The shear senses from structures identified in the field, from such structures as shear bands, verging folds and offset markers, were also considered in correlation with the thin section samples. In many cases, the sense of shear was not reliably indicated and ambiguous samples have not been assigned a shear sense so as to avoid misinterpretation. Finally, scaled microphotographs of the textures and fabrics in the thin sections were taken using a Nikon Eclipse LV100POL polarizing microscope as visual aids to the microstructural descriptions.

In conjunction with the thin section descriptions, several hand specimens were described in the context of their fabrics and overprinting relationships. The hand specimens chosen for study correspond to thin sections that showed unique or ambiguous textures and therefore benefitted from study at the hand sample scale. Photographs and sketches of the hand specimens were taken in order to visualise the fabrics and structural relationships represented in the samples.

4.4 Fault Rock Definitions

The following fault rock definitions (Sibson, 1977; Brodie et al., 2007; Fossen, 2010) are included to make clear the classifications assigned to the fault rock samples in this study.

Fault Breccia – Cohesive or non-cohesive fault rocks consisting of randomly oriented fragments resulting from brittle fracturing. Breccia fragments must constitute > 30% of the rock.

Fault Gouge – Fine grained and clay-rich non-cohesive rock located in fault cores and formed by crushing and chemical alteration of the host rock. Breccia fragments constitute <30% of the rock.

Cataclasite – Cohesive and fine-grained fault rock with a poorly developed or absent schistosity.

Schist – A metamorphic rock displaying schistose structure, or a well-developed schistosity.

Gneiss – A metamorphic rock displaying a gneissose structure, or broadly spaced schistosity on the centimetre-scale.

Mylonite – A fault rock which is cohesive and characterised by a well-developed foliation resulting from tectonic reduction of grain size.

Protomylonite – A mylonite in which less than 50% of the rock volume has undergone grain size reduction.

Ultramylonite – A mylonite in which more than 90% of the rock volume has undergone grain size reduction.

Phyllonite – A phyllosilicate-rich mylonite that has a lustrous sheen and is typically strongly sheared.

a)

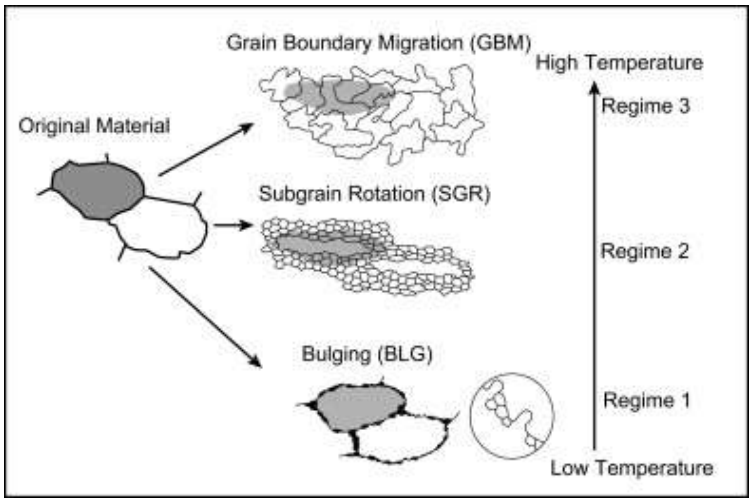

b)

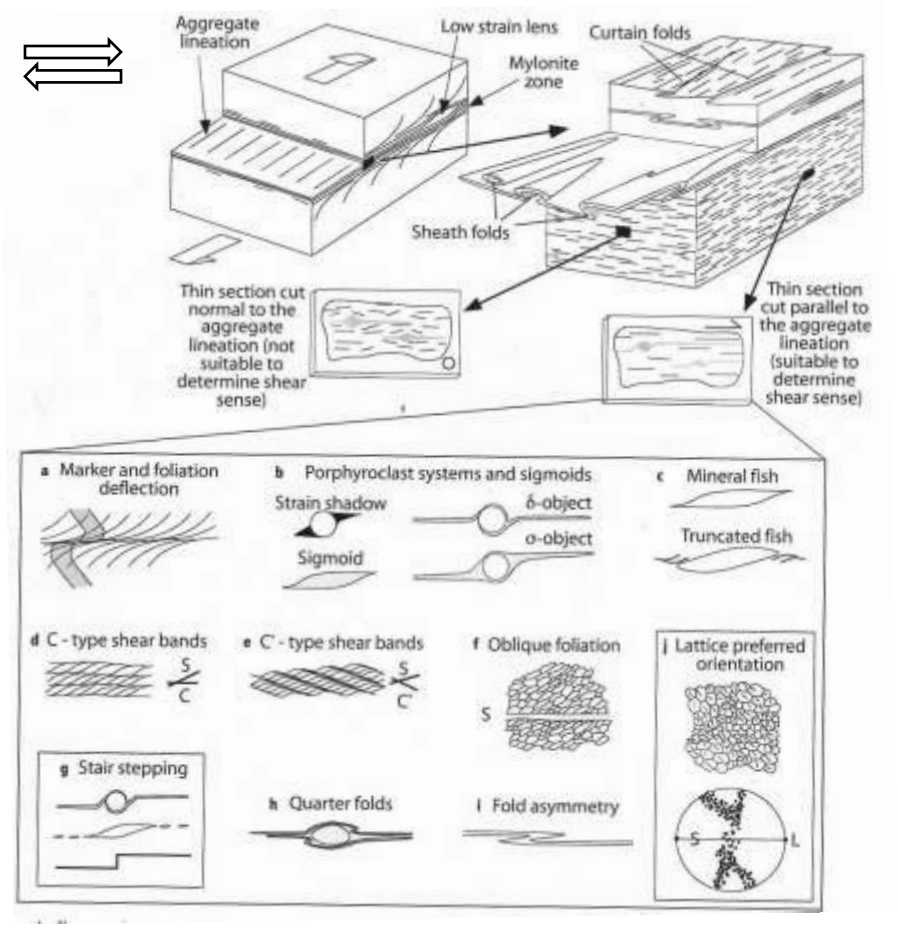

Figure 4.3: schematic diagrams taken from Passchier & Trouw (2005) to show a) the characteristic textures of the different dynamic recrystallization regimes given in Table 4.2 and b) shear sense indicator textures in thin section and hand specimen. All of the examples are given for a dextral shear sense.

Basics:								Brittle Structures:			
Mineral:	Proportion (%):	Place in lattice/slide:	Grain Size			Grain Shape:	Shear sense:	Fractures:			Cataclasis:
Mineral 1			Av.	Min	Max			Inter- or intra-:	Av. Length:	Orientation:	

Crystal Plasticity:										Grain Boundaries:							
Intracrystalline:			Other:	Recrystallisation:						Shape:		Angles		GBAR?	Fluids:		
Undulose extinction	Lamellae	Twinning:		BLG	SGR	GBM	Av. New size	New Shape	CPO?	Relict:	New:	Same phase:	Other phase:		Dissolution:	Precipitation:	Alteration:
(Mineral 1 cont.)																	

Table 4.1 Standard table for optical microscopy descriptions including mineralogy, grain size, brittle fractures, crystal plastic textures and grain boundary textures.

Dislocation Creep Regime	Dominant Recrystallisation Mechanism	Favoured Conditions	Common Microstructural Characteristics
Regime 1	Strain induced bulging (BLG) grain boundary migration	Low temp, high strain rates	Irregular and patchy undulose extinction, very fine recrystallized grain size, absence of aligned subgrains
Regime 2	Subgrain rotation (SGR) recrystallisation	Moderate temp, moderate strain rates	Sweeping undulose extinction, homogeneously flattened original grains, subgrains often with strong crystallographic preferred orientation (CPO), core and mantle structures
Regime 3	Grain boundary migration (GBM) recrystallisation	High temp, low strain rates	Large grain sizes with lobate or sutured grain boundaries, high proportion of recrystallized grains, weak CPO of recrystallized grain.

Table 4.2: Summary table of the microstructures and conditions of deformation associated with the deformation regimes of dislocation creep identified by Hirth & Tullis (1992) and adapted from Smith (2007).

Inferred Metamorphic Grades:	Characteristic textures:	Inferred temperature range:
Diagenesis	Brittle fractures, cataclasis, compaction, dissolution and precipitation	<200°C
Sub-Greenschist	Quartz: brittle fracture, limited undulose extinction and dissolution-precipitation at grain boundaries Feldspar: brittle fracture, cataclasis	200-300°C
Lower Greenschist	Quartz: brittle fracture, BLG recrystallisation, undulose extinction, deformation lamellae Feldspars: brittle fracture, cataclasis	300-400°C
Upper Greenschist	Quartz: SGR and limited GBM recrystallization, pressure solution Feldspar: brittle fracture, undulose extinction, subgrains, twinning, kinking	400-450°C
Amphibolite	Quartz: GBM recrystallization, lobate boundaries, pinning Feldspar: BLG recrystallization, core and mantle fabrics, myrmekites	>450°C

Table 4.3: Descriptions of the microstructural textures used to infer the metamorphic grade and temperature range represented in a thin section (adapted from Passchier and Trouw, 2005).

5 Chapter 5: Gander Zone Results

5.1 Gander Zone Field Relationships

Within the Gander Zone, field observations suggest a progressive eastward increase in deformation, strain intensity and retrogressive alteration across the zone towards the boundary with the Avalon Zone. Following the approach of Holdsworth (1994), the structures observed in the field can be classified by their relative ages and overprinting textures. Early Ductile structures are overprinted by Late Ductile structures, which are in turn overprinted by Late Brittle structures.

5.1.1 Maccles Lake

The Maccles Lake area, shown in Figure 5.1.1, represents the best exposure in the Gander Zone of fault rocks within the DFSZ and is the area that is least affected by later brittle faulting. Consequently, most of the thin section samples (16) from the Maccles Lake area were located in the Gander Zone. The majority of the exposure occurs along road cuttings (often in the road bed itself) and the shorelines of Maccles Lake and smaller ponds in the area, in addition to quarry and railway cutting exposures north of Maccles Lake. Within the area, the Gander-Avalon boundary, represented by the ductile Dover fault, trends NNE-SSW and is exposed on islands in Maccles Lake and to the north of the area, as shown in Figure 5.1.1. Otherwise, the ductile boundary itself is not exposed or has been removed from the sequence by faulting. The HBG occurs in a NE-SW trending lithological belt that terminates at the Gander-Avalon boundary. Several NE-SW to N-S trending granitic plutons contained wholly in the HBG, such as the DFG and LBG, run parallel to the orientation of the Gander-Avalon boundary. The foliation fabric in the Maccles Lake area consistently has a N-S trend and dips steeply to the east or west in all of the Gander Zone lithologies (see Figure 5.1.2). A stretching mineral lineation on the foliation planes generally plunges shallowly to the north or south, as shown in Figure 5.1.3.

The Early Ductile structures in the Maccles Lake area occur in outcrops of the HBG. At the far western boundary of the HBG where it contacts the Gander Group outside of the mapped area to the north of Maccles Lake, the strain intensity shows a marked, stepped increase. Whilst the Gander Group preserves flat lying folds and pressure solution fabrics, the HBG shows a

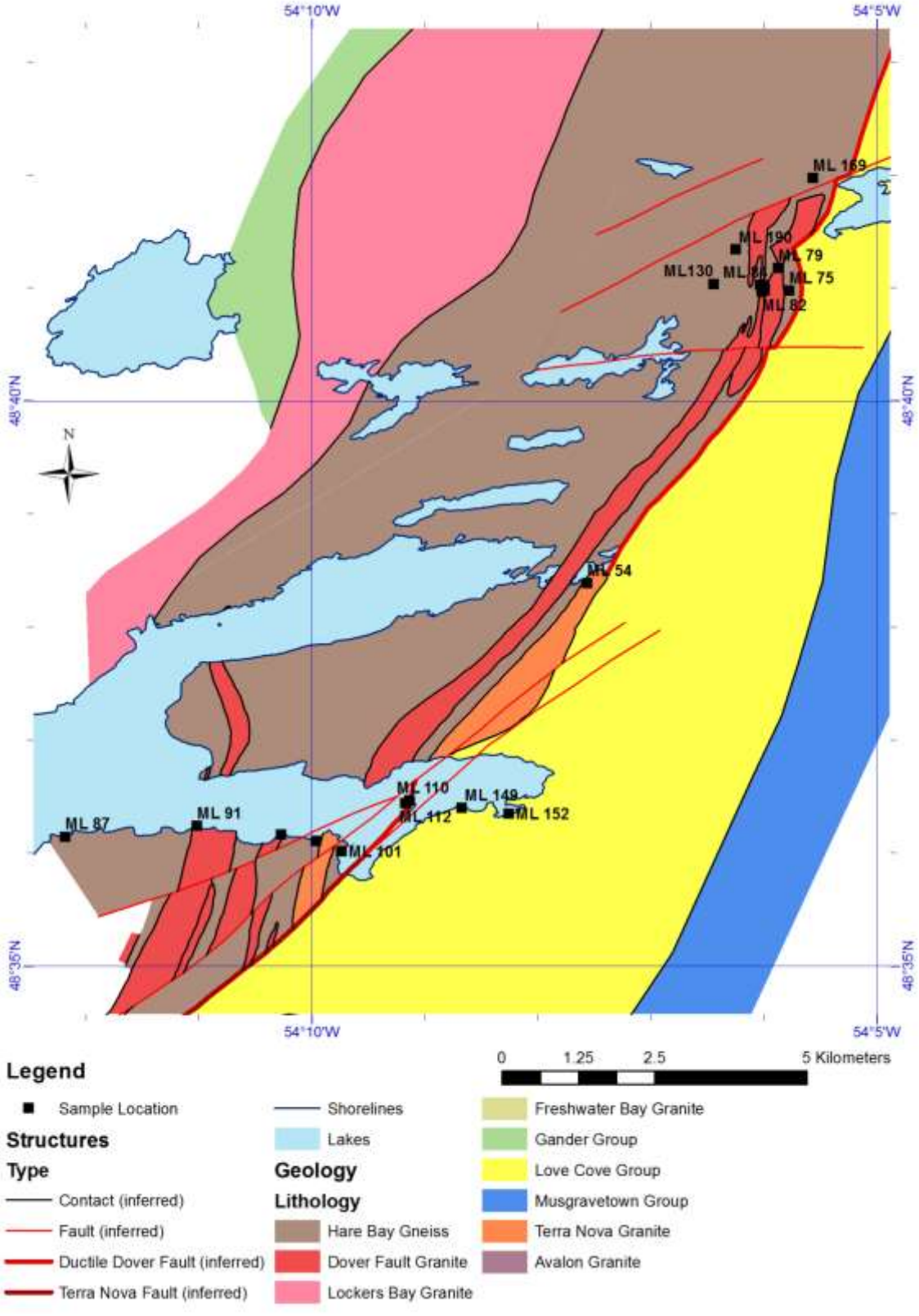

Figure 5.1.1: A geological map of the Maccles Lake study area showing the locations of the thin section and hand specimen samples.

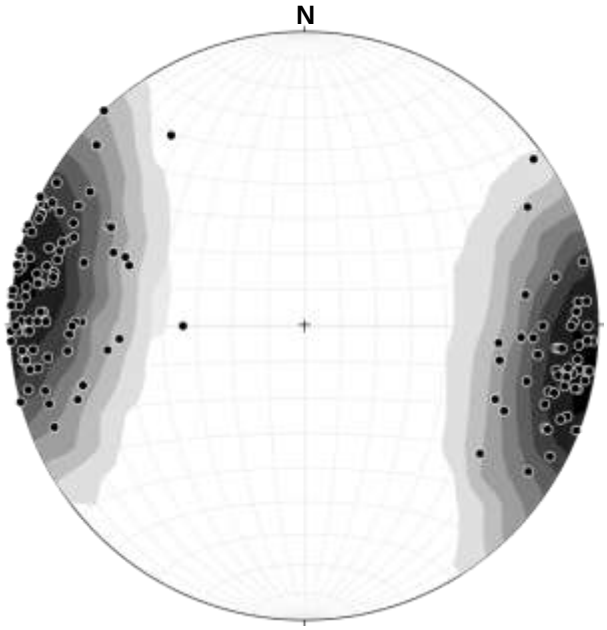

Figure 5.1.2: Stereonet representing the orientations of poles to foliation planes in the Gander Zone of Maccles Lake (HBG and DFG lithologies).

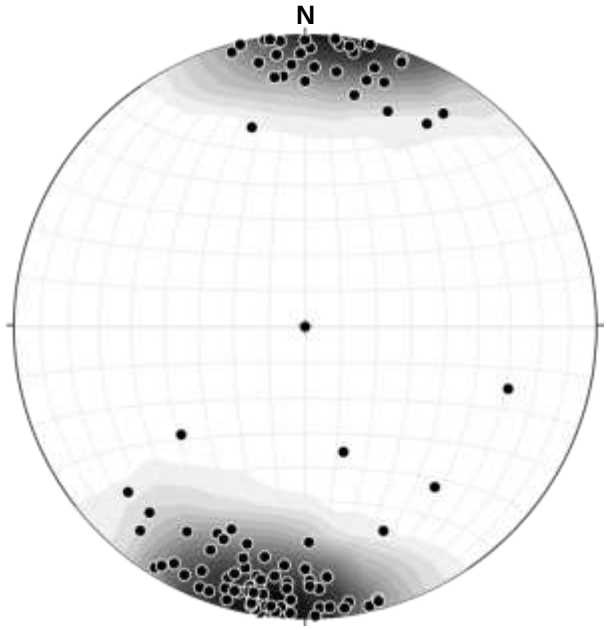

Figure 5.1.3: Stereonet representing the orientations of stretching mineral lineations in the Gander Zone of Maccles Lake (HBG and DFG lithologies).

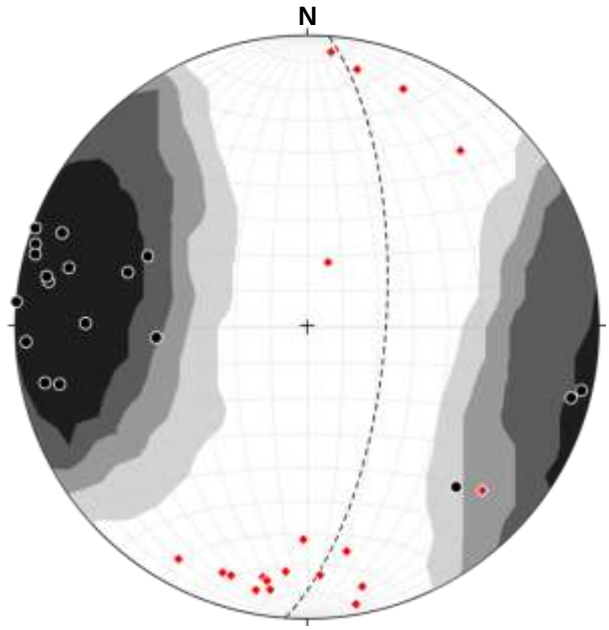

Figure 5.1.4: Stereonet representing the orientations of Early Ductile folds in the Gander Zone of Maccles Lake (HBG and DFG lithologies). Black – poles to axial planes, Red – fold vergence, dashed line – representative axial plane.

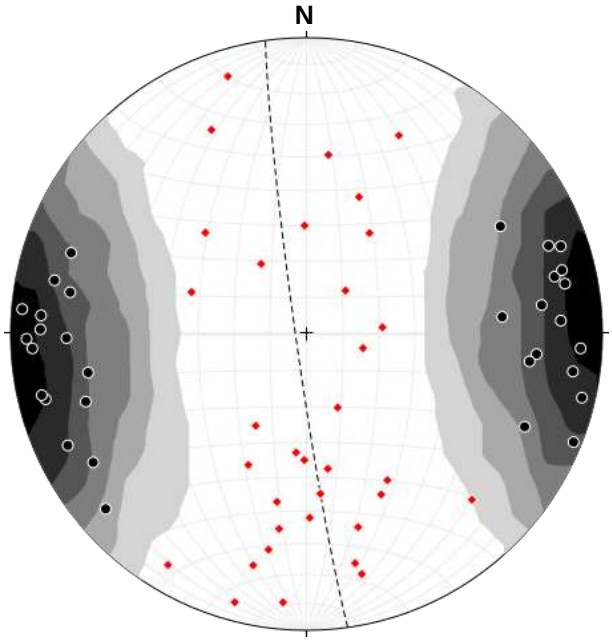

Figure 5.1.5: Stereonet representing the orientations of Late Ductile curvilinear folds in the Gander Zone of Maccles Lake (HBG and DFG lithologies). Black – poles to axial planes, Red – fold vergence, dashed line – representative axial plane.

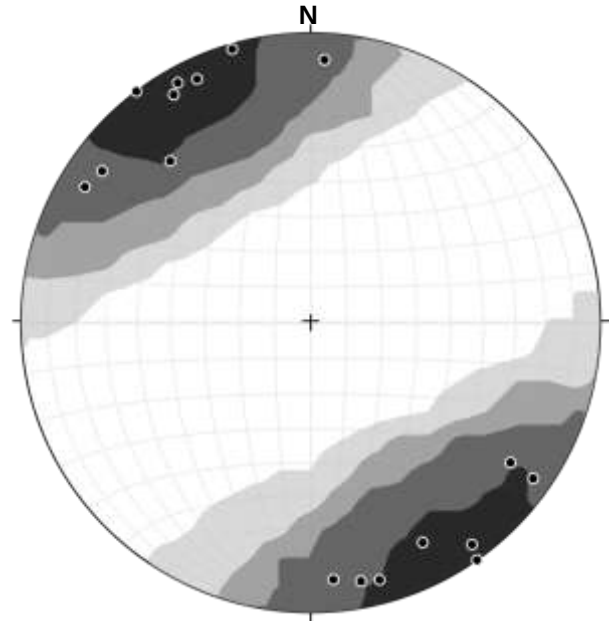

Figure 5.1.6: Stereonet representing the orientations of poles to brittle fault planes showing dextral offset in the Gander Zone of Maccles Lake (HBG and DFG lithologies).

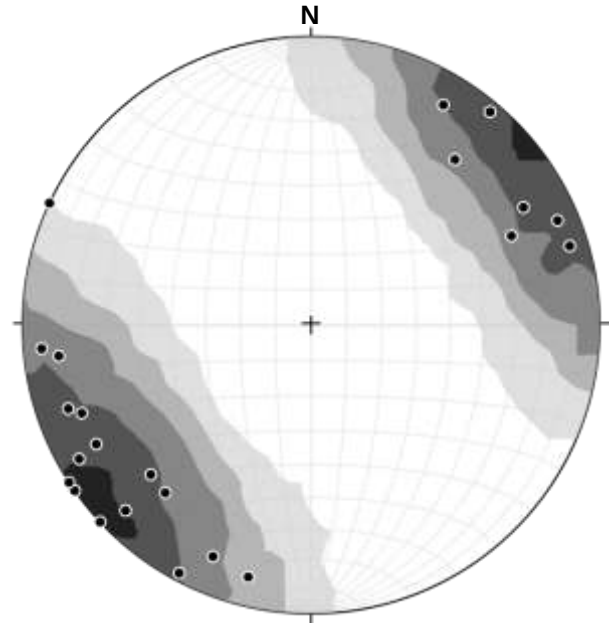

Figure 5.1.7: Stereonet representing the orientations of poles to brittle fault planess showing sinistral offset in the Gander Zone of Maccles Lake (HBG and DFG lithologies).

discontinuous and chaotic form of the lithological units. For example, the amphibolites can occuras continuous interlayers or elliptical pods with sharp contacts. Early Ductile structures in the HBG include mm- to km-scale folds with steeply dipping to vertical northeast-trending axial planes (see Figure 5.1.4), in which minor folds are curvilinear with up to 180° of curvature around the mineral lineation. Sinistral shear sense indicators are common in Early Ductile structures including shear bands, asymmetric wrapping of xenoliths, σ-porphyroblasts and offset markers.

Within 1-2km of the Gander-Avalon boundary, there is a progressive increase in the intensity of structures that overprint the HBG high temperature textures. Whilst the Early Ductile textures in the HBG are fairly ubiquitous, the overprinting Late Ductile structures are mostly restricted to localised shear zones. The Late Ductile structures in Maccles Lake include open to tight curvilinear folds of the mylonitic foliation and lineation on the scale of millimetres to centimetres with N-S trending axial planes (see Figure 5.1.5 for fold orientation and Figure 5.1.8). A dextral shear sense is indicated in Late Ductile structures by the vergence of the curvilinear folds, dextral shear bands and σ-porphyroblasts (see Figure 5.1.9). Chlorite, epidote and other alteration products become progressively more apparent towards the Gander-Avalon boundary so that both the HBG and intrusive lithologies become strongly phyllonitic. The Dover Fault Granite (DFG) in the Maccles Lake area is a narrow, elongate, sheeted intrusion of mylonitic granite with strongly wrapped feldspar porphyroclasts clearly visible in the field. Networks of conjugate sinistral and dextral phyllonitic shear zones occur within the DFG together with rarer coarse-grained amphibolites and gabbros. The DFG exposures within 1-2km of the Gander-Avalon boundary display solid-state recrystallization fabrics, such as S-C textures and compositional banding.

Minor faulting is also concentrated around the ductile Dover Fault, especially in pre-existing shear zones. The faults are steeply dipping with shallowly plunging slickenlines, suggesting strike-slip fault movement. Using the stereonets in Figure 5.1.6 and 5.1.7, it is apparent that there are conjugate sets of faults that show both sinistral and dextral displacement. Often, these minor faults are marked by narrow veins of epidotic cataclasite or broader zones of breccias. In association with the faults are other brittle structures that include kink- and box-folds and calcite and quartz veining.

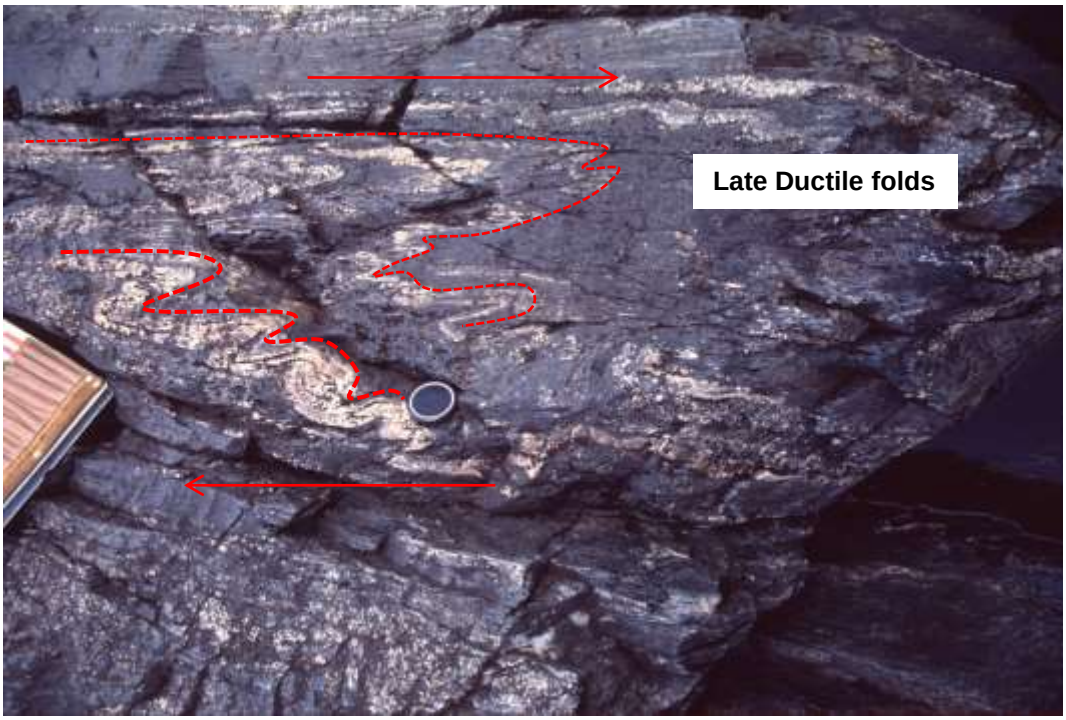

Figure 5.1.8: field photograph of disharmonic Late Ductile folds of granitic veins in a unit of pelitic HBG at locality 40 at Maccles Lake. Lens cap for scale.

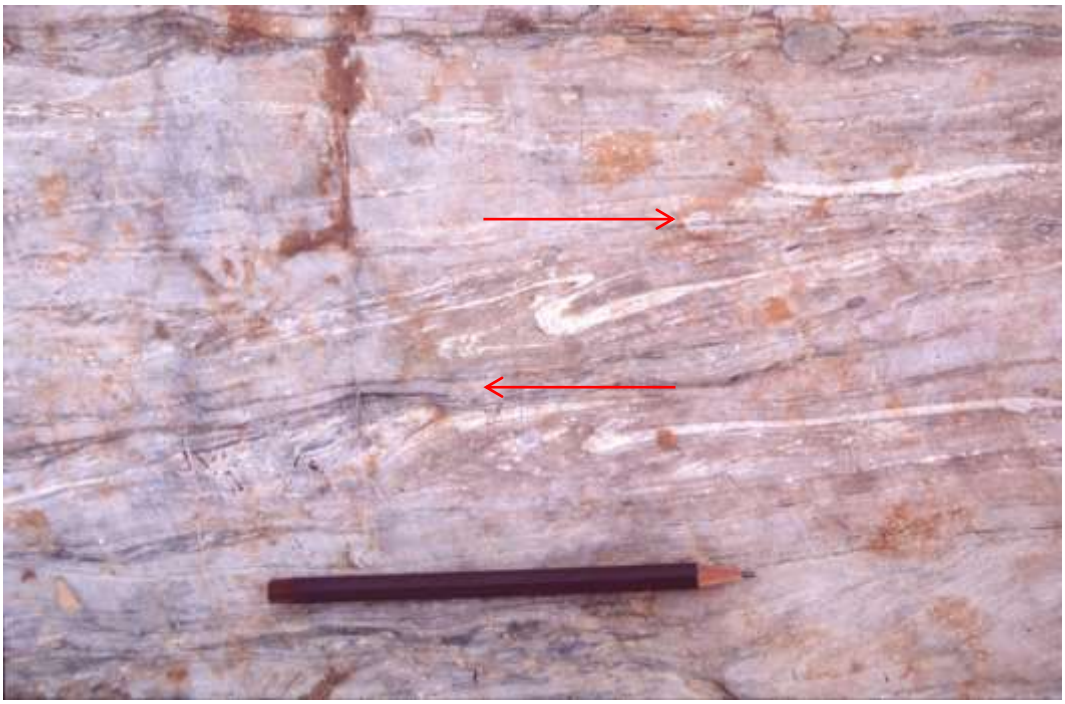

Figure 5.1.9: field photograph of Late Ductile, dextral, asymmetrical folds in mylonitic DFG at locality 10 at Maccles Lake. Pencil for scale.

5.1.2 Bay du Nord

Shown in Figure 5.1.10, the Bay du Nord study area covers a distance of 38km from Terra Nova Lake in the north to Island Pond West in the south. Exposure is relatively poor so the sample collection was limited to isolated hill top, river bank and lake shoreline exposures visited by helicopter. The brittle Terra Nova fault trends NNE-SSW across the area and it represents the Gander-Avalon boundary in Bay Du Nord as the DFSZ has been excised from the sequence by the later faulting. The boundary also shows evidence of later offset at scales of 400m to 2km that indicates the presence of a series of major, dextral strike-slip faults that are not exposed. In the Bay du Nord area, the HBG is in contact with the majority of the Gander-Avalon boundary as well as several narrow, elongate Locker's Bay (LBG)-type granite bodies that parallel and terminate at the boundary. The megacrystic granites are often interlayered on the metre-scale with screens and sheets of HBG pelites, semi-pelites and gneisses. The foliation in the Bay du Nord area generally trends NNE-SSW with steep dips to the ESE or WNW (see Figure 5.1.11). The associated stretching lineations show a range of shallow to steep plunges and trend NE or SW (see Figure 5.1.12).

Early Ductile structures in exposures of HBG and LBG are best represented at localities >1km from the Gander-Avalon boundary in the Bay du Nord area. The HBG and LBG contain sinistral σ-porphyroclasts, gneissic layering and close folds on the millimetre to centimetre-scale around the mineral lineation (see Figure 5.1.14). The Late Ductile structures in close proximity to the Gander-Avalon boundary in the Bay du Nord area differ from the other study areas in that the dominant shear sense indicators are sinistral. The shear indicators include σ-porphyroclasts, shear bands and S-C fabrics (see Figure 5.1.15). Towards the boundary, the HBG and LBG contain fine grained mylonitic shear zones that include progressively higher proportions of chlorite and muscovite. The earlier ductile structures are complicated by the Late Brittle overprinting faults, fractures and folds in the Bay du Nord area. For example, very open to close Late Brittle folds that show a dextral shear sense (see Figure 5.1.13) were observed to distort the earlier foliation and lineation fabrics.

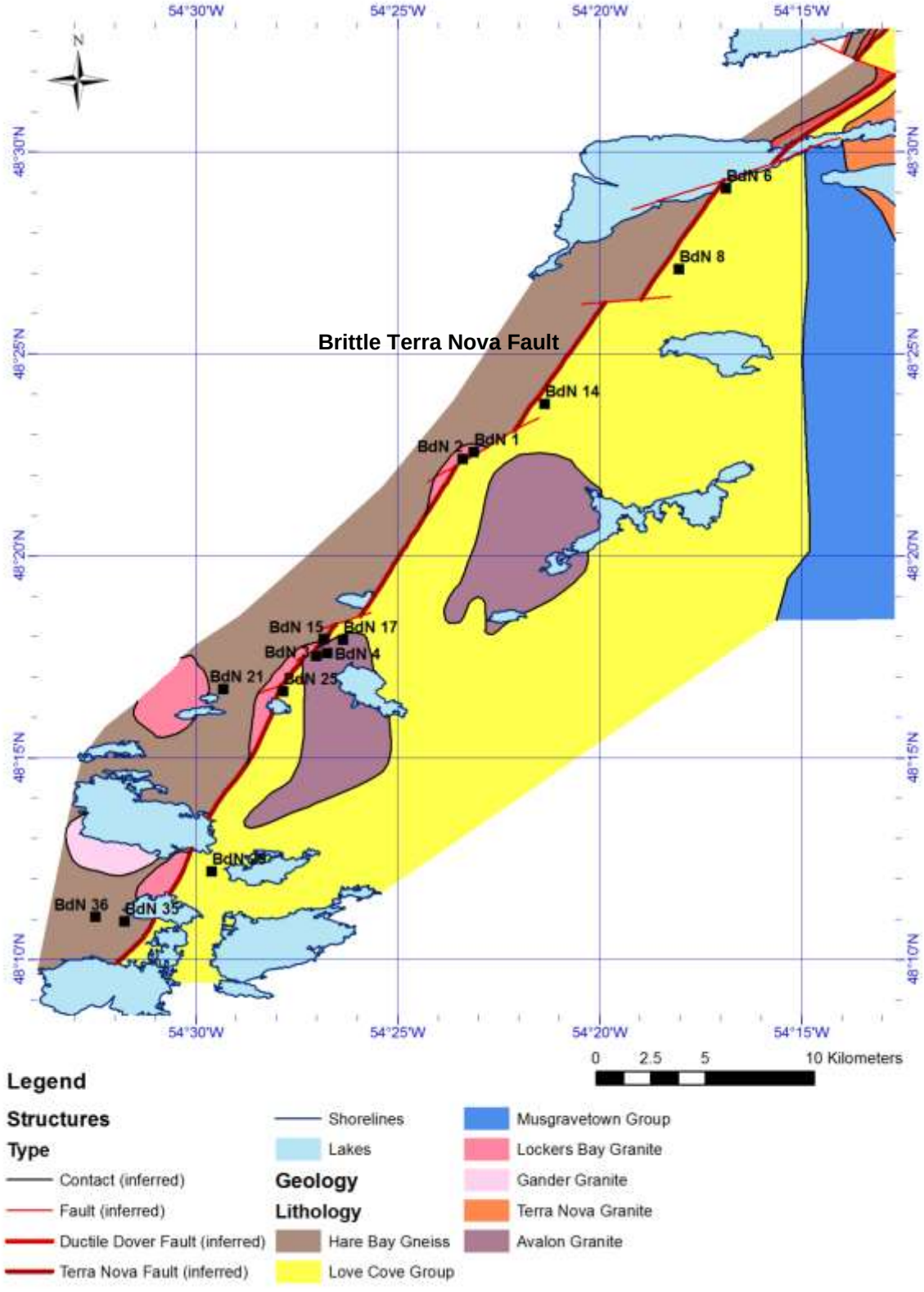

Figure 5.1.10: a geological map of the Bay du Nord area showing the locations of the thin section and hand specimen samples

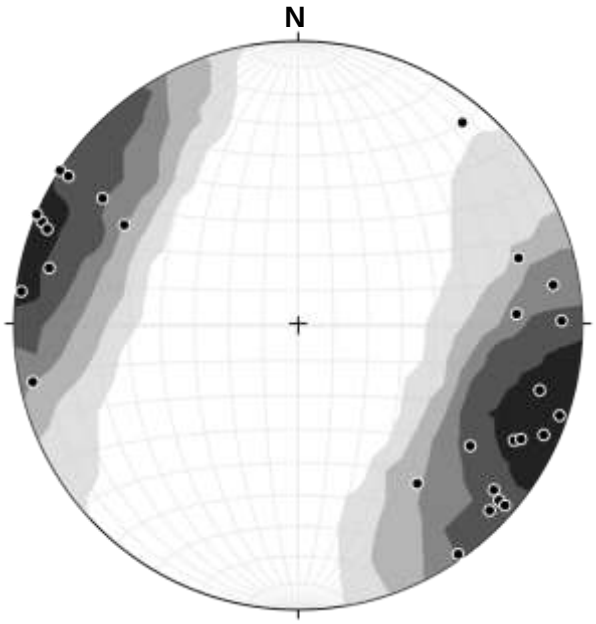

Figure 5.1.11: Stereonet representing the orientations of poles to foliation planes in the Gander Zone of Bay du Nord (HBG and LBG lithologies)..

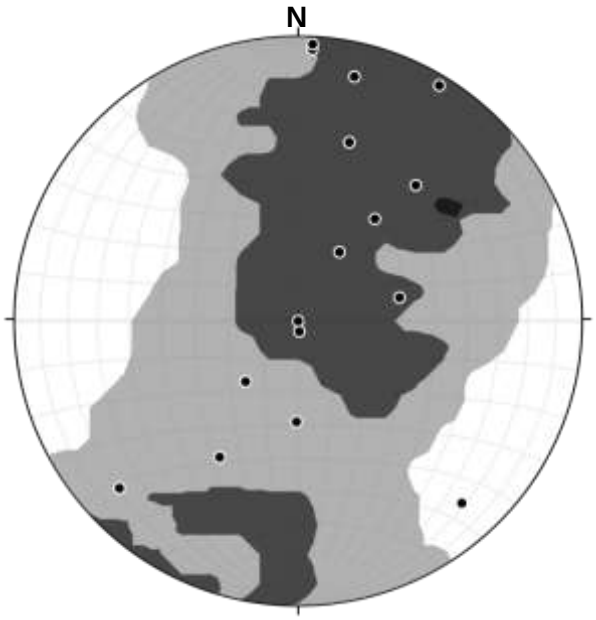

Figure 5.1.12: Stereonet representing the orientations of stretching mineral lineations in the Gander Zone of Bay du Nord (HBG and LBG lithologies).

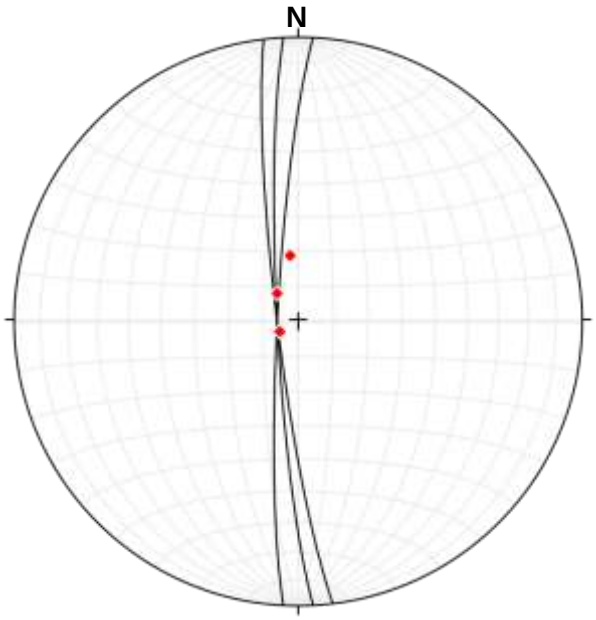

Figure 5.1.13: Stereonet representing the orientations of Late Brittle folds in the Gander Zone of Bay du Nord (HBG and LBG lithologies). The upright folds have steep N-S trending axial planes.

Figure 5.1.14: field photograph of gneissic granite at locality 22 in the Bay du Nord study area. Pencil for scale.

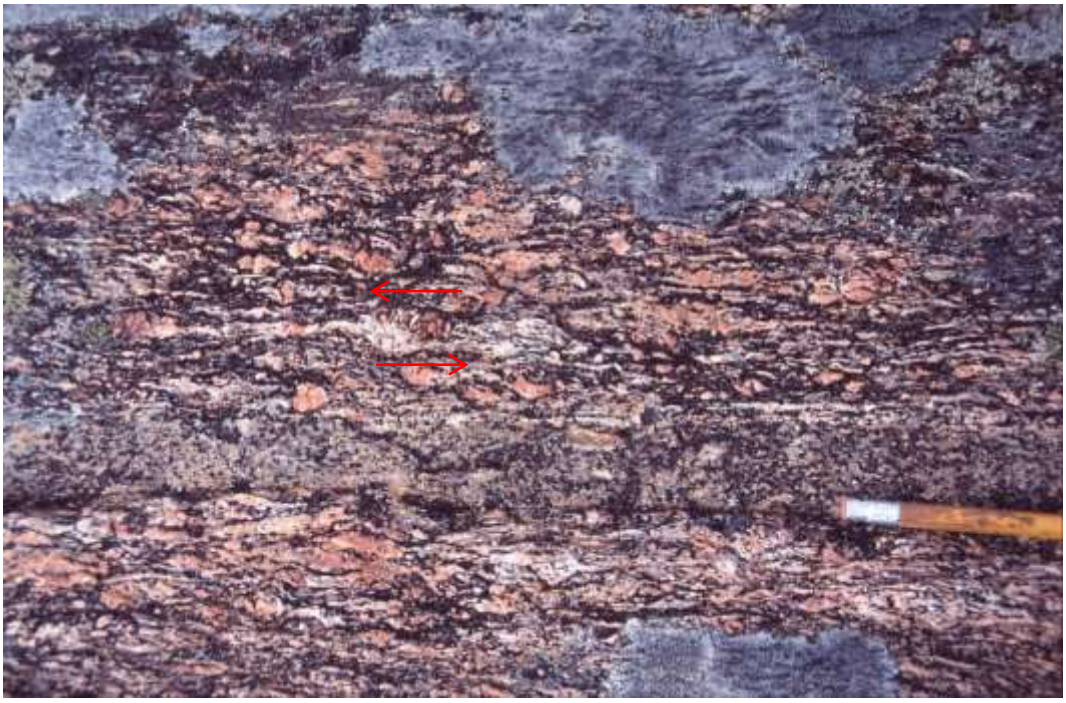

Figure 5.1.15: field photograph of the mylonitic granite at locality 2 in the Bay du Nord study area. Pencil for scale.

5.1.3 Freshwater Bay

The Freshwater Bay study area extends around the north and south coasts of the inlet in Content Reach with the samples spread out over 12km from west to east, shown in Figure 5.1.16. Sampled exposures of the Gander Zone lithologies in Freshwater Bay are confined to coastal outcrops. At the Gander-Avalon boundary a narrow, sharply-defined ravine indicates the trace of the brittle-ductile Dover Fault. The first-order Dover Fault trends NE-SW to the north of Freshwater Bay but then shows a significant change in trend to almost N-S to the south of Freshwater Bay. Along the southern shore of Freshwater Bay, the DFG is in direct contact with the Gander-Avalon boundary and to the west the mylonitic DFG passes into exposures of the HBG. The north shore of Freshwater Bay is dominated by exposures of the HBG and another inter-sheeted pluton – the Locker's Bay Granite (LBG). The foliation fabric in Freshwater Bay generally has a N-S trend and dips steeply to the east or west (see Figure 5.1.17). The stretching mineral lineation on the foliation planes shows some variation but it generally plunges at a shallow angle to the north or south (see Figure 5.1.18).

The Early Ductile structures in the HBG and LBG of Freshwater Bay are well preserved at more than 1km from the Gander-Avalon boundary. Lithological units in the Freshwater Bay HBG have a similar discontinuous form to that observed in Maccles Lake. Strain in the HBG exposures is heterogeneous as low shear zones were observed that preserve lenticular xenoliths of pelites, skarns and amphibolites. Early Ductile, isoclinal to open folds on the millimetre to centimetre-scale (orientation in Figure 5.1.19) indicate a sinistral sense of shear. Migmatites and mobilised gneisses were observed at several localities, especially along the northern shore of Freshwater Bay, that associate with chaotic banding and irregular open folds on the metre-scale.

Within 1km west of the Gander-Avalon boundary, Late Ductile structures become evident as narrow (m-scale) mylonitic zones and brittle faults surrounding low strain augen. In addition, there is a general increasing trend in phyllonitisation of the outcrops from west to east. The Late Ductile structures in the HBG, DFG and LBG all indicate a dextral sense of shear from structures such as σ-porphyroclasts, asymmetrical and curvilinear folds (orientation in Figure 5.1.20), shear bands and S-C fabrics. In the sheeted LBG and DFG intrusions, the Late Ductile structures include

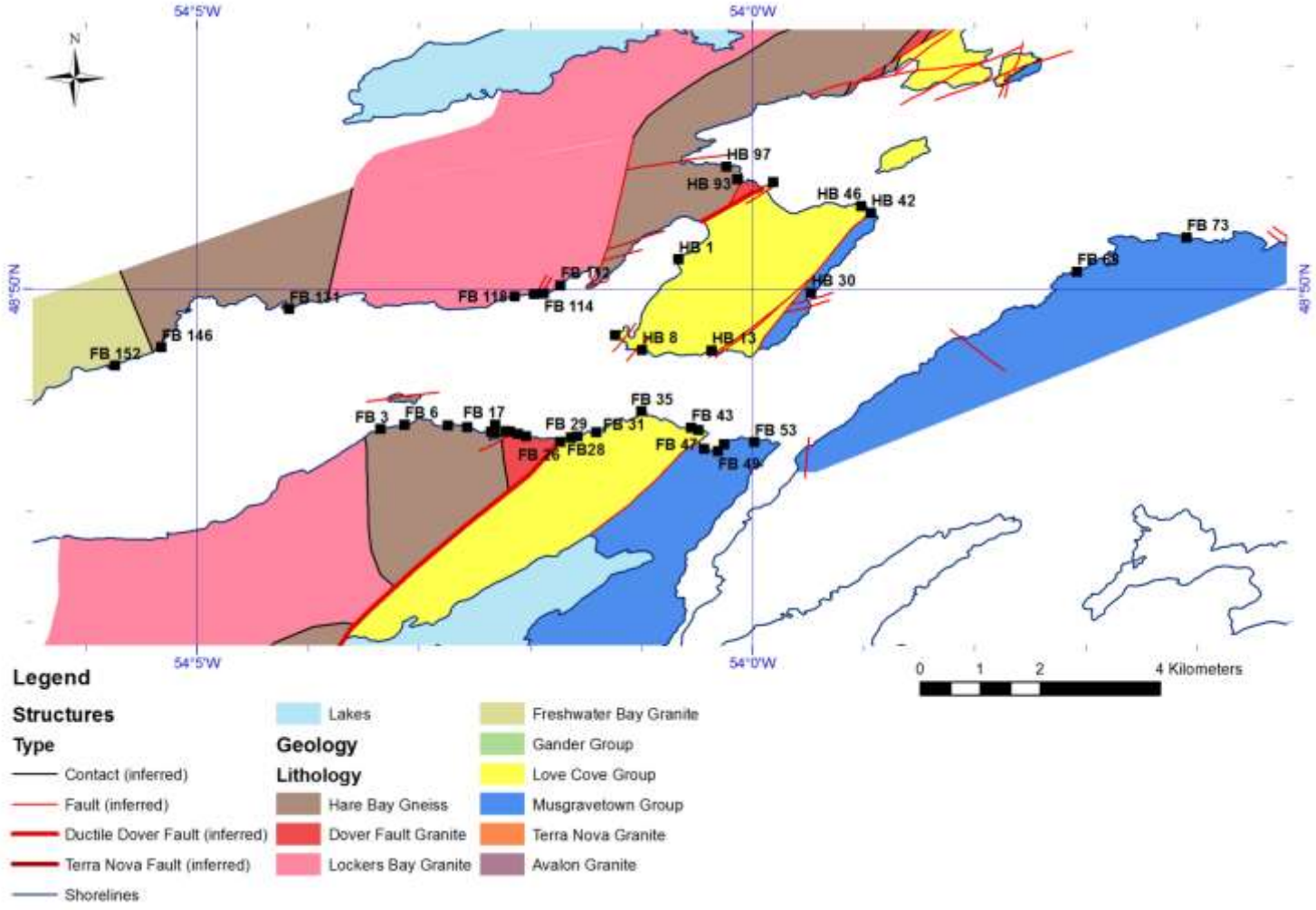

Figure 5.1.16: a geological map of the Freshwater Bay and Hare Bay study areas showing the locations of thin section and hand specimen samples.

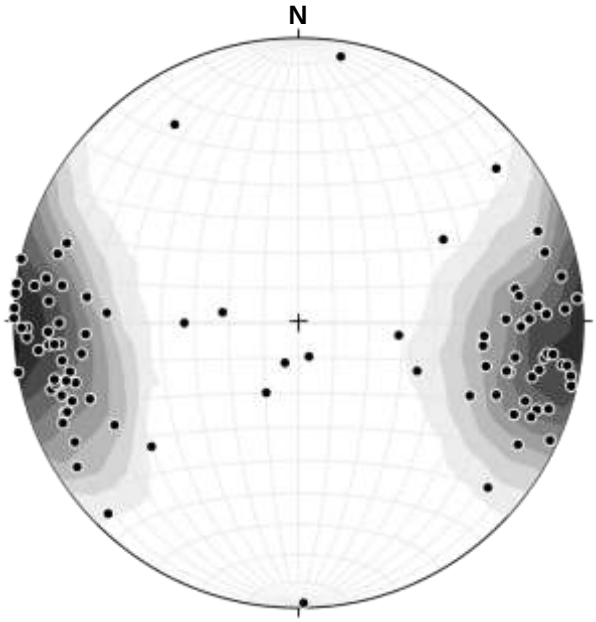

Figure 5.1.17: Stereonet representing the orientations of poles to foliation planes in the Gander Zone of Freshwater Bay (HBG, DFG and LBG lithologies).

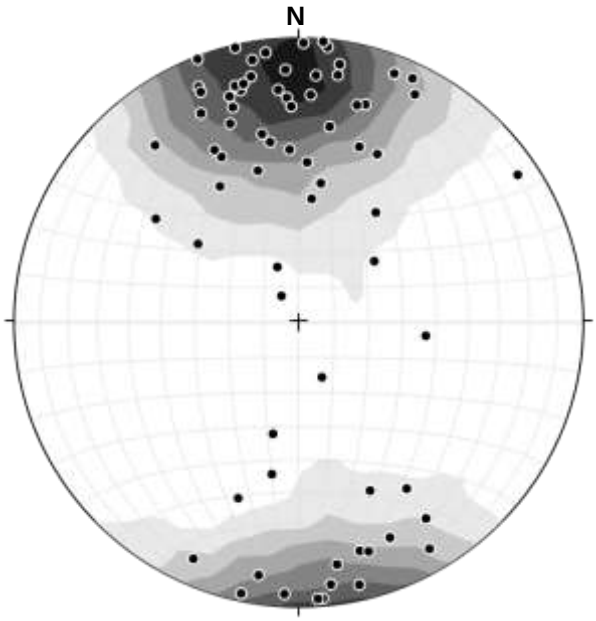

Figure 5.1.18: Stereonet representing the orientations of stretching mineral lineations in the Gander Zone of Freshwater Bay (HBG, DFG and LBG lithologies).

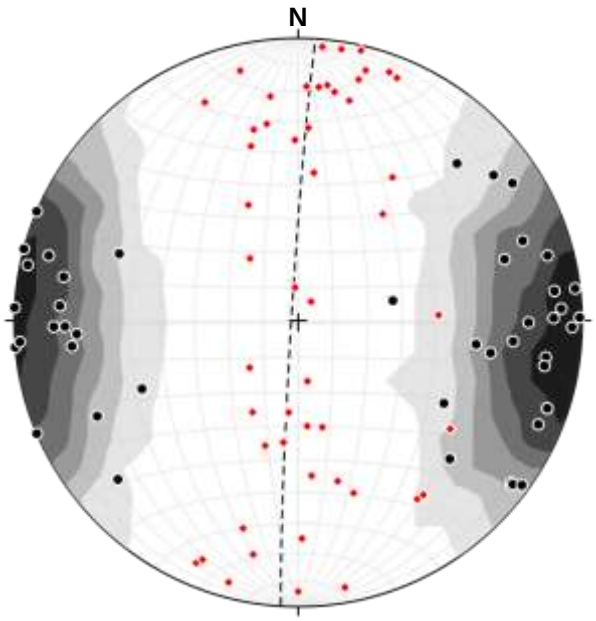

Figure 5.1.19: Stereonet representing the orientations of Early Ductile Folds in the Gander Zone of Freshwater Bay (HBG, DFG and LBG lithologies). Black – poles to axial planes, Red – fold vergence, dashed line – representative axial plane.

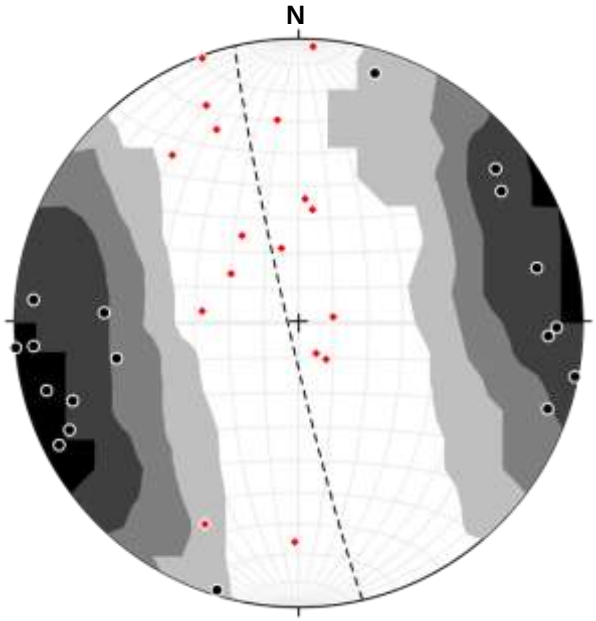

Figure 5.1.20: Stereonet representing the orientations of Late Ductile Folds in the Gander Zone of Freshwater Bay (HBG, DFG and LBG lithologies). Black – poles to axial planes, Red – fold vergence, dashed line – representative axial plane.

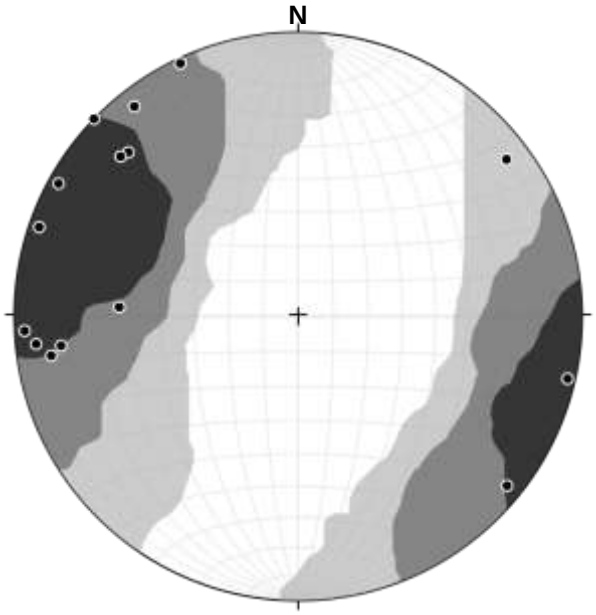

Figure 5.1.21: Stereonet representing the orientations of poles to dextral shear bands in the Gander Zone of Freshwater Bay (HBG, DFG and LBG lithologies). The shear bands have a NE-SW trend and dip steeply to the SE and NW.

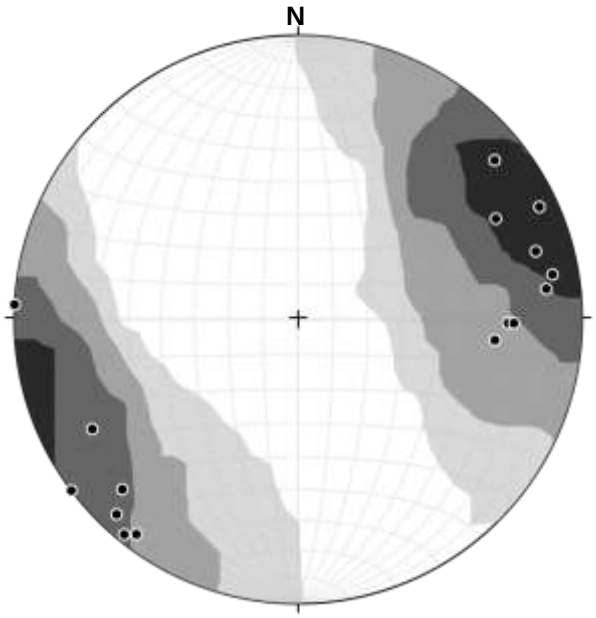

Figure 5.1.22: Stereonet representing the orientations of poles to sinistral shear bands in the Gander Zone of Freshwater Bay (HBG, DFG and LBG lithologies). The shear bands have a NW-SE trend and dip steeply to the NE and SW.

narrow (m-scale) phyllonitic shear zones with solid-state recrystallisation fabrics and open cm-scale folds. The highest density of Late Brittle structures in Freshwater Bay occurs at the brittle Dover Fault so that the exposures either side of the fault are pervasively fractured and brecciated. Brittle shear bands indicate both dextral (Figure 5.1.21) and sinistral (Figure 5.1.22) senses of shear whereas Late Brittle open folds generally indicate a dextral shear sense. Networks of calcite and quartz veins (mm-cm scale) are common in close proximity to the Dover Fault.

5.1.4 Hare Bay

The study area of Hare Bay is located to the northeast of Freshwater Bay in the vicinity of the town of Hare Bay. Exposure in this area is limited to shoreline and wave-cut platform outcrops along the coastline. The majority of this exposure is within the Avalon Zone to the southeast of Hare Bay so only three samples located within the town are from the Gander Zone (see Figure 5.1.16). In the Hare Bay area, the Gander-Avalon boundary shows a trend of NE-SW from the outskirts of the town of Hare Bay across to the centre of Boutcher's Cove. The siting and orientation of the Gander-Avalon boundary therefore changes significantly across Freshwater Bay. This offset of the Gander-Avalon boundary may indicate the presence of a later, major, dextral, brittle strike-slip fault that runs through Freshwater Bay. The foliation has a NNE-SSW trend similar to the Gander-Avalon boundary and a steep dip to the east or west (see Figure 5.1.23). The mineral lineations consistently plunge shallowly to the NE or SW (see Figure 5.1.24).

Early Ductile structures in Hare Bay are similar to those described in the preceding sections. Exposures of the HBG include isoclinal to open, intrafolial folds on millimetre to centimetre-scales, sinistral shear bands and enclaves of amphibolites and metasediments. At 500m from the Gander-Avalon boundary in the town of Hare Bay, Late Ductile structures such as overprinting dextral shear bands begin to appear and become more intense moving SE towards the boundary. Increasingly phyllonitic shear zones cross cut the Early Ductile structures and the curvilinear Late Ductile folds (see Figure 5.1.25) clearly fold the mineral lineation and foliation fabrics. Dextral shear sense indicators, such as fold vergence, shear bands and σ-porphyroclasts are ubiquitous The Late Brittle deformation is revealed by fault block rotation and brittle folds and is most intense within 100m of the Gander-Avalon boundary. Brecciated and heavily altered outcrops in contact

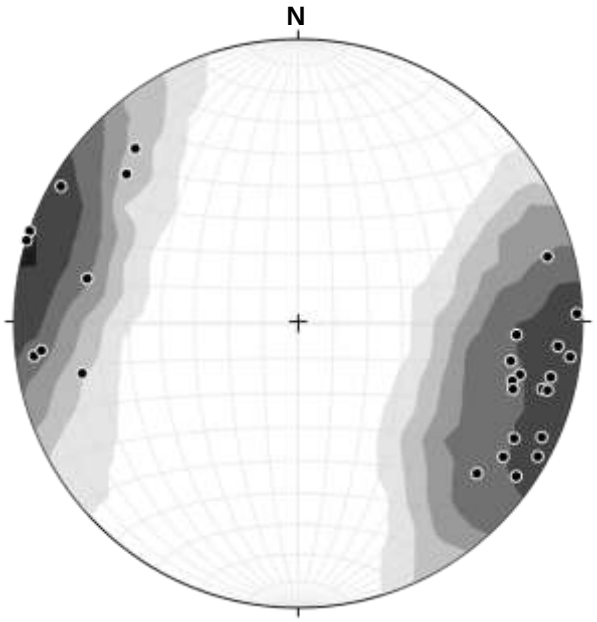

Figure 5.1.23: Stereonet representing the orientations of poles to foliation planes in the Gander Zone of Hare Bay (HBG and DFG lithologies).

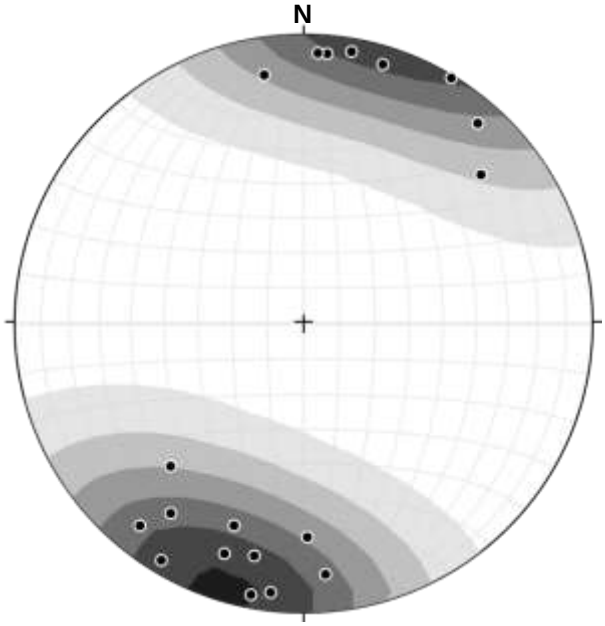

Figure 5.1.24: Stereonet representing the orientations of stretching mineral lineations in the Gander Zone of Hare Bay (HBG and DFG lithologies).

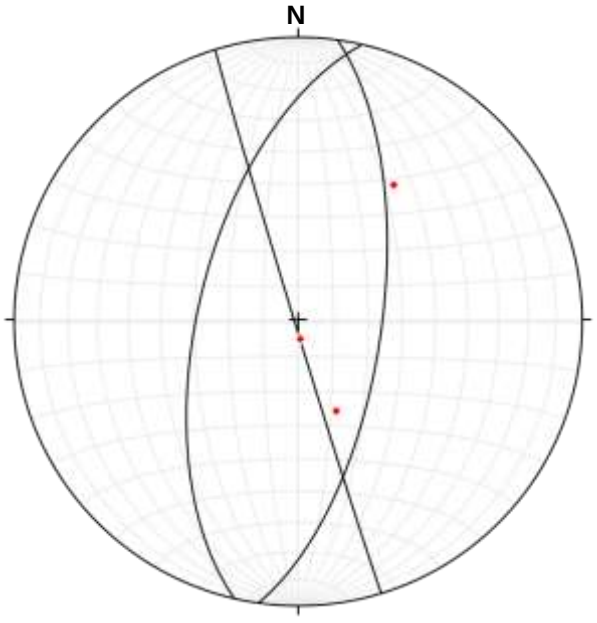

Figure 5.1.25: Stereonet representing the orientations of Late Ductile Folds in the Gander Zone of Hare Bay (HBG and DFG lithologies). Black lines – axial planes, Red points – fold vergence.

with the fault include epidote-rich cataclastic bands (mm to cm thickness) parallel to the foliation.

5.1.5 Shoal Bay

The study area of Shoal Bay extends along the coastline north of Hare Bay with 14 samples from the Gander Zone (see Figure 5.1.26). The Gander-Avalon boundary trends ENE-WSW across the Shoal Bay area to the Locker's Bay area and separates the Avalon LCG from mostly the HBG and part of the DFG in the Gander Zone. The offshore position of the Dover Fault is unknown and so complicates any interpretations drawn from the samples based on the distance from the Gander-Avalon boundary. The foliations in all Gander Zone lithologies have a NE-SW trend and the foliation planes are steeply dipping to the NW or SE (see Figure 5.1.27). The stretching mineral lineations generally plunge to the SW at shallow to steep angles.

In general, observations in the field show an increase in strain from the west to the east of Shoal Bay. This is shown by increasing foliation and lineation fabric intensity, folding intensity and brittle fracturing to the degree that several outcrops are extensively brecciated. Locally, however, the strain intensity can be highly variable with weak fabrics in xenoliths, lower strain pods and high strain mylonites at the boundaries of granite bodies. The Early Ductile structures recognised in the HBG in Shoal Bay include intrafolial, isoclinal to open folds and sinistral shear bands. At several localities, the Early Ductile structures have become irregular and chaotic due to mobilisation of the HBG. Late Ductile structures are most intense in narrow (m-scale) shear zones at the boundaries of intrusions or low-strain rafts. A dextral sense of shear in the Late Ductile structures is indicated by folds (see Figure 5.1.29), S-C fabrics, σ-porphyroclasts and shear bands. The lithologies affected by Late Ductile shearing show intense alteration so that the outcrops comprise pink-green phyllonites (see Figure 5.1.31)

Across the Shoal Bay area, a network of brittle faults cross cut the lithologies and the faults dextrally offset the DFG, HBG and the Gander-Avalon boundary, as shown in Figure 5.1.30. The overall structure of Shoal Bay is complicated by this overprinting fault network as well as by the presence of xenoliths and low strain augen within the HBG. The faults form distinct patterns of R, P and R' faults that constitute arrays of rotating fault blocks that are typical of brittle strike slip fault zones. Shoal Bay is the area that is most affected by Late Brittle structures so that the

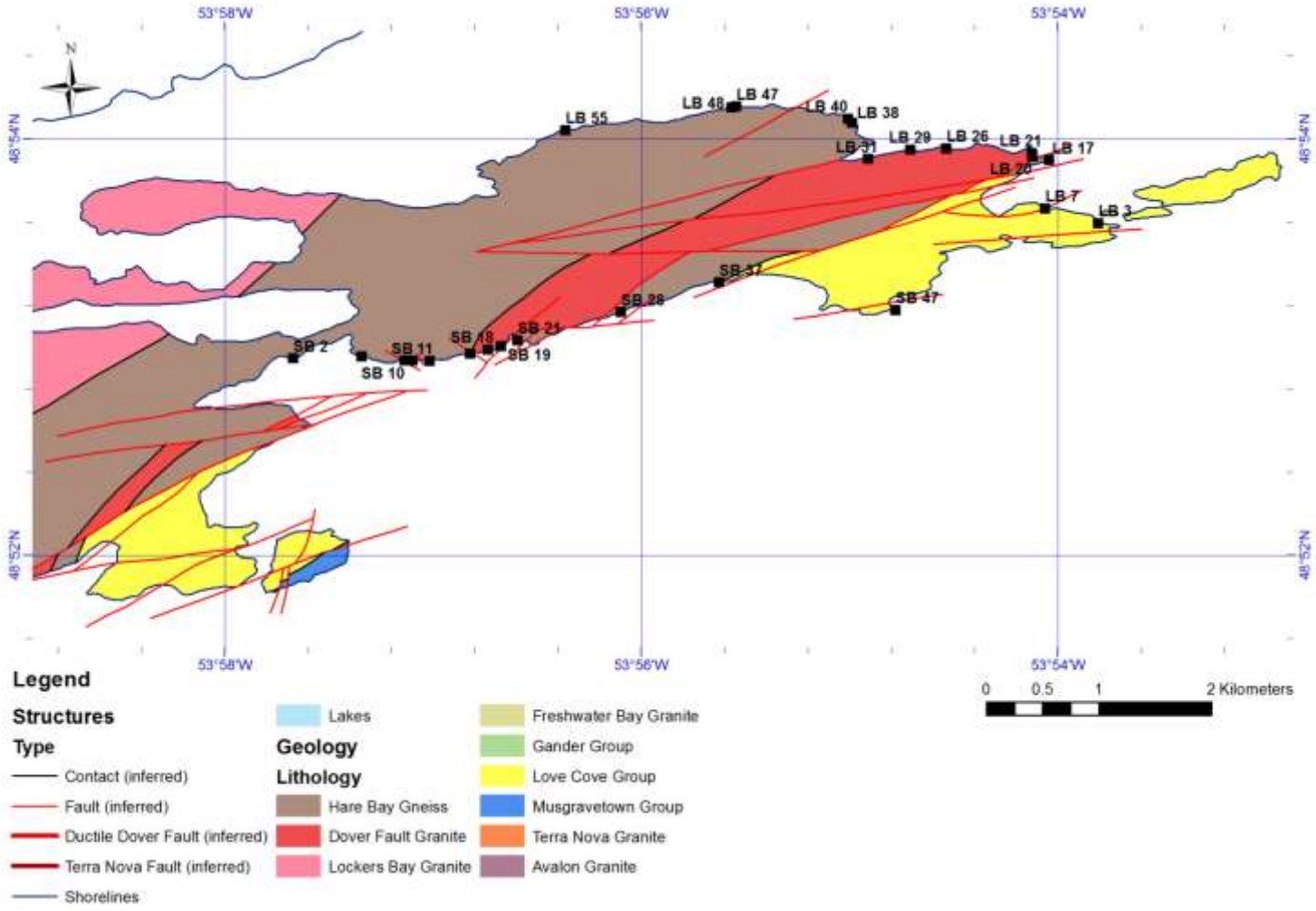

Figure 5.1.26: a geological map of the Shoal Bay and Lockers Bay study areas showing the locations of the thin section and hand specimen samples.

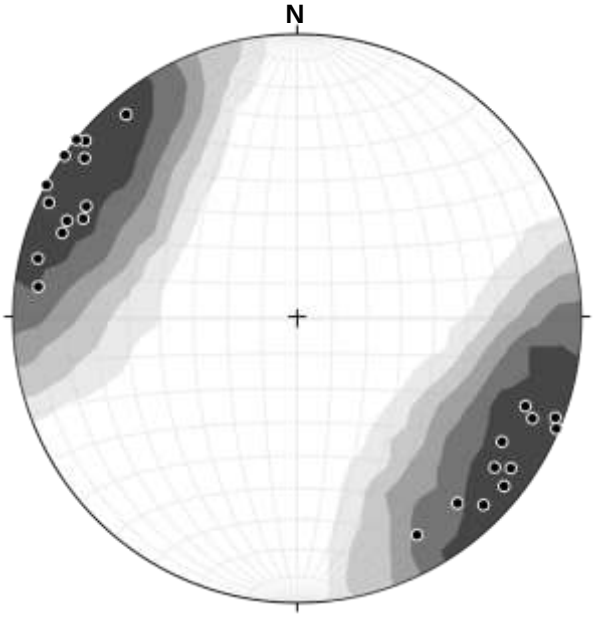

Figure 5.1.27: Stereonet representing the orientations of poles to foliation planes in the Gander Zone of Shoal Bay (HBG and DFG lithologies).

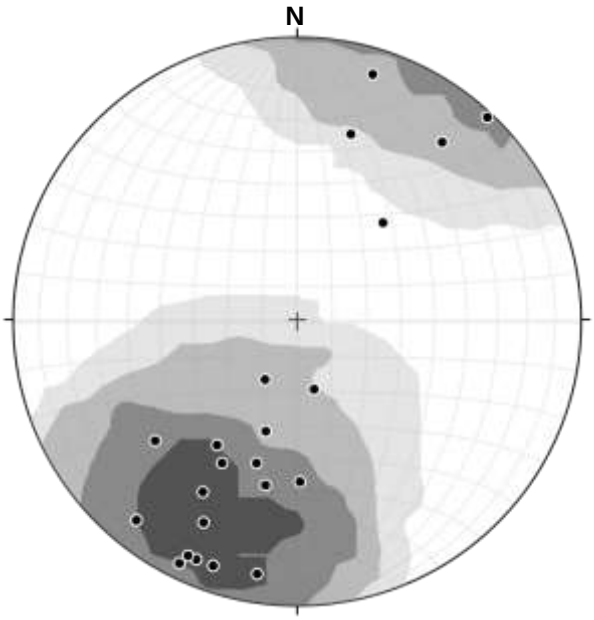

Figure 5.1.28: Stereonet representing the orientations of stretching mineral lineations in the Gander Zone of Shoal Bay (HBG and DFG lithologies).

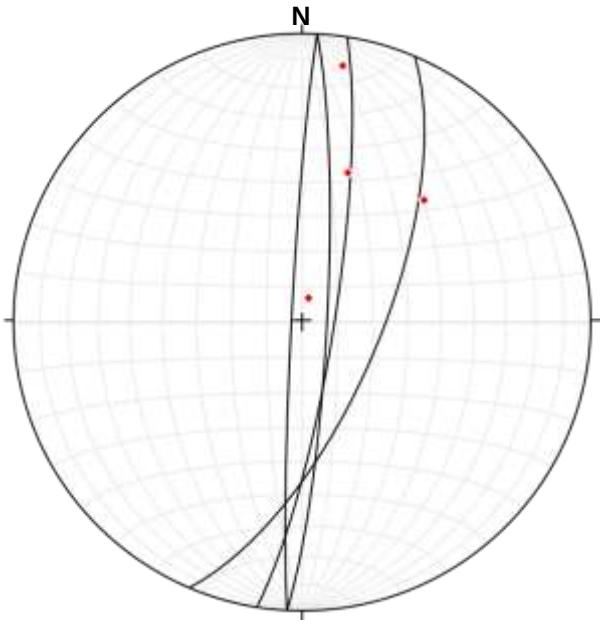

Figure 5.1.29: Stereonet representing the orientations of Late Ductile Folds in the Gander Zone of Shoal Bay (HBG and DFG lithologies). Black lines – axial planes, Red points – fold vergence.

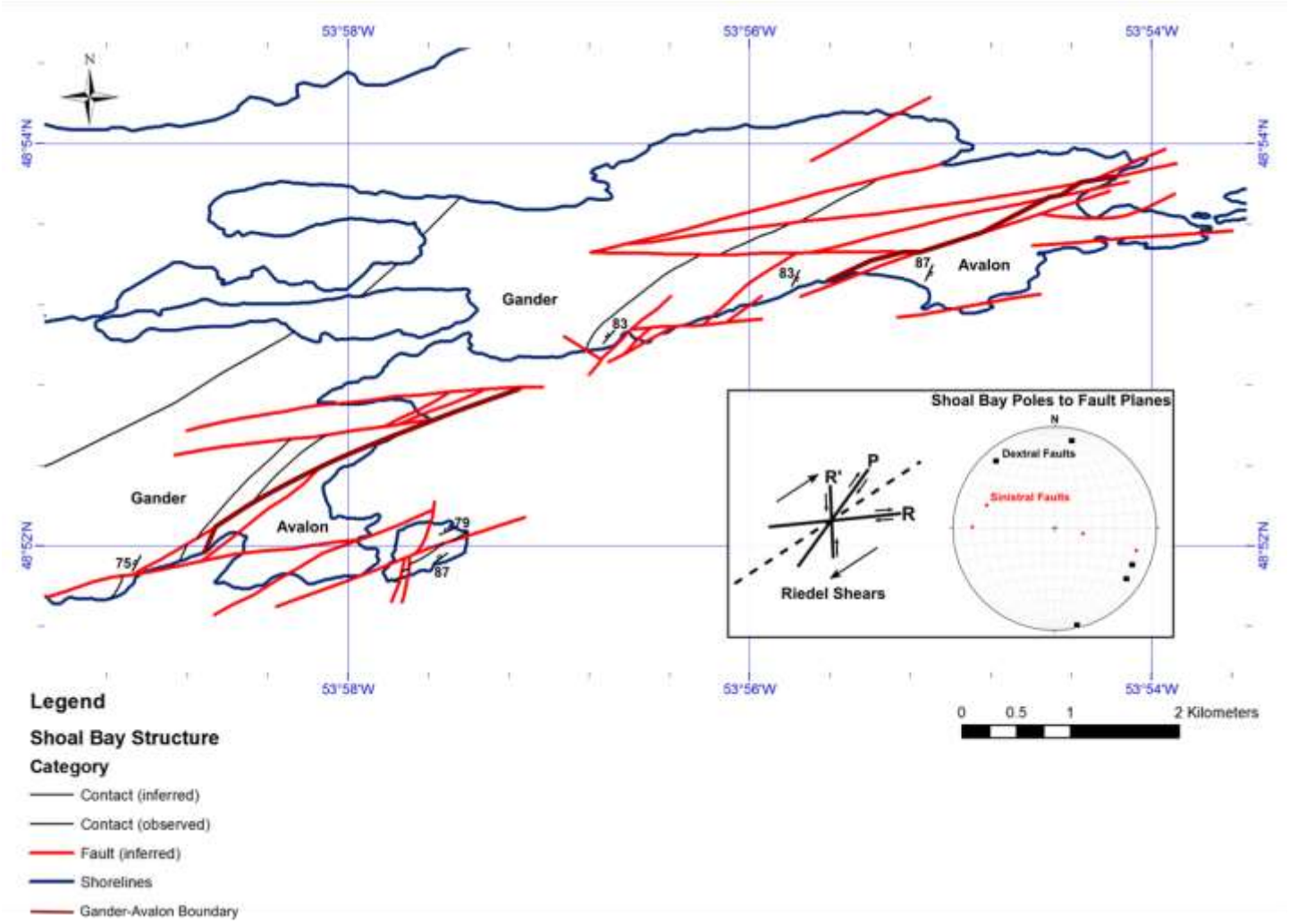

Figure 5.1.30: a structural map of the Shoal Bay and Locker's Bay study areas highlighting the overprinting brittle faulting.

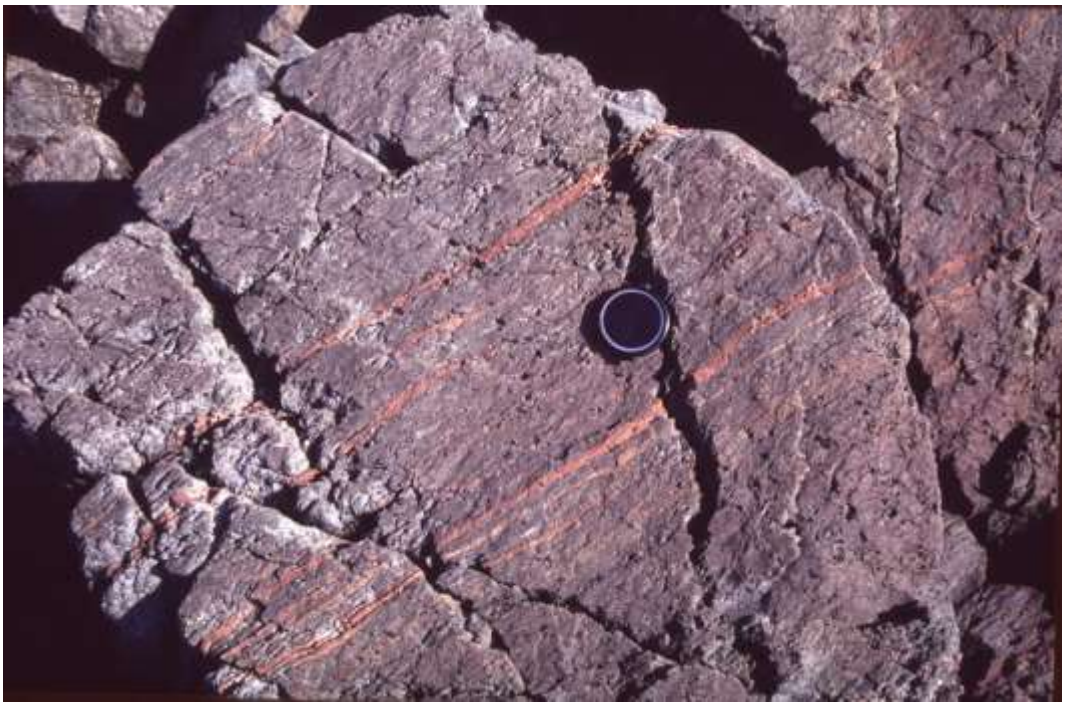

Figure 5.1.31: field photograph of a typical pink-green streaky phyllonite in the HBG at locality 27 in the Shoal Bay area. Lens cap for scale

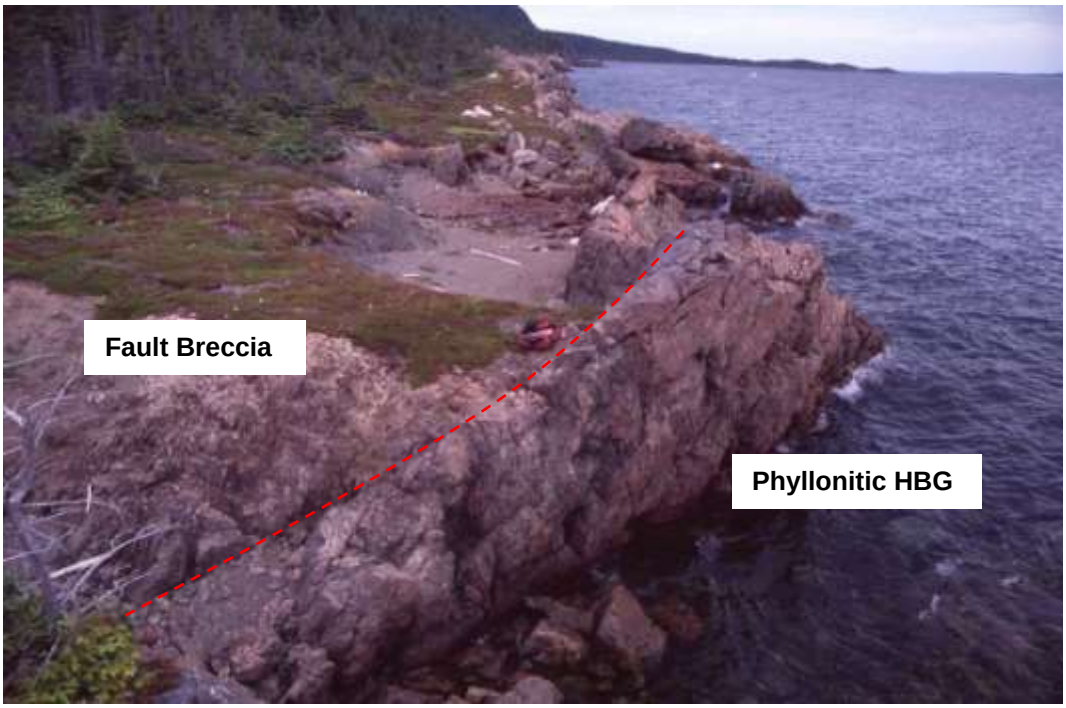

Figure 5.1.32: field photograph of a brittle fault (101/77 S) separating fault breccias and phyllonitic HBG at locality 24 in the Shoal Bay area. Backpack for scale.

lithologies are highly disrupted from the centimetre to kilometre scale.

5.1.6 Locker's Bay

Locker's Bay extends along the southern shore of the Locker's Bay inlet north of Shoal Bay. To the north of Locker's Bay, the Dover Fault that marks the Gander-Avalon boundary moves offshore and it is only exposed on a few small islands within Contents Reach, such as Frying Pan Island. As in the other study areas, the exposure is limited to shoreline outcrops and 12 samples were collected in southern Locker's Bay. The faults that dextrally offset the Gander-Avalon boundary in Shoal Bay continue into the Locker's Bay area, as shown in Figure 5.1.30. The foliations in the HBG and DFG have a NE-SW trend and the foliation planes are steeply dipping to the NW or SE (see Figure 5.1.33). The stretching mineral lineations generally plunge to the WSW at shallow to steep angles (see Figure 5.1.34).

Early Ductile structures are well represented in the HBG of Locker's Bay, but the sampled exposures also often contain overprinting m-scale Late Ductile phyllonitic shear zones. The HBG exposures contain millimetre to centimetre-scale isoclinal to tight Early Ductile folds (see Figure 5.1.35) that are cross cut by cm-scale apolgranite and granite veins. A sinistral sense of shear for the Early Ductile structures is indicated by shear bands, wrapping of rigid pods (see Figure 5.1.37) and fold vergence. Migmatisation of the HBG in western Locker's Bay and the presence of syn-kinematic sillimanite needles indicate that the HBG experienced relatively high temperatures (>500-700°C) during deformation.

The Late Ductile shear zones are generally composed of phyllonitic and mylonitic HBG and DFG veins and sheets (see Figure 5.1.38). Open to close curvilinear folds were observed to refold the Early Ductile folds and the main foliation and mineral lineation fabrics (see Figure 5.1.36). The dominant shear sense indicated by Late Ductile shear bands, folds and σ-porphyroclasts is dextral. The phyllonitic shear zones that overprint the Early Ductile structures are generally overprinted in turn by Late Brittle structures. Brittle faults, fractures and shear bands disrupt the earlier ductile fabrics and Late Brittle folds were observed to refold the ductile foliation and mineral lineation. As in Shoal Bay, the first order fault arrays in the Locker's Bay area indicate a dextral sense of strike-slip on the brittle Dover Fault.

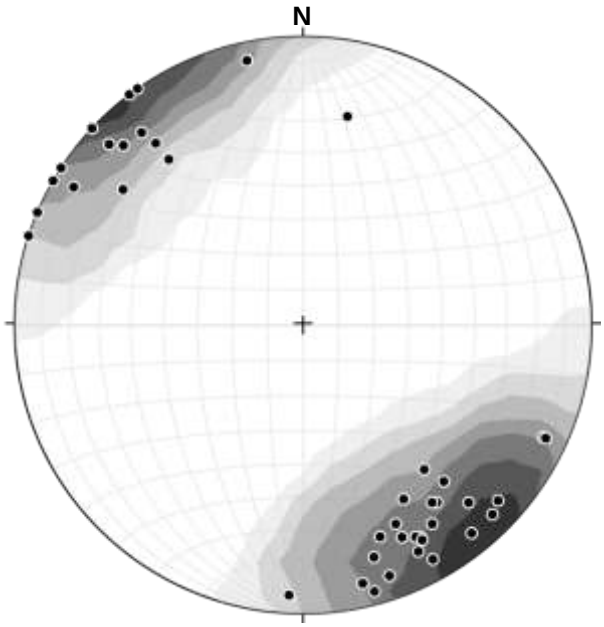

Figure 5.1.33: Stereonet representing the orientations of poles to foliation planes in the Gander Zone of Locker's Bay (HBG and DFG lithologies)..

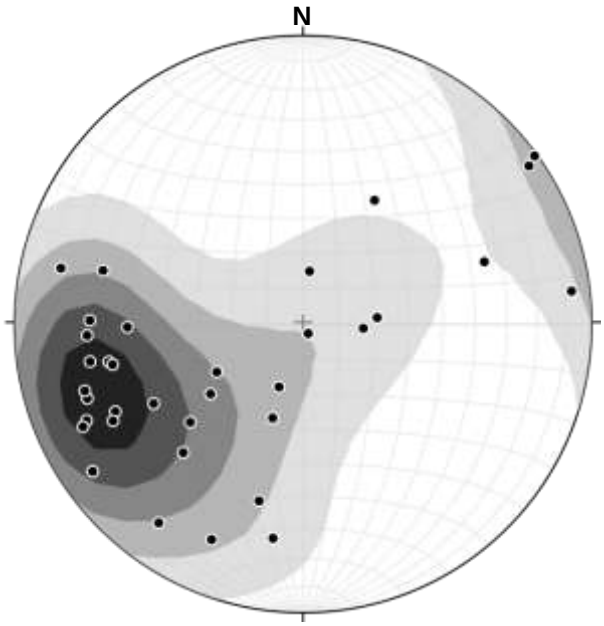

Figure 5.1.34: Stereonet representing the orientations of stretching mineral lineations in the Gander Zone of Locker's Bay (HBG and DFG lithologies).

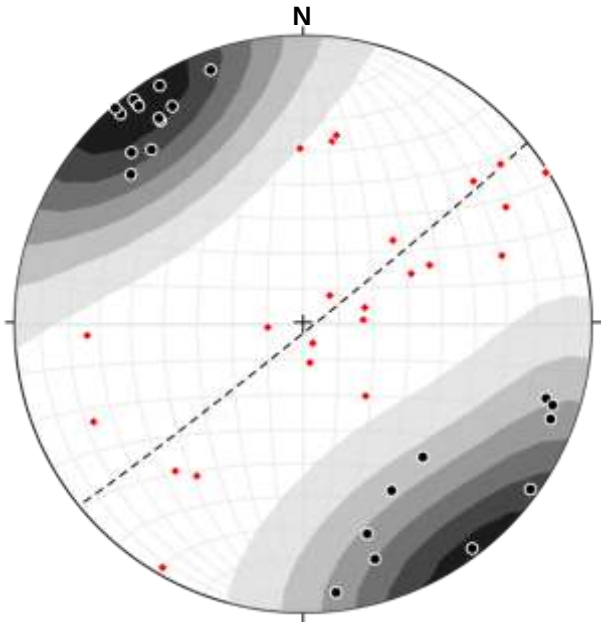

Figure 5.1.35: Stereonet representing the orientations of Early Ductile Folds in the Gander Zone of Locker's Bay (HBG and DFG lithologies). Black – poles to axial planes, Red – fold vergence, dashed line – representative axial plane.

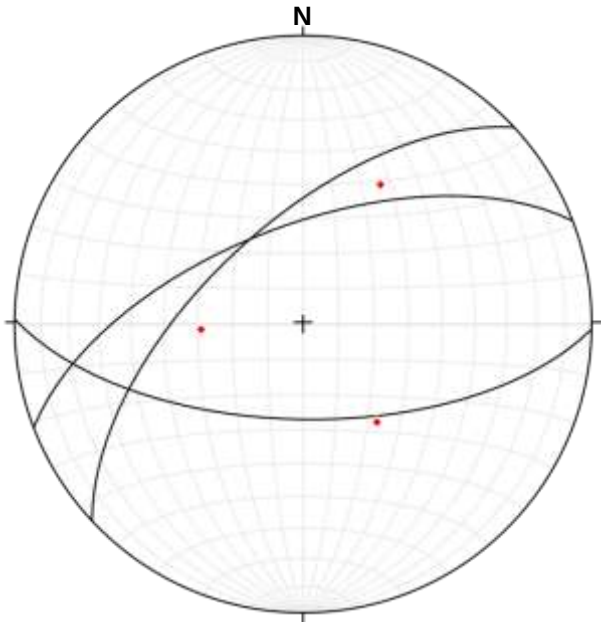

Figure 5.1.36: Stereonet representing the orientations of Late Ductile Folds in the Gander Zone of Locker's Bay (HBG and DFG lithologies). Black lines – axial planes, Red points – fold vergence.

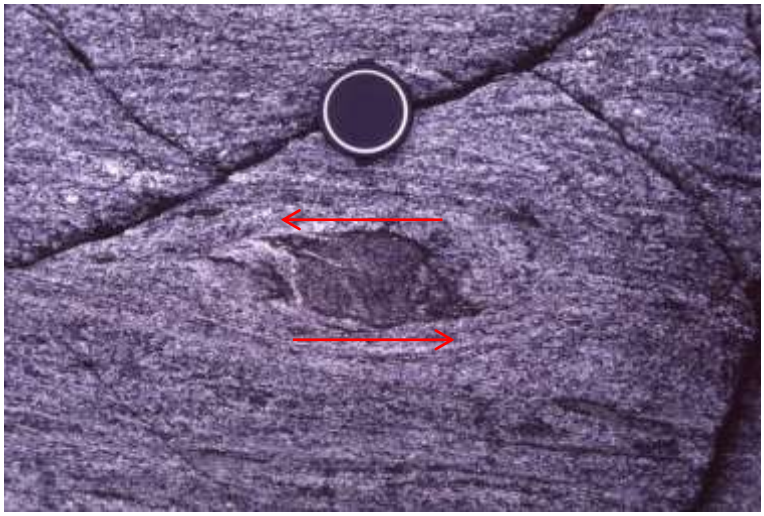

Figure 5.1.37: field photograph of HBG at Locker's Bay locality 41 showing sinistral folding around a rigid amphibolite enclave.

Figure 5.1.38:field photograph of dextrally sheared inter-layered mylonitised quartz veins and phyllonite at Locker's Bay locality 17.

5.1.7 Frying Pan Island

Frying Pan Island is a 400m long island in the north of Bonavista Bay located 9km to the north-east of Locker's Bay (see Figure 5.1.39). It is included here because it is the most northeastern onshore expression of the brittle Dover Fault. The only lithology that outcrops on Frying Pan Island is the Newport Granite, which occurs as a coarse-grained (up to 2cm grain size), megacrystic granite containing K-feldspar, plagioclase, quartz and biotite. The structure of Frying Pan Island is dominated by brittle faulting and associated fractures.

At field locations more than 50m from the faults the granite appears intact and undeformed (see Figure 5.1.34). With closer proximity to the fault zones, the feldspars within the granite become increasingly altered and epidote occurs along joint surfaces. Highly fractured fault damage zones surround the fault slip surfaces at 2-10m widths (see Figure 5.1.40). Within the fault damage zones, the Newport Granite shows extensive alteration to chlorite and epidote that produces a grey-green colour in the field. The actual fault surfaces are sharply defined and can be highly polished with slickenlines that generally indicate strike slip movement (see Figure 5.1.41). A component of dip-slip is also indicated by the slickenlines although the timing relative to the strike-slip movement is not clear. The hanging wall to the west of the fault is less extensively fractured than the eastern footwall. The fracture sets form on the metre, centimetre to millimetre scale and form in characteristic Riedel shear configurations (see Figure 5.1.42). A dextral sense of strike-slip movement is clearly indicated by the configuration of the fracture sets and by offset markers.

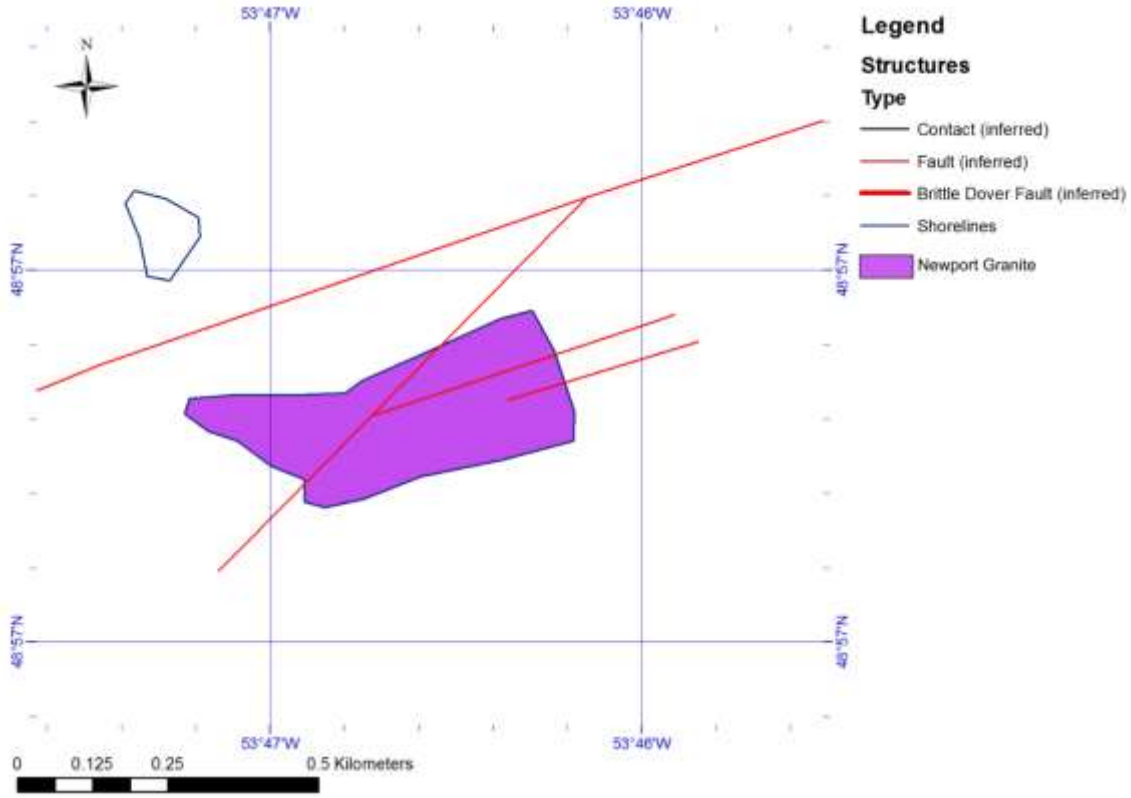

Figure 5.1.39: a geological map of the Frying Pan Island study area.

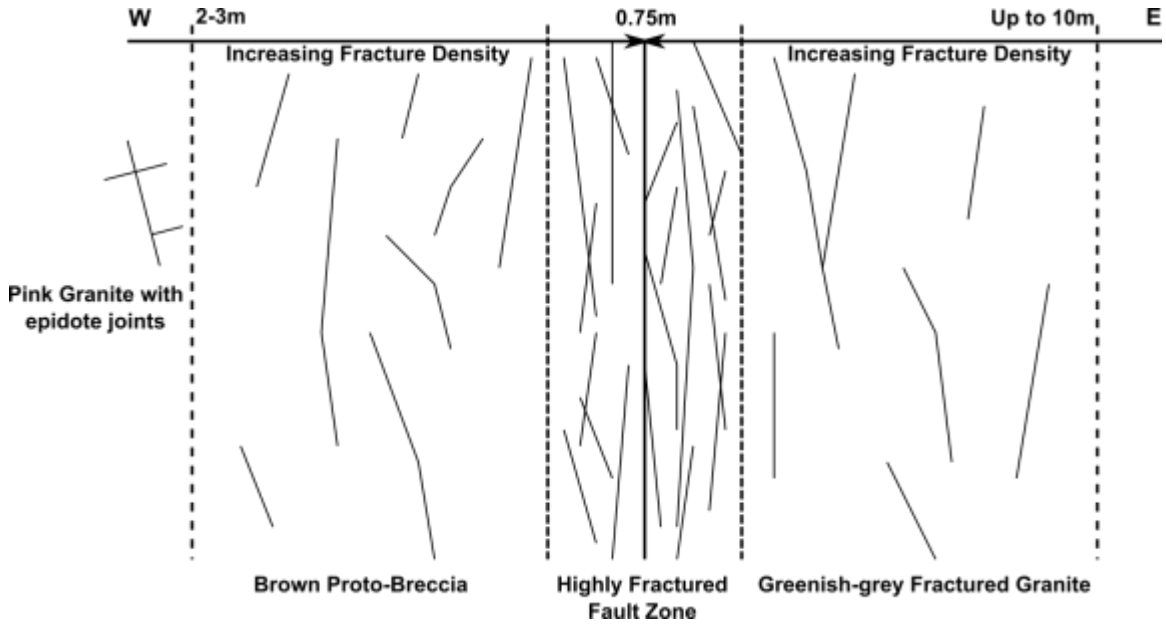

Figure 5.1.40: Schematic sketch of the structure of the fault zones on Frying Pan Island.

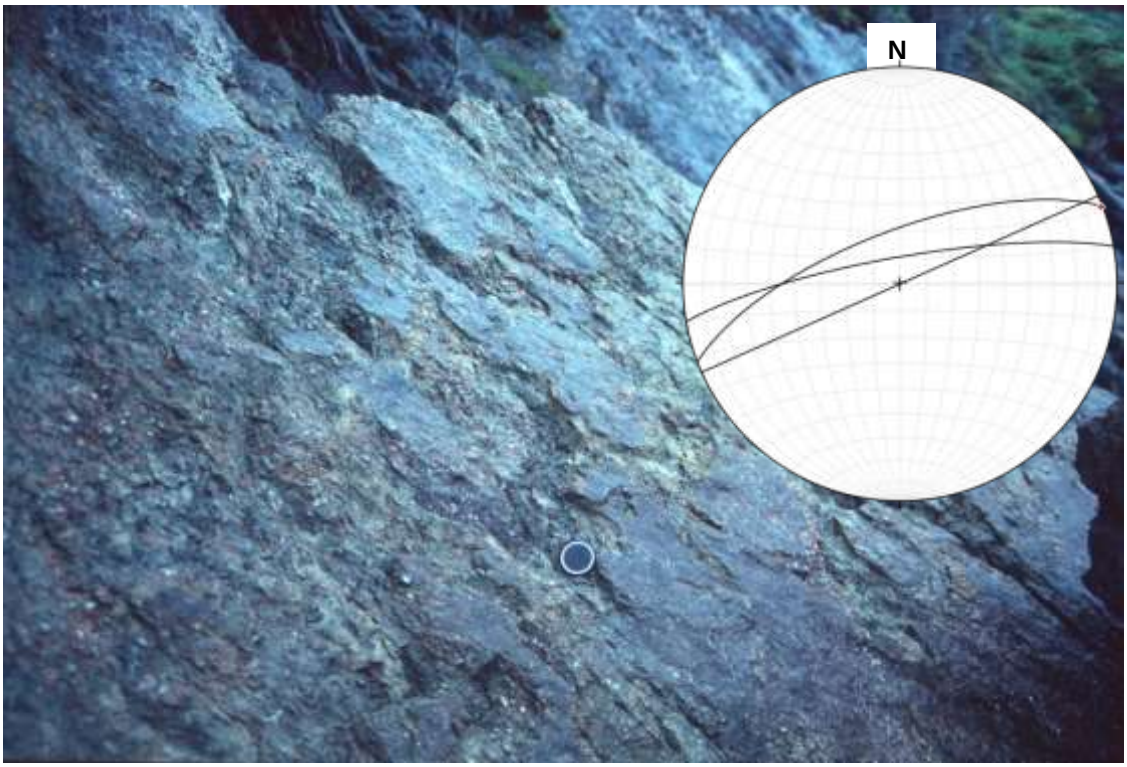

Figure 5.1.41: Field photograph of a polished fault surface in the Newport Granite on Frying Pan Island. Insert: Stereonet representing the orientations of faults on Frying Pan Island. Black – fault planes; Red – slickenlines.

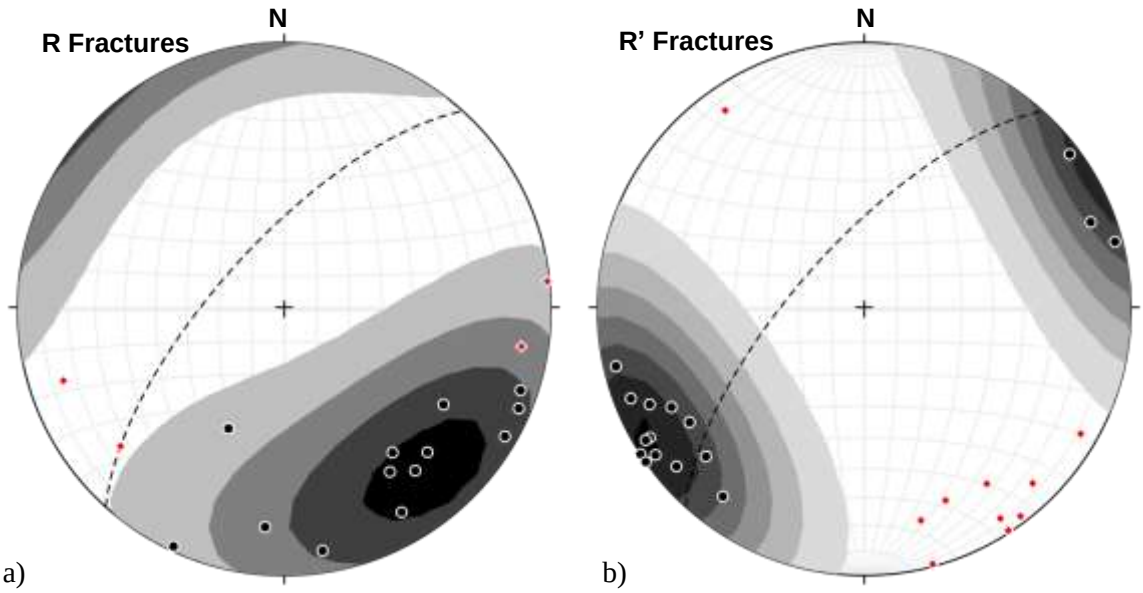

a) b)

Figure 5.1.42: Stereonets representing the orientations of poles to a) R fractures and b) R' fractures and the associated slickenlines (red). Dashed line – representative master fault orientation.

5.1.8 Summary of Gander Zone Field Observations

The analysis of field data shows that three main deformation phases are recorded in the rocks of the DFSZ. In the Gander Zone, the fault rocks at distances of more than 1km record an early, high temperature, sinistral deformation phase in the form of the Early Ductile structures. The intensity of fabrics in these samples is relatively low compared to those in close proximity to the Gander-Avalon boundary. The development of a gneissose texture in the HBG as well as irregular isoclinal folds, sinistral shear bands and limited mobilisation of the gneisses support the interpretation of a high temperature sinistral deformation phase.

A later, dextral, lower temperature deformation phase can be recognised in the Gander Zones of almost all of the field study areas. The Bay du Nord area records a coeval, sinistral, upper-greenschist grade deformation event in both the thin section and field observations. This upper-greenschist grade event is represented by the Late Ductile structures identified in the field including curvilinear folds that refold the earlier fabric. In the in the DFG of the Gander Zone, there is a first order structure (100m-1km) of central zones of less-deformed granite that separate highly-strained phyllonites, which are derived mostly from the highly altered HBG (see Figure 5.1.43). Several shear criteria in the field, such as shear bands, σ-structures and verging folds, also indicate a dextral shear sense.

The latest deformation phase is recorded in all of the study areas but is most intense at the Gander-Avalon boundary. The brittle deformation phase shows a dextral shear sense at the regional-scale as shown by the orientation of the subordinate fault sets, such as those on Frying Pan Island. The damage caused by the brittle deformation is highly localised, although the fracture and fault networks can reach several kilometres from the Gander-Avalon boundary. Conjugate sets of dextral and sinistral minor faults appear to accommodate a late component of compression at a high angle (~90°) to the Gander-Avalon boundary. The change in trend of the Gander-Avalon boundary from N-S to NE-SW across Freshwater Bay is inferred to reflect a primary structure rather than brittle reactivation because the earlier ductile foliations reflect this change in orientation.

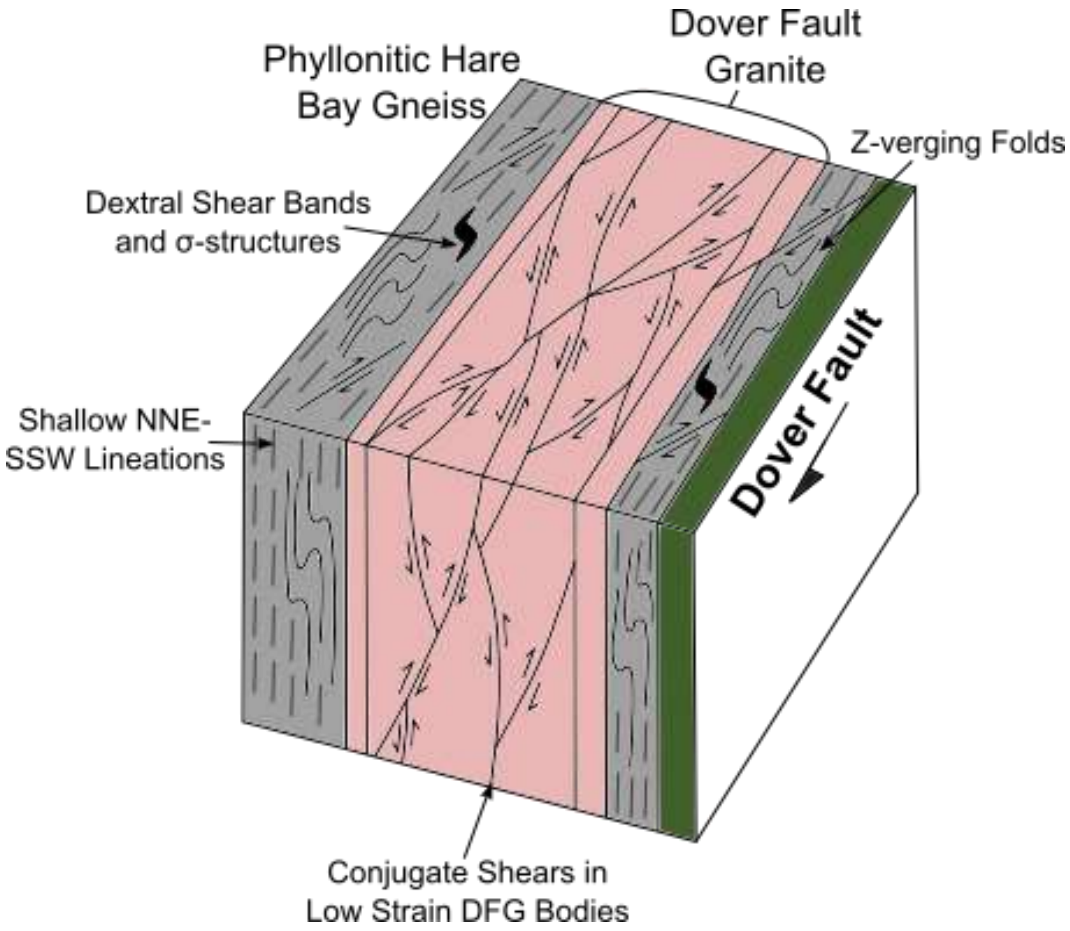

Figure 5.1.43: a 3-dimensional block diagram depicting the geometry of structures within the DFSZ and <1km from the Dover Fault (adapted from Holdsworth, 1991).

5.2 Gander Zone Microstructual Analysis

5.2.1 Maccles Lake

The samples in the west of the Maccles Lake study area consist predominantly of quartzofeldspathic orthogneisses in the HBG and foliated megacrystic granites. Quartz is relatively coarse grained (>0.5mm) in the samples and the grains display interlobate grain boundaries with low intracrystalline deformation. Although the quartz mostly occurs in compositional bands, the grains show only weak to moderate CPO under a tint plate. Plagioclase and K-feldspar grains in the orthogneisses and granites both show partial alteration (0-50%) to extremely fine grained sericite mica (see Figure 5.2.1.b). Whilst the alteration partially masks the feldspar grains, a core-and-mantle texture can be recognised in many samples with coarse relict grains surrounded by a mantle of very fine grained (<50μm) new grains. The new grains of feldspar are also often concentrated along intergranular fractures within the millimetre-scale relict grains. In addition to intra- to inter-granular fractures, the relict grains of feldspar show undulose extinction patterns, myrmekites and flame perthite textures.

Phyllosilicate phases within the samples, including biotite, muscovite and limited chlorite, are strongly aligned in either discrete or continuous foliations and can form strain caps or mica beards on feldspar porphyroclasts (see Figure 5.2.1). Mica grains have elongated to tabular shapes or form relatively coarse grained (0.5-1mm) mica fish and can show kinking textures with sweeping undulose extinction. Retrogressive alteration and the subsequent formation of sericite and epidote is relatively limited in the samples from the west of the Maccles Lake study area. Sinistral shear sense indicators, such as stair stepping on σ-porphyroclasts, S-C fabrics and mica fish, are common in the HBG orthogneisses.

ML91 is a sample of megacrystic granite and ML95 and ML87 are examples of gneisses from the HBG, both of which are located over 1km from the Gander-Avalon boundary. In hand specimen, ML91 displays coarse feldspar-rich bands with porphyroclasts that have an average grain size of 15 mm as well as thin quartz compositional bands that are 1-3 mm thick (see Figure 5.2.1.c). The fractures in the feldspar grains are visible in both the hand specimen and thin section of ML91 at 15-30mm in length. ML95 in hand specimen displays mica-rich foliation planes with low

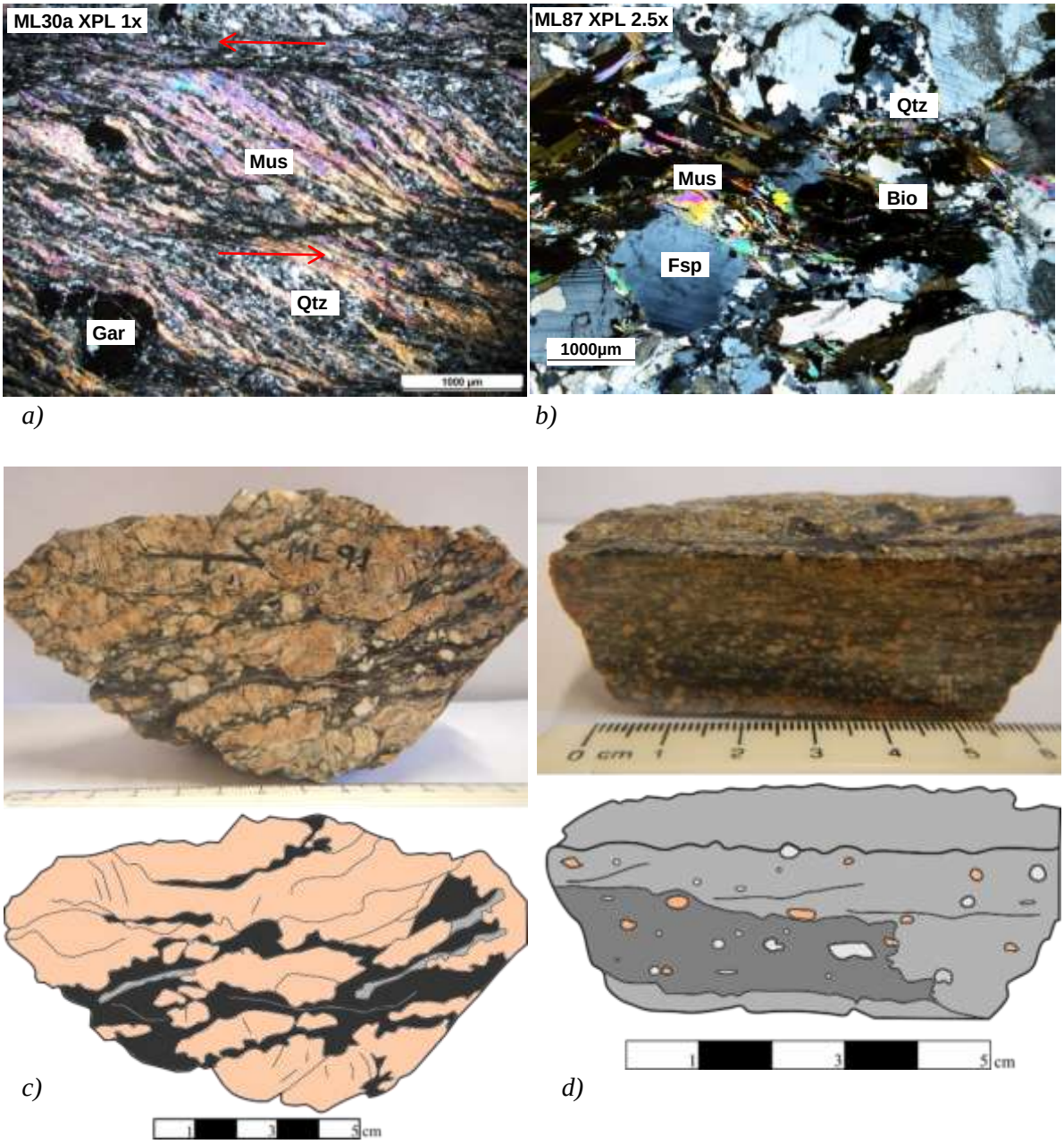

Figure 5.2.1: a) thin section photomicrograph of ML30a at 1x zoom under crossed-polars. A clear sinistral sense of shear is indicated by the S-C fabric and the stair stepping of the mica wings on the garnet porphyroblasts. b) thin section photomicrograph of ML87 at 2.5x zoom under crossed-polars. The K-feldspar and plagioclase clasts show partial alteration to sericite. c) photo and sketch of ML91 in hand specimen showing the compositional zoning of the sample and the pervasive fracturing of feldspars. d) photo and sketch of ML95 showing the feldspar porphyroclasts and mica-rich foliation fabric.

amplitude folds and quartz and feldspar porphyroclasts ranging from 1-4mm in size with mica beards. ML87 contains sinistral stair-stepping mica strain shadows and the K-feldspar and plagioclase grains show partial alteration to sericite (see Figure 5.2.1.b).

The textures identified in the samples of HBG and megacrystic granites in the west of the Maccles Lake area are indicative of high temperature deformation at amphibolite grade conditions. Recrystallization of quartz occurred through grain boundary migration (GBM) in regime 3 of Table 4.2 whereas both calcic plagioclase and K-Feldspar display textures characteristic of intracrystalline plastic deformation and bulging (BLG) recrystallization from regime 1. This contrast in textures indicates an estimated temperature range of 450-500°C for the preserved deformation fabric. Mica beards and strain caps on porphyroclasts indicate dissolution of mineral phases that are more soluble than the micas and are thought to represent the operation of diffusive mass transfer (DMT) during deformation. The majority of these high temperature samples show a sinistral sense of shear.

Within 500m of the Gander-Avalon boundary, there is a clear change in microstructural fabric in samples of both the HBG and DFG. Quartz grains show generally finer grain sizes with irregular or straight grain boundaries and moderate to strong CPO under a tint plate. The quartz grains also show strong intracrystalline deformation textures such as sweeping or patchy undulose extinction and elongate to rounded subgrains. In contrast, feldspar grains in samples from both the HBG and DFG display strong brittle deformation fabrics including intra- and inter-granular fractures and kinking of tapered deformation twins. There is no evidence of recrystallization of the coarse relict grains of feldspar, but they do display a relatively high degree of alteration to sericite mica at 25-100%. Along the grain boundaries of the feldspar porphyroclasts, micas form strain caps and strain shadows. Most of the foliation and S-C fabrics in the samples are defined by the alignment of these phyllosilicates in discrete cleavage domains.

Retrogressive alteration of the mylonites and granites is more pervasive within 500m of the brittle Dover Fault and phyllonitic fault rocks are increasingly common. The intergrowth textures between biotite and chlorite is evidence of the hydrous alteration of the biotite. In the sample ML75, chlorite occurs in synkinematic overgrowths in the strain shadows of feldspar porphyroclasts, as shown in

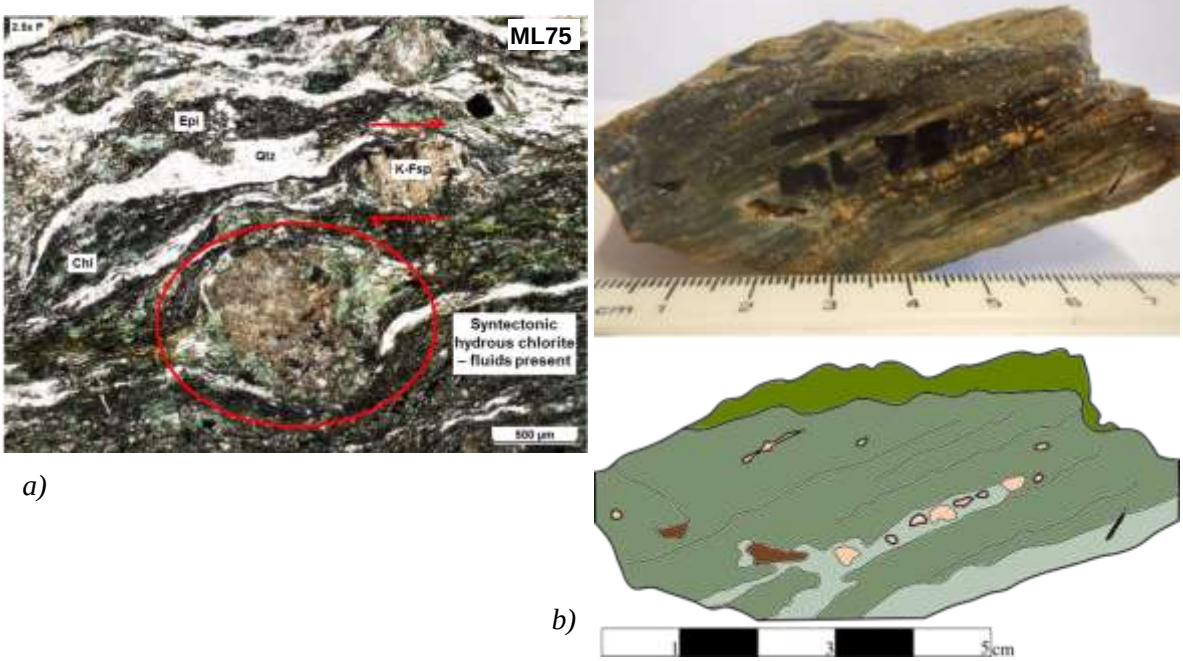

Figure 5.2.2: a) thin section photomicrograph of sample ML75 at 2.5x zoom under plane polarised light. The chlorite overgrowths on the feldspar indicated display a dextral kinematic fabric that is inferred to have formed syntectonically. b) photo and sketch of ML75 in hand specimen showing the distinctive green colour derived from the high degree of retrogressive alteration. c) thin section photomicrograph of sample ML112 at 1x zoom under crossed polarised light. The mylonitic fabric in ML112 has been folded into tight to isoclinal folds that show a dextral shear sense from the asymmetrical fold shape. d) photo and sketch of ML112 in hand specimen on mirrored cut face so that the asymmetrical folding of the foliation fabric appears sinistral but is actually dextral.

Figure 5.2.2.a. Dextral shear sense indicators, such as those in ML112 (see Figure 5.2.2.c and d), are common in samples within 500m of the Gander Avalon boundary. These indicators include stair stepping σ-porphyroclasts, oblique fabrics, asymmetric folds, S-C fabrics and mineral fish.

Within 500m of the Gander-Avalon boundary in the Maccles Lake area, the earlier higher temperature fabric has been obliterated by a lower temperature deformation phase with a dextral sense of shear. Quartz textures within the samples indicate that the dominant recrystallization mechanism for quartz was subgrain rotation (SGR) from regime 2 of Table 4.2. As feldspar microstructures are dominated by brittle and crystal plastic deformation mechanisms, this brittle-plastic deformation regime implies that the synkinematic conditions were at mid- to upper-greenschist grade and occurred at temperatures of 350-450°C.

In all of the Maccles Lake samples, there are brittle microstructures that overprint all of the earlier ductile microstructures. ML30b, shown in Figure 5.2.3, contains examples of these brittle microstructures including transgranular fractures, microfaults, quartz and calcite veins and rare cataclastic shear zones. The orientations of the brittle fractures and faults often follow three different trends: parallel to foliation, perpendicular to the foliation and oblique (~60° anticlockwise) to foliation. This represents a Riedel fracture array for sinistral shear in ML30b. Within the mineralised veins, quartz and calcite do not show evidence of deformation or recrystallization. Opaque minerals occur in most of the thin sections and are concentrated along fracture planes and rare stylolitic surfaces. These textures represent the latest phase of deformation that is recorded in the Maccles Lake samples and the dominance of brittle textures in all mineral phases shows that the conditions of deformation were at sub-greenschist grade (<300°C). The mineralisation of fractures indicates that hydrothermal fluids were present during this phase of deformation and that the brittle fracture network likely acted as fluid flow pathways. The concentration of opaque minerals in fractures is a consequence of dissolution of less soluble phases and lends further evidence to support the presence of fluids in the fracture network.

The results of microstructural analysis of the thin section samples from Maccles Lake are given in Table 5.2.1. The samples show evidence of an early, amphibolite grade sinistral deformation phase that is preserved in samples at more than 500-600m west of the Gander-Avalon boundary. This is

Sample No.	Distance from Boundary (m)	Rock Type	Mineral Assemblage (descending order of %)	Quartz Fabric	Feldspar Fabric	Metamorphic Grade	Shear Sense
87	3440	Orthogneiss	K-fsp, Qtz, K-fsp (ser), Bio, Mus	GBM	BF + DMT (?)	Upper greenschist-amphibolite	Sinistral
91	2113	Megacrystic granite	K-fsp (ser), Qtz, K-fsp (neo), Plag, Bio, Mus, Chl, Epi, Ox	GBM	BLG-SGR	Amphibolite	-
95	1121	Orthogneiss	Qtz, K-fsp (ser), Mus, Chl, Plag, Ox	GBM	CP + BLG	Amphibolite	Dextral
130	951	Banded Orthogneiss	K-fsp (ser), Qtz, Mus, Bio, Chl, Plag	GBM	BLG-SGR	Amphibolite	Sinistral
97	668	Phyllonitic mylonite	Chl, Qtz, Epi, Bio, K-fsp (ser), Epi	SGR	Alt	Lower Greenschist	Dextral
190	621	Phyllonitic orthogneiss	K-Fsp (ser), Qtz, Bio, Chl, Epi, Ox	GBM	BLG-SGR	Amphibolite	Sinistral
30a	443	Phyllonitic Gneiss (HBG)	Qtz, Mus, Chl, K-Fsp (ser), Gar, Cal	SGR	Alt	Lower Greenschist	Sinistral
30b	443	Othogneiss and cataclasite (HBG)	Qtz, K-Fsp (ser), Mus, Epi, Cal, Ox	SGR-GBM	CP + BLG	Upper Greenschist	-
82	422	Mylonite	Qtz, K-Fsp (ser), Plag, Bio, Mus, Epi	SGR	BF + CP + BLG	Upper Greenschist	Dextral
84	402	Phyllonitic mylonite	Qtz, Chl, K-Fsp (ser), Epi, Bio, Mus, Ox	SGR-GBM	BF + CP (DMT?)	Upper Greenschist	Both indicated
83	394	Phyllonitic mylonite	Qtz, K-Fsp (ser), Plag, Mus, Chl, Ox	SGR-GBM	BF + CP	Upper Greenschist	Dextral
169	290	Altered gabbro	Chl, K-Fsp (ser), Plag, Bio, Mus, Qtz, Ox	-	Mag?	-	-
101	283	Altered granite	Chl, K-Fsp (ser), Qtz, Cal	SGR	Alt	Lower Greenschist	-
79	232	Megacrystic granite	K-Fsp (ser), K-Fsp, Chl, Qtz, Mus, Epi, Ox	SGR-GBM	BF + CP	Mid Greenschist	-
54	174	Weakly foliated granite	Qtz, Plag, K-Fsp (ser), Mus, Ox	BLG-SGR	BF + CP	Lower Greenschist	-
75	133	Phyllonite	Chl, Qtz, K-Fsp (ser), Epi, Ox	SGR-GBM	Alt	Upper Greenschist	Dextral

Sample No.	Distance from Boundary (m)	Rock Type	Mineral Assemblage (descending order of %)	Quartz Fabric	Feldspar Fabric	Metamorphic Grade	Shear Sense
112	62	Phyllonite	Qtz, Chl, K-Fsp (ser), Mus, Cal, Epi	SGR-GBM	CP + BLG (DMT?)	Upper greenschist-amphibolite	Dextral

Table 5.2.1: Table of results for samples from the Gander Zone in the Maccles Lake area with inferred metamorphic grade and shear sense. Mineral phase codes: Qtz – Quartz, K-Fsp (ser) – K-Feldspar altered to sericite, K-Fsp (neo) – recrystallized K-Feldspar, Plag – Plagioclase, Mus – Muscovite, Bio – Biotite, Chl – Chlorite, Epi – Epidote, Ox – Oxides, Cal – Calcite, Gar – Garnet.

Figure 5.2.3: thin section composite photomicrograph of sample ML30b at 2.5x zoom under plane polarised light. The earlier foliation fabric running horizontal across the picture has been offset by an overprinting brittle fracture network showing both sinistral and dextral offsets. To the left of the image, the large vein sinistrally offsetting the foliation at a high angle contains undeformed calcite and quartz grains.

then overprinted by a later, greenschist, ductile dextral deformation phase that is preserved within 500m of the Gander-Avalon boundary. The final brittle, sub-greenschist grade deformation phase overprints both of the earlier ductile fabrics and is associated with the operation of hydrothermal fluids within the fracture network. Both the early amphibolite and later greenschist deformation phases preserve evidence of fluid-assisted DMT and both the greenschist and brittle sub-greenschist grade deformation phases display pressure solution textures.

5.2.2 Bay du Nord

The samples BdN36a (gneiss) and BdN21 (granitic gneiss) are both located more than 1km from the Gander-Avalon boundary and display similar microstructural fabrics. Quartz grains in BdN36a and BdN21 are a relatively coarse size at 0.4mm and the grain boundaries can be straight, irregular or lobate. BdN21 quartz grains display even extinction patterns, include trails of fluid inclusions (tuttle lamellae) and the grain boundaries occur at 120° in triple junctions, as shown in Figure 5.2.4.a. In contrast, quartz grains in BdN36a contain subgrains and show sweeping undulose extinction. Feldspar grains in both BdN36a and BdN21 occur as relatively coarse (~1mm) relict grains and porphyroclasts. The feldspar grains have been partially altered to sericite mica at 0-70% of individual grains, especially along intragranular fractures. Intracrystalline deformation microstructures, such as sweeping undulose extinction, rare myrmekites and flame perthites, can still be recognised despite the partial alteration of the feldspar grains.

Relatively coarse grained (0.5-1mm) phyllosilicate minerals define a discrete foliation in BdN21 and a continuous foliation in BdN36a. Muscovite and biotite grains are elongate in shape and show kinking textures with sweeping undulose extinction. Both chlorite and epidote are present in low proportions in BdN36a and BdN21 and chlorite shows intergrowth textures with biotite within individual grains. Opaque minerals in the thin sections are concentrated in brittle fractures, rare stylolitic surfaces and the cleavage domains of the foliation. Shear sense indicators in the sample BdN21 were ambiguous whilst the stair stepping strain shadows and mica fish structures in BdN36a indicated a dextral sense of shear.

Within 1km of the Gander-Avalon boundary, the sample BdN1 and the BdN location 2 samples display a different microstructural fabric. At only 88m from the Gander-Avalon boundary, the

mylonitic granites at BdN2 contain discrete foliations defined by the alignment of phyllosilicate minerals, compositional bands or lenses of quartz and feldspar porphyroclasts (see Figure 5.2.5.a). The quartz grain sizes in BdN2a and 2b are finer than the other samples from the Bay du Nord area at 0.1-0.2mm. Elongate to irregular quartz grain shapes have a strong CPO as well as irregular to lobate grain boundary shapes, undulose extinction and subgrains. The feldspar porphyroclasts have been pervasively altered to sericite mica (50-100%) in BdN1, BdN2a and 2b so that any other microstructures present have been partially masked. In the less altered grains, intragranular fractures can be seen to break up the grains to the point that they form mosaic fracture networks in BdN1 (see Figure 5.2.4.b). BdN2a has rare core and mantle textures on the feldspar porphyroclasts and rare flame perthite structures.

Chlorite, muscovite and biotite can form strain caps, mica beards and stair-stepping wings in the strain reduction shadows of the feldspar porphyroclasts, as shown in Figure 5.2.5. The mica grains often show sweeping undulose extinction and in BdN,1 the chlorite grains have been sheared to form boudin structures. Opaque minerals, as well as epidote, are fairly common and occur in association with the foliations, fractures and a few rare stylolitic surfaces within the samples. The shear sense indicated in BdN1 is dextral and differs from the clear sinistral shear sense shown in BdN2a and 2b by stair-stepping strain reduction shadows, oblique foliations, mica fish and C' fabrics. The sinistral sense of shear shown by these samples and the field observations in close proximity to the Gander-Avalon boundary contrasts with the dextral shear sense observed in all of the other study areas.

Similar to the Maccles Lake study area, all of the ductile fabrics are overprinted by a brittle fabric including brittle fractures, calcite and quartz veins and rare stylolitic surfaces. The calcite veins in BdN1 (seeFigure 5.2.5.c) show no recrystallization textures, which suggests they were precipitated after ductile deformation had ceased. Of the few brittle structures that show offset, the dominant shear sense indicated is sinistral and the orientations of the brittle structures are similar to those in Maccles Lake including parallel to, perpendicular to and oblique to the ductile foliation fabric.

All of the samples in the Bay du Nord area contain textures that indicate mid-upper greenschist grade conditions during deformation at estimated temperatures between 400-450°C. The quartz

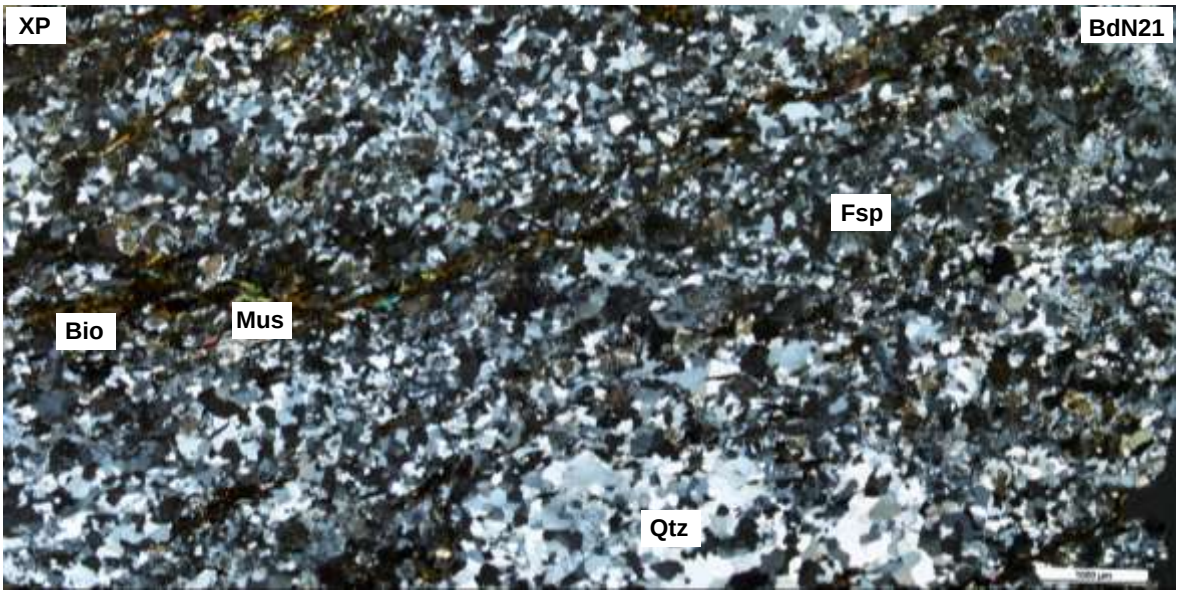

a)

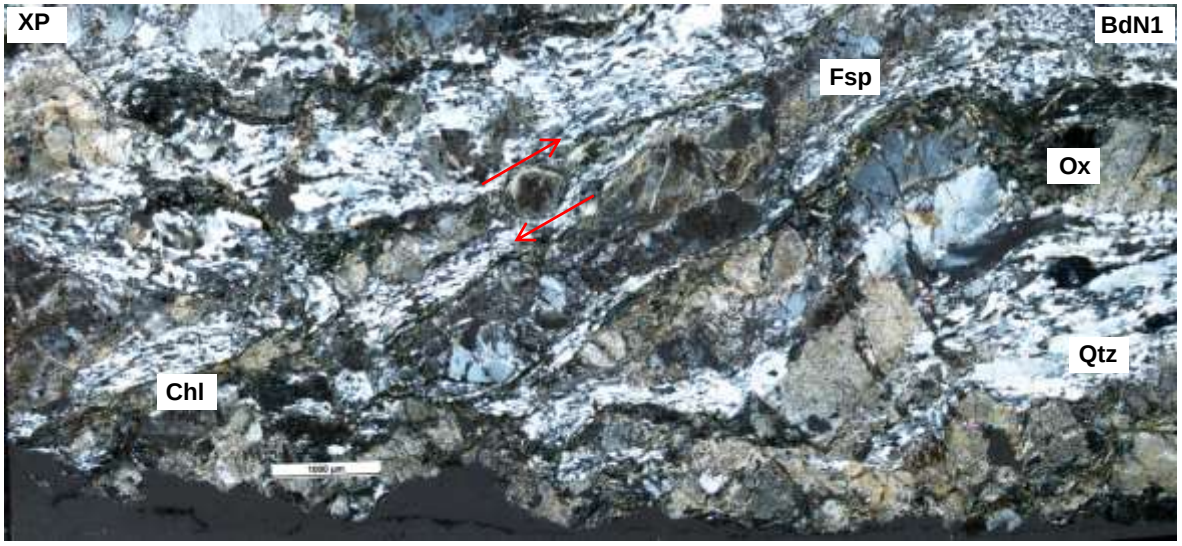

b)

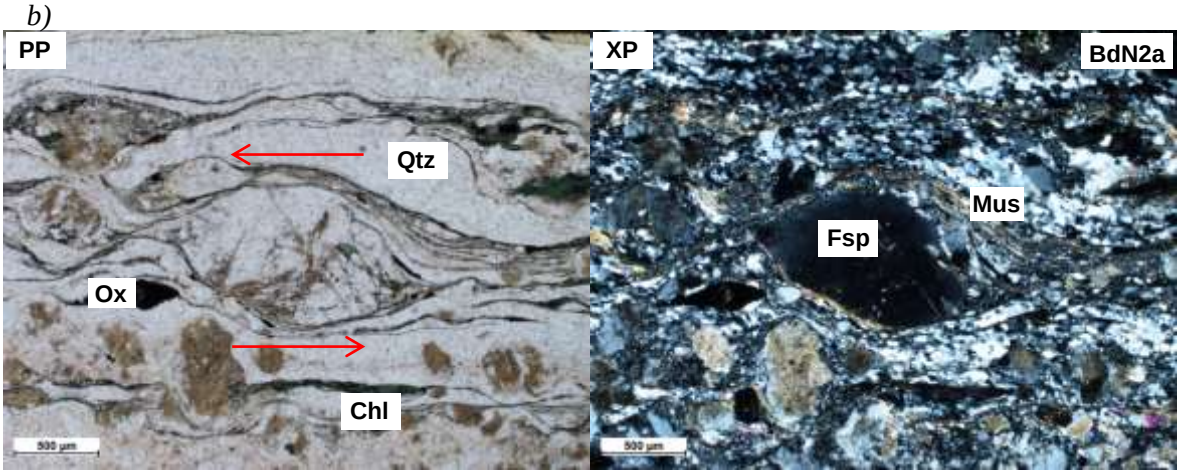

c) *d)*

Figure 5.2.4: a) thin section photomicrograph of BdN21 at 1x zoom under crossed polars. The quartz grains show the polygonal to irregular shapes and straight grain boundaries that are indicative of recovery. b) thin section photomicrograph of BdN1 at 1x zoom under crossed polars. The minerals show clear compositional zoning with bands of relict feldspar grains that are heavily fractured and bands of elongate quartz grains and subgrains indicative of SGR recrystallization. c) and d) thin section photomicrographs of BdN2a at 2.5x zoom and under plane and crossed polars respectively. The feldspar porphyroclast is surrounded by a mica beard that indicates a sinistral sense of shear and the quartz grains display textures associated with SGR recrystallization.

a)

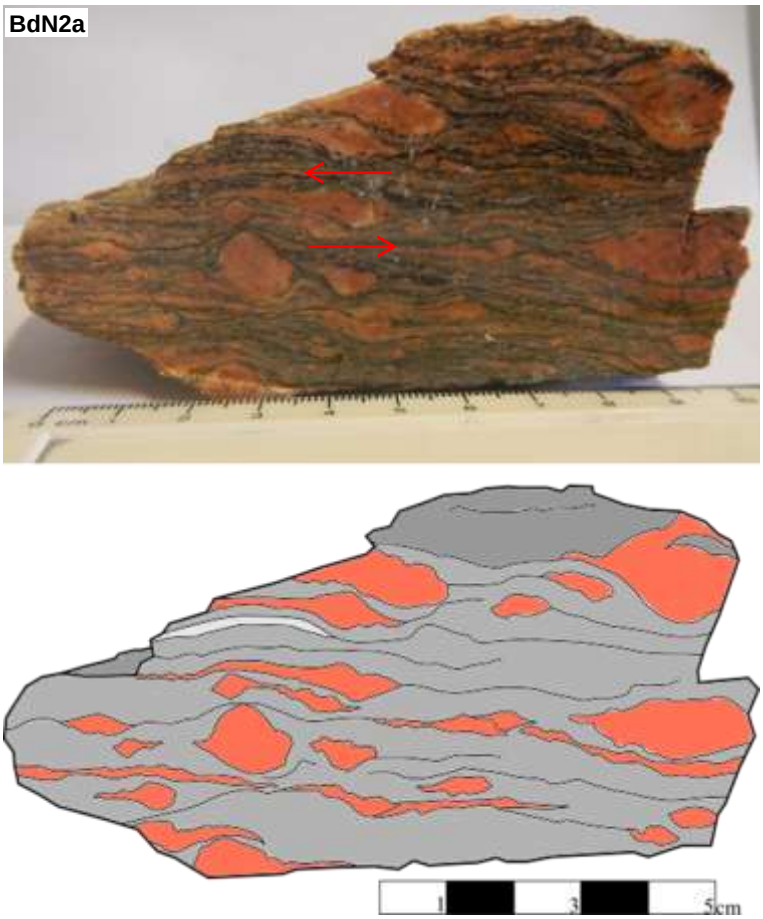

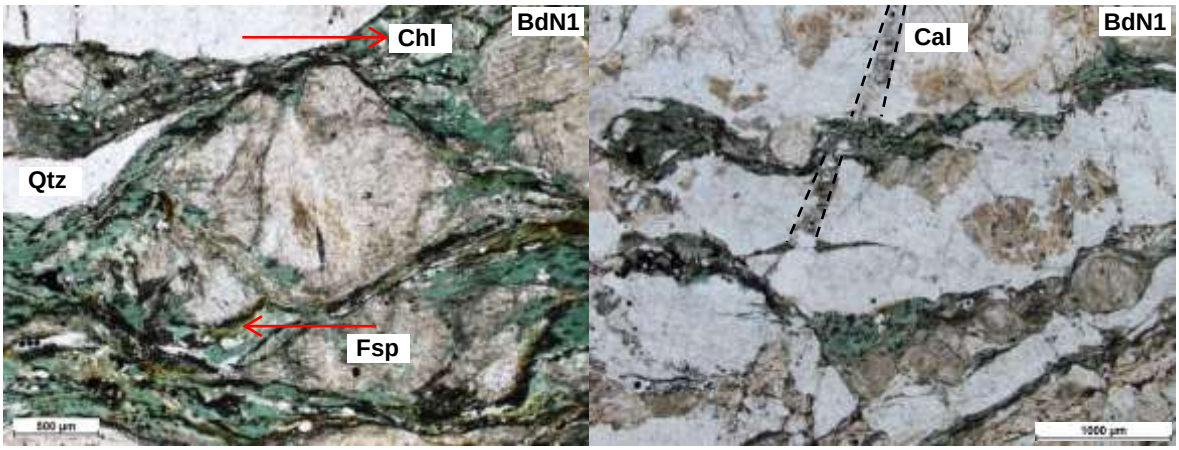

b) *c)*

Figure 5.2.5: a) photo and sketch of BdN2a in hand specimen showing the strong mylonitic fabric and sinistral stair stepping fabric on the feldspar porphyroclasts. b) thin section photomicrograph of BdN1 at 2.5x zoom under plane-polarised light. The overgrowth of chlorite in the strain reduction shadows of the feldspar porphyroclast contains the same dextral kinematic fabric as the rest of the sample and so is inferred to have formed synkinematically. c) thin section photomicrograph of BdN1 at 1x zoom under plane-polarised light. A calcite vein containing fractured host rock cross cuts the section at a high angle (~80°) to the earlier ductile foliation fabric. Intergranular fractures cross cut the quartz compositional bands and the feldspar porphyroclasts.

Sample No.	Distance from Boundary (m)	Rock Type	Mineral Assemblage (descending order of %)	Quartz Fabric	Feldspar Fabric	Metamorphic Grade	Shear Sense
36a	1701	Gneiss	Qtz, K-Fsp (ser), Mus, Bio, Chl, Ox	GBM	BF + CP	Upper Greenschist	Dextral
21	1649	Granitic Gneiss	Qtz, K-Fsp (ser), Bio, Mus, Chl, Ox	GBAR + GBM??	BF + CP	Upper Greenschist	Unknown
1	108	Granitic Mylonite	K-Fsp (ser), Qtz, Chl, Mus, Ox, Epi (Cal)	SGR + lim BLG	BF + CP	Mid-Greenschist	Dextral
2a	88	High Strain (?) Mylonite	Qtz, K-Fsp (ser), Chl, Mus, Bio, Ox, Epi	SGR + GBM + lim DMT	BF + CP + BLG	Upper Greenschist - Amphibolite	Sinistral
2b	88	Ultramylonite	K-Fsp (ser), Qtz, Chl, Epi, Bio, Mus, Ox	SGR + lim DMT	Alt + BF + CP	Mid-Greenschist	Sinistral

Table 5.2.2: Table of results for samples from the Gander Zone in the Bay du Nord area with inferred metamorphic grade and shear sense. Mineral phase codes: Qtz – Quartz, K-Fsp (ser) – K-Feldspar altered to sericite, Mus – Muscovite, Bio – Biotite, Chl – Chlorite, Epi – Epidote, Ox – Oxides, Cal – Calcite

fabrics in BdN21 are characteristic of recovery and grain-boundary-area-reduction (GBAR) so could potentially mask higher temperature fabrics. The presence of mylonites and ultramylonites with relatively fine grain sizes in close proximity to the Gander-Avalon boundary could reflect a higher degree of accommodated strain. The sinistral shear sense indicated in the samples at locality BdN2 may represent a sinistral shear zone that was coeval with the greenschist grade dextral shear zones in the other study areas. Similarly to the Maccles Lake area, there are many microstructures present in the Bay du Nord samples that imply that fluids were present during deformation. The growth of chlorite and other fibrous minerals in synkinematic strain shadows requires hydrous conditions during the ductile deformation phase. Several other microstructural fabrics indicate that fluids were present during brittle deformation, including the hydration alteration of biotite and feldspar grains, hydrothermal mineralisation in veins and dissolution along rare stylolitic surfaces.

5.2.3 Freshwater Bay

At more than 1km from the Gander-Avalon boundary, the dominant rock type are gneisses that contain a well-defined gneissic fabric, open to isoclinal folds and enclaves of amphibolites and metasediments in outcrop. The orthogneisses are relatively coarse grained as quartz grains show sizes of 0.5-1.5mm, feldspar grains at an average size of 1mm and mica grain sizes range from 0.4-1.5mm. Compositional bands of quartz contain microstructures such as irregular to interlobate. grain boundaries, occasional subgrain development, tuttle lamellae and pinning effects from mica grains. The HBG samples contain both plagioclase and K-feldspar as porphyroclasts or relict grains that have been altered at a low degree to sericite mica (0-25%). The feldspar grains often show undulose extinction and can contain tabular subgrains and myrmekites that bulge inwards from the grain boundaries. Several samples show core and mantle textures with very fine (<0.1mm) new feldspar grains that form thin mantles around the deformed relict grains. Biotite and muscovite in the HBG samples often define continuous or discrete foliation fabrics or they occur in strain caps and mica beards on the feldspar porphyroclasts. The elongate or fish-shaped mica grains often show sweeping undulose extinction patterns. Chlorite and epidote are present in these orthogneisses, but in relatively low proportions (<10%) and the chlorite usually occurs within biotite grains as an inter-grown alteration product. The shear senses recorded in the HBG samples

can be ambiguous, especially in samples with a weak continuous foliation fabric, but a sinistral sense of shear can be identified from mica fish and oblique foliation microstructures.

The fabrics observed in the gneiss samples further than 1km from the Gander-Avalon boundary indicate deformation conditions at amphibolite grade with sinistral shear. The microstructures in the quartz grains are characteristic of GBM recrystallization whereas the feldspars have deformed by BLG recrystallization and crystal plastic mechanism. This contrast in deformation mechanism between quartz and feldspar provides an estimated temperature range of 450-500°C.

Within 1km of the Gander-Avalon boundary, the rock types become more variable with gneisses, schists, foliated granites and phyllonites recognised in the field and thin sections. There are two main microstructural textures that occur within 1km of the Dover Fault that are here termed Type 1 and Type 2. The Type 1 fabric includes strong discrete foliations defined by the alignment of mica grains, compositional bands of quartz and plagioclase and K-feldspar porphyroclasts (see Figure 5.2.6.a). It is therefore similar to the orthogneisses in the HBG, but there are several major differences, such as the more intense foliation fabric. The grain sizes are generally finer in the Type 1 fabric with quartz grains at an average size of 0.5mm, feldspars at 0.6-1mm and mica grains from 0.3-0.7mm. Similarly to the orthogneiss samples, the quartz grains have irregular to lobate boundaries, often contain subgrains and show pinning effects from mica grains. The feldspar grains often show core and mantle structures with very fine new grains as well as myrmekites, flame perthites and relatively strong alteration to sericite (10-75%). Chlorite and muscovite can occur as mica beards on the feldspar porphyroclasts and, as shown in Figure 5.2.6.a, the mica grains can define a strong S-C-C' sinistral shear band fabric. Chlorite and epidote occur in generally higher proportions in the Type 1 samples (chlorite 20% in FB15a and 15% in FB20) and opaque oxide minerals occur at low proportions (<10%) in association with the foliation cleavage domains and overprinting fractures.

Samples that contain the Type 2 fabric are located within narrow mylonitic zones containing steeply plunging, tight to isoclinal, dextral folds that often separate low-strain lenses of weakly foliated rock. The grain sizes are slightly finer again than in Type 1 with quartz grains at sizes of 0.1-0.4mm, feldspar grains at averages of 0.5-1mm and mica grains at 0.2-0.7mm. The quartz

a)

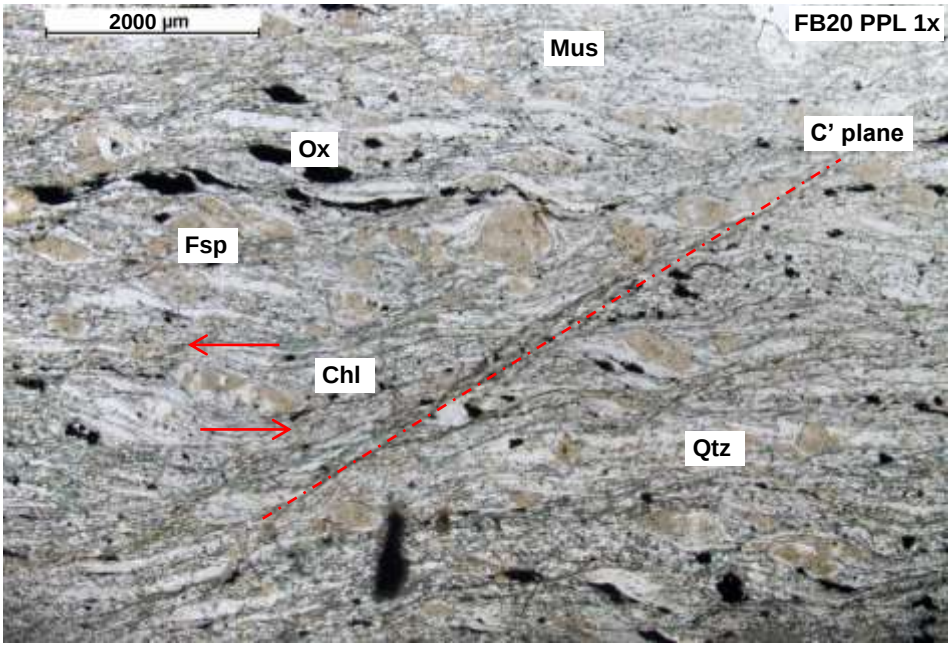

b)

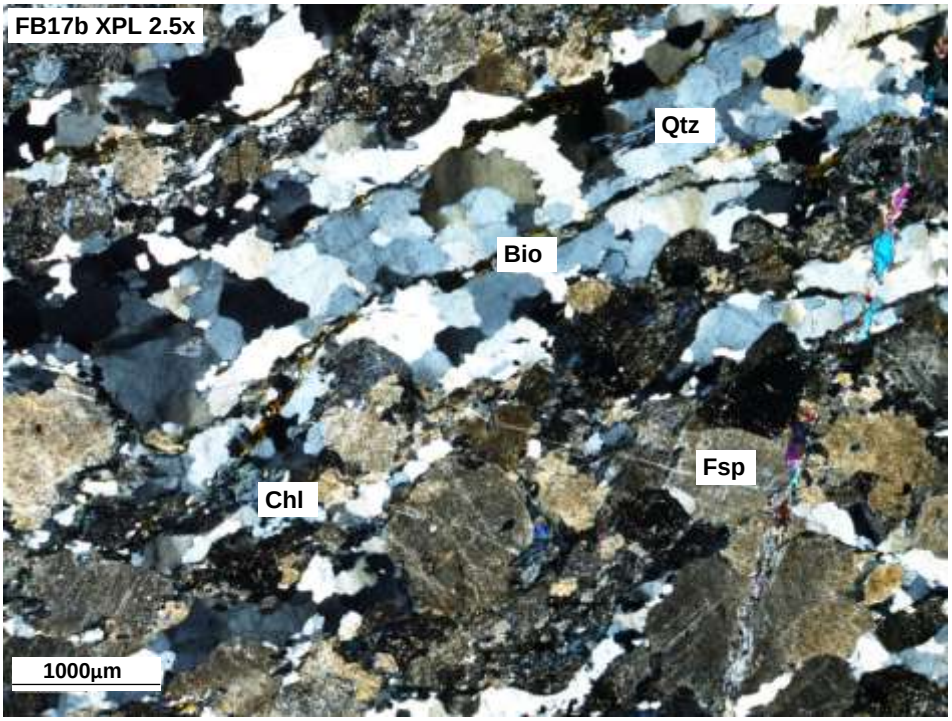

Figure 5.2.6: a) thin section composite photomicrograph of FB20 at 1x zoom under plane polarised light (Type 1). The chlorite and muscovite grains in FB20 are aligned in a strong S-C fabric with a C' plane fabric that indicates a sinistral sense of shear. All of the highly altered feldspar porphyroclasts have a mica beard texture that is indicative of the action of DMT. b) thin section composite photomicrograph of FB17b at 2.5x zoom under crossed polarised light (Type 2). The quartz grains have the interlobate grain boundaries and relatively low intracrystalline deformation that are characteristic of GBM recrystallization. The feldspar porphyroclasts have been highly altered to sericite and are overprinted by an epidote-rich vein.

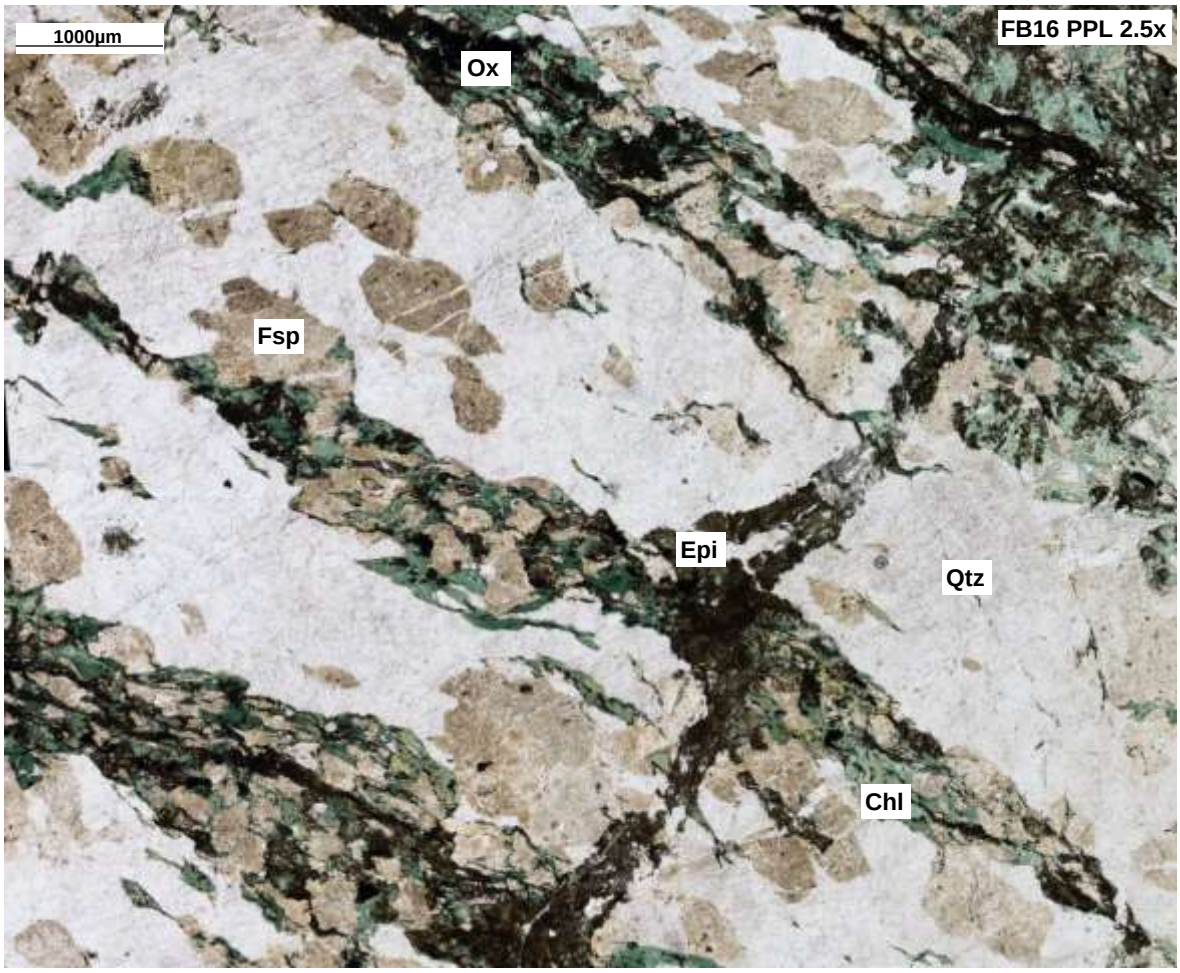

Figure 5.2.7: thin section composite photomicrograph of FB16 at 2.5x zoom under plane polarised light. A quartz- and epidote-rich vein cuts across the thin section at a perpendicular orientation to the foliation. Another set of fractures run parallel to the foliation and have opaque oxide minerals concentrated on the fracture surface.

occurs in compositional bands or microlithons with lobate grain shapes and a weak to moderate CPO under a tint plate. In the feldspar porphyroclasts, the dominant microstructures are brittle intra- to inter-granular fractures and intracrystalline deformation textures including tapered deformation twins and sweeping and patchy undulose extinction (see Figure 5.2.6.b). There are also a few rare and limited core and mantle textures and myrmekites in the feldspar grains. Discrete foliation fabrics defined by the mica grains are very strong in Type 2 samples and chlorite can count for up to 20% of the thin sections. As in the type 1 samples, chlorite and muscovite can form in mica beards around the feldspar porphyroclasts. The shear senses indicated in the thin section samples are variable with both sinistral and dextral shear indicated. At the outcrop scale, however, almost all of the structures indicate a dextral sense of shear.

Across all of the samples in the Gander Zone of Freshwater Bay there is a brittle overprint that offsets and reactivates the earlier ductile fabric. At the outcrop scale, these structures include brittle box folds at the centimetre-scale, dextral shear bands and fractures in Riedel configurations. In thin section, the brittle overprint can be recognised in transgranular fractures and mineralised veins. In FB16, shown in Figure 5.2.7, epidote- and calcite-rich veins can be seen to cut across the thin section almost perpendicular to the foliation, whereas oxide-rich transgranular fractures follow the chlorite cleavage domains. In cross polarised light, the quartz grains in FB16 show core and mantle textures of very fine new grains (<0.1mm) that overprint the coarse grains in the compositional bands.

The results of the microstructural analysis of the thin sections from the Gander Zone in Freshwater Bay are given in Table 5.2.3 below. Interpreting these results shows that the earlier amphibolite grade deformation phase observed in the HBG orthogneisses is also preserved in the Type 1 samples. The recrystallization of quartz by GBM and feldspar by BLG mechanisms indicates that amphibolite grade conditions were prevalent during deformation. The higher intensity of the mylonitic fabric and finer grain size may reflect increasing strain towards the Gander-Avalon Boundary. An upper-greenschist to amphibolite boundary grade (400-450°C) with a dextral sense of shear is inferred for the Type 2 samples based on the recrystallization of quartz by GBM compared to the brittle and crystal plastic deformation of feldspar. The brittle overprinting

Sample No.	Distance from Boundary (m)	Rock Type	Mineral Assemblage (descending order of %)	Quartz Fabric	Feldspar Fabric	Metamorphic Grade	Shear Sense
152	4680	Orthogneiss	Qtz, K-Fsp, Bio, Epi, Chl	GBM	BF + CP (unknown)	Upper Greenschist - Amphibolite	Unclear
146	4677	Orthogneiss	K-Fsp (ser), Qtz, Bio, Plag (ser), Chl, Epi	GBM	BF + CP (GBM?)	Amphibolite	Unclear
131	3400	Weakly deformed granite	K-Fsp (ser), Plag (ser), Bio, Qtz, Chl, Epi	GBM	BF + CP + BLG?	Amphibolite	Unclear
3a	1744	Orthogneiss	K-Fsp (ser), Qtz, Mus, Bio, Plag, Chl, Ox	SGR + GBM	CP + DMT?	Upper Greenschist	Sinistral
3b	1744	Orthogneiss	K-Fsp (ser), Qtz, Plag, Mus, Bio, Chl, Cal, Ox	SGR + GBM	CP (DMT?)	Upper Greenschist	Unclear
6	1585	Orthogneiss	Bio, Qtz, K-fsp (ser), Chl, Ox	SGR + GBM	Alt	Upper Greenschist	Sinistral
11	1188	Orthogneiss	Qtz, K-fsp, Bio, Epi	GBM	BLG	Lower Amphibolite	Sinistral
118	1106	Weakly deformed granite	K-Fsp (ser), Qtz, Bio, Chl, Epi	GBM	BLG + SGR	Amphibolite	Unclear
13	999	Orthogneiss	K-Fsp, Qtz, Mus, Bio, Chl	GBM	BLG+SGR (DMT?)	Amphibolite	Sinistral
116	920	Gabbro	Chl, Bio, K-Fsp (ser), Plag (ser), Epi	-	BF + CP	Lower- or sub-Greenschist	Unclear
114	824	Phyllonitic granite	Qtz, K-fsp, Mus, Bio, Chl, Ox	GBM	BLG + DMT?	Upper Greenschist - Amphibolite	Dextral
17a	750	Striped Schist	K-Fsp (ser), Qtz, Chl, Epi, Bio, Ox	GBM	SGR	Amphibolite	Unclear
17b	750	Granite	K-Fsp (ser), Qtz, Chl, Plag (ser), Epi, Bio	GBM	CP + BF	Upper Greenschist	Unclear
15a	725	Orthogneiss	K-Fsp (ser), Qtz, Chl, Epi, Mus (Vein: Qtz, Epi, Ser)	SGR+GBM	BLG (DMT)	Amphibolite	
15b	725	High Strain Orthogneiss	K-Fsp (ser), Qtz, Plag, Bio, Mus, Epi, Chl	GBM	Lim BLG + DMT?	Upper Greenschist	Dextral ?
112	715	Weakly foliated granite	K-Fsp (ser), Qtz, Bio, Chl, Epi	GBM	BLG + SGR	Amphibolite	Unclear

Sample No.	Distance from Boundary (m)	Rock Type	Mineral Assemblage (descending order of %)	Quartz Fabric	Feldspar Fabric	Metamorphic Grade	Shear Sense
16	687	Altered mylonite	Qtz, K-Fsp (ser), Chl, Epi, Plag (ser), Cal, Ox	GBM (overprint BLG)	CP + BF + lim BLG	Upper Greenschist	Unclear
19	591	Phyllonitic gneiss	K-fsp (ser), Bio, Epi, Chl, Qtz, Ox	SGR	BF + CP + BLG	Upper Greenschist - Amphibolite	Sinistral
20	550	High strain phyllonite	Qtz, K-fsp (ser), Mus, Chl, Ox	GBM + DMT	BLG + SGR + DMT	Amphibolite	Sinistral
21	458	Weakly foliated granite	K-fsp (ser), Qtz, Plag, Chl, Mus, Ox	SGR + GBM	BF + CP + lim BLG	Upper Greenschist - Amphibolite	Unclear
22	360	Mylonitic zone in granite	K-fsp (ser), Qtz, Mus, Chl, Epi, Plag, Ox	SGR + GBM (late BF)	CP + BLG (late BF)	Upper Greenschist - Amphibolite	Sinistral

Table 5.2.3: Table of results for samples from the Gander Zone in the Freshwater Bay area with inferred metamorphic grade and shear sense. Mineral phase codes: Qtz – Quartz, K-Fsp (ser) – K-Feldspar altered to sericite, Plag – Plagioclase, Mus – Muscovite, Bio – Biotite, Chl – Chlorite, Epi – Epidote, Ox – Oxides, Cal – Calcite.

deformation is inferred to have occurred at lower- to sub-greenschist at temperatures of <300°C, as shown by the limited BLG recrystallization of quartz in FB16. It is clear from the number of mica beards on porphyroclasts, chlorite syn-kinematic overgrowths and the concentration of opaque minerals on fracture surfaces that the fluid assisted mechanisms of DMT and pressure solution were active during all of the deformation phases. Through these mechanisms, the presence of fluids during deformation appears to have aided in the formation of the mylonitic and gneissic fabrics. Overall, the fabrics in the samples show a down-temperature trend in overprinting deformation phases with increasing strain towards the Dover Fault and the centre of the DFSZ.

5.2.4 Hare Bay

Of the three Gander Zone samples, only the samples from locality HB93 are of use in determining the conditions during metamorphism and deformation. Sample HB97 contains only chlorite and oxide minerals that form no clear deformation fabric. Whilst HB97 as a heavily altered gabbro does offer evidence of retrogressive alteration, it does not contain any microstructures that are characteristic of a metamorphic grade.

The samples taken from locality HB93 are sited only 270m from the Gander-Avalon boundary and the samples HB93a and 93b were sampled, respectively, in planes both parallel and perpendicular to the mineral lineation. Observations of these lithologies in the field indicated that they were derived from the HBG and that the outcrops included structures such as dextral shear bands and dextral wrapping of the foliation fabric around pods of mafic material. At the thin section scale, both HB93 and b have strongly defined fabrics with compositional bands of quartz, strong discrete foliations defined by phyllosilicate minerals and K-Feldspars form porphryoclasts. The quartz grains in both HB93a and b are elongate to irregular in shape and the grains are relatively fine grained at an average grain size of 0.1mm. The microstructures in the quartz grains include subgrains or sweeping undulose extinction patterns, irregular grain boundaries and a weak to moderate CPO. Porphyroclasts of K-feldspar have an average grain size of 0.5mm in both HB93 samples, but the grain size can reach a maximum of 3mm, as shown in Figure 5.2.8 and 5.2.9. The feldspar grains contain brittle intragranular fractures with an average length of 0.1mm but they also show evidence of intracrystalline deformation including sweeping extinction patterns and fluid

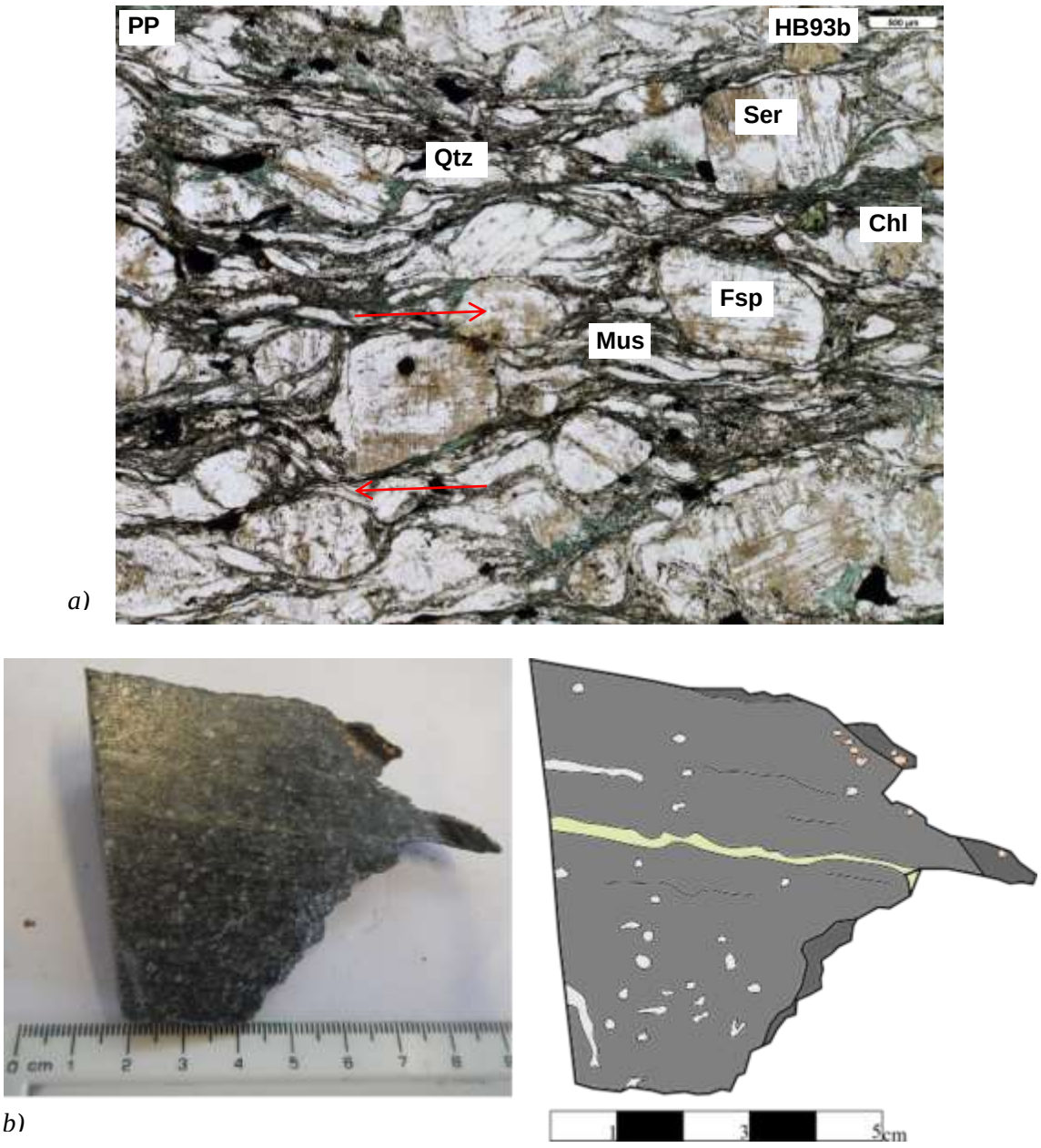

Figure 5.2.8: a) thin section composite photomicrograph of sample HB93b at 2.5x zoom under plane polarised light. The partially altered K-Feldspar porphyroclasts show dextral shear senses from the stair stepping of the mica minerals in their strain reduction shadows. b) photo and sketch of the sample HB93b in hand specimen. The well-defined foliation fabric and K-feldspar porphyroclasts are clearly visible in hand specimen and retrogressive alteration of the sample has imparted a green-grey colour to the specimen.

inclusion trails. Myrmekite textures are rare in the HB93 samples and occur only at feldspar grain boundaries whereas partial alteration of the feldspar clasts to sericite is widespread.

Muscovite and chlorite grains within the samples form mica beards, strain caps and stair-stepping strain shadows on almost all of the feldspar porphyroclasts in the HB93 samples (see Figure 5.2.8 and 5.2.9). The micas form elongate or mineral fish shapes and generally there is a sweeping extinction pattern in the mica grains. The shear sense indicated by the stair-stepping strain shadows and S-C fabrics formed by the micas is clearly dextral. In sample HB93b, the chlorite grains show an anomalous blue interference colour under crossed polarised light that is characteristic of iron-rich chlorite phases. Oxide minerals in HB93b are associated with these iron-rich chlorite clasts in a portion of the thin section that has undergone a greater degree of alteration. In the field, a brittle overprinting fabric was identified at locality HB93, as shown by brittle box- and kink-folds. At the thin section scale, both samples contain transgranular fractures and the sample HB93a contains a mineralised quartz vein that all cross cut the ductile foliation fabric.

As shown by the samples HB93a and b, the Gander Zone mylonites and phyllonites in the Hare Bay area record a mid-greenschist grade, dextral shear deformation phase within close proximity to the Gander-Avalon boundary. An estimated temperature during deformation of 350-400°C was derived from the quartz microstructures that are indicative of SGR recrystallization, in contrast with the brittle and crystal plastic deformation of the feldspar grains. Both HB93a and b contain microstructures that indicate that DMT was an active deformation mechanism during the greenschist deformation phase. Mica beards around feldspar porphyroclasts are evidence of the precipitation of new fibrous mineral grains around the feldspars and the syntectonic overgrowth of hydrous chlorite minerals on the feldspar grains is a process that requires fluids to be present during deformation. The overprinting of the ductile fabrics with brittle structures is evidence of a later, sub-greenschist grade deformation phase that produced pervasive fracturing in close proximity to the brittle Dover Fault. This pattern of deformation fabrics concurs well with evidence from the Maccles Lake, Bay du Nord and Freshwater Bay areas. The microstructural analysis results are summarised in Table 5.2.4 below.

Sample No.	Distance from Boundary (m)	Rock Type	Mineral Assemblage (descending order of %)	Quartz Fabric	Feldspar Fabric	Metamorphic Grade	Shear Sense
97	517	Chloritised Amphibolite	Chl, Ox	-	-	-	-
93a	273	Gneissic Mylonite	Qtz, Mus, K-Fsp, Plag	SGR + DMT	CP + DMT	Mid-Greenschist	Dextral
93b	273	Phyllonitic Gneiss	Qtz, K-Fsp, Mus, Chl, Ox, Plag	SGR + DMT	CP + DMT	Mid Greenschist	Unclear

Table 5.2.4: Table of results for samples from the Gander Zone in the Hare Bay area with inferred metamorphic grade and shear sense. Mineral phase codes: Qtz – Quartz, K-Fsp – K-Feldspar, Plag – Plagioclase, Mus – Muscovite, Chl – Chlorite, Ox – Oxides.

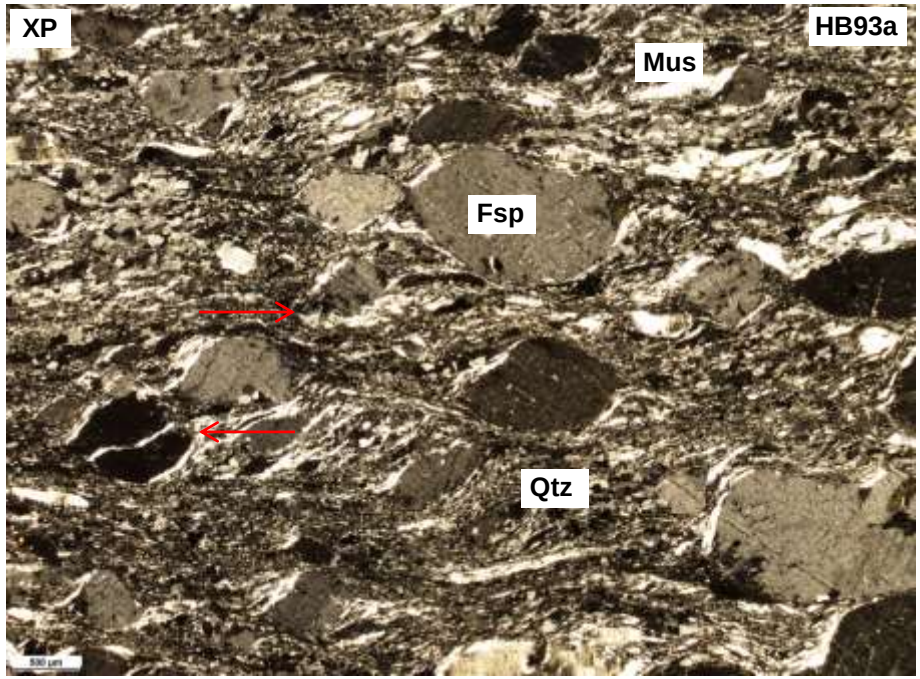

Figure 5.2.9: thin section composite photomicrograph of sample HB93a at 2.5x zoom under crossed-polarised light. Almost every plagioclase and K-feldspar porphyroclast in the sample has a mica beard or strain cap texture. This is indicative of the action of DMT processes in the presence of fluids during deformation. The dextral sense of shear is shown by the shape of the mica fish and the stair stepping on the porphyroclasts.

5.2.5 Shoal Bay

In samples of HBG located more than 1km from the onshore Gander-Avalon boundary, the dominant rock types are gneisses with subordinate metasediments and marbles. Quartz grains in the gneisses occur either in microlithons or in monomineralic compositional bands with the grain sizes generally coarser in the bands (1-2mm). The anhedral to amoeboid shaped quartz grains (see Figure 5.2.10) often contain elongate subgrains that can define intragranular deformation bands. Under a sensitive tint plate, the quartz grains show a weak to moderate CPO. Relict clasts of K-Feldspar and plagioclase are variable altered to sericite (0-100%) and they show average grain sizes in the range of 0.3-1mm. The feldspars show moderate intracrystalline deformation with sweeping extinction, tapered deformation twins and rare myrmekites at grain boundaries. In sample FB10b there are rare core and mantle textures with very fine (<0.1mm) new grains of feldspar. Biotite, muscovite and chlorite usually occur in continuous foliations with relatively low intracrystalline deformation shown by weakly sweeping extinction patterns. The proportion of chlorite is variable (0-50%) and the chlorite usually occurs in intergrowth textures as an alteration product of biotite. Shear senses in the gneiss samples are ambiguous with only SB13 indicating a reliable dextral shear sense from stair stepping on porphyroclast strain shadows. Sample 10a, shown in Figure 5.2.10, shows examples of tight, upright folding of the compositional fabric and shows a steeply plunging lineation on the foliation planes. The samples 11a, b and c were collected from a pod of skarn in the HBG that contained amphibolites, marbles and pelitic marbles. The lack of quartz or feldspar in these samples complicates interpretations of the metamorphic grade experienced by the samples. Using the thick, straight calcite twins that show twins within twins a temperature estimate for these skarn samples at 150-300°C can be inferred (Burkhard, 1993).

Samples of the DFG at more than 1km from the Gander-Avalon boundary show similar textures to those in the HBG. The fabric is formed by continuous or discrete foliations of the mica grains with coarse grained, lobate quartz grains in the intervening microlithons. Porphyroclasts of K-Feldspar show core and mantle textures with very fine (<0.1mm) new grains and myrmekites that bulge into the grain from irregular boundaries (see Figure 5.2.11). Only sample SB19 contains reliable shear sense indicators, which show a dextral sense of shear from the stair-stepping of strain shadows.

Sample SB28, shown in Figure 5.2.11.b, is the closest located sample to the Dover Fault in the Gander Zone. The locality SB28 is located in a zone of phyllonites and the outcrop contains a prominent dextral shear band fabric. In the thin section there is a very strong fabric with the foliation defined by compositional banding that is extensively overprinted by brittle fractures and calcite veins. Quartz grains in SB28 are very fine grained (<0.1mm) with irregular shapes, subgrains and a strong CPO. Epidote occurs as coarse porphyroblasts with apparent dextral stair-stepping on chlorite strain shadows in σ-type structures. The sample SB28 is classified as an epidote-chlorite-schist and represents the most intense example of the brittle overprinting phase in Shoal Bay.

Shoal Bay displays a more complicated Gander Zone structure than in the other study areas. A relatively high temperature, upper-greenschist to amphibolite grade (400-500°C) deformation phase is recorded in the samples more than 1km from the Dover Fault. The shear sense is not often indicated at the thin section scale with a dextral shear sense shown in the few samples that do. In the field, sinistral shear senses were identified for many of the sampled exposures more than 1km from the Gander-Avalon boundary (e.g. SB10). At less than 1km from the Dover Fault, the strain and phyllonitisation in the rocks generally increases and a dextral, upper-greenschist grade deformation phase is preserved. The brittle, sub-greenschist deformation phase can be identified in all of the Shoal Bay samples but the intensity of the fabric is much higher in close proximity to the Dover Fault. Both sinistral and dextral shear senses are indicated for the brittle structures at the thin section scale. However, the dextral offsetting of the Gander-Avalon boundary suggests that, at a regional scale, the deformation had an overall dextral shear sense. The Shoal Bay microstructural results are summarised in Table 5.2.5.

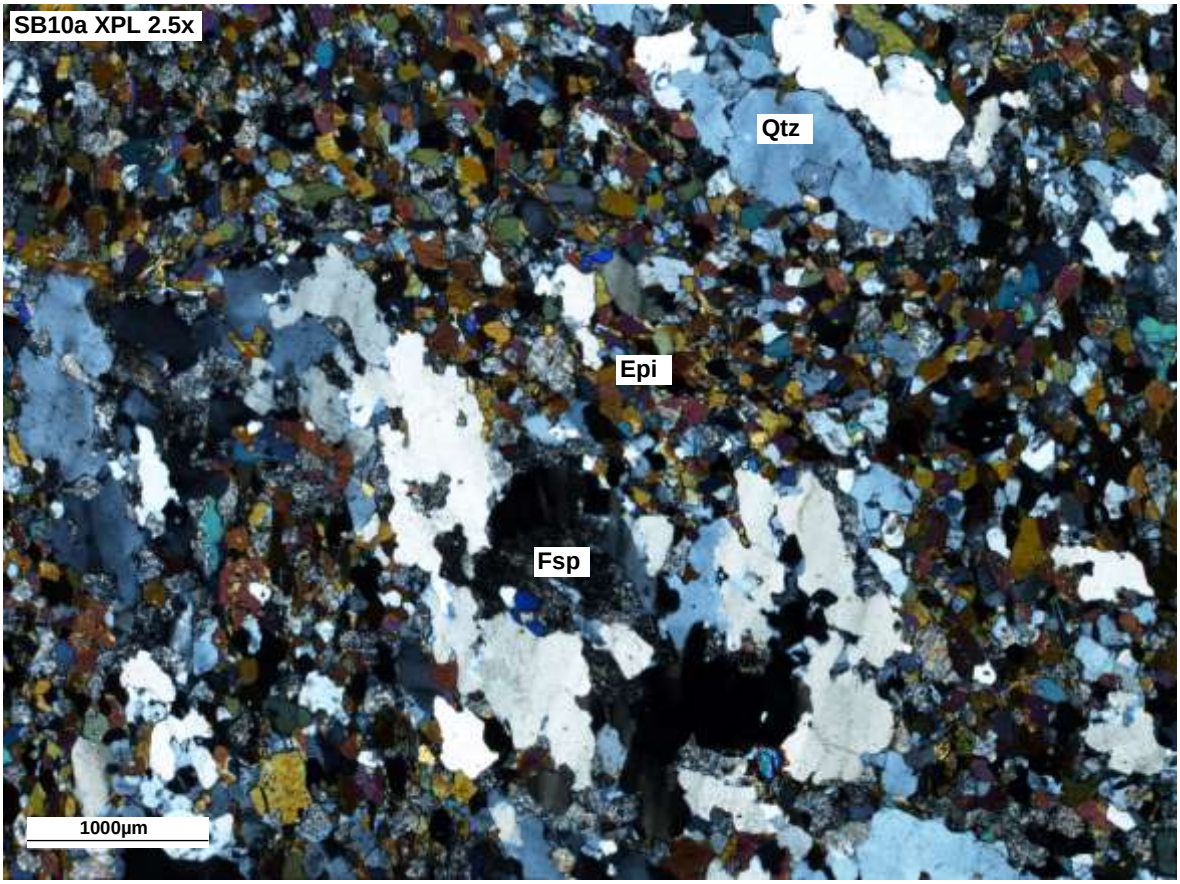

a)

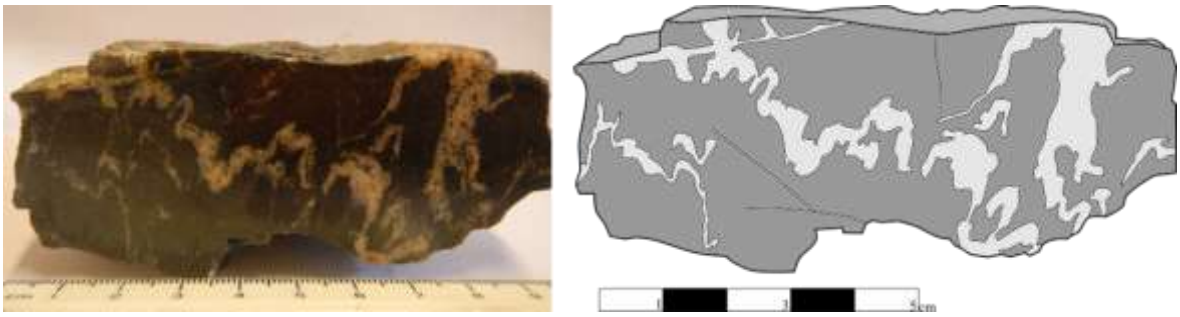

b)

Figure 5.2.10: a) thin section composite photomicrograph of SB10a under crossed polarised light. Quartz grains show coarser grain sizes and lobate to amoeboid grain shapes in the quartz-rich compositional bands. This sample has undergone strong alteration as the feldspar grains are almost entirely replaced with sericite. b) photo and sketch of SB10a in hand specimen. Quartz compositional bands can be seen to be complex and tightly folded with wavelengths of 3-7mm. There is a well-defined lineation fabric on the foliation surfaces and mineralised fractures overprint the earlier folds.

a)

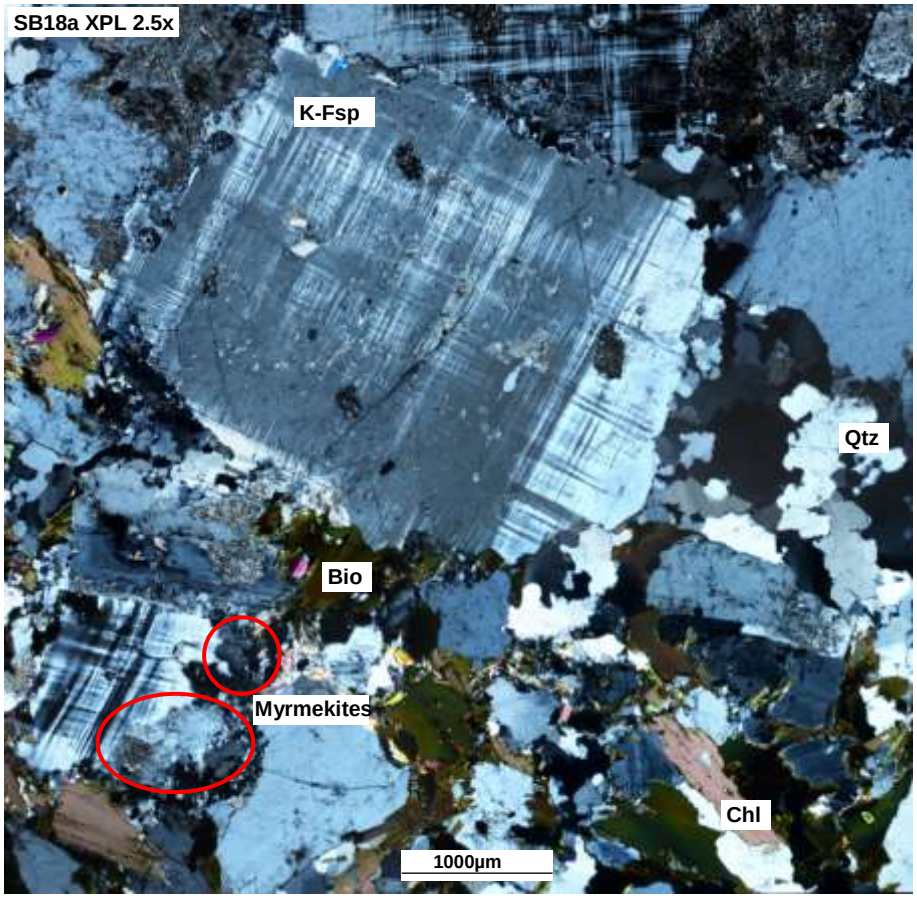

b)

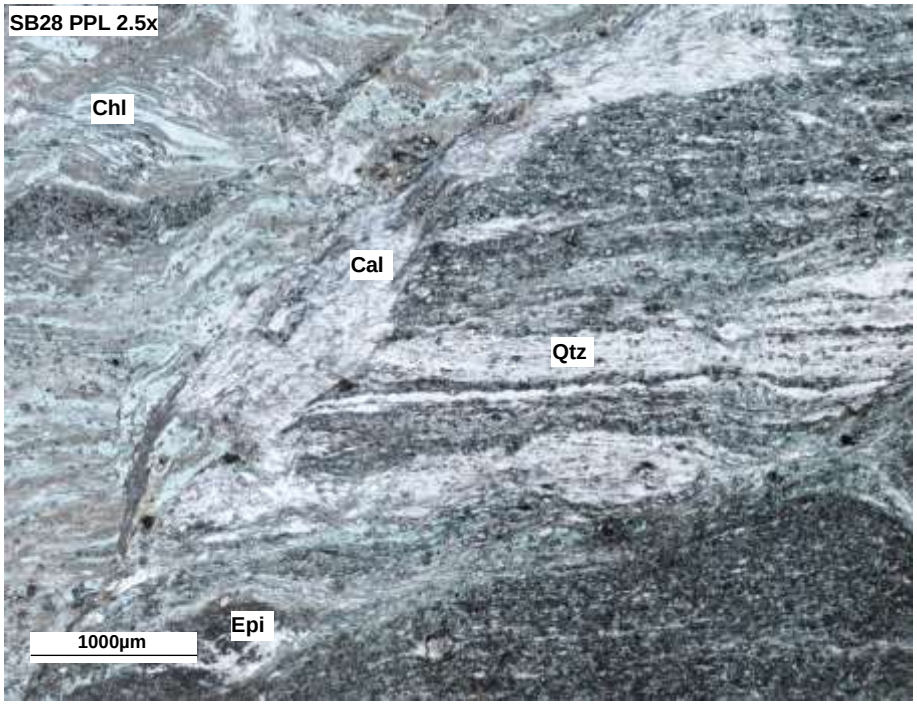

Figure 5.2.11: a) thin section composite photomicrograph of SB18a at 2.5x zoom under crossed polarised light. The coarse relict grains of K-feldspar show irregular to weakly lobate grain boundaries and some grains contain myrmekites that bulge inwards from the grain boundaries. As the quartz grains show textures indicative of GBM recrystallization, this indicates relatively high temperature conditions during deformation. b) thin section composite photomicrograph of SB28 at 2.5x zoom under plane polarised light. High proportions of SB28 are formed of chlorite and epidote, which shows a high level of retrogressive alteration. The ductile foliation fabric is strongly overprinted and offset by mineralised micro-faults, fractures and calcite veins.

Sample No.	Distance from Boundary (m)	Rock Type	Mineral Assemblage (descending order of %)	Quartz Fabric	Feldspar Fabric	Metamorphic Grade	Shear Sense
2	2600	Gneiss	Qtz, K-Fsp (ser), Bio, Plag, Ox, Chl, Epi	GBM	CP	Upper Greenschist-Amphibolite	Unclear
6	2212	Altered Diorite	Bio, K-Fsp (ser), Ox, Chl, Epi	-	Alt + CP + BF	-	Unclear
10a	1986	Feldspar-Quartz-Epidote Schist	Epi, Qtz, K-Fsp, Mus, Bio, Chl	GBM	Alt + CP	Upper Greenschist-Amphibolite	Unclear
10b	1986	Granitic Gneiss	K-Fsp (ser), Qtz, Bio, Chl, Epi, unknown	GBM	BLG + CP + BF	Amphibolite	Unclear
11a	1943	Amphibolite	K-Fsp (ser), Bio, Chl, Epi	-	Alt + CP + BF	?	Unclear
11b	1943	Pelitic Marble ?	Cal, Epi, Mus, K-Fsp (ser), Qtz	CP + BF	Alt + CP + BF	?	Unclear
11c	1943	Marble	Cal, Mus, Epi, K-Fsp, Qtz	CP	CP	?	Unclear
13	1849	Mylonitic Gneiss	K-Fsp (ser), Qtz, Chl, Bio, Ox, Epi	GBM	CP + BF + lim BLG	Amphibolite	Dextral
17	1607	Amphibolite	Chl, Bio, Qtz, K-Fsp (ser), Ox, Epi	SGR	Alt + CP	Greenschist	Unclear
18a	1489	Gneissic Granite	K-Fsp (ser), Qtz, Bio, Epi, Chl	GBM	CP + BF + lim BLG	Amphibolite	Unclear
18b	1489	Chloritised Diorite	Chl, K-Fsp (ser), Qtz, Bio, Epi, Clz	SGR + GBM	Alt + CP	Upper Greenschist	Unclear
19	1421	Granitic Gneiss	K-Fsp (ser), Qtz, Bio, Chl, Mus, Epi, Ox	GBM	BLG + CP + BF	Amphibolite	Dextral
21	1301	Gneiss	Qtz, K-Fsp (ser), Bio, Plag, Chl, Epi	GBM	Alt + CP	Upper Greenschist	Maybe sinistral
28	648	Epidote-Chlorite-Schist	Chl, Qtz, Epi, Cal	SGR + lim GBM?	-	Upper Greenschist	Dextral

Table 5.2.5: Table of results for samples from the Gander Zone in the Shoal Bay area with inferred metamorphic grade and shear sense. Mineral phase codes: Qtz – Quartz, K-Fsp – K-Feldspar, K-Fsp (ser) – K-Feldspar altered to sericite, Plag – Plagioclase, Mus – Muscovite, Bio – Biotite, Chl – Chlorite, Epi – Epidote, Ox – Oxides, Cal – Calcite.

5.2.6 Locker's Bay

At more than 600m from the Gander-Avalon boundary in Locker's Bay, the exposures of the HBG are dominated by gneisses that have been overprinted by phyllonitic shear zones. The shear zones are highly localised and contain many dextral shear sense indicators, such as dextral shear bands. Within the gneiss samples, the grain sizes are relatively coarse with quartz grain sizes at an average of 0.5mm, feldspars at 0.5-1.5mm and micas at 0.1-1mm. The quartz grains have lobate grain shapes and often contain subgrains and the quartz grains show both pinning effects from mica grains and a weak to moderate CPO under a tint plate. Relict grains of K-feldspar and plagioclase in the gneisses are variably altered to sericite and they often contain myrmekites and show core and mantle textures of very fine (<0.1mm) new grains (see Figure 5.2.12.a). Mica grains in the gneisses mostly define continuous foliation fabrics with a sinistral shear sense and they show strong kinking textures and sweeping extinction patterns (see Figure 5.2.12.a).

In samples that were collected from the phyllonitic shear zones there is a much stronger mylonitic fabric in that the mica grains define discrete foliations, quartz grains occur in compositional bands and the feldspar grains form porphyroclasts. The quartz grains in the mylonitic samples are generally finer than in the gneisses (0.1-0.2mm) and they show irregular to elongate ribbon grain shapes with a moderate CPO. Core and mantle textures on the feldspar grains are rare in the mylonitic samples but mica beards around the porphyroclasts are much more common (see Figure 5.2.12.b). Chlorite occurs in low to moderate proportions in most of the samples with a range of 0-15% and the intergrowth structures between biotite and chlorite show that the alteration of biotite is incomplete. Both epidote and opaque oxide minerals occur in very low proportions (<5%) and both phases associate with the phyllosilicate minerals in thin section. Sinistral senses of shear are indicated in two of the samples (out of 12) using mica fish, oblique foliation and stair-stepping strain shadow structures but the field observations suggests that dextral shear is dominant.

Locker's Bay samples within 600m of the Gander-Avalon boundary are more pervasively mylonitic to phyllonitic and the rocks can be pervasively fractured to fully brecciated in outcrop. In the samples, quartz occurs in compositional bands with grain sizes ranging from 0.1-0.5mm and irregular to amoeboid grain shapes. In crossed polarised light, the quartz shows sweeping to patchy

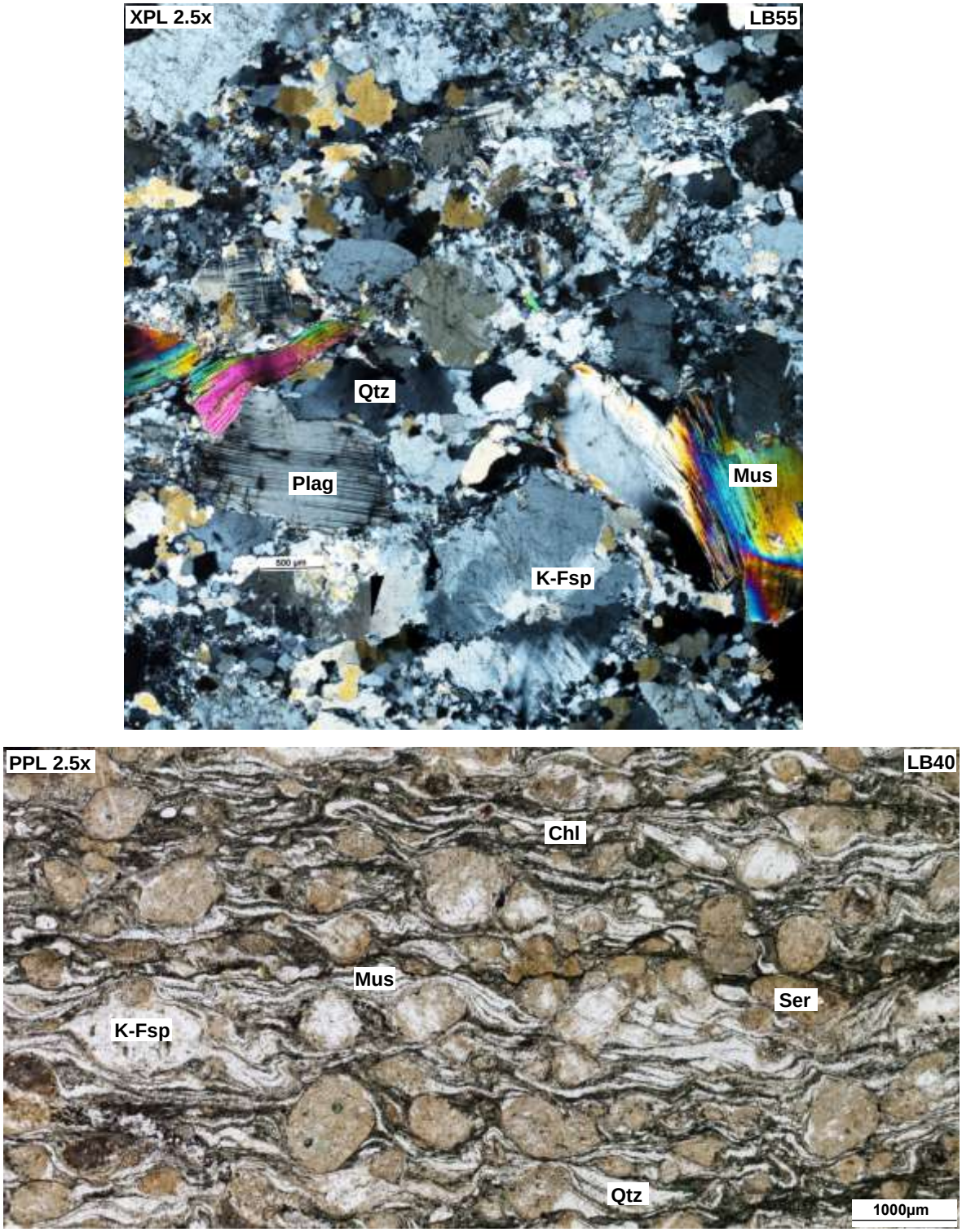

Figure 5.2.12: a) thin section composite photomicrograph of LB55 at 2.5x zoom under crossed polarised light. Several of the Plagioclase and K-Feldspar relict clasts show core and mantle textures of very fine new grains, whereas the muscovite grains have strongly sweeping undulose extinction and the quartz grains have lobate grain boundaries and low intracrystalline deformation. These textures indicate that deformation took place under amphibolite grade conditions. b) thin section composite photomicrograph of LB40 at 2.5x zoom under plane polarised light. The strong, discrete foliation fabric has been folded into complex asymmetrical folds around the highly altered feldspar porphyroclasts. The sense of shear is uncertain due to the presence of both dextral and sinistral shear sense indicators within LB40.

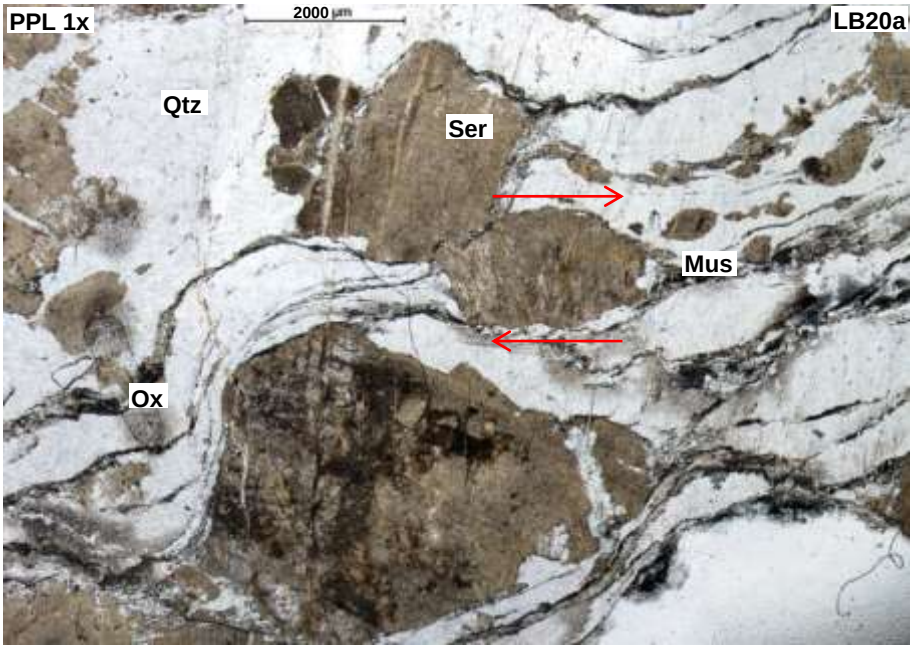

a)

b)

Figure 5.2.13:a) thin section composite photomicrograph of LB20a at 1x zoom under plane polarised light. The feldspar porphyroclasts have been almost entirely altered to sericite mica and opaque oxide minerals in LB20a. Muscovite mica in the discrete foliation fabric and mica beards around the porphyroclasts show a clear dextral sense of shear. b) photo and sketch of LB20a in hand specimen. The mylonitic fabric in this specimen is clearly evident with phyllosilicate-rich foliations separating domains rich in feldspar porphyroclasts.

extinction and the grains often contain elongate subgrains. The feldspar porphyroclasts range in size from 0.4-2mm and the degree of alteration to sericite can be high in the feldspar grains at 20-100%. The typical microstructures in the feldspars include intragranular fractures, sweeping undulose extinction and very rare core and mantle textures. Biotite, chlorite and muscovite define strong discrete foliations and S-C fabrics in the mylonitic samples, in addition to forming mica beards around the feldspar porphyroclasts (see Figure 5.2.13). Chlorite again occurs in moderate proportions in the samples (<15%) in intergrowth textures with biotite. Most of the samples within 600m of the Gander-Avalon boundary display dextral senses of shear that were derived from structures such as stair-stepping strain shadows on the porphyroclasts, S-C fabrics and asymmetric folds. Samples 21 and 20b, however, show sinistral senses of shear that are inferred to relate to more conjugate sinistral shear zones that have been offset by local brittle faults observed in the field to have disrupted the original sequence. Opaque oxide minerals are preferentially located along foliation, shear and fracture planes in the samples.

This brittle overprinting is best represented in the Locker's Bay area by sample LB17, as shown in Figure 5.2.14. This mylonitised quartz vein contains polygonal shaped quartz grains that have straight edges, 120° grain boundary junctions and common tuttle lamellae. These textures are characteristic of recovery and GBAR after peak metamorphism and deformation. This earlier moderate to high temperature fabric is overprinted by dextral asymmetric folds that closely associate with core and mantle textures in the recovered quartz grains (see Figure 5.2.14). The extremely fine (<0.05mm) new quartz grains are indicative of BLG recrystallization, which relates to a sub- to lower-greenschist grade of deformation. As shown in the hand specimen of LB17 (Figure 5.2.14.b), the asymmetrical folds associate with brittle fractures.

In the Locker's Bay Gander Zone, the samples located more than 600m from the Gander-Avalon boundary preserve a high temperature, amphibolite grade deformation phase with a sinistral sense of shear. The textures of GBM recrystallization in quartz and BLG recrystallization in feldspar give an estimated temperature range of 450-500°C. This earlier fabric has been overprinted by a dextral, upper-greenschist to amphibolite boundary grade deformation phase that is recorded extensively in rocks within 600m of the Gander-Avalon boundary and in localised shear zones in rocks that are

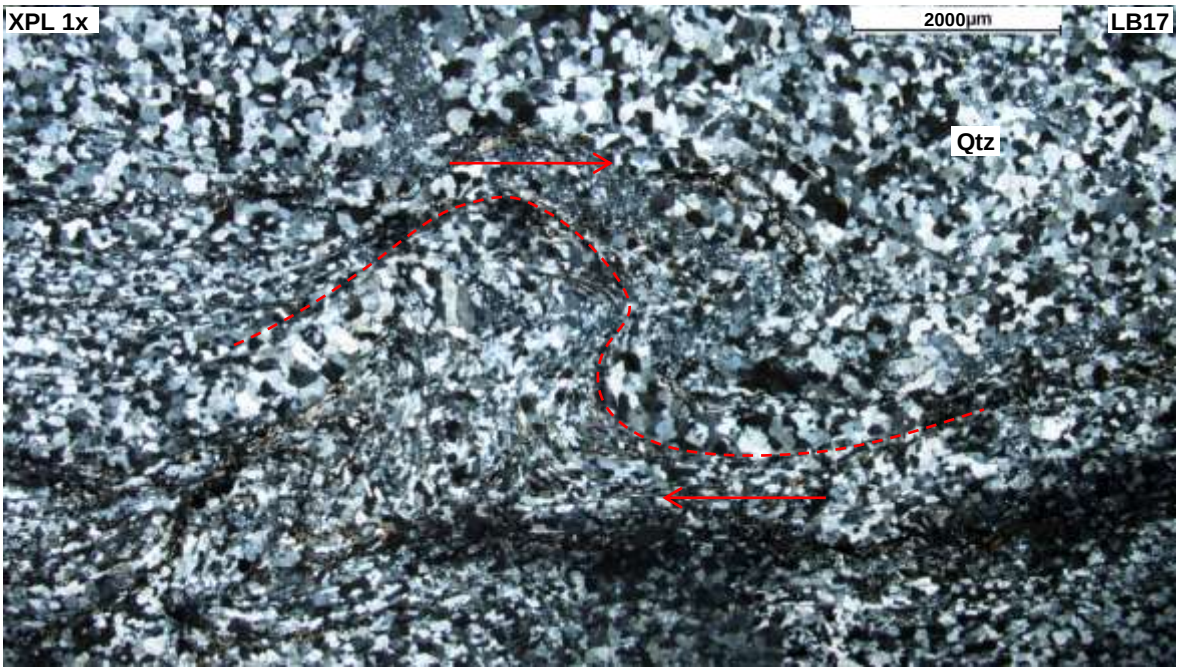

a)

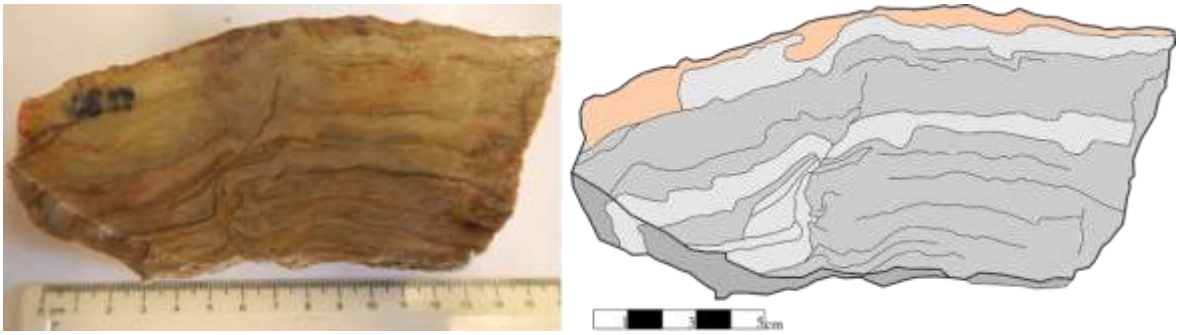

b)

Figure 5.2.14: a) thin section composite photomicrograph of LB17 at 1x zoom under crossed polarised light. The quartz grains in the majority of the section have a texture indicative of recovery including a polygonal shape, fluid inclusions and straight grain boundaries. The dextral asymmetrical fold highlighted in the centre of the photo has overprinted the fabric with relatively low temperature (~300°C) BLG recrystallization. b) photo and sketch of LB17 in hand specimen. The asymmetrical folds in the hand specimen clearly relate to brittle fracturing and overprinting of the earlier ductile fabric.

Sample No.	Distance from Boundary (m)	Rock Type	Mineral Assemblage (descending order of %)	Quartz Fabric	Feldspar Fabric	Metamorphic Grade	Shear Sense
55	1622	Mylonitic Aplogranite	Qtz, K-Fsp (ser), Mus, Plag (ser), Ox, Gar	GBM	BF + CP + BLG + lim DMT	Amphibolite	Sinistral
48	1354	Phyllonite	Qtz, K-Fsp (ser), Bio, Mus, Chl, Plag, Ox	SGR + GBM	BF + CP + lim DMT	Upper Greenschist	Sinistral
47	1343	Gneiss	Qtz, K-Fsp (ser), Bio, Mus, Plag, Chl, Ox	GBM	Alt + CP + BF	Upper Greenschist	Unclear
40	903	Mylonite	Qtz, K-Fsp (ser), Chl, Mus, Epi, Ox	SGR + GBM	CP + BLG + lim DMT	Amphibolite	Unclear
38	862	Mylonitic Granodiorite	K-Fsp (ser), Qtz, Bio, Chl, Plag, Hnb, Epi	GBM	Alt + BF + CP + lim BLG	Upper Greenschist-Amphibolite	Unclear
31	550	Phyllonite	Qtz, Mus, Bio, Chl, K-Fsp (ser), Epi, Ox, Cal	SGR	BF + CP + DMT	Mid-Greenschist	Dextral
29	453	Protomylonitic Granodiorite	K-Fsp (ser), Bio, Qtz, Hnb, Ox, Epi	GBM	BF + CP + BLG + lim SGR	Amphibolite	Unclear
26	359	Phyllonitic Mylonite	Qtz, K-Fsp (ser), Mus, Chl, Plag, Cal, Epi	SGR + lim GBM	BF + CP + lim DMT	Upper Greenschist	Unclear
17	194	Quartz Mylonite	Qtz, Mus, Ox	GBAR	-	Pro: upper greenschist. Retro: sub-lower- greenschist	Dextral
21	181	Phyllonitic Mylonite	Qtz, K-Fsp (ser), Mus, Chl, Epi, Cal	Lim SGR + GBM	BF + CP + BLG + lim DMT	Upper Greenschist – Amphibolite	Sinistral
20b	156	Meta-Gabbro	Mus, Pyx, Plag, Ox, Qtz	CP	Mag + BF	Unclear	Sinistral
20a	156	Mylonite	Qtz, Plag/K-Fsp (ser), Mus, Chl, Ox, Clz, Cal	GBM	Alt + BF + CP + DMT + BLG	Upper Greenschist - Amphibolite	Dextral

Table 5.2.6: Table of results for samples from the Gander Zone in the Locker's Bay area with inferred metamorphic grade and shear sense. Mineral phase codes: Qtz – Quartz, K-Fsp (ser) – K-Feldspar altered to sericite, Plag – Plagioclase, Plag (ser) – Plagioclase altered to sericite, Mus – Muscovite, Bio – Biotite, Chl – Chlorite, Epi – Epidote, Clz – Clinozoisite, Pyx – Pyroxene, Hnb – Hornblende, Gar – Garnet, Ox – Oxides, Cal – Calcite.

further from the boundary. The textures in the samples indicate that quartz experienced SGR and GBM recrystallization and the feldspars primarily deformed through brittle fracture, intracrystalline plasticity and limited BLG recrystallization. As many of the samples contain mica beards and syn-tectonic chlorite overgrowths, it can be inferred that DMT was active during both of these deformation phases. As chlorite is a hydrous phase, it suggests that the operation of DMT was fluid-assisted. The later brittle overprinting recognised in the samples and in the field occurred at lower- to sub-greenschist grade and likely relates to the final stages of cooling in the Gander Zone. A summary of the results of the microstructural analysis for the Gander Zone in Locker's Bay is given in Table 5.2.6.

5.2.7 Frying Pan Island

Only one sample (FP3) from Frying Pan Island was studied. FP3 was collected 50m from the major ENE-WSW trending fault on the island and was located within the footwall. Exposures of the Newport Granite showed pervasive fracturing across multiple scales (mm-cm-m) so that the outcrop was extensively brecciated. Shear fracture surfaces associated with 1-2mm width cataclasite fault rocks. The hand specimen sample FP3 lacks a foliation fabric and is highly fractured from the grain scale (~1mm) to the centimetre-scale (see Figure 5.2.15). Narrow cataclastic bands (1-2mm width) can be recognised in the sample by the very fine grain size and discolouration. The green-grey colour of the sample is evidence of the pervasive alteration of the Newport Granite protolith.

In thin section, FP3 has no overriding foliation or layering fabrics and the grains are randomly orientated. Quartz grains in FP3 occur as either angular, coarse relict grains at up to 10mm in size or pervasively broken, fine grains (<0.1mm) in the matrix. The quartz grains are highly fractured with fracture sizes ranging from <0.1 – 3mm. The relict grains contain deformation lamellae that are defined by elongate subgrains visible in crossed polarised light (see Figure 5.2.16). Feldspar grains in FP3 are pervasively altered to sericite by 50-100% in individual grains. The relict grains of K-feldspar and plagioclase have average grain sizes of 0.5 – 1mm but they are often broken into mosaic grains by sericite-filled fractures (see Figure 5.2.16). Under crossed polarised light, the feldspars have sweeping undulose extinction patterns and the plagioclase grains show distortion

Sample No.	Distance from Boundary (m)	Rock Type	Mineral Assemblage (descending order of %)	Quartz Fabric	Feldspar Fabric	Metamorphic Grade	Shear Sense
3	50	Breccia	Qtz, K-Fsp (ser), Ser, Plag (ser), Chl	BF + CP	BF + CP	Sub-greenschist	Not indicated

Table 5.2.7: Table of results for samples from the Gander Zone in the Frying Pan Island area with inferred metamorphic grade and shear sense. Mineral phase codes: Qtz – Quartz, K-Fsp (ser) – K-Feldspar altered to sericite, Plag (ser) – Plagioclase altered to sericite, Chl – Chlorite, Ser – Sericite.

Figure 5.2.15: photo and sketch of FP3 in hand specimen.

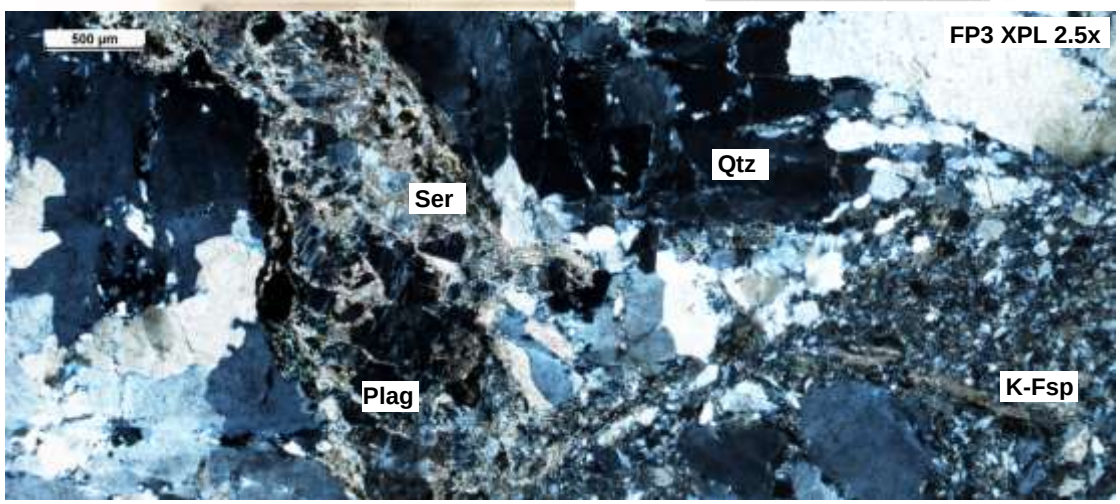

Figure 5.2.16: thin section composite photomicrograph of FP3 at 2.5x zoom under crossed polarised light. Pervasive fracturing of the feldspar and quartz grains has occurred to produce mosaic relict grains and very fine broken grains in the matrix. Extensive alteration of the feldspars to sericite suggests that H_2O-rich fluid was present during deformation.

and kinking of the original twins. Chlorite is generally located at relict grain boundaries and is subordinate in proportion to sericite, which constitutes 25% of FP3. The sericite grains are very fine grained at <0.1mm and they dominate the rock matrix.

FP3 is inferred to be a fault breccia based on the relative proportions of clasts to matrix (<30% matrix). Deformation of the sample was dominated by brittle fracturing at sub-greenschist grade conditions (<300°C), although the presence of subgrains in quartz and the undulose extinction in the feldspars indicates that deformation was also accommodated by intracrystalline plasticity. The extensive alteration of the feldspars in the Newport Granite protolith is evidence that an H_2O-rich fluid was present within the fault and fracture network.

5.2.8 Summary of Gander Zone Microstructural Analysis

The Gander Zone thin section samples record textures from three main deformation phases. The field observations suggest that the sinistral Early Ductile structures correspond to a sinistral, amphibolite grade event. This early amphibolite texture is best preserved in samples located more than 1km from the Gander-Avalon boundary. Deformation at the grain-scale was accommodated in the early, amphibolite grade event by dynamic recrystallization and DMT mechanisms.

The Late Ductile field structures correlate with the dextral, mid- to upper-greenschist grade deformation phase that is recorded in many of the samples of the HBG, DFG and LBG within 1km of the tectonic boundary. Deformation at the grain-scale during this later, lower temperature phase was accommodated by dynamic recrystallization, grain size reduction, brittle fracturing, DMT and the formation of localised shear zones and fabrics.

The Late Brittle deformation structures correlate to the dextral sub-greenschist grade textures observed from samples across the Gander Zone. Deformation was accommodated during the brittle phase by brittle fracturing, pressure solution, limited dynamic recrystallization and folding. The widespread evidence of the action of DMT, hydration alteration, hydrothermal mineralisation and pressure solution indicates that fluids were present in the DFSZ during at least a portion of all three deformation phases.

6 Chapter Six: Avalon Zone Results

6.1 Avalon Zone Field Relationships

In a mirror of the Gander Zone, the lithologies in the Avalon Zone show a progressive increase in strain intensity and retrogressive alteration to the west, towards the Gander-Avalon boundary.

6.1.1 Maccles Lake

In the Avalon Zone of the Maccles Lake area, the LCG contacts the N-S trending Gander-Avalon boundary. As the MSG outcrops 3km east of the boundary, it lies outside of the Maccles Lake study area. The Terra Nova Granite to the southeast of Maccles Lake is the only major intrusion in the area but minor intrusions including m-scale basaltic dykes and cm-scale granitic veins were observed in the sampled exposures. The foliations in the LCG show a NNE-SSW trend and are steeply dipping to both the east and west (see Figure 6.1.1). The stretching mineral lineations on the foliation planes are moderately steep and dip to the north (see Figure 6.1.2). A cleavage fabric was recognised in several locations that has a steep dip and the cleavage planes trend NNE-SSW (see Figure 6.1.3).

Outcrops of the LCG comprise of felsic crystal tuffs, agglomerates and phyllonitic tuffs in the Maccles Lake area. The outcrops that were studied in the Avalon Zone were all located within 500m of the Gander-Avalon boundary as a result of limited exposure. The structures that were observed may therefore only represent a part of the DFSZ. In the sampled outcrops of LCG, the foliation and mineral lineation fabric was generally well-developed and many of the fault rocks had accommodated a high degree of strain. Ductile structures within the fault rocks include dextral σ-porphyroclasts and dextral wrapping of epidote-rich pods and volcanic clasts. The degree of alteration is variable in the LCG exposures so that several outcrops are formed of epidote-rich, high strain phyllonites whereas other outcrops preserve the original volcanic clasts and mineral phases. Exposures in close proximity to the Gander-Avalon boundary contain prominent fracture sets, brittle shear bands and oblique dextral-opening mineralised veins to the degree that many of the lithologies have become extensively brecciated.

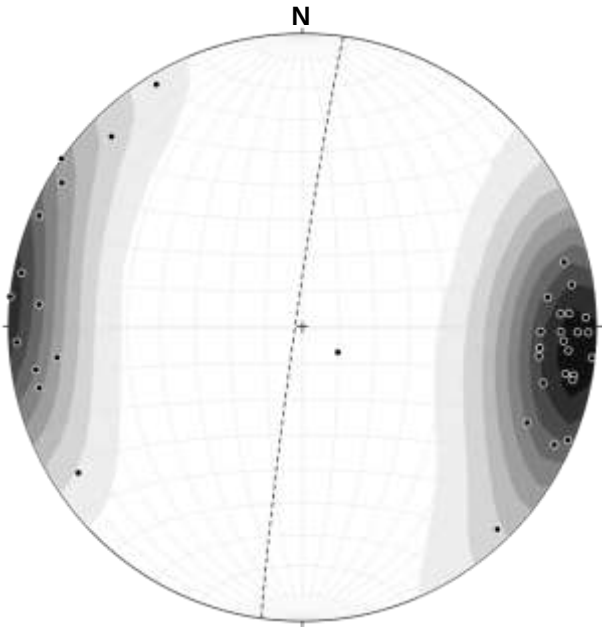

Figure 6.1.1: Stereonet representing the orientations of poles to foliation planes in the Avalon Zone of Maccles Lake (LCG lithology). Dashed line – representative foliation.

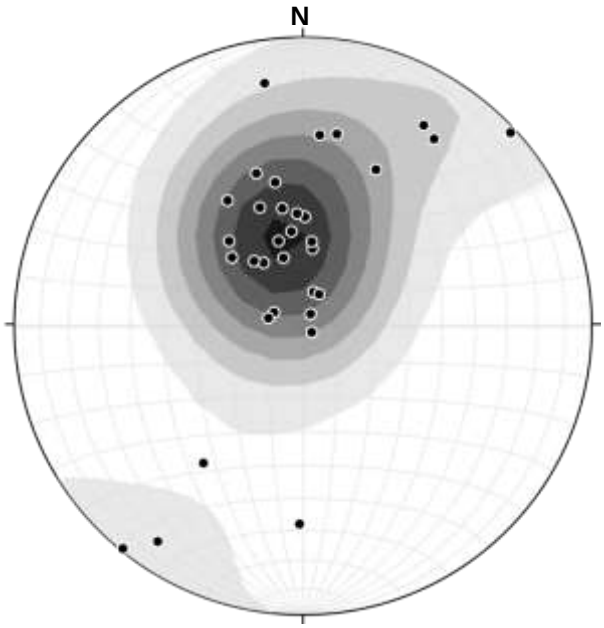

Figure 6.1.2: Stereonet representing the orientations of stretching mineral lineations in the Avalon Zone of Maccles Lake (LCG lithology).

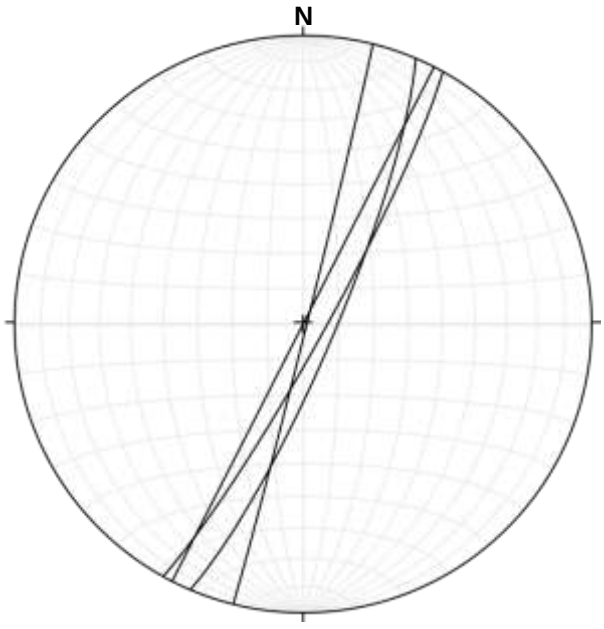

Figure 6.1.3: Stereonet representing the orientations of cleavage planes in the Avalon Zone of Maccles Lake (LCG lithology).

6.1.2 Bay du Nord

As in the Gander Zone of the Bay du Nord area, exposure in the Avalon Zone occurs mostly in river beds, bare hilltops and lake shorelines. All of the twelve samples from the Avalon Zone in Bay du Nord are located within 900m of the Gander-Avalon boundary. The dominant rock type along the brittle Dover Fault is the LCG as well as several unnamed granitic plutons that trend roughly N-S that occur close to, or terminate at, the brittle boundary. Within the LCG exposures sampled, the foliations have a NNE-SSW trend and are steeply dipping to both the east and west (see Figure 6.1.4). The orientation of the stretching mineral lineations is variable with shallow to steep dips to the NNE or SSW (see Figure 6.1.5).

In the LCG, a variable intensity of folding was observed in the field with centimetre to millimetre scale, open to tight, intrafolial, mm-cm-scale folds that fold the mylonitic foliation. The intensity of folding generally increases to the west of the Avalon Zone towards the tectonic boundary. Exposures of the LCG are dominantly phyllonitic within 1km of the brittle Dover Fault but they also comprise platy acidic and mafic tuffs and pink mylonitic tuffs. The outcrops contain dextral ductile structures such as shear bands and σ-porphyroclasts. At locality 15 (see Figure 6.1.6), the tuffs in the LCG show reactivation by Late Brittle dextral shear bands and mm-cm-scale folds. There is also evidence of pressure solution at locality 15 as localised dextral crenulation cleavage was observed in the LCG tuffs.

The granitic intrusions in the Avalon Zone follow the same pattern as the LCG of increasing mylonitisation and retrogression towards the Gander-Avalon boundary. All of the Avalonian granites in close proximity to the Dover Fault display solid-state deformation fabrics and the plutons trend N-S, which is subparallel to the banding in the LCG. This indicates that these intrusions were emplaced whilst the Gander-Avalon boundary was still active. Within the granite outcrops, the strain is highly variable between massive low strain zones and narrow (m-scale) phyllonitic or platy shear zones. A dextral sense of shear was derived from S-C solid state fabrics and σ-porphyroclasts. The Avalonian-type granites also contain Late Brittle structures that overprint the ductile structures such as cm-scale folds, fractures and faults. At locality 3, a set of mylonitic quartz veins that contain potentially sinistral shear bands and σ-porphyroclasts may

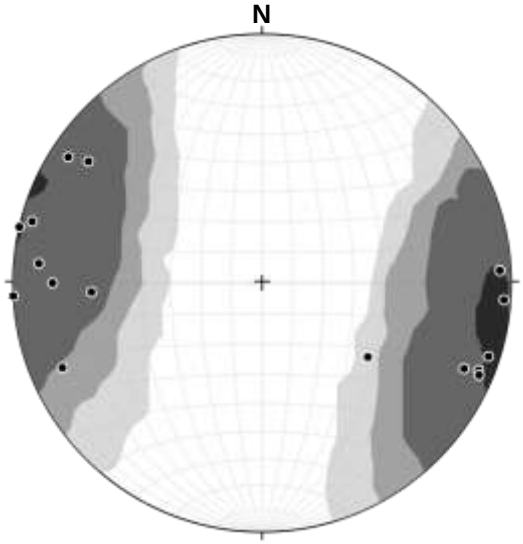

Figure 6.1.4: Stereonet representing the orientations of poles to foliation planes in the Avalon Zone of Bay du Nord (LCG and Avalon Granite lithology).

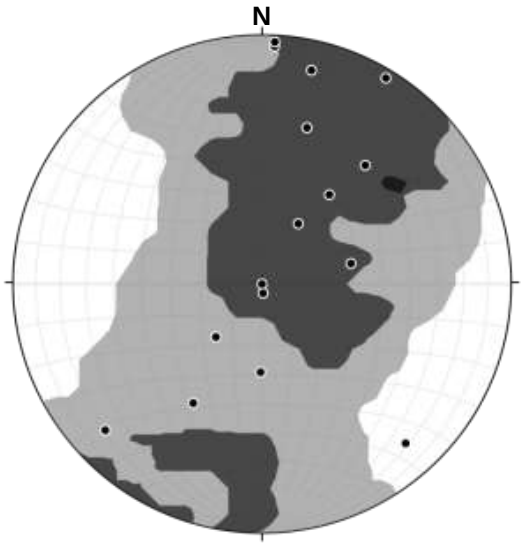

Figure 6.1.5: Stereonet representing the orientations of stretching mineral lineations in the Avalon Zone of Bay du Nord (LCG and Avalon Granite lithology).

Figure 6.1.6: Field photograph of platy mafic and acidic tuffs in the LCG at locality 15 in the Avalon Zone of Bay du Nord. Hammer for scale. Outcrop contains a mylonitic fabric that has been reactivated in dextral shear bands (marked in red).

represent an earlier brittle structure that was then reactivated by late stage ductile deformation.

6.1.3 Freshwater Bay

The 16 samples in the Avalon Zone around Freshwater Bay were collected from coastal exposures at up to almost 5km from the Dover Fault, which represents the widest region of the Avalon Zone sampled in this study. Moving east from where the LCG contacts the DFG across the Dover Fault, the LCG passes into the MSG across a northeast-trending faulted contact. The foliation planes that are predominately within the LCG exposures are steep to moderately dipping and trend NE-SW (see Figure 6.1.7). The mineral lineations on the foliation planes generally plunge to the NE at shallow to moderate angles (see Figure 6.1.8). The cleavage planes were observed in all of the lithologies in the Avalon Zone in Freshwater Bay and the cleavage has a NE-SW trend and steep to moderate dips (see Figure 6.1.9).

In a contrast with the Gander Zone, the Avalon Zone in Freshwater Bay does not have as broad a region of deformation associated with the Gander-Avalon boundary. Beyond a distance of 1-1.5km, the rocks of the MSG record very little strain and contain only rare deformation structures. The structures that do occur in the MSG include a weak to moderate, upright, slatey cleavage and an occasionally present steeply-plunging lineation. Gentle folding with NE or SW plunging axes also occurs in the MSG at a kilometre-scale along with very rare minor (m-scale) folds. Exposures of the MSG from the shores of the Cat Gut channel towards Content Reach preserve the original sedimentary bedding structures including bedding (see Figure 6.1.10), cross bedding and soft sediment sedimentation.

As with the Gander Group-HBG contact in the Gander Zone, there is a significant increase in strain intensity towards the Dover Fault across the contact between the MSG and LCG. Across the faulted contact, the cleavage intensifies and a variably steep to shallow south-west plunging lineation becomes well developed on cleavage plane surfaces (see Figure 6.1.8). In addition, minor folding becomes more common in the lower LCG so that two phases of folding can be identified. The Early Ductile fold set (see Figure 6.1.12) are overprinted by the Late Ductile fold set (see Figure 6.1.11) that is curvilinear around the lineation. Both fold sets in the LCG are tighter than the single fold set in the MSG.

Within the lower LCG, at >500-600m from the brittle Dover Fault, the minor Early Ductile folds seen lie parallel to the mineral lineation and the overprinting Late Ductile folds are still relatively rare. The Early Ductile tight to isoclinal fold structures fold the original compositional layering in the LCG lithologies but the folds are in turn overprinted by all other fabrics. A northwest-up, sinistral sense of shear is indicated by the shear bands and asymmetric wrapping of volcanic clasts in the lower LCG.

In close proximity to the Gander-Avalon boundary (<500m), intense retrogressive alteration has produced a sequence of intensely cleaved, green-grey phyllonites from the LCG volcanics. The LCG contains strong lithological banding of mafic and silicic layers, a strong cleavage fabric and isoclinal folding. The Late Ductile overprinting fold set becomes more common within the phyllonites and refolds the earlier mineral lineation. Many lithologies also display a steep, north-northeast trending slatey cleavage that is parallel to the lithological banding in the volcanics. A dextral shear sense is indicated within the LCG phyllonites by the vergence in the minor fold sets and by the common S-C fabrics.

Similarly to the Gander Zone, brittle deformation overprints all other structures and lithologies in the Avalon Zone. Brittle faulting mostly associates with the Dover Fault and with lithological contacts, such as the boundary between the MSG and LCG. Many of the faults have steep strike-slip orientations, trend northeast and indicate dextral shear senses as shown by marker offset. As in the Gander Zone, the minor faults are commonly associated with kink and box folds, brittle fracturing and calcite and quartz veining (see Figure 6.1.12). At the tectonic boundary, brittle faults and dilatational vein networks show a predominantly dextral sense of shear.

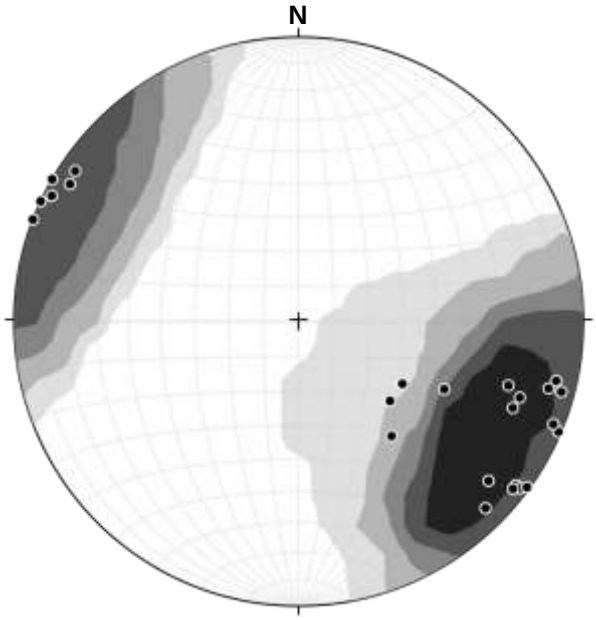

Figure 6.1.7: Stereonet representing the orientations of poles to foliation planes in the Avalon Zone of Freshwater Bay (LCG and MSG lithologies).

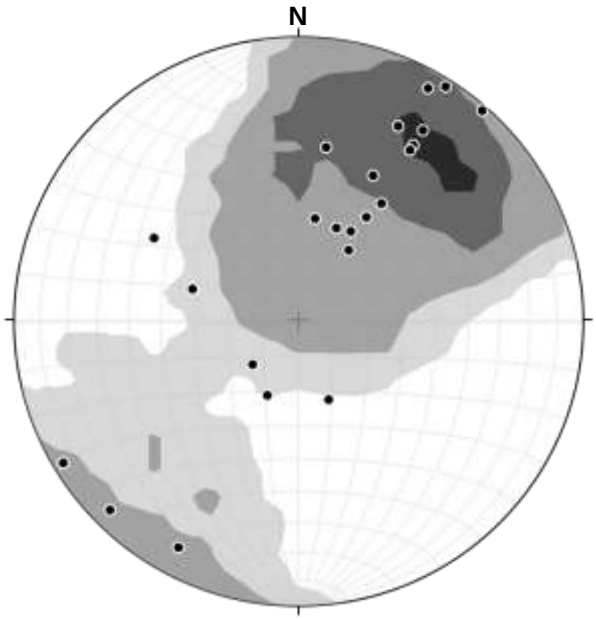

Figure 6.1.8: Stereonet representing the orientations of stretching mineral lineations in the Avalon Zone of Freshwater Bay (LCG and MSG lithologies).

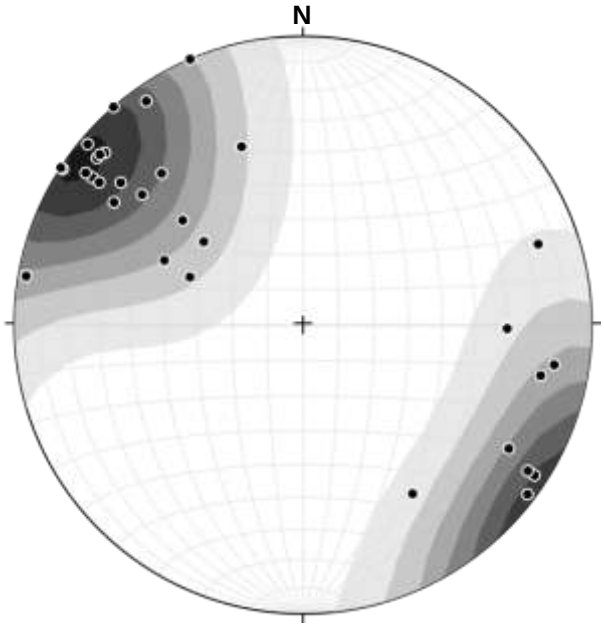

Figure 6.1.9: Stereonet representing the orientations of poles to cleavage planes in the Avalon Zone of Freshwater Bay (LCG and MSG lithologies).

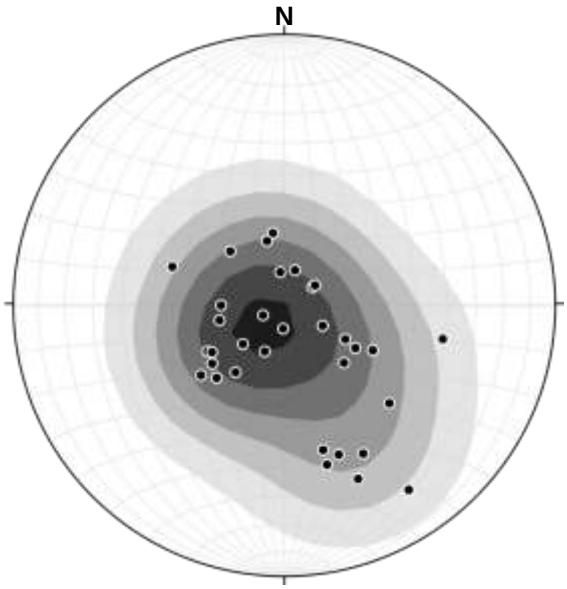

Figure 6.1.10: Stereonet representing the orientations of poles to bedding planes in the Avalon Zone of Freshwater Bay (MSG lithology). The bedding planes are generally shallowly dipping to the NW or SE.

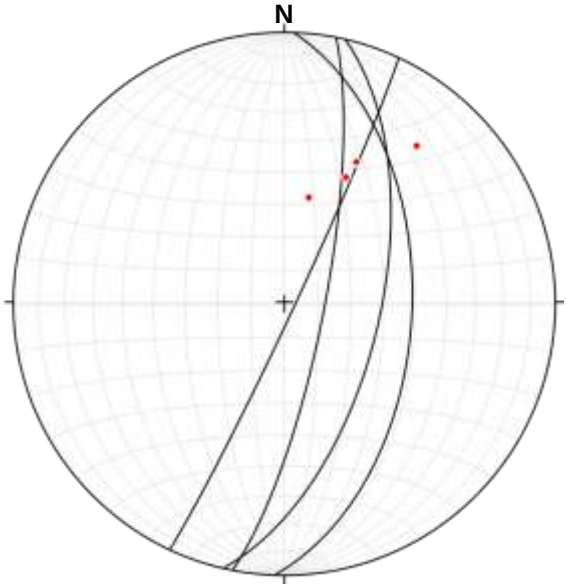

Figure 6.1.11: Stereonet representing the orientations of Late Ductile Folds in the Avalon Zone of Freshwater Bay (LCG lithology). Black lines – axial planes, Red points – fold vergence.

Figure 6.1.12: field photograph of mylonitic acidic and mafic tuffs in the LCG at locality 31 in Freshwater Bay. The foliation and tight Early Ductile cm-scale folds are disrupted by Late Brittle shear fractures filled with calcite

6.1.4 Hare Bay

In the Hare Bay area, the 11 Avalon Zone samples were collected from coastline exposures around the headland to the south of the town of Hare Bay. The majority of the headland is formed of the LCG with a narrow band of the MSG that outcrops along the eastern shore. Multiple brittle faults with associated fracture damage zones were identified in the Hare Bay Avalon Zone in both the LCG and MSG. The foliation planes in the LCG and MSG have a NE-SW trend and dip steeply to the NW or SE (see Figure 6.1.13). In the Hare Bay area, the mineral lineation within the LCG can be seen to rotate anticlockwise towards a shallower plunge with increasing proximity to the Dover Fault (see Figure 6.1.14). This indicates a clear overprint of dextral shear on pre-existing sinistral shear textures. The cleavage planes in both lithologies are steeply dipping and have a NE-SW trend (see Figure 6.1.15).

The MSG exposures are located over 1.5km from the Gander-Avalon boundary and they generally preserve original sedimentary structures such as bedding planes (see Figure 6.1.16), cross laminations and normal or reverse grading of grain size. Within 1.5km of the Gander-Avalon boundary, the LCG shows increasing strain intensity and alteration towards the boundary. Early Ductile, tight to isoclinal, upright centimetre-scale folds are present in the sampled exposures of both the LCG and MSG. Early Ductile folds can be distinguished from later folds by their foliation-parallel axial planes (see Figure 6.1.17). A sinistral sense of shear for the Early Ductile structures was inferred from the shear bands present. Late Ductile irregular folds in the MSG appear to be focused on quartz vein structures. The Late Ductile folds were observed to fold the main foliation fabric and a shear fibre fabric and they occur on the cm-scale with highly variable plunges (see Figure 6.1.18). A centimetre-spaced crenulation cleavage was also observed in the MSG exposures that overprints the Early Ductile structures. A dextral sense of shear is inferred for the Late Ductile structures using σ-porphyroclasts of epidote and dextral shear bands in the LCG. The Late Brittle structures in both the LCG and MSG indicate a dominant dextral shear sense and the structures include brittle faults, open to tight folds and unfolded mineral veins.

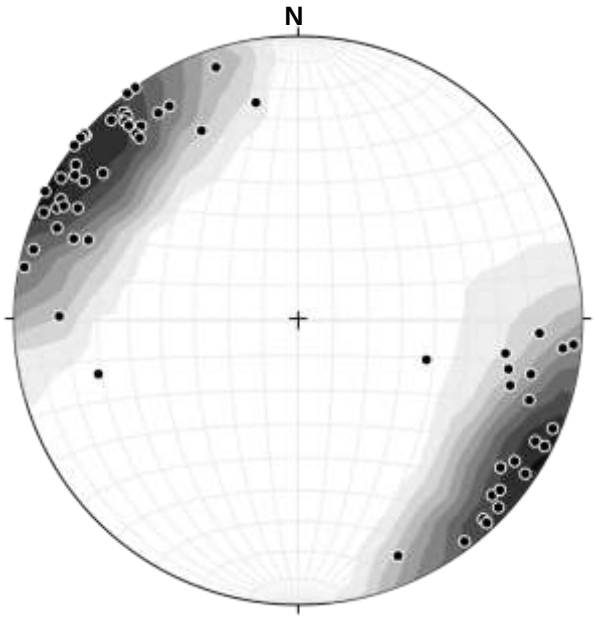

Figure 6.1.13: Stereonet representing the poles to foliation planes in the Avalon Zone of Hare Bay (LCG and MSG lithologies).

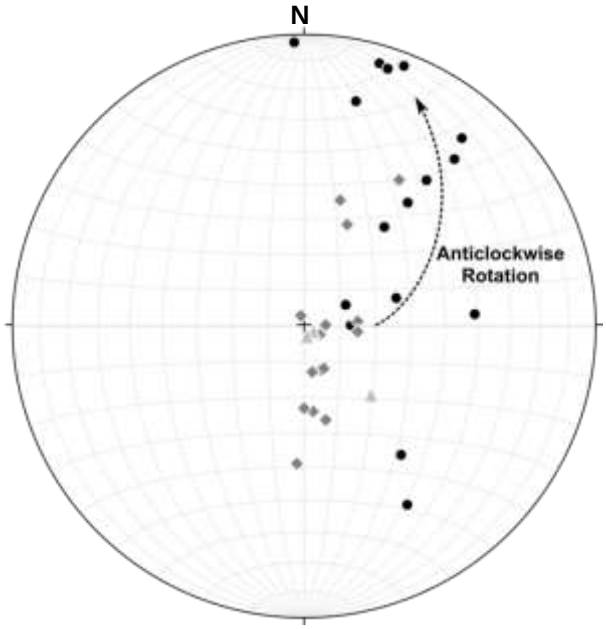

Figure 6.1.14: Stereonet representing the orientations of stretching mineral lineations in the Avalon Zone of Hare Bay (LCG and MSG lithologies). The MSG lineations (light grey triangles) are steep but the LCG lineations (grey diamonds >500m from Gander Avalon boundary; black circles <500m) show reactivation through an anticlockwise rotation.

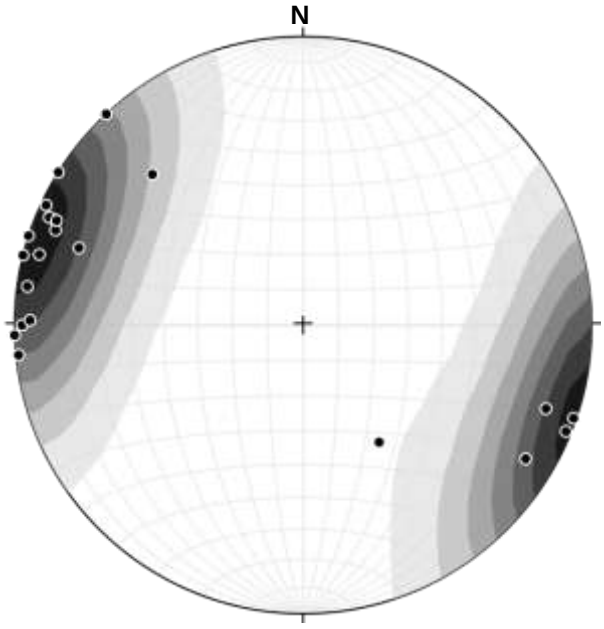

Figure 6.1.15: Stereonet representing the orientations of poles to cleavage planes in the Avalon Zone of Hare Bay (LCG and MSG lithologies).

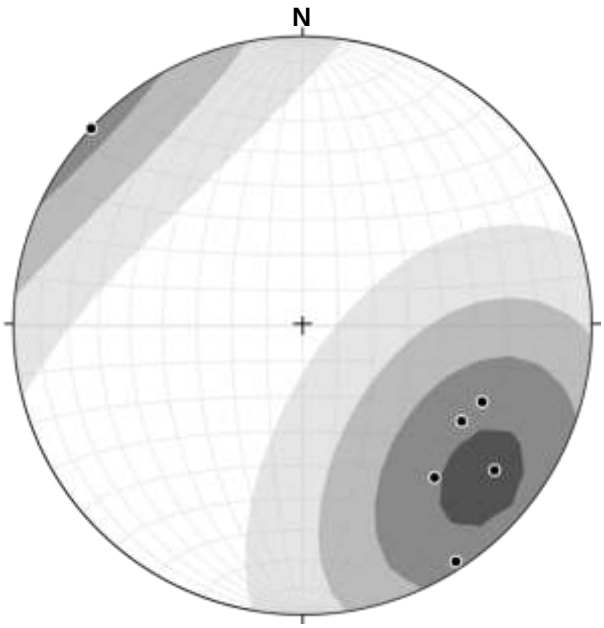

Figure 6.1.16: Stereonet representing the orientations of poles to bedding planes in the Avalon Zone of Hare Bay (MSG lithology). The bedding planes show moderate dip angles and trend NE-SW.

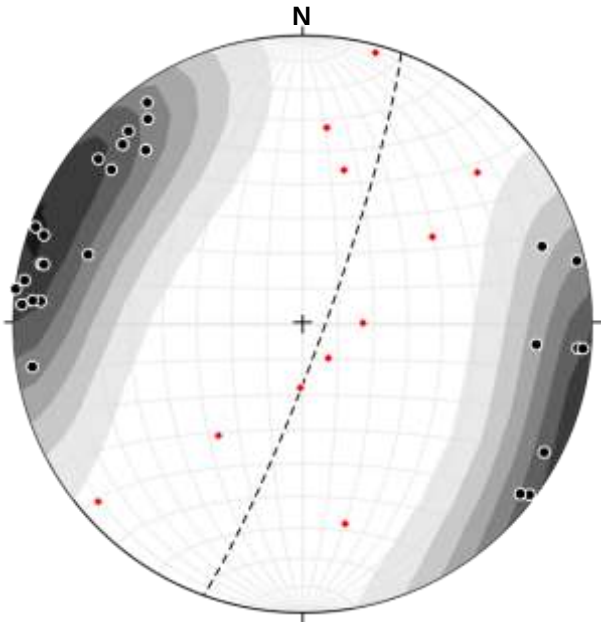

Figure 6.1.17: Stereonet representing the orientations of Early Ductile folds in the Avalon Zone of Hare Bay (LCG lithology). Black – poles to axial planes, Red – fold vergence, dashed line – representative axial plane.

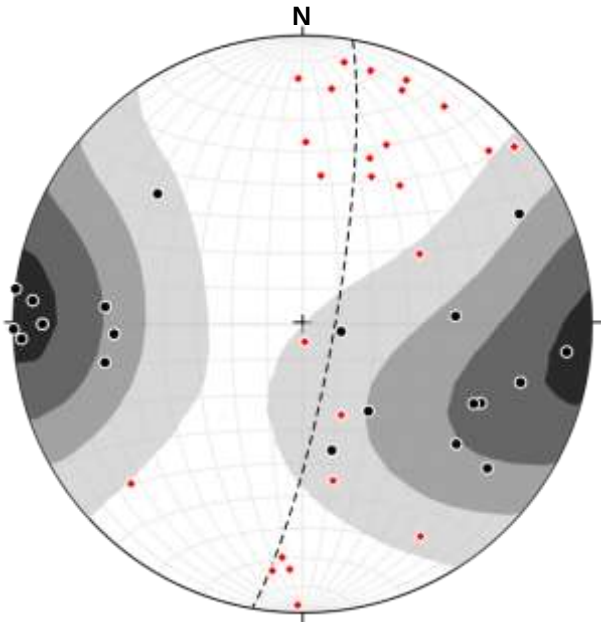

Figure 6.1.18: Stereonet representing the orientations of Late Ductile folds in the Avalon Zone of Hare Bay (LCG lithology) Black – poles to axial planes, Red – fold vergence, dashed line – representative axial plane.

6.1.5 Shoal Bay

As in the Gander Zone, the Avalon Zone contains excellent exposures and examples of Late Brittle structures and faults. Only the LCG was observed in outcrop around the shoreline of Shoal Bay and the lithologies exposed included platy to phyllonitic mylonites and acidic to mafic tuffs. The foliations in the LCG have a NE-SW trend and dip steeply to the NW or SE (see Figure 6.1.19). The mineral lineations in the LCG are consistently steeply dipping to the north (see Figure 6.1.20).

Early Ductile structures are relatively rare when observed in outcrop in the Shoal Bay area. The only Early Ductile structures that were recognised were centimetre-scale isoclinal early folds that had axial planes that were parallel to the mineral lineation and the sinistral wrapping of the mylonitic fabric around rigid clasts in the LCG (see Figure 6.1.21). Late Ductile structures are most prevalent at localities in close proximity to the Gander-Avalon boundary in Shoal Bay. At the boundary itself at locality 37, a series of quartz veins were seen to be mylonitised so that they represent an early phase of brittle deformation that has been overprinted by ductile deformation.

Late Brittle structures, such as folds, kinks and faults, are common throughout the exposures sampled in Shoal Bay. A dextral sense of shear for the Late Brittle structures was inferred using the offset of markers along the brittle faults, as well as the vergence of folds, crenulation cleavage and shear bands. As there are multiple generations of veins, the Late Brittle structures are recognised by their overprinting relationships with all other structures and the Late Brittle veins have altered the mylonites that they cross cut. Kink bands occur on centimetre to metre-scales and they disrupt the earlier foliation fabrics. Late Brittle folds have open to tight forms with a dominant dextrally verging fold set and a subordinate sinistral fold set.

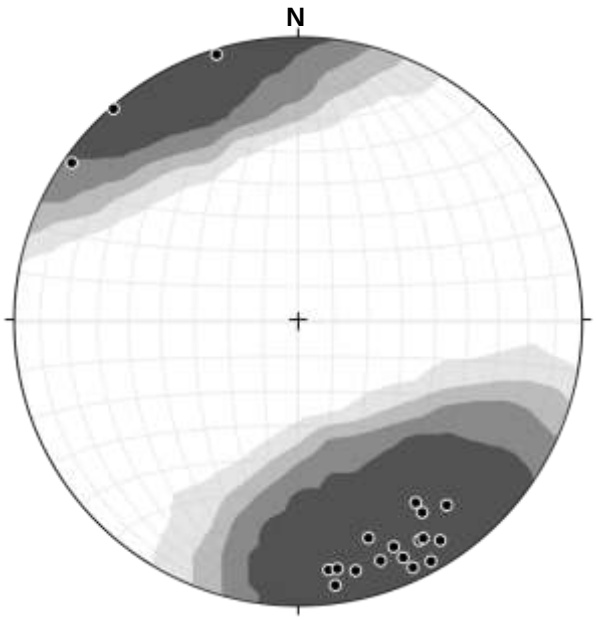

Figure 6.1.19: Stereonet representing the orientations of poles to foliation planes in the Avalon Zone of Shoal Bay (LCG and MSG lithologies).

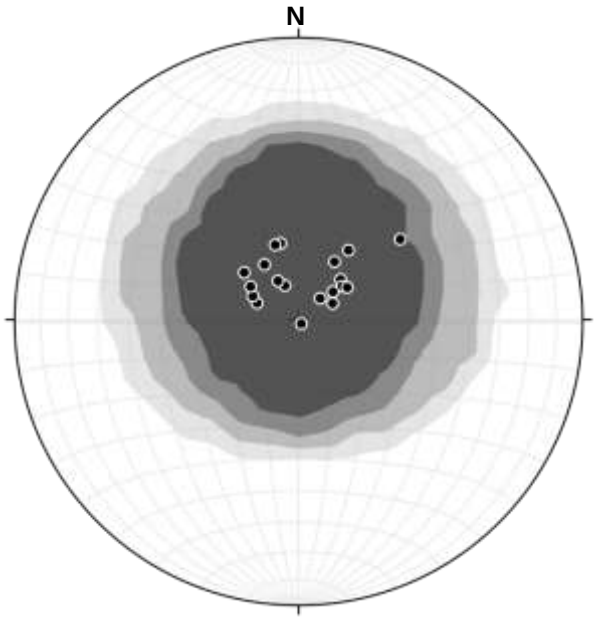

Figure 6.1.20: Stereonet representing the orientations of stretching mineral lineations in the Avalon Zone of Shoal Bay (LCG and MSG lithologies).

Figure 6.1.21: field photograph of sinistral wrapping around a rigid pod in a LCG mylonite at locality 37 in Shoal Bay.

6.1.6 Locker's Bay

The extent of the Avalon Zone in the Locker's Bay study area is very limited so that only 15 localities were visited and 2 samples were collected. The section is highly disrupted by Late Brittle faulting so that very few Early Ductile or Late Ductile structures could be reliably identified other than the mylonitic to phyllonitic fabric. The foliation planes in the LCG in Locker's Bay have a NE-SW to ENE-WSW trend and dip steeply to the SSE or NW (see Figure 6.1.22.a). As in Shoal Bay, the mineral lineations show a rotation from steep to shallow plunges with increasing proximity to the Gander-Avalon boundary (see Figure 6.1.22.b). In outcrops in contact with the boundary, this reactivation of the mineral lineation has brought it parallel to the Gander-Avalon boundary. The Late Brittle faults show a dextral sense of shear from offset of markers and the orientations of subordinate fracture networks. Other Late Brittle structures include centimetre-scale open folds, millimetre to centimetre-scale kink structures and carbonate or quartz veins. In the exposures sampled in close proximity to the brittle Dover Fault, the rocks are extensively fractured and are comprised of proto-breccias and breccias.

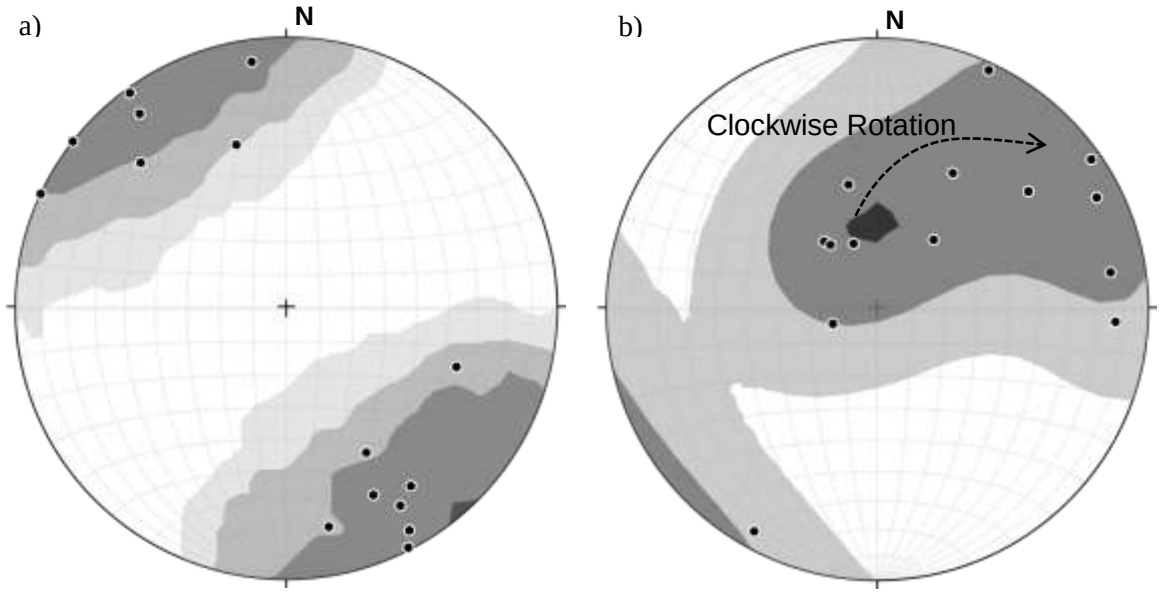

Figure 6.1.22: a) Stereonet representing the orientations of poles to foliation planes in the Avalon Zone of Locker's Bay (LCG lithology). b) Stereonet representing the orientations of stretching mineral lineations in the Avalon Zone of Locker's Bay (LCG lithology).

6.1.7 Summary of Avalon Zone Field Observations

As in the Gander Zone, the field observations in the Avalon Zone identified three main deformation phases along the Gander-Avalon boundary. In a contrast with the Gander Zone, the earliest Avalon Zone structures result from a moderate to low temperature deformation phase, the effects of which extend up to 2km from the boundary. The Early Ductile structures do have a sinistral SE to the top sense of shear similar to that in the Gander Zone but the lower temperatures suggest that the exposed tectonic terranes may have been at different tectonic levels.

The earlier sinistral deformation phase is overprinted by a moderate temperature, dextral deformation phase that is recorded in exposures within 1km of the Gander-Avalon boundary. Highly localised phyllonitic shear zones contain Late Ductile structures such as curvilinear folds, dextral shear bands and mylonitised quartz veins. Reactivation of the earlier sinistral fabric can be recognised by the rotation of the mineral lineation from steep to shallow plunges that run parallel to the brittle-ductile Dover Fault.

The latest deformation phase is represented by the Late Brittle structures of faults, brittle folds and fracture networks that occur in all of the study areas. As in the Gander Zone, the damage from these brittle structures is highly localised into fault zones that often reactivate pre-existing shear zones. The regional-scale faults that cross cut the Gander-Avalon boundary have dextral offsets and the conjugate sets of dextral and sinistral faults recognised in the Gander Zone are also present in the Avalon Zone.

6.2 Avalon Zone Microstructural Analysis

The high angles and rotation of the mineral lineations in the Avalon Zone samples complicates the interpretation of shear sense from microstructures in the thin sections. Hence, the shear senses have been inferred with respect to the orientation of the hand specimens and mineral lineations, which are included in the summary results tables for clarity.

6.2.1 Maccles Lake

The only sample from the Avalon Zone in the Maccles Lake area, ML110, was collected from an island within Maccles Lake. The brittle Dover Fault trends N-S through the island and separates phyllonitic HBG to the west from Love Cove Group (LCG) phyllonites in the east. In the sample ML110, the quartz grains in microlithons between the discrete foliation domains are extremely fine grained at <0.05mm. Under a high power of magnification, the quartz grains can be seen to have irregular shapes, sweeping undulose extinction and contain elongate subgrains. A moderate CPO in the quartz grains can be observed using a sensitive tint plate. The mica grains in the discrete foliation domain are also fine grained at 0.1mm grain size and the mineralogy includes a high proportion of chlorite (~35%). Open, asymmetric folds of the foliation fabric indicate a dextral sense of shear. As shown in Figure 6.2.1, the sample ML110 records the same brittle overprinting fabric as observed in the field. Calcite veins that dextrally offset the foliation fabric are common throughout the sample and cross cut the fabric at high angles (70-90° clockwise).

The textures preserved in the quartz and mica grains in ML110 indicate a mid-greenschist grade during deformation with a dextral sense of shear. Recrystallisation of the quartz grains is inferred to have been dominated by SGR as shown by the irregular grain shapes, strong intracrystalline deformation and moderate CPO. ML110 is classified as a phyllonite due to the high proportion of hydrous chlorite, epidote and the strong mylonitic fabric. The brittle overprinting deformation phase is assigned a sub-greenschist grade of deformation with a dextral shear sense. As most of the brittle structures have experienced calcite mineralisation, it is suggested that the brittle Dover Fault may have acted as a conduit for fluids rather than a barrier for at least part of its active life span. As there are currently no dates available for the calcite veins, only a relative age can be determined for these brittle structures that form the latest observed deformation phase.

Sample No.	Distance from Boundary (m)	Rock Type	Mineral Assemblage (descending order of %)	Quartz Fabric	Feldspar Fabric	Metamorphic Grade	Shear Sense	Mineral Lineation
110	26	Phyllonite	Qtz, Chl, Cal, Mus, Epi	SGR	-	Mid-Greenschist	Dextral	16-351

Table 6.2.1: Table of results for samples from the Avalon Zone in the Maccles Lake area with inferred metamorphic grade and shear sense. Mineral phase codes: Qtz – Quartz, K-Fsp (ser) – K-Feldspar altered to sericite, Mus – Muscovite, Chl – Chlorite, Epi – Epidote, Cal – Calcite.

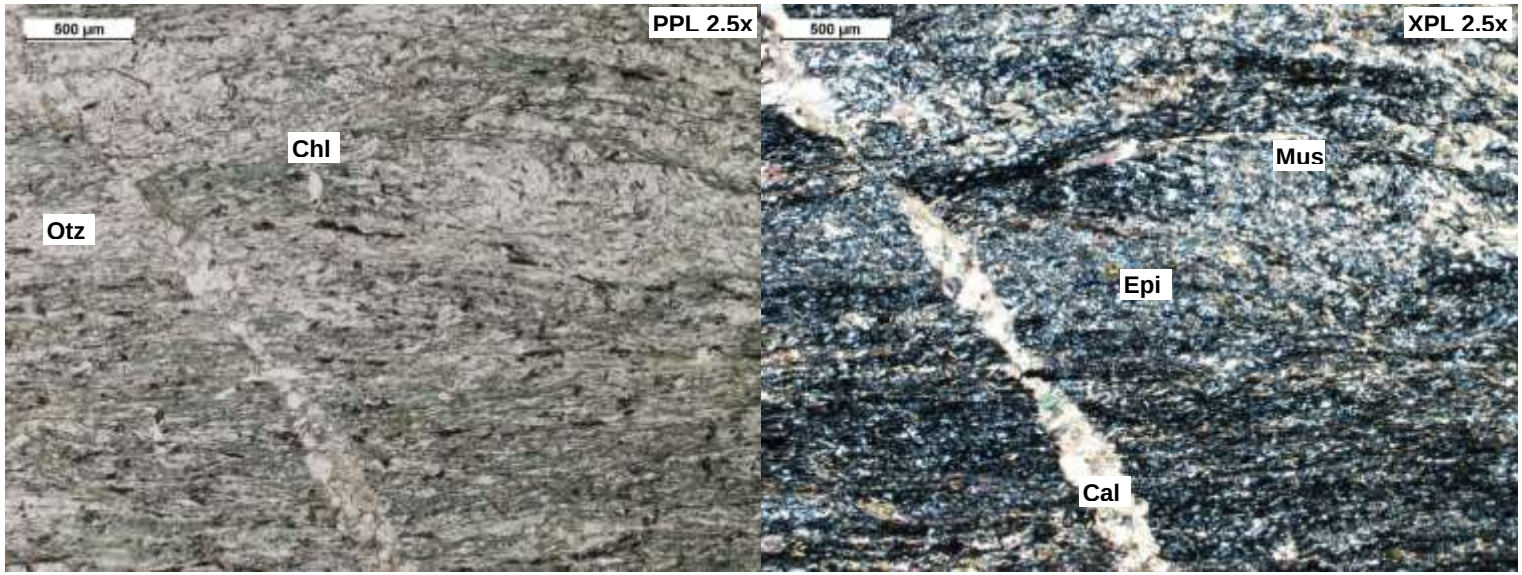

a) *b)*

Figure 6.2.1: thin section photomicrographs of ML110 at 2.5x zoom under (a) plane polarised and (b) cross polarised light. ML110 is very fine grained with a strong foliation fabric defined by the alignment of chlorite and muscovite mica grains. The calcite vein to the left of the photos cross cuts the ductile foliation fabric and contains no evidence of ductile deformation of the calcite grains.

6.2.2 Bay du Nord

In the Bay du Nord LCG samples, the phyllosilicate minerals form strongly defined discrete foliations and S-C fabrics with quartz and feldspar-rich compositional bands or microlithons (see Figure 6.2.2.b). The porphyroclasts in the sampled LCG include partially altered feldspars, highly altered hornblende clasts and epidote porphyroblasts. Quartz grains in the LCG are very fine grained at <0.05-0.1mm and form elongate to ribbon grains that have undergone pervasive subgrain development. The grain boundaries of quartz grains range in shape from irregular to weakly lobate and often have a shape affected by mica pinning. Alteration of the feldspar grains to sericite is generally high at 50-100% as shown by a brown discolouration in Figure 6.2.2.a. Despite the high degree of alteration, it is possible to recognise other textures in the feldspar grains, including even to sweeping undulose extinction, tapered deformation lamellae and intragranular fractures. Several thin sections include porphyroclasts with chlorite and muscovite mica beard structures. The other mica grains situated in the cleavage domains of the foliation are generally fine grained (<0.1-0.2mm) and show even to strongly sweeping extinction in crossed polarised light. Chlorite can form a high proportion of these LCG samples at up to 40% and epidote is also a major constituent at up to 20% of the samples. Opaque oxide minerals within the samples can associate with strongly altered relict clasts or can be concentrated along fracture or foliation surfaces. Almost all of the samples show a dextral sense of shear from such indicator textures as oblique foliations, S-C fabrics, domino fractures and stair stepping strain shadows.

The mylonitic samples taken from granitic lithologies were located both in major plutons and from granitic layers or veins that are interlayered with the LCG phyllonites. Quartz grains in compositional bands in the granite samples are generally coarser than those in the LCG samples at 0.3-0.8mm average grain size. This may reflect differences in the grain sizes of the protoliths rather than resulting from deformation. The irregular to elongate quartz grains record moderate intracrystalline deformation as shown by sweeping to patchy undulose extinction and pervasive subgrain development. In some quartz grains, the intracrystalline deformation is intense so that the subgrains form a chessboard-type texture. Porphyroclasts in the Avalon granite samples are predominantly K-feldspar or plagioclase grains and they are relatively coarse in size at 1-6mm. The

a)

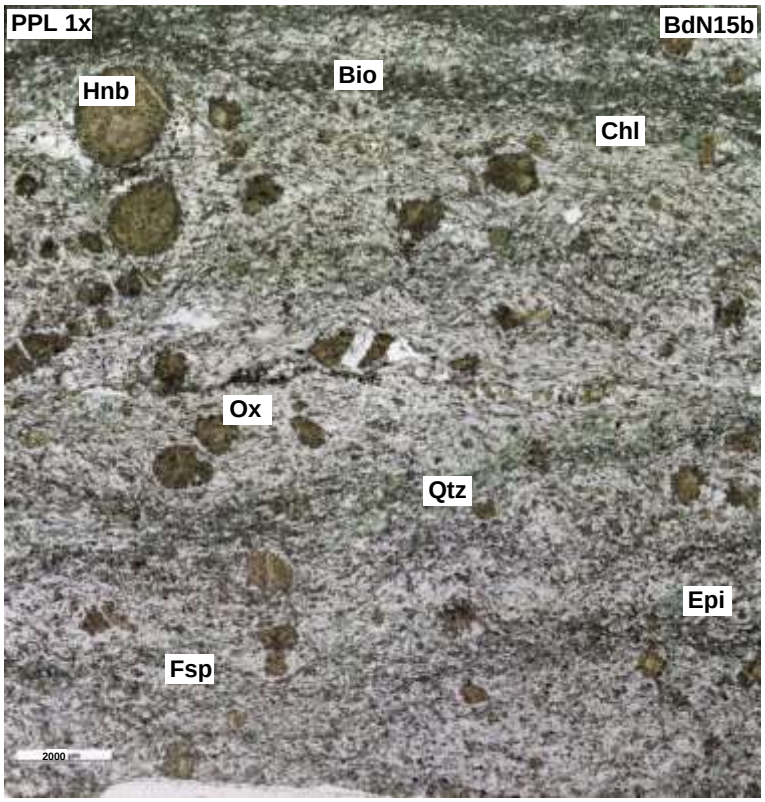

b)

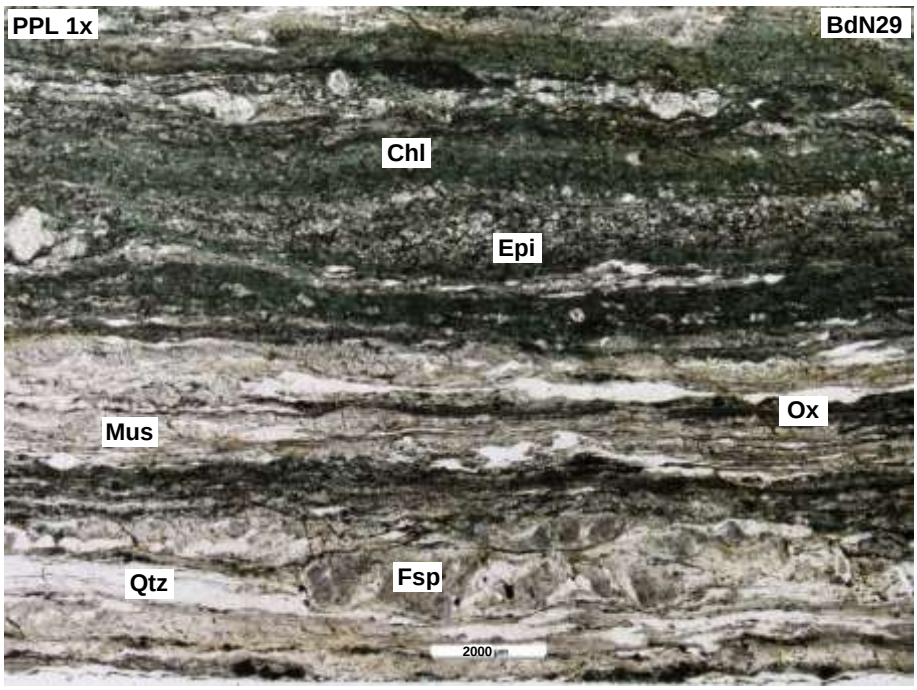

Figure 6.2.2: a) thin section composite photomicrograph of BdN15b at 1x zoom under plane polarised light. Coarse, highly altered mafic clasts form porphyroclasts in the phyllonitic fabric in BdN15b and micas in the foliation fabric and strain shadows show dextral shear senses. b) thin section composite photomicrograph of BdN29 at 1x zoom under plane polarised light. The compositional banding is clear in this photo, with chlorite, epidote and oxide-rich bands at the top and quartz and feldspar-rich bands at the bottom. A strongly dextral sense of shear is indicated by oblique foliation in the quartz grains as well as strain shadow stair stepping and domino fracture patterns in the feldspar porphyroclasts. Brittle fractures clearly overprint the earlier ductile fabric.

alteration of feldspar to sericite mica is much more variable in the granites than in the LCG phyllonites with individual grains altered by 0-70%. A few rare core and mantle structures occur on the feldspar porphyroclasts but brittle intragranular fractures are the more common microstructure in the feldspar grains.

As in the LCG samples, the phyllosilicate minerals define a strong discrete foliation fabric in the granite samples and chlorite and muscovite mica often occur as strain caps or mica beards (see Figure 6.2.3). The mica grains in the granite samples are coarser than those in the LCG samples at 0.2-0.3mm but they do show similar sweeping extinction patterns. Chlorite occurs at a lower proportion in the mylonitic granites (5-10%) and it also shows intergrowth textures with biotite that have resulted from hydration alteration of the biotite grains. Stair stepping of the mica overgrowths and strain shadows on the feldspar porphyroclasts indicate a dextral sense of shear in almost every sample.

As shown in Figure 6.2.3, the Bay du Nord samples contain brittle fractures and veins that overprint the earlier ductile fabric, regardless of lithology. Micro-faults offset the foliation fabrics in both sinistral and dextral movements and the fractures occur in predominantly three different orientations: parallel, perpendicular and oblique (45-60° clockwise) to the foliation fabric. The concentration of oxide minerals along fractures (see Figure 6.2.3) and rare stylolitic surfaces suggests that dissolution of more soluble mineral phases has taken place. In addition, the presence of calcite and quartz veins that cross cut the ductile foliation is evidence of the presence of fluids within the fracture network during the brittle deformation phase.

All of the samples in the Bay du Nord Avalon Zone display textures derived from dextral shear under mid-upper greenschist grade conditions, as shown in Figure 6.2.3. The quartz grains have undergone SGR and GBM recrystallization whilst the feldspar grains have deformed primarily by brittle fracturing and crystal plastic mechanisms. As all of the samples display similar metamorphic grades, dextral shear senses and relatively high strain fabrics, it can be inferred that the ductile DFSZ extends at least 900m from the brittle Dover Fault into the Avalon Zone in the Bay du Nord area. The extensive alteration of the samples plus the presence of mica and chlorite overgrowths provides evidence of fluids being present during both ductile and brittle deformation. This suggests

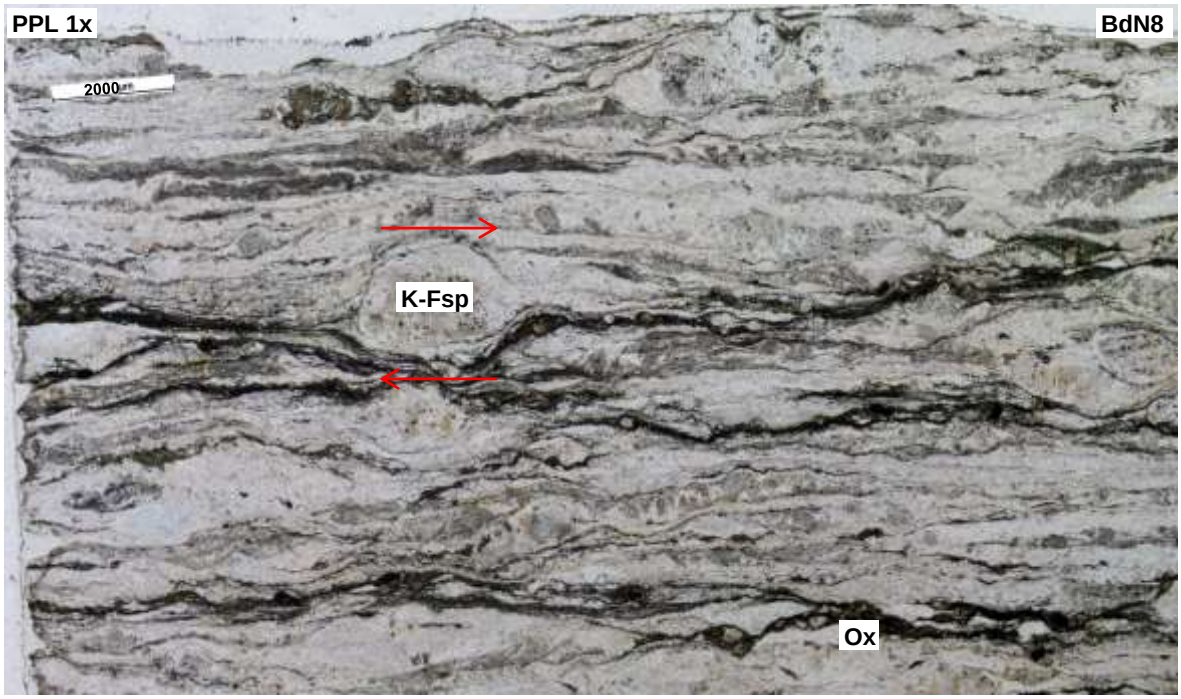

a)

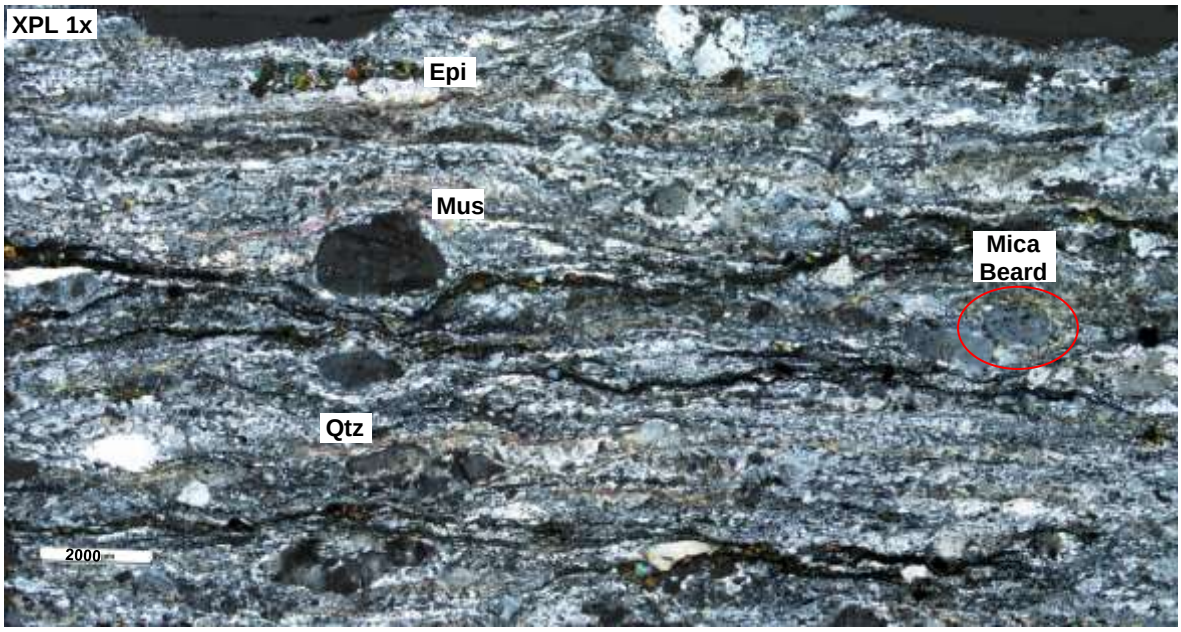

b)

Figure 6.2.3: thin section composite photomicrographs of the mylonitic granite BdN 8 at 1x magnification in a) plane polarised and b) cross polarised light. The K-feldspar grains form coarse porphyroclasts that have undergone partial alteration to sericite and have dextrally stair stepping strain shadows and mica beards (as indicated). Opaque oxide minerals and epidote grains strongly associate with transgranular fractures that parallel the foliation fabric.

Sample No.	Distance from Boundary (m)	Rock Type	Mineral Assemblage (descending order of %)	Quartz Fabric	Feldspar Fabric	Metamorphic Grade	Shear Sense	Mineral Lineation
29	868	Phyllonite	Chl, Qtz, K-Fsp (ser), Mus, Epi, Ox, Hnb	SGR	BF + CP	Mid-Greenschist	Dextral	02-358
35	811	Volcanic Phyllonite	Qtz, Mus, Ash, K-Fsp (ser), Ox	CP + BLG	BF + CP	Sub- to Lower Greenschist	Dextral	15-227
17	522	Mylonitic Granite	Qtz, K-Fsp (ser), Mus, Plag, Bio, Epi, Ox	GBM + lim DMT	BF + CP + lim BLG	Upper Greenschist - Amphibolite	Dextral	37-041
8	498	Mylonitic Granite	K-Fsp (ser), Qtz, Mus, Chl, Epi, Ox	GBM + lim DMT	Alt + CP + BLG	Amphibolite	Dextral	60-077
4	418	Protomylonite	Qtz, K-Fsp (ser), Mus, Chl, Bio, Epi, Ox	SGR + GBM	BF + CP	Upper Greenschist	Dextral	13-013
14	343	Granitic Mylonite	Qtz, K-Fsp (ser), Mus, Bio, Chl, Hnb, Ox, Epi	GBM + overprint CP + SGR	Alt + CP + BF	Upper Greenschist - Amphibolite	Unknown	87-173
3b	252	Banded Granite/ Granodiorite	Bio, Qtz, Hnb, Plag (ser), K-Fsp (ser)	GBM?	Alt + BF + CP	Upper Greenschist	Unknown	15-138
6	236	Phyllonite	Chl, Qtz, Epi, K-Fsp (ser), Ox, Cal	SGR + DMT	BF + CP + DMT	Upper Greenschist	Sinistral	39-213
25a	151	Mylonite	Qtz, K-Fsp (ser), Mus, Chl, Epi, Ox	SGR + lim GBM	BF + CP	Mid- to Upper-Greenschist	Dextral	67-221
25b	151	Phyllonite	Qtz, K-Fsp (ser), Chl, Mus, Epi, Ox	SGR + lim GBM	BF + CP	Mid- to Upper-Greenschist	Dextral	67-221
15a	11	Mylonite	Qtz, Mus, K-Fsp (ser), Bio, Chl, Ox, Cal	SGR + GBM + DMT	Alt + CP + BF + DMT	Upper Greenschist	Dextral	05-357
15b	11	Mafic Phyllonite	Chl, Qtz, K-Fsp, Mafics, Oxi, Bio, Epi	SGR	BF + CP	Mid-Greenschist	Dextral	05-357

Table 6.2.2: Table of results for samples from the Avalon Zone in the Bay du Nord area with inferred metamorphic grade and shear sense. Mineral phase codes: Qtz – Quartz, K-Fsp (ser) – K-Feldspar altered to sericite, Plag – Plagioclase, Mus – Muscovite, Bio – Biotite, Chl – Chlorite, Epi – Epidote, Ox – Oxides, Cal – Calcite, Hnb – Hornblende.

that the DFSZ may have been a conduit for fluid flow for significant periods of its active history.

6.2.3 Freshwater Bay

Samples of the MSG in Freshwater Bay are located more than 1.5km from the Gander-Avalon boundary and observations in the field show that they preserve mostly primary sedimentary textures in a range of sandstones and siltstones. Quartz grains in the MSG are generally well rounded relict grains of 0.1-0.5mm in size. They show very few microstructures with most samples only showing even to sweeping undulose extinction. Samples FB73a and b do show some core and mantle structures of very fine (<0.1mm) new grains. Similarly, the feldspar grains in the MSG are relatively low strain relict grains with intragranular fractures, partial alteration to sericite and grain sizes from 0.1-0.5mm. In most of the MSG samples, mica grains are extremely fine grained (<0.05mm) and form part of the sedimentary matrix. In the samples FB73a and b, however, the mica grains are aligned in a weak cleavage fabric and can form fibrous overgrowths on the coarser relict grains (see Figure 6.2.4.a). Overall, the MSG samples record sub- to lower-greenschist grades of metamorphism with little or no strain accommodated. Only the samples at FB73 show a weak deformation fabric, although they lack any mineral lineation, and FB73a indicates a sinistral sense of shear when correctly oriented. Hence it is clear that the MSG samples are only weakly affected by the DFSZ.

Across the faulted contact between the MSG and LCG, there is a marked change in the deformation fabric and intensity. Outcrops of the LCG within 1.5km of the Gander-Avalon boundary show strong compositional layering and a well-defined foliation fabric. As the LCG volcanic protolith is itself strongly layered and is often fine grained, this is reflected in the siting of deformation and the textures of the overprinting fault rocks. The quartz grains in the LCG samples are very fine grained (<0.05-0.1mm) and form elongate to ribbon shaped grains with patchy to sweeping undulose extinction. Subgrain development within the quartz grains is extensive, especially in monomineralic bands where the quartz grains are generally coarser and the grain boundaries are irregular to lobate. Under a sensitive tint plate, the quartz grains show a moderate CPO. The feldspar porphyroclasts tend to be coarser, at ~0.5mm as compared to 0.2-0.3mm, in samples that are over 500m from the tectonic boundary. The alteration of the feldspar grains to sericite is also

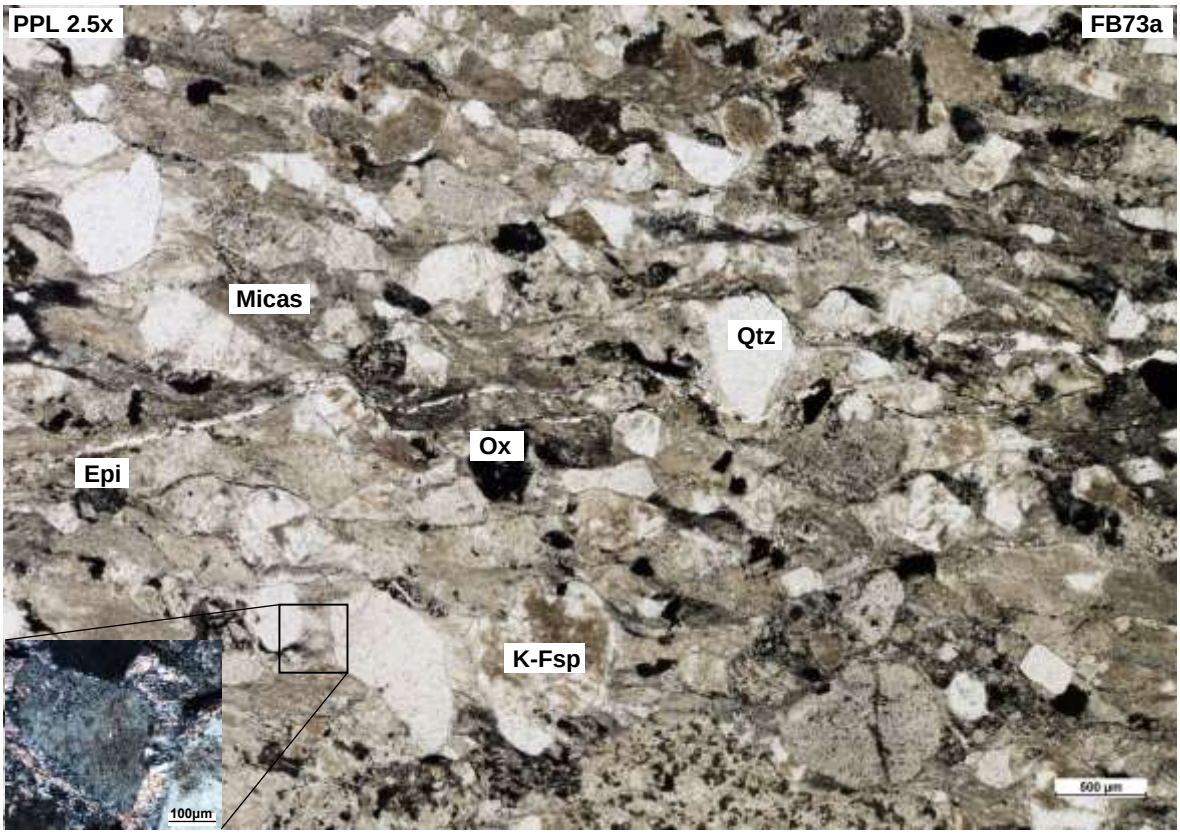

a)

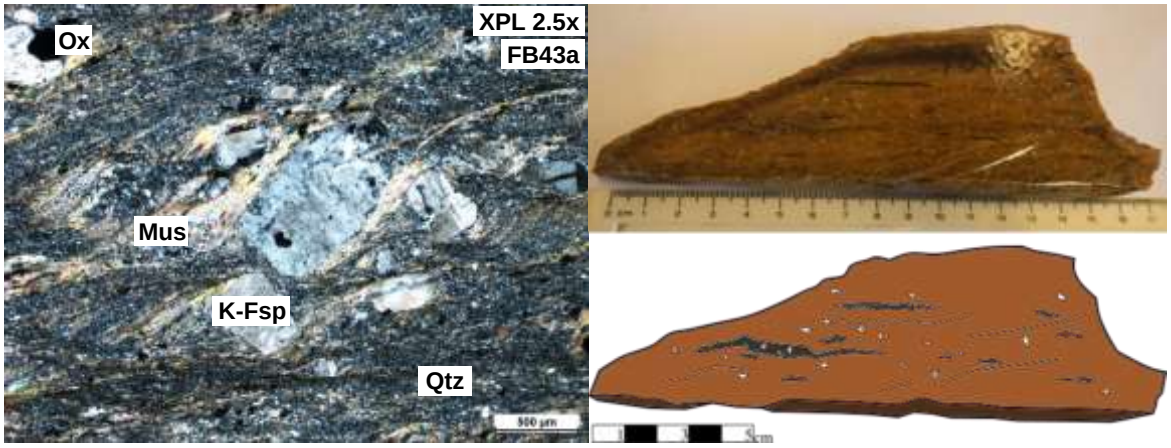

b) *c)*

Figure 6.2.4: a) thin section composite photomicrograph of the MSG sandstone FB73a at 2.5x zoom under plane polarised light. The quartz and feldspar relict grains preserve the original sedimentary texture but a weak cleavage has developed and is defined by the alignment of mica grains. The photo insert was taken at 10x zoom under crossed polarised light and shows the fibrous overgrowths of muscovite mica on the relict grains. b) thin section photomicrograph of FB43a at 2.5x zoom under crossed polarised light. Muscovite mica forms relatively wide strain caps and mica beards on the K-feldspar porphyroclasts. When correctly oriented to the hand specimen the apparent dextral shear in thin section is shown to be evidence of sinistral shear in the LCG mylonites. c) photo and sketch of FB43a in hand specimen showing the well-defined foliation fabric, porphyroclasts and compositional partitioning.

highly variable (0-100%), but most samples include the feldspar microstructures of intra- to inter-granular fractures, sweeping undulose extinction and a few rare core and mantle textures.

Muscovite and chlorite grains form both discrete and continuous foliations in the LCG samples. The fine grained micas (0.1-0.2mm) can occur in strain caps or mica beards on the feldspar porphyroclasts and they often show strongly sweeping extinction patterns (see Figure 6.2.4.b). Chlorite can form a significant proportion of the samples at up to 30% whilst epidote can occur at proportions as high as 40%. The epidote grains commonly form in compositional bands with chlorite or as coarse porphyroblasts that disrupt the mylonitic fabric. The samples within the LCG in Freshwater Bay at more than 1km from the Gander-Avalon boundary (FB35b, 43a and 43b) generally show sinistral shear senses from stair stepping strain shadows, mica fish and C' fabrics.

Brittle structures in the LCG are most intense in samples that are in close proximity to the Dover Fault, such as FB26a in Figure 6.2.5. Brittle faults down to the centimetre-scale can be seen to offset the ductile mylonitic fabric in both apparently dextral and sinistral shear senses. As shown by FB26a, there are several different generations of brittle fracturing events as the earlier calcite and quartz veins are offset by later fractures, which themselves terminate along other fracture sets. Only the relative ages of the fracture sets can be determined in this study, as no absolute dates currently exist for the mineralised veins.

The Avalon Zone samples in the Freshwater Bay area show similar trends to the other study areas. In samples closest to the tectonic boundary, there are textures indicative of an upper-greenschist grade of deformation with a dextral shear sense inferred from both the field and thin section observations. At more than 1km from the Gander-Avalon boundary, the samples record an upper greenschist grade, sinistral deformation phase that relates to Early Ductile structures identified in the field. Strain intensity and the metamorphic grade decreases eastwards across the Avalon Zone to a lower- or sub-greenschist grade and finally to little deformed sediments in the MSG. A late brittle deformation phase is recognised in most of the samples but it is most obvious in samples located close to the Dover Fault. As the earlier calcite and quartz veins are overprinted by brittle shear fractures, it can be inferred that hydrothermal fluids were present in the fracture network at least during the early phases of the brittle deformation. In addition, the brittle deformation phase

likely involved episodic fracturing associated with the Dover Fault as evidenced by the multiple generations of fractures.

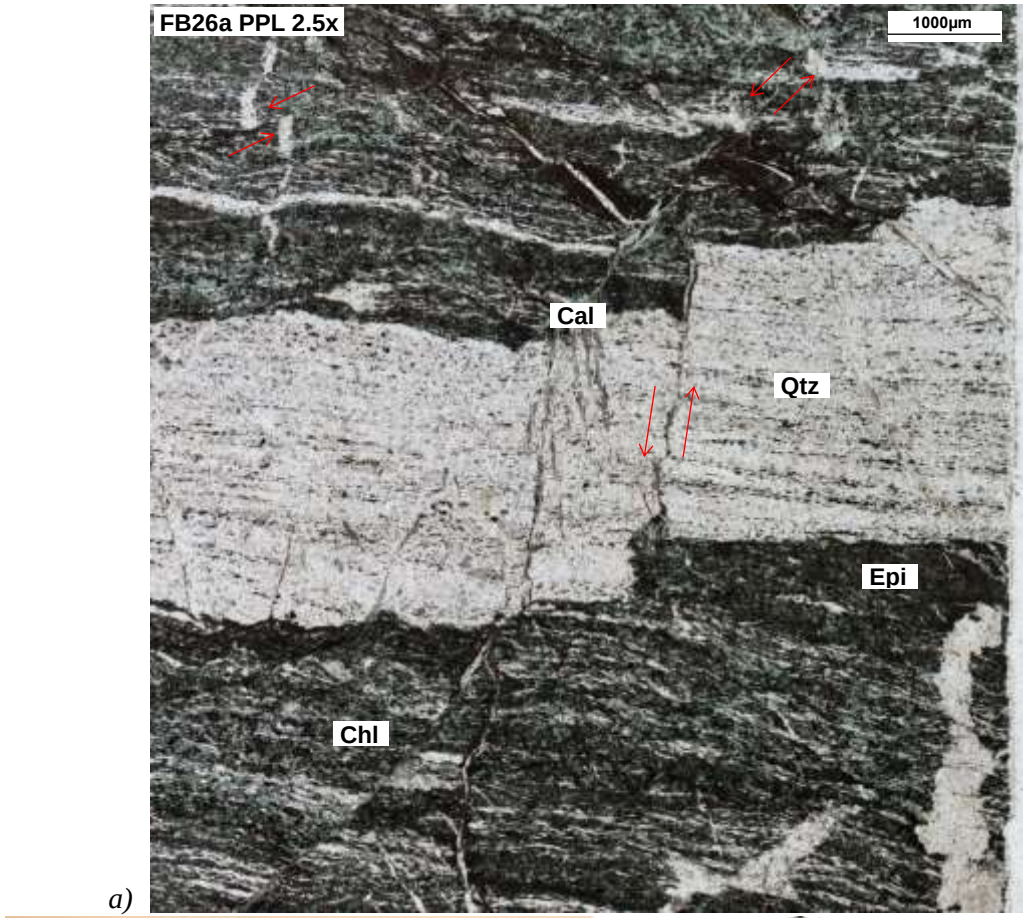

a)

b)

Figure 6.2.5: a) thin section composite photomicrograph of FB26a at 2.5x zoom under plane polarised light. The strong phyllonitic fabric and the mylonitised quartz vein in this sample have been overprinted and offset by networks of brittle micro-faults and calcite veins. Whilst all the offsets in this image are sinistral, both shear senses are recorded in the thin section. Several generations of brittle fracturing events are recorded here, as shown by the relative cross cutting relationships. b) photo and sketch of FB26a in hand specime with the offset quartz veins and phyllonitic fabric clearly visible. The sample records a high level of both ductile and brittle strain as shown by the high intensity of foliation and fracturing.

Sample No.	Distance from Boundary (m)	Rock Type	Mineral Assemblage (descending order of %)	Quartz Fabric	Feldspar Fabric	Metamorphic Grade	Shear Sense	Mineral Lineation
73a	4745	Metasandstone	Qtz, Mus, Ox, K-Fsp (ser), Epi, Unknown	BLG + DMT?	CP + DMT?	Lower- or sub-Greenschist	Sinistral	-
73b	4745	Feldspathic wacke with deformation bands	Qtz, Mus, K-Fsp (ser), Ox, Epi	BLG + lim SGR	CP + BF	Lower- or sub-Greenschist	Unclear	-
68	2133	Conglomerate	Comp Grain, Micas, Qtz, K-Fsp (ser), Epi, Ox	BF?	BF?	Diagenesis	-	-
53	2027	Brecciated siltstone	Cal, Mus, Qtz, Ox, K-Fsp (ser), Epi	-	-	Diagenesis	-	-
49	1676	Siltstone	Clay, K-Fsp (ser), Qtz, Mus	-	-	Diagenesis	-	-
47	1523	Siltstone	Qtz, K-Fsp (ser), Mus, Ox, Chl, Epi	-	-	Diagenesis	-	-
44	1380	Mylonite (fold hinge in tuffs)	Qtz, Mus, Epi, K-Fsp (ser), Ox, Chl	SGR	CP + BLG	Upper Greenschist	Unclear	41-300
43a	1292	Mylonite (from acidic tuffs)	K-Fsp (ser), Mus, Qtz, Chl, Ox	SGR	BF + CP + BLG	Upper Greenschist	Sinistral	67-203
43b	1292	Mylonite (from purple tuffs)	Qtz, K-Fsp (ser), Mus, Ox, Cal	SGR	BF + CP + BLG	Upper Greenschist	Sinistral	67-203
35a	710	Mylonite	Qtz, Chl, Epi (?), K-fsp (ser), Cal	SGR	BF	Greenschist	Dextral	48-035
35b	710	Mylonite with Qtz-Cal Veins	Qtz, K-fsp, Chl, Epi (Vein: Qtz, Cal)	SGR (late BF)	BF + CP + BLG	Upper Greenschist	Sinistral	48-035
31 slide 1	305	Weakly deformed volcanic tuff	Qtz, K-fsp, Mus, Cal, Epi, Chl	BF + CP	BF + CP	Sub-Greenschist	Unclear	27-033

Sample No.	Distance from Boundary (m)	Rock Type	Mineral Assemblage (descending order of %)	Quartz Fabric	Feldspar Fabric	Metamorphic Grade	Shear Sense	Mineral Lineation
29	145	Mylonitic volcanics	Qtz, K-fsp (ser), Mus, Chl, Epi, Cal	SGR + GBM? (late BF)	CP + BLG + DMT (late BF)	Upper Greenschist - Amphibolite	Sinistral	07-029
28	90	Mylonite	Qtz, K-fsp (ser), Chl, Epi, Cal	SGR	CP + BLG (DMT?	Upper Greenschist	Sinistral	02-041
26a	12	Phyllonitic mylonite	Qtz, Epi, Chl, Cal, K-fsp	SGR + GBM (late BF)	(late BF)	Upper Greenschist	Dextral	38-009
26b	12	Fold hinge in mylonite qtz veins	Qtz, Mus, Chl, K-Fsp (ser), Ox, Cal	SGR + GBM	CP + BF	Upper Greenschist	Unclear	38-009

Table 6.2.3: Table of results for samples from the Avalon Zone in the Freshwater Bay area with inferred metamorphic grade and shear sense. Mineral phase codes: Qtz – Quartz, K-Fsp (ser) – K-Feldspar altered to sericite, Plag – Plagioclase, Mus – Muscovite, Bio – Biotite, Chl – Chlorite, Epi – Epidote, Ox – Oxides, Cal – Calcite.

6.2.4 Hare Bay

At more than a kilometre from the Gander-Avalon boundary, the MSG samples were collected from metasediments that partially preserve the original sedimentary structures as well as deformation textures. Observations in the field identified structures including a steep cleavage, irregular folding of quartz veins and rare crenulation cleavage. Quartz grains within the MSG form coarse (average 1.5mm) relict grains and they often contain strong undulose extinction patterns, fluid inclusions and tabular subgrains. In HB30, the relict quartz grains have core and mantle textures of very fine (<0.1mm) new grains at the grain boundaries. K-feldspar also forms angular relict grains in the MSG samples at an average grain size of 0.1mm. Relatively low alteration to sericite (10-40%) has preserved the microstructures in the feldspars including intragranular fractures and even to sweeping extinction patterns. Fine grained (~0.1mm) muscovite and chlorite grains are aligned in either discrete or continuous foliations and the elongate mica grains often show sweeping extinction patterns. Whilst chlorite occurs in relatively low proportions (<15%), opaque oxide minerals are relatively common in the MSG samples and, as shown in Figure 6.2.6.a, the oxide minerals are often concentrated in fracture or cleavage planes.

In the field, the LCG lithologies displayed interlayered bands of mafic and silicic material and the outcrops included a shallow mineral lineation in close proximity to the Dover Fault. Phyllonitic or mylonitic textures are dominant in the LCG with strong foliation fabrics defined by the alignment of micas, porphyroclasts of feldspar and epidote and recrystallized quartz groundmass, as shown in Figure 6.2.6. All of the mineral phases are generally fine grained with quartz at <0.1mm, K-feldspar at 0.1-0.2mm and mica grains at <0.1mm. The quartz grains have irregular shapes with irregular to weakly lobate grain boundaries. The intracrystalline deformation is moderate in the quartz grains as evidenced by the patchy to sweeping undulose extinction, elongate subgrains and a moderate CPO under a tint plate. Porphyroclasts of K-feldspar and plagioclase commonly contain intragranular fractures and they have been affected by a relatively low degree of sericite alteration (average of 10%). Muscovite and chlorite are elongate in shape with sweeping undulose extinction. In addition to forming the discrete cleavage domains, the mica grains also form mica beard overgrowths on the porphyroclasts. Chlorite occurs in variable proportions from 5-40% and epidote

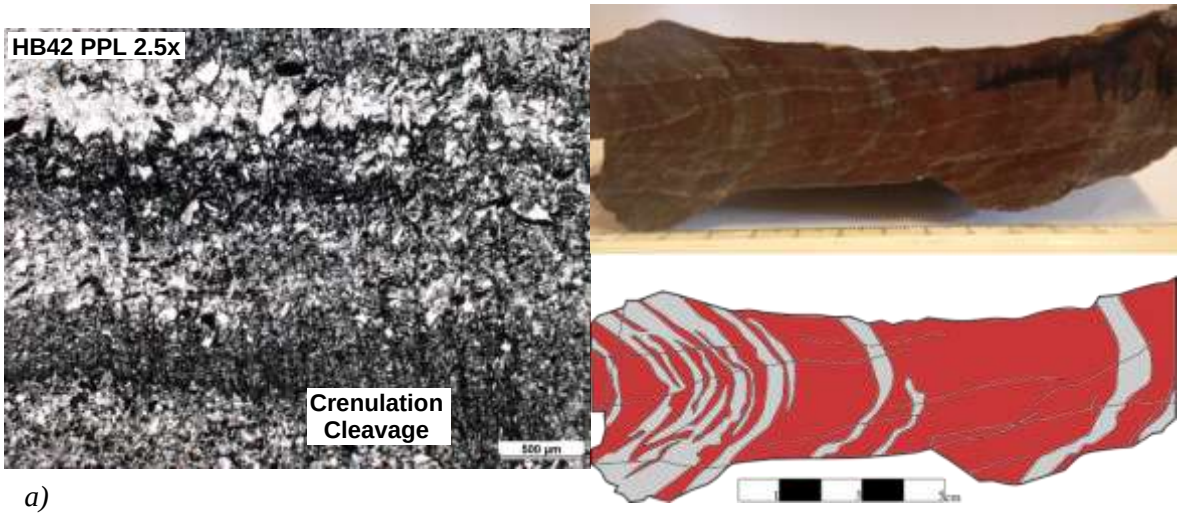

a)

b)

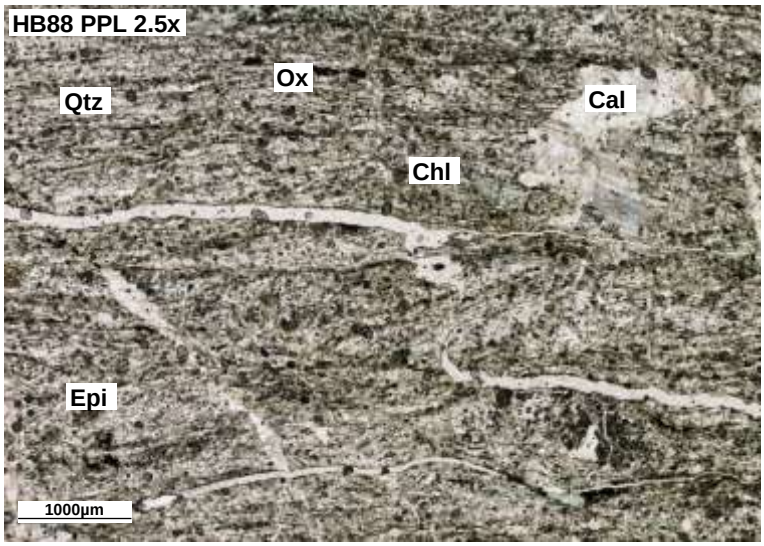

c)

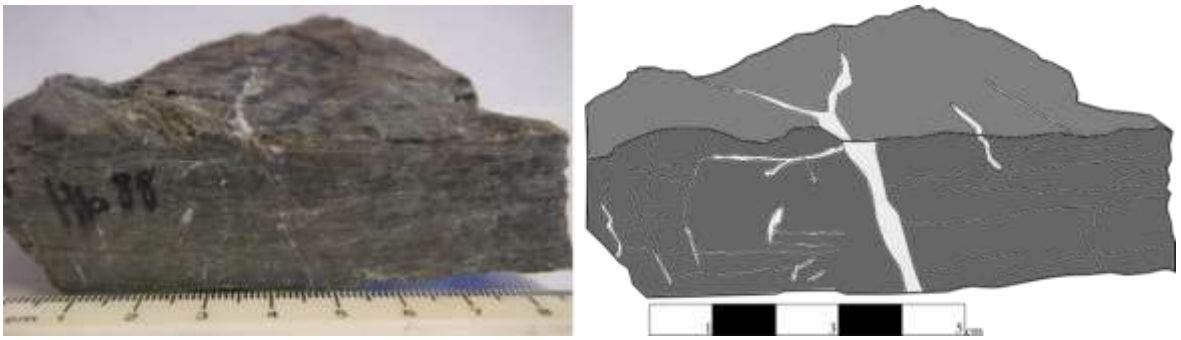

d)

Figure 6.2.6: a) thin section photomicrograph of MSG sandstone HB42 at 2.5x zoom under plane polarised light. The earlier compositional layering is overprinted by a perpendicular crenulation cleavage fabric with opaque oxide minerals concentrated on the cleavage planes. b) photo and sketch of HB42 in hand specimen. Centimetre-scale tight folds in the fine grained siltstone are overprinted by brittle fractures that trend sub-parallel to the axial plane of the folds. c) thin section composite photomicrograph of HB88 (LCG protolith) at 2.5x zoom under plane polarised light. The fine grained mylonitic fabric in this thin section has been overprinted by many mineralised calcite veins and brittle shear zones. d) photo and sketch of HB88 in hand specimen showing pervasive fracturing of the sample with associated mineralisation.

forms 5-20% of the thin sections, either located in the cleavage domain or as porphyroblasts. Interpreting shear senses in the Hare Bay samples is difficult as the senses are not strongly indicated and can be ambiguous. When oriented correctly with respect to the hand specimens, the samples HB13a and 13b, located more than 1km from the Gander-Avalon boundary, indicate a sinistral sense of shear from the stair stepping of σ-porphyroclasts. Within 1km of the tectonic boundary, the samples HB1b and HB8 indicate a dextral sense of shear, which was derived from the stair stepping of σ- and δ-type porphyroclasts, mica fish and weak dextral vergence on folds.

Similarly to the other study areas, a brittle deformation fabric overprints the earlier ductile structures and it is most intense in close proximity to the Dover Fault. HB88, shown in Figure 6.2.6.c and d, was collected from a pervasively brecciated damage zone only 10m from the Dover Fault and the sample shows several generations of calcite and quartz veins and fractures at both thin section and hand specimen scale. Whilst this brittle deformation is most obvious in HB88, fracturing and mineral veins can also be observed in the MSG samples at over 1.5km from the brittle Dover Fault.

In the samples closest to the Gander-Avalon boundary, the structures indicate a dextral lower-greenschist grade with a high degree of strain shown by the intensity of the fabrics and the extensive reduction in grain size. Further from the tectonic boundary, the LCG samples record a sinistral lower greenschist grade deformation phase that associates with the Early Ductile structures observed in the field. The samples in the MSG record sub-greenschist grade conditions during deformation, which shows that the ductile DFSZ is approximately a kilometre in width in the Hare Bay study area. The brittle overprinting deformation phase is also inferred to have occurred at sub-greenschist grade conditions. The multiple generations of veins and fractures indicate a prolonged period of activity on the Dover Fault, although only the relative ages have been identified in the samples. As the presence of mica beards indicate that fluid-assisted DMT was active during deformation, it is suggested that fluids were present within both the ductile and brittle DFSZ during the different deformation phases. Table 6.2.4 summarises the microstructural analysis results for the Hare Bay samples.

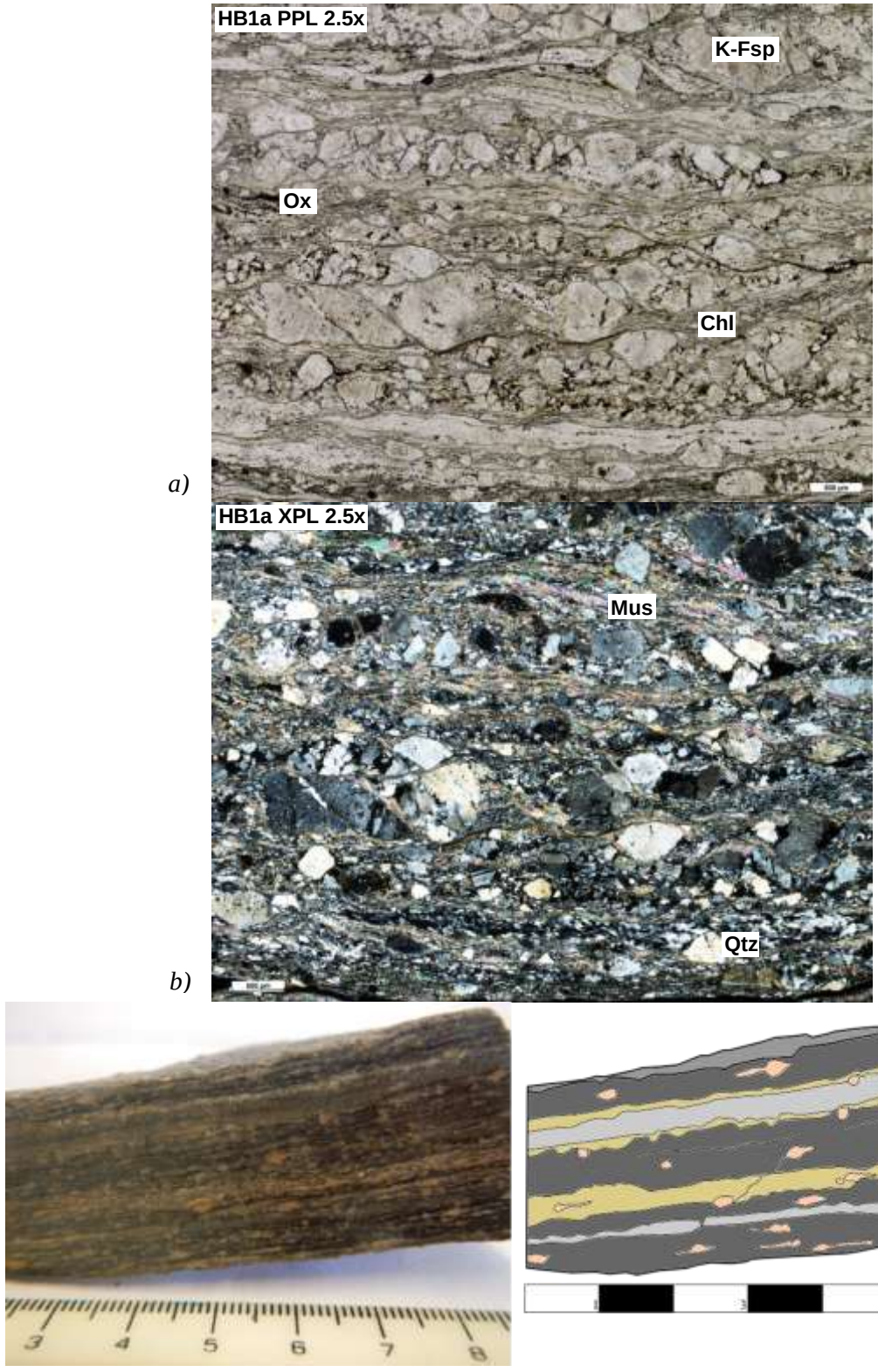

a)

b)

c)

Figure 6.2.7: thin section composite photomicrographs of HB1a at 2.5x zoom under a) plane polarised and b) crossed polarised light. HB1a displays a mylonitic fabric with a well-defined discrete cleavage domain, K-Feldspar porphyroclasts and recrystallized quartz compositional bands. The strain caps and mica beards on the porphyroclasts indicate a sinistral sense of shear. c) photo and sketch of HB1a in hand specimen. The quartz-, feldspar- and mica-rich compositional layers, mylonitic fabric and porphyroclasts are clearly visible in hand specimen. Several brittle fractures can be seen to disrupt and offset the earlier ductile fabric.

Sample No.	Distance from Boundary (m)	Rock Type	Mineral Assemblage (descending order of %)	Quartz Fabric	Feldspar Fabric	Metamorphic Grade	Shear Sense	Mineral Lineation
30	1688	Semipelite	Qtz, Mus, Chl, Cal, K-Fsp (ser), Epi, Woll	CP + BLG	CP + BF	Sub- to Lower Greenschist	Dextral? (unclear)	-
13a	1455	Mylonite	Qtz, Mus, Epi, K-Fsp, Chl, Ox	SGR	BF + DMT	Lower Greenschist	Sinistral	59-023
13b	1455	Mylonite	Qtz, Mus, Ox, K-Fsp, Chl, Epi	SGR	BF + DMT	Lower Greenschist	Sinistral	59-023
42	1110	Metasandstone	Qtz, Mus, K-Fsp (ser), Ox, Epi	CP + DMT?	CP + DMT?	Sub-Greenschist	Dextral	-
46	991	Meta-rhyolite	Qtz, Mus, Chl, K-Fsp (ser), Ox	BLG + SGR	CP + DMT	Sub- to Lower Greenschist	Unclear	77-170
8	830	Mylonitic tuff	Qtz, Mus, K-Fsp, Epi, Chl, Cal	SGR	CP + BF	Lower Greenschist	Dextral? (unclear)	24-042
2	520	Phyllonitic tuff	Qtz, Mus, Chl, Ox, Epi, K-Fsp (ser), Cal	SGR	BF (+ lim DMT?)	Lower Greenschist	Unclear	41-086
1a	340	Mylonite	Qtz, Mus, K-Fsp (ser), Plag, Chl, Cal, Epi	SGR	CP + BF + DMT	Lower Greenschist	Sinistral	03-358
1b	340	Phyllonite	Chl, Epi, Qtz, Cal, Mus	SGR	-	Lower Greenschist	Dextral	03-358
85	20	Brecciated Mylonite	Qtz, Epi, Cal, Chl, Ox	SGR + BF	-	(Pro) Low - Mid Greenschist (Retro) sub-Greenschist	Unclear	-
88	10	Mylonite	Qtz, Chl, Epi, K-Fsp, Ox, Cal	SGR	CP + BF	Lower Greenschist	Unclear	09-041

Table 6.2.4: Table of results for samples from the Avalon Zone in the Hare Bay area with inferred metamorphic grade and shear sense. Mineral phase codes: Qtz – Quartz, K-Fsp – K-Feldspar, K-Fsp (ser) – K-Feldspar altered to sericite, Plag – Plagioclase, Mus – Muscovite, Chl – Chlorite, Epi – Epidote, Ox – Oxides, Cal – Calcite, Woll - Wollastonite.

6.2.5 Shoal Bay

Only two samples (SB37 and SB47) were collected from the Avalon Zone from the coastline of Shoal Bay. The sample SB37 is located close to the brittle Dover Fault where the HBG contacts the LCG. The contact is marked in outcrop by mylonitised quartz veins, purple to green mylonitic tuffs and a fractured damage zone. In both of the samples, quartz grains occur in a relatively fine (0.1-0.2mm) grained groundmass with tabular to irregular grain shapes. The size and shape of the quartz grains show some pinning effects from mica grains so that the quartz grains are coarser in areas of lower mica proportions. Subgrains within the quartz grains, as well as sweeping extinctions, are very common and under a sensitive tint plate the quartz grains show a moderate CPO. Feldspar grains also occur at relatively fine sizes (0.1-0.2mm) as relict clasts. Mica beards are fairly common around the feldspar grains, although some grains instead display a core and mantle texture with very fine (<0.1mm) new grains. The relict clasts often contain intragranular fractures and have undergone partial alteration to sericite (50-100%). Muscovite and chlorite are also fine grained (0.1mm) and their alignment defines both discrete and continuous foliation fabrics. Chlorite forms a moderate proportion of SB47 at 15% and occurs with muscovite in strain shadows on epidote porphyroblasts, as shown in Figure 6.2.8. Brittle overprinting structures occur in both SB37 and SB47 as shown in Figure 6.2.8 and 6.2.9. Pervasive fracturing in SB37 disrupts the earlier ductile foliation and opaque oxide minerals are concentrated along the fracture surfaces. Calcite occurs in both samples as vein and void infill material. The dextral, asymmetrical fold in SB47 appears to associate with brittle fracturing and so may represent a brittle kink fold.

Both samples are inferred to have deformed at mid-upper greenschist grade conditions. Quartz fabrics in the samples are characteristic of recrystallization by dominantly SGR with subordinate GBM mechanisms. Whilst there is some rare BLG feldspar recrystallization in SB37, the more dominant deformation mechanism in the feldspar grains is brittle fracture. The mica beards and oxides in fractures are evidence that DMT and pressure solution were also active deformation mechanisms in these samples and they were likely fluid assisted. As shown by the pervasive fracturing in SB37, the brittle overprinting deformation is most intense in close proximity to the

brittle Dover Fault. Brittle fractures and folds are still present at more than 600m from the Dover Fault in SB47, but at a much lower intensity.

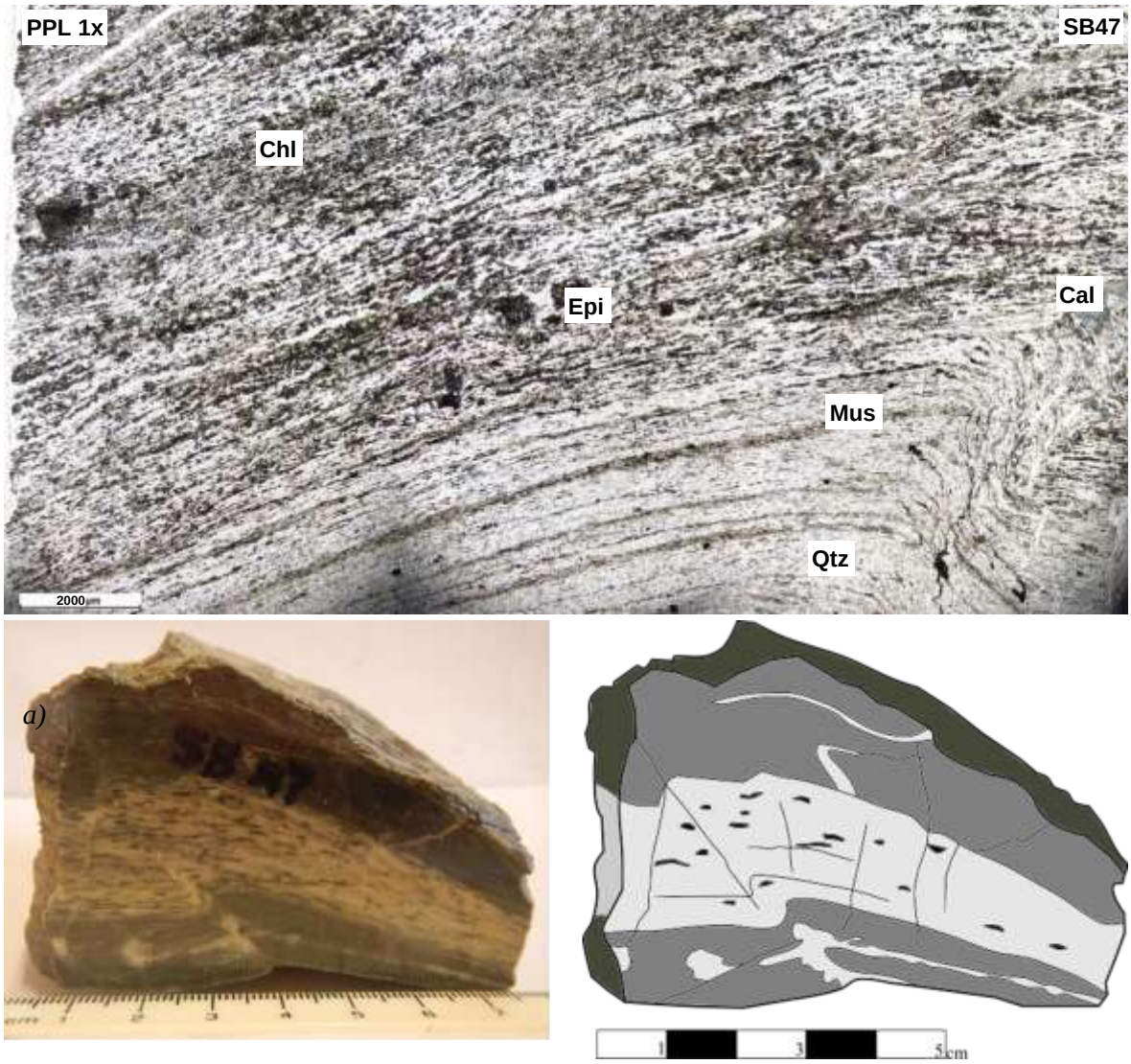

Figure 6.2.8: a) thin section composite photomicrograph of SB47 at 1x zoom under plane polarised light. The strong mylonitic fabric has been folded into a dextral asymmetric fold with calcite mineralisation concentrated around the hinge of the fold. b) photo and sketch of SB47 in hand specimen. The (mirrored) fold structures are also visible in hand specimen, as are the brittle fractures and mineralised veins that overprint the earlier ducile fabric.

Sample No.	Distance from Boundary (m)	Rock Type	Mineral Assemblage (descending order of %)	Quartz Fabric	Feldspar Fabric	Metamorphic Grade	Shear Sense	Mineral Lineation
47	674	Mylonite	Qtz, K-Fsp (ser), Chl, Epi, Cal, Ox	SGR	Alt + CP	Mid Greenschist	Dextral	75-299
37	16	Mylonite	Qtz, Mus, K-Fsp (ser), Cal, Ox, Chl	SGR + lim GBM?	CP + BF + v lim BLG	Upper Greenschist-Amphibolite	Unclear	-

Table 6.2.5: Table of results for samples from the Avalon Zone in the Shoal Bay area with inferred metamorphic grade and shear sense. Mineral phase codes: Qtz – Quartz, K-Fsp (ser) – K-Feldspar altered to sericite, Mus – Muscovite, Chl – Chlorite, Epi – Epidote, Ox – Oxides, Cal – Calcite.

a)

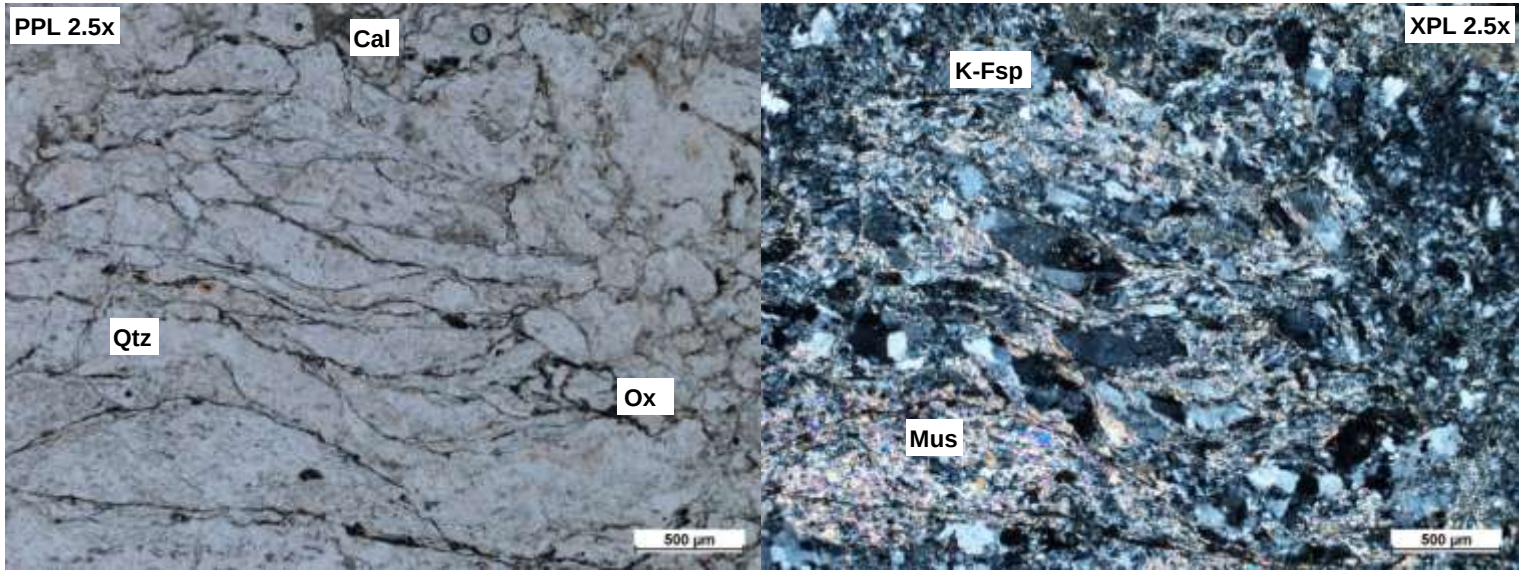

b)

Figure 6.2.9: thin section photomicrographs of SB37 at 2.5x under a) plane polarised and b) crossed polarised light.

6.2.6 Locker's Bay

As in the Shoal Bay area, only two samples were collected from the Avalon Zone in the east of the Locker's Bay area. LB7 is a sample of phyllonitic LCG whilst LB3 is a sample of a granitic vein that cross cuts the LCG fabric. Shown in Figure 6.2.10, LB3 contains coarse (2mm) relict grains of quartz with core and mantle textures of very fine (<0.1mm) new grains. The quartz grains in LB3 also commonly contain fluid inclusions and show strong intracrystalline deformation with elongate subgrains, sweeping extinction and deformation lamellae. In contrast, the quartz grains in LB7 are very fine grained (<0.1mm) with an irregular shape, sweeping to patchy extinctions, elongate subgrains and a moderate CPO under a tint plate. The feldspar grains are also coarser in LB3 than in LB7 at average grain sizes of 1.5mm to 0.2mm respectively. The microstructures in the feldspar grains are similar in both samples, however, with intra- to inter-granular fractures, even to sweeping extinctions and rare elongate subgrains. Alteration of feldspar to sericite mica is relatively limited in both samples at up to 30% of the individual grains. Whilst LB3 only contains sericite, LB7 contains both muscovite and chlorite grains that are aligned in a continuous foliation fabric (see Figure 6.2.10.b). The micas in LB7 are fine grained (average 0.1mm) and show sweeping undulose extinctions under crossed polars. Chlorite forms a relatively high proportion of LB7 at ~20% and it often forms synkinematic overgrowths on the feldspar grains that indicate a sinistral sense of shear. Brittle fracturing overprints the ductile fabrics in both samples, with cross cutting quartz and calcite veins in LB7 and oxide-rich fractures in LB3.

The two Avalon samples in the Locker's Bay area record different conditions during deformation as the granitic vein of LB3 records lower-greenschist grade conditions while LB7 contains textures characteristic of mid-greenschist grade conditions with a sinistral sense of shear. The recrystallization of quartz grains in LB7 was dominated by SGR and the brittle deformation of the K-Feldspar grains indicates temperatures during deformation were in the range of 350-400°C. As the granitic vein of LB3 cross cuts the fabric in the LCG, it can be inferred as relatively younger and may record part of the cooling history of the Locker's Bay area. As the brittle structures overprint ductile fabrics in both samples, it is inferred to post-date the deformation of LB3 and occurred at sub-greenschist grade conditions.

Sample No.	Distance from Boundary (m)	Rock Type	Mineral Assemblage (descending order of %)	Quartz Fabric	Feldspar Fabric	Metamorphic Grade	Shear Sense	Mineral Lineation
3	634	Altered Granitic Vein	Qtz, K-Fsp, Plag, Ox	CP + BLG	BF + CP	Lower Greenschist	Unclear	64-322
7	347	Phyllonitic Mylonite	Qtz, Epi, Chl, K-Fsp (ser), Woll, Cal	SGR	BF + CP	Mid-Greenschist	Sinistral	30-052

Table 6.2.6: Table of results for samples from the Avalon Zone in the Locker's Bay area with inferred metamorphic grade and shear sense. Mineral phase codes: Qtz – Quartz, K-Fsp – K-Feldspar, K-Fsp (ser) – K-Feldspar altered to sericite, Plag – Plagioclase, Chl – Chlorite, Epi – Epidote, Woll – Wollastonite, Ox – Oxides, Cal – Calcite.

a)

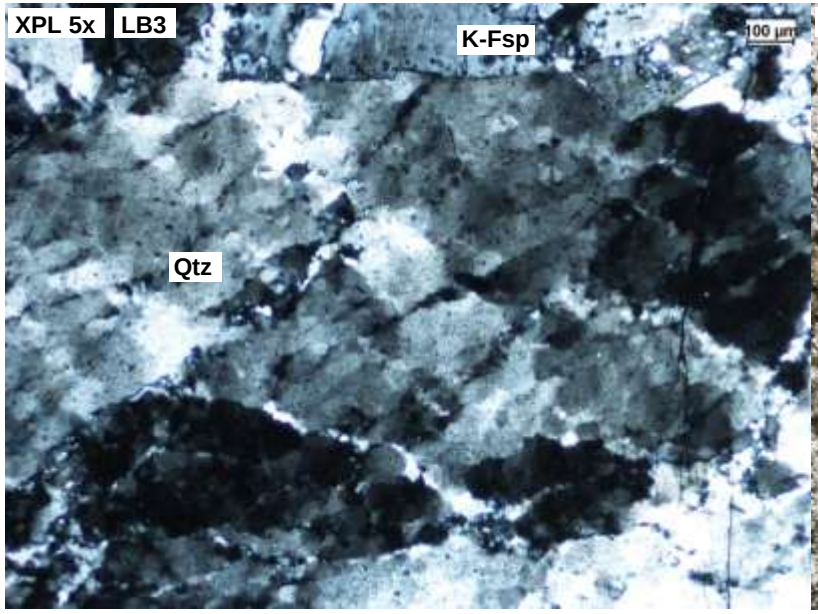

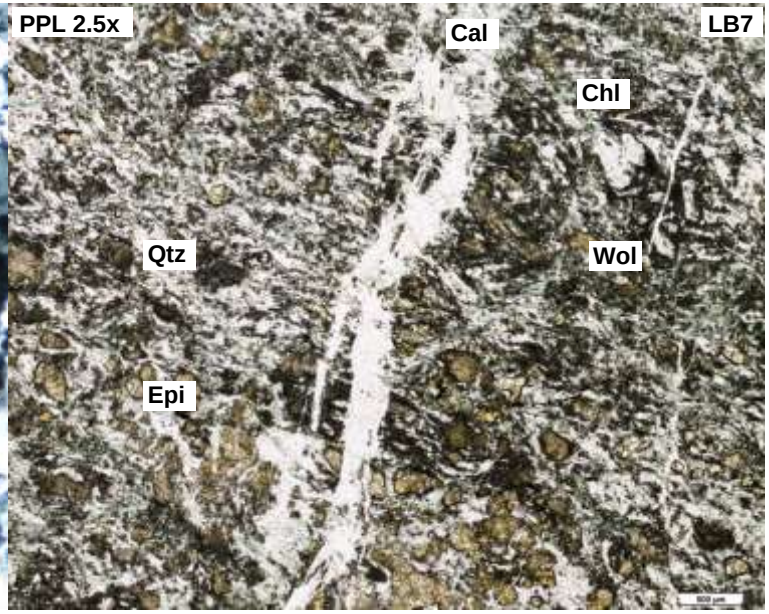

b)

Figure 6.2.10: a) thin section photomicrograph of LB3 at 5x zoom under crossed polarised light. The coarse grains of quartz display very strong intracrystalline deformation including elongate subgrains, sweeping extinction and BLG recrystallization at grain boundaries. b) thin section composite photomicrograph of LB7 at 2.5x zoom under plane polarised light. LB7 is phyllonitic in texture with a high proportion of chlorite and epidote and calcite and quartz veins cross cut the foliation fabric.

6.3 Summary of Avalon Zone Microstructural Analysis

In the Avalon Zone, the Early Ductile structures identified in the field correlate to a sub- to mid-greenschist grade, sinistral deformation phase that is recorded in samples of the MSG and LCG at more than 1km from the tectonic boundary. Grain-scale deformation during this low temperature sinistral event was accommodated by brittle fracture, pressure solution and dynamic recrystallisation.

A dextral, mid- to upper-greenschist grade deformation phase is recorded in all of the study areas within 1km of the Gander-Avalon boundary, which correlates with the Late Ductile structures observed in the field. Deformation at the grain-scale during this later, lower temperature phase was accommodated by dynamic recrystallization, grain size reduction, brittle fracture, DMT and the formation of localised shear zones and fabrics (see Figure 6.3.1).

Deformation was accommodated during the brittle phase by brittle fracturing, pressure solution, limited dynamic recrystallization and folding. As in the Gander Zone, the action of DMT, hydration alteration, hydrothermal mineralisation and pressure solution indicates that importance of fluids in the DFSZ during all three deformation phases (see Figure 6.3.2).

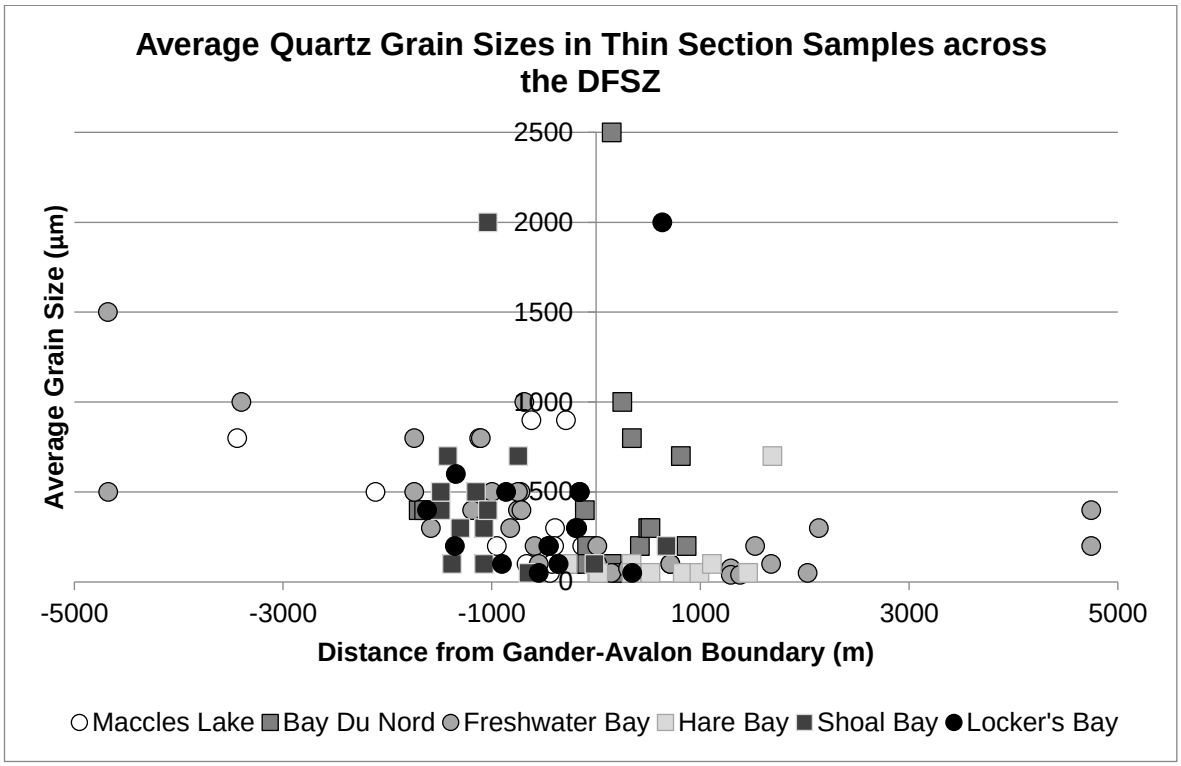

Figure 6.3.1: a graph showing the average quartz grain sizes in thin section across all of the study areas in both tectonic terranes. There is no clear grain size trend other than that the finest grain sizes occur in close proximity to the Gander-Avalon boundary.

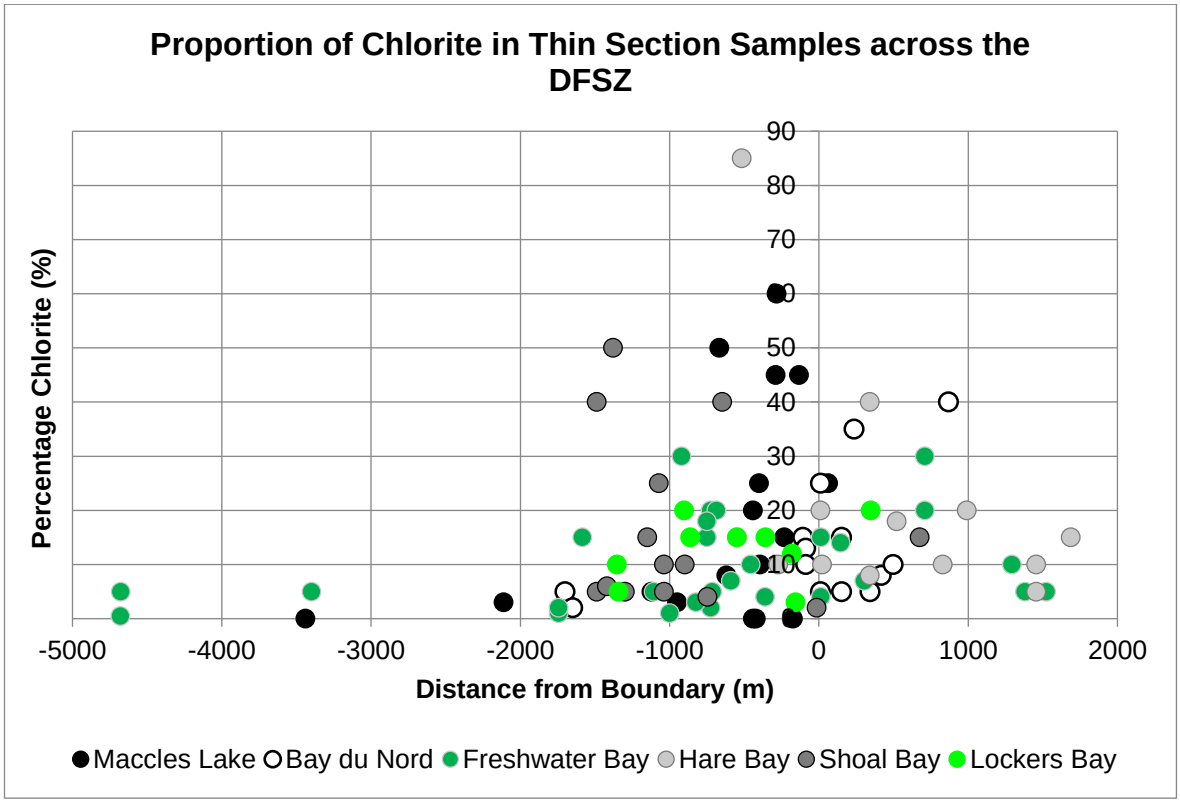

Figure 6.3.2: a graph showing the proportion of chlorite in thin section across all of the study areas in both tectonic terranes. As with Figure 6.3.1, there are no clear trends in the proportion of chlorite other than that the greatest variation and highest values occur in close proximity to the tectonic boundary. There are likely other controls on grain size and the proportion of chlorite than just distance from the centre of the DFSZ.

7 Chapter 7: Discussion

This chapter aims to synthesise the observations of the fault rocks in the DFSZ and to integrate the findings in this research with the structural history of Newfoundland outlined in the scientific literature. The weakening mechanisms that were active during deformation along the Gander-Avalon boundary and the implications of fault weakening will also be discussed. Finally, several suggestions will be given for further work on the subjects of deformation weakening and the DFSZ.

7.1 The Structural History of the DFSZ

In order to understand the history of weakening in the DFSZ, the observations in this study will first be correlated with the literature on the tectonic history of northeast Newfoundland to produce a detailed structural history. The depth estimates that are given for the fault rock assemblages and inferred deformation phases are based on an assumed typical shear zone geothermal gradient of 30°C per km depth.

Prior to the Silurian, the Gander and Avalon Zones in Newfoundland record different geological and structural histories. In the Avalon Zone, O'Brien (1983) identified variably dispersed Precambrian deformation structures in southeast Newfoundland that were thought to be related to compression in a volcanic arc-type setting. The distribution and significance of these Precambrian structures remain uncertain but the low grade deformation and metamorphism appears highly localised along long lived fault zones (O'Brien, 1987) It is unclear whether these events affected the rocks close to the present day boundary with the Gander Zone, but the limited preserved evidence suggests that the protoliths of the DFSZ rocks in the western Avalon Zone record little or no deformation.

In contrast, the Gander Zone records multiple deformation phases prior to the Silurian that are thought to be related to the obduction of the Dunnage Zone onto western Ganderia and the early Salinic accretion of the leading edge of Ganderia to Laurentia (King, 1997; Valverde-Vaquero et al., 2006; van Staal et al., 2009; Pollock et al., 2012). The protolith of the HBG in the Gander Zone is the Gander Group, a sequence of metasediments that record a greenschist grade deformation phase identified as the regional D2 event by King (1997). It is unknown whether the pre-existing

D2 structures had any influence on the siting of later deformation and metamorphism in the eastern Gander Zone at the tectonic boundary.

The first deformation phases associated with the Gander-Avalon boundary predate the ductile DFSZ and show a strong temperature and texture contrast across the tectonic boundary. In the Gander Zone, the amphibolite grade, sinistral deformation phase identified in the field is termed the Early Ductile phase by Holdsworth (1991, 1994) and is inferred to represent temperatures during deformation of at least 500°C and up to 700°C (Dallmeyer et al., 1981). The Early Ductile structures in the Gander Zone relate to a sinistral transpressional shear zone that was sited at depths of at least 15km in the viscous crust. The high temperatures and ductile mode of deformation produced a broad region (~4km) of partially melted gneisses and migmatites in the HBG. In this Early Ductile phase, the peak temperatures of 750°C at pressures of 4.5kbar would require a geothermal gradient in excess of 50°C km^{-1} (Schofield and D'Lemos, 2000). This high temperature-low pressure metamorphism can be explained due to an abnormally high heat flow as a result of abundant magmatism (Schofield and D'Lemos, 2000). Langille (2012) proposed that the HBG are not simply the high temperature metamorphic equivalents of the Gander Group metasediments and in fact include partial melt-derived intrusions into the eastern Gander Zone. Holdsworth (1994) also inferred that the orthogneisses in the HBG represented early intrusive phases. The geochemical signatures of LREE enrichment relative to HREE and negative Nb and Ti anomalies in the deformed granitic bodies and orthogneisses in the HBG indicate a sedimentary source of melting (Langille, 2012). Silurian granitic plutons, such as the LBG, also record high temperature, sinistral, pre-full crystallisation fabrics that suggest relatively high ambient temperatures were prevalent during pluton emplacement (Schofield and D'Lemos, 1998; Kellett et al., 2014). In addition, a lack of contact metamorphic aureoles at the margins of the Silurian granites is evidence that the emplacement of the Silurian plutons occurred at mid-crustal depths (Schofield and D'Lemos, 1998; Kellett et al., 2014).

The amphibolite grade, sinistral Early Ductile (or D3) phase in the Gander Zone represents the regional peak metamorphic conditions and it is generally correlated with the final stages of the Salinic orogeny (Holdsworth, 1994; King, 1997; van Staal et al., 2009; Pollock et al., 2012; Kellett

et al., 2016). The trailing passive edge of the Ganderian microcontinent that equates to the eastern Gander Zone was separated from the leading edge by the Tetagouche-Exploits Basin and a westwards facing subduction zone in the early Salinic orogeny, as shown in Figure 7.1 (van Staal et al., 2009; Pollock et al., 2012). Accretion of the trailing edge of Ganderia to the Laurentian margin is generally dated at 430-422 Ma due to the closure of the Tetagouche-Exploits basin (van Staal et al., 2009; Kellett et al., 2016). The Silurian syn-collisional magmatism in the Gander Zone (433-423 Ma) has been proposed to relate to break-off of the subducted Tetagouche-Exploits slab (Whalen et al., 2006).

In the Avalon Zone, the earliest deformation phase identified in the samples and the field is the greenschist grade, sinistral deformation phase that was correlated by Holdsworth (1991) with the Early Ductile phase in the Gander Zone. The Avalon greenschist grade sinistral deformation phase relates to temperatures of 300-400°C, which corresponds to depths of 10-13km in the FVTZ in the continental crust. Holdsworth (1991,1994) the correlated two early deformation phases across the Gander-Avalon boundary using the same SE to the top, sinistral kinematics and the relative ages of the Early Ductile structures compared to later overprinting structures. However, during the late stages of the Salinic orogeny the Gander and Avalon Zones are thought to have been separated by the Acadian seaway (van Staal et al., 2009; Pollock et al., 2012). The effects of the accretion of the passive eastern Gander Zone are therefore unlikely to have produced the sinistral greenschist grade shear zone observed in the Avalon Zone. The sinistral shear zone in the Avalon Zone is therefore inferred to post-date the Salinic orogeny and the Early Ductile structures in the Gander Zone.

The presence of several greenschist grade sinistral shear zones in the Gander Zone that post-date the Early Ductile structures are here correlated with the early, greenschist grade sinistral shear zones in the Avalon Zone. In the Bay du Nord region south of Maccles Lake, there is a mid-upper greenschist, sinistral transpressive shear zone located in the Gander Zone (see Figure 7.2). The Bay du Nord shear zone clearly post-dates the Early Ductile Salinic deformation as the early foliation and mineral lineation are reactivated by later, sinistral, ductile fold structures. North of the study area, there is another sinistral shear zone that is sited at the western margin of the Cape Freels Granite, which also overprints the earlier, peak metamorphism Salinic deformation

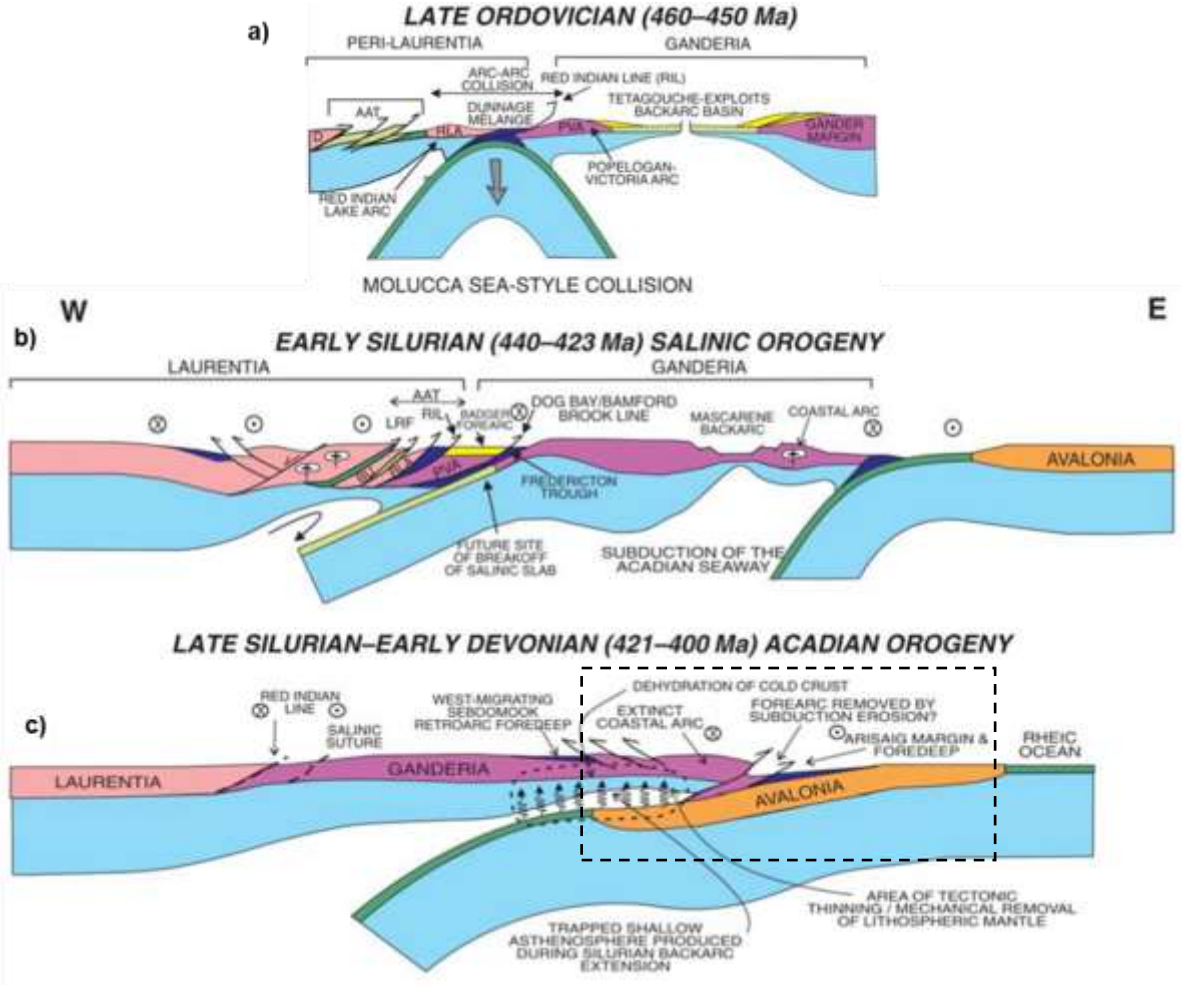

Figure 7.1: schematic tectonic models of the Appalachian orogeny showing: a) Accretion of the leading edge of Ganderia and the opening of the Tetagouche-Exploits basin. b) Late Ordovician-Silurian closure of the Tetagouche-Exploits back-arc basin in the Salinic orogeny. c) Silurian closure of the Acadian seaway that separated Ganderia and Avalonia in the Acadian orogeny. (adapted from van Staal et al., 2009). Box marks Gander-Avalon boundary region.

(Holdsworth et al., 1993). It is unclear exactly how these greenschist grade sinistral shear zones relate to the Late Ductile (dextral) DFSZ; the similar metamorphic grades and the orientation of the Cape Freels Shear Zone to the DFSZ might suggest that they are contemporaneous but in the Bay du Nord area the shear zones are parallel, which would be unlikely in a conjugate system. Field evidence in the Cape Freels Shear Zone also suggests that the sinistral shear zones may have been somewhat earlier than the dextral shear zones, including overprinting of dextral structures on sinistral and higher (>450°C) deformation temperatures (Holdsworth et al., 1993). The sinistral greenschist shear zones in both the Avalon and Gander Zones are inferred to be contemporaneous because they share the same top to the SE kinematics, greenschist grade of metamorphism and a phyllonitic fault rock assemblage.

In order to understand the timing of this later sinistral ductile deformation phase, the study by Kellett et al. (2016) is considered, which focused on the sinistral, post-peak metamorphism Wing Pond Shear Zone (WPSZ) in the Gander Zone that is to the west of and overprinted by the DFSZ. The WPSZ is taken to be broadly contemporaneous with the early sinistral greenschist shear zones (Kellett et al., 2016). Although, the WPSZ may have been active earlier and recorded more of the regional post-peak cooling as the fault rocks record a down temperature gradient from amphibolite to greenschist conditions (Jones et al., 2006). Using U-Pb dating in zircon and monazite and Ar-Ar dating in white mica, Kellett et al. (2016) were able to constrain the shear in the WPSZ to between 423-395 Ma. The deformation phase that produced sinistral greenschist grade shear zones in the Avalon and Gander Zones is now therefore termed the *Late Sinistral Ductile phase*.

The mid-upper greenschist, Late Sinistral Ductile (and later dextral) transpression is generally correlated with the end Silurian-early Devonian Acadian orogeny (422-394 Ma) that resulted from the accretion of Avalonia to Ganderia (van Staal et al., 2009; Pollock et al., 2012; Kellett et al., 2016). Avalonia is commonly taken to be the down-going plate in westwards subduction beneath Ganderia in the closure of the intervening Acadian seaway, as shown in Figure 7.1 (van Staal et al., 2009). Van Staal et al. (2009) proposed that the subduction angle progressively shallowed towards a flat-slab- like subduction zone during the Acadian orogeny so as to explain the production of syn-Acadian, upper-plate arc-like magmatism in the Gander Zone.

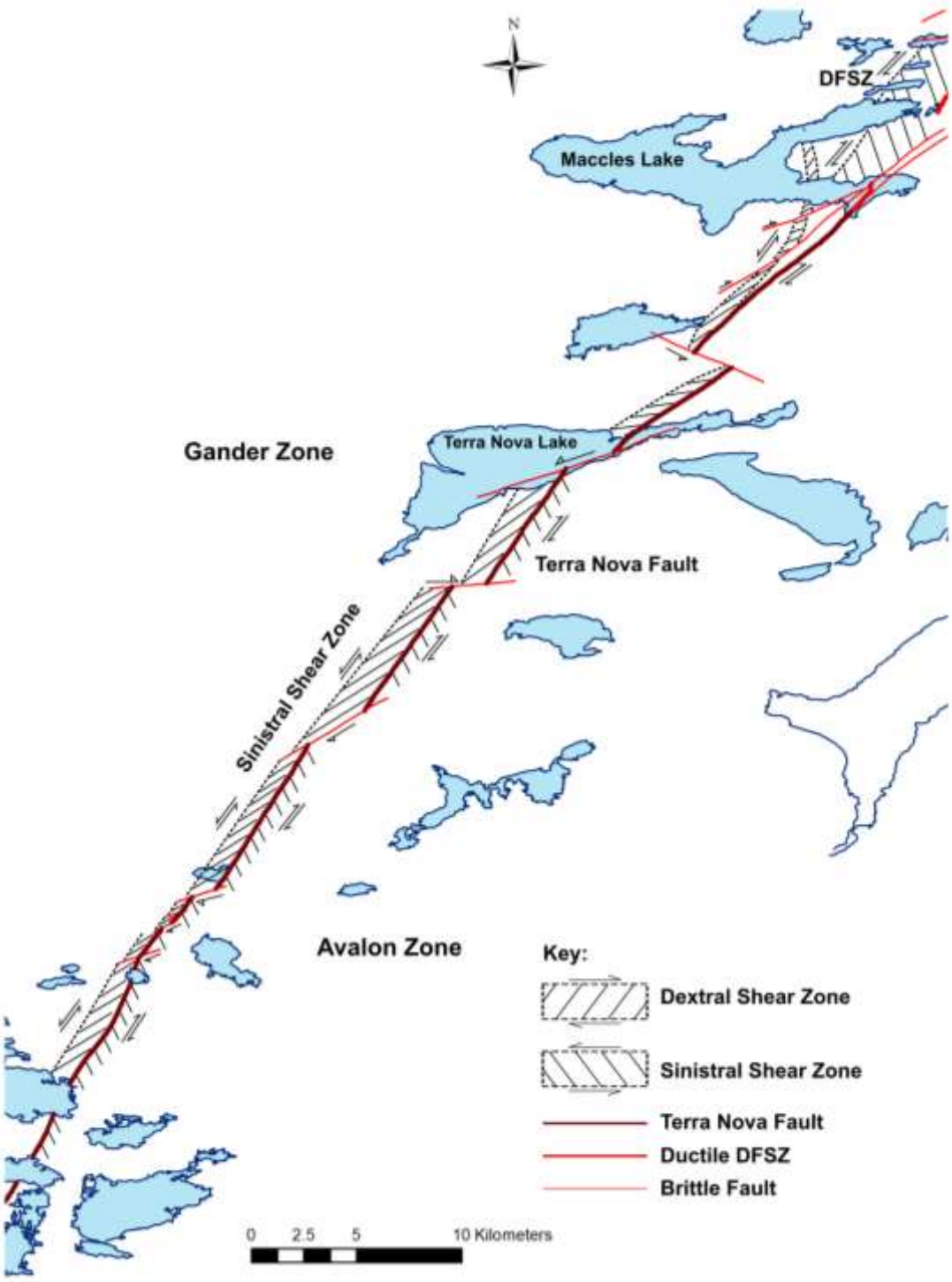

Figure 7.2: a schematic map showing the distribution of Late Ductile shear zones along the Gander-Avalon boundary in the Maccles Lake to Bay du Nord region (adapted from Holdsworth, 1994).

The ductile DFSZ reactivated the existing Early Ductile structures in the northern part of the Gander Zone and the Late Sinistral Ductile structures in the Avalon Zone. In both the Gander and Avalon Zones, the DFSZ records a mid-upper greenschist grade, dextral, NW to the top transpressional deformation phase termed the Late Ductile phase by Holdsworth (1991, 1994) and represents the D5 phase in the Gander Zone (King, 1997). The temperatures recorded in the Late Ductile samples and fault rocks range from 350-450°C, which corresponds to depths of 11-15km in the FVTZ. This interpretation is supported by the operation of both frictional and plastic deformation mechanisms at the grain-scale in the studied samples. In addition, an inferred greenschist grade of deformation in the Late Ductile DFSZ is supported by a quartz c-axis fabric derived temperature of 385 ± 50°C at 397-399 Ma calculated by Kellett et al (2016). The ductile DFSZ extends 500-1000m either side of the Gander-Avalon boundary as a series of localised mylonitic to phyllonitic shear zones. Between Maccles Lake and the southern shore of Freshwater Bay, the ductile boundary between the Gander and Avalon terranes is preserved and is not substantially disrupted by later brittle faulting as in other regions. Correlation of structures across the tectonic boundary is clearer for the Late Ductile phase as both terranes record the same metamorphic grade, kinematics and similar textures. To update the terminology used by Holdsworth (1991, 1994), the deformation phase that produced the ductile DFSZ is here referred to as the *Late Dextral Ductile phase*.

Holdsworth (1994) originally proposed a Silurian age for the ductile DFSZ but recent Ar-Ar dating of white mica (Kellett et al., 2016) constrains the formation of the DFSZ to prior to 385 Ma (Mid-Devonian). The kinematic reversal of the Gander-Avalon boundary from sinistral to dextral has been linked to the accretion of another terrane in the Appalachian orogeny, namely the Meguma terrane that forms most of southwest Nova Scotia (Kellett et al., 2016). The accretion of the Meguma terrane here in the Neoacadian orogeny occurred along a dextral transpressional boundary, which correlates well with the dextral shear senses in the DFSZ (Pollock et al., 2012; Kellett et al., 2016).

Devonian plutons that were emplaced in both the Gander and Avalon Zones are inferred to post-date the ductile DFSZ as they contain little or no solid-state deformation fabrics (Holdsworth,

1991; Schofield and D'Lemos, 1998; Kellett et al., 2014). The post-tectonic plutons, including the Newport and Ackley Granites, cross cut the regional structures and have well developed contact aureoles that are typical of shallower crustal emplacement levels (King, 1997; Schofield and D'Lemos, 1998; Kellett et al., 2014). Granophile-type mineralization (Mo, W, F, base metals) is present within the contact aureoles of both Gander and Avalon Zone plutons younger than 380 Ma, which is also associated with high-level structural settings (Kellett et al., 2014)The contrast in emplacement depths between the Silurian and Devonian granites in the Gander Zone indicates that an extended period of exhumation occurred between the Late Silurian (430-422 Ma) and the Late Devonian (~380-377 Ma) with an estimated removal of 12-15km of Ganderian crust (D'Lemos et al., 1997; Kellett et al., 2014). In addition, the sequence of overprinting and progressively lower temperature and retrogressive shear zones at the Gander-Avalon boundary is indicative of a shear zone that has remained active throughout exhumation.

The final deformation phase that is recorded in the samples from the Gander-Avalon boundary is the sub-greenschist, dextral brittle deformation phase termed the Late Brittle phase by Holdsworth (1991) and D6 in the Gander Zone by King (1997). On a regional scale, this phase is represented by the dextral strike-slip Dover and Terra Nova faults, which overprint the ductile DFSZ on both sides of the Gander-Avalon boundary. The Late Brittle samples record temperatures below 300°C and so reflect depths of less than 10km in the frictional upper crust. The brittle dextral Dover Fault is best represented in Frying Pan Island, Locker's Bay and Shoal Bay whereas south of Maccles Lake to the Ackley Granite, the brittle Terra Nova Fault has excised the ductile terrane boundary. Kellett et al. (2016) used a K-Ar date for a clay fraction of fault gouge at 351 ± 7 Ma as a maximum age for the latest motion along the co-linear Hermitage Bay Fault. No dates currently exist for the brittle Dover and Terra Nova faults, but it is clear that they are the youngest deformation structure as they overprint all other structures and igneous intrusions.

The frictional slip on the Hermitage Bay fault has been linked to the reactivation of a regional network of reactivated Appalachian-trend structures during the Carboniferous formation of the transtensional Maritimes Basin to the west of Newfoundland (Hibbard and Waldron, 2009; Waldron et al., 2015). Hibbard and Waldron (2009) calculated that at least 245km of slip along the

Appalachian trend strike-slip fault network is required to explain the extent of crustal thinning in the Maritimes Basin. It is unclear how this Carboniferous transtension relates to northeast Newfoundland and the reactivation of the ductile DFSZ. As the ductile DFSZ is preserved between Maccles Lake and Freshwater Bay, it is unlikely that the brittle Dover and Terra Nova faults accommodated offsets on the order of hundreds of kilometres. However, the Late Brittle strike-slip faulting does reactivate and truncate the ductile DFSZ to accommodate top to the NW shear and a component of compression normal to the ductile DFSZ. The movement along the brittle faults in NE Newfoundland is therefore likely to be a result of the larger slip offsets along the regional network of Appalachian strike-slip faults in the late Neoacadian orogeny (Kellett et al., 2016).

King (1997) inferred an overall clockwise P-T-t-D metamorphic path for the Gander Zone with the Early Ductile phase representing the peak metamorphic conditions (see Figure 7.3). The rapid exhumation of the Gander Zone resulted in pressure decreasing more rapidly than temperature to produce the clockwise P-T-t-D paths (King, 1997). The repeated reactivation of the Gander-Avalon Zone over a period of ~70Ma is clear evidence that it represents a relatively weak structure compared to the intact continental crust.

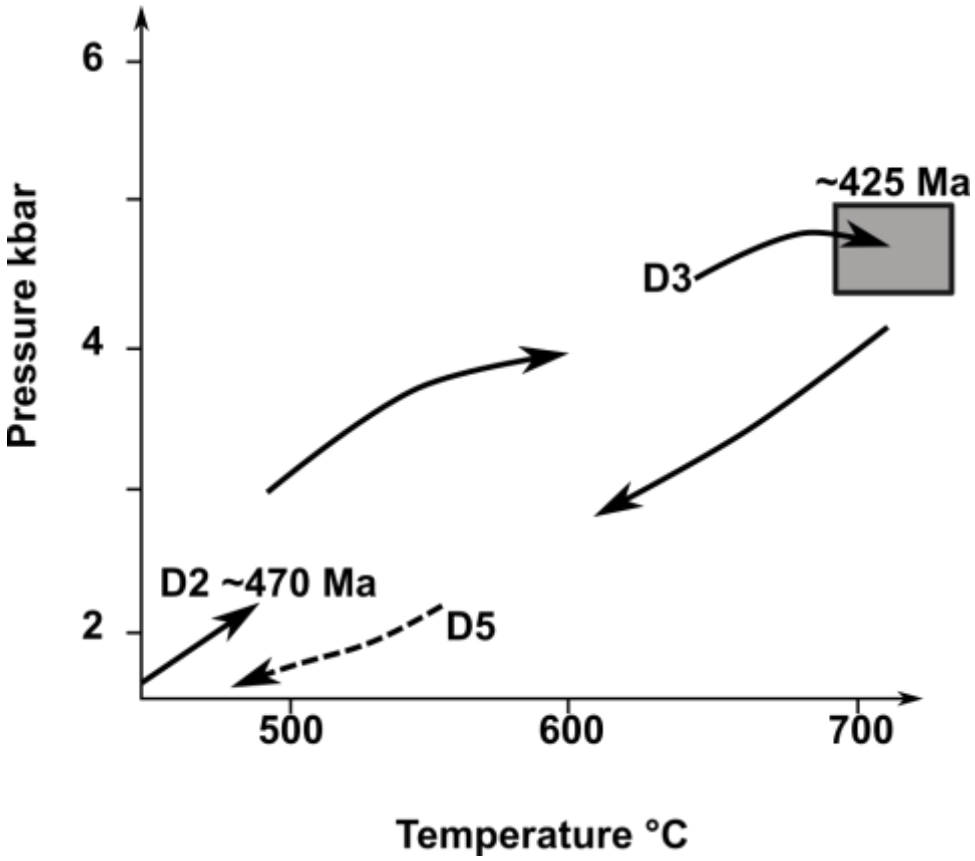

Figure 7.3: A summary P-T-t-D evolution paths for the Gander Zone (adapted from King, 1997)

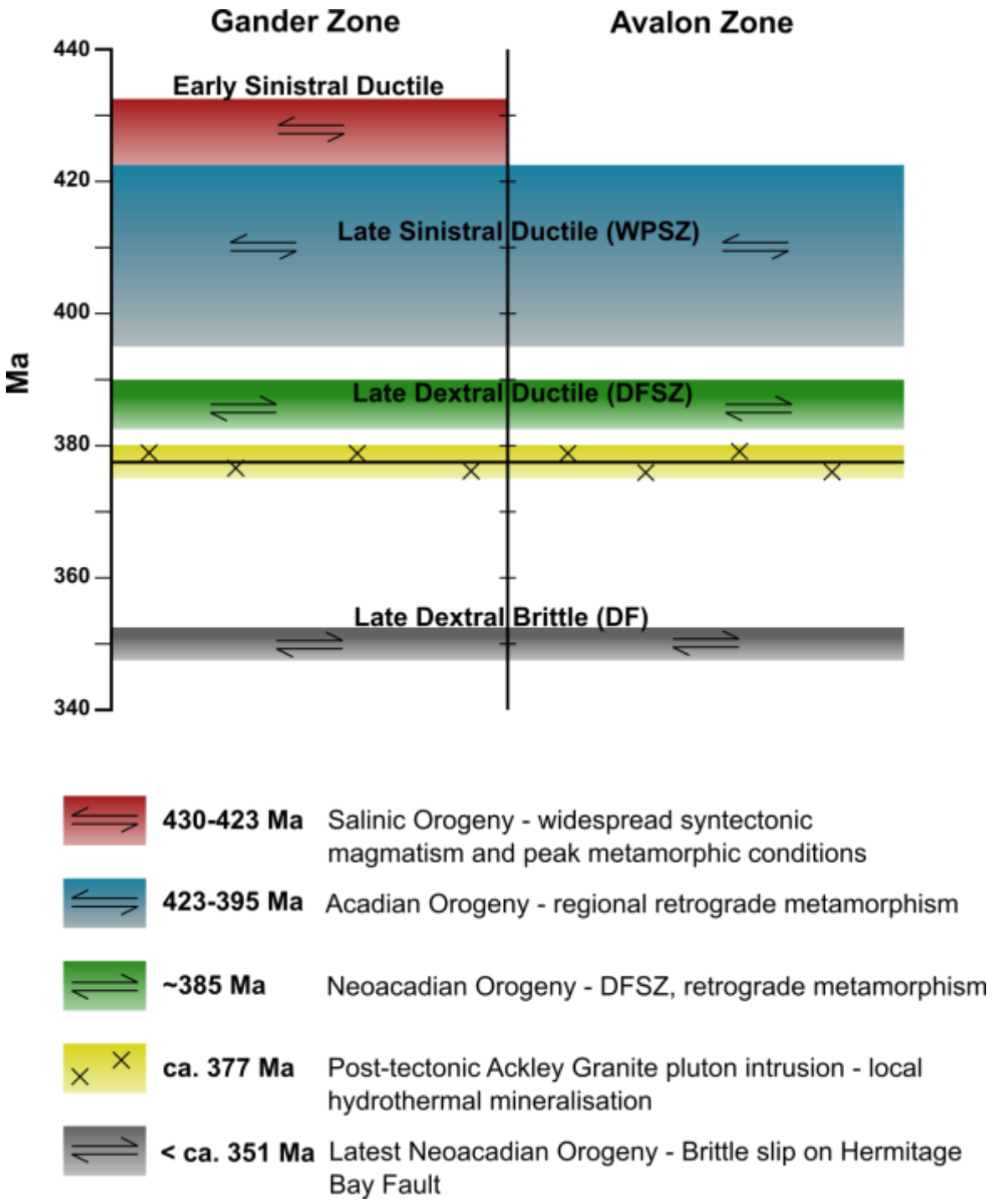

Figure 7.4: A summary of the structural and tectonic history of the Gander-Avalon boundary (adapted from Kellett et al., 2016).

7.2 Deformation Weakening

The main focus area for this study is the subject of deformation weakening and through the study of structures in the outcrop to microstructural scale, the evidence of strain weakening can be seen on a regional scale in both the Gander and Avalon Zones. Both tectonic zones show increasing structural complexity and metamorphic grade towards the tectonic boundary and successive deformation phases produced progressively narrower shear zones, thus indicating that deformation was progressively localised into the shear zone. Reactivation is also evident at the outcrop-scale as narrow, metre-scale shear zones and brittle faults are preferentially located at sites of rheological contrasts, such as granite margins or pre-existing deformation structures. Even at the microstructural-scale, the samples from the Gander-Avalon boundary region show reactivation and overprinting relationships, such as shear fractures along foliation planes and mylonitised quartz veins. The reactivation across all scales of observation indicates that significant weakening of the Gander-Avalon boundary has occurred.

The Gander Zone in northeast Newfoundland shows a more strongly retrograde down-temperature history than the Avalon Zone, which is significant in terms of the deformation weakening in the region. The amphibolite grade Early Ductile phase is only present in the Gander Zone and at these conditions quartz and feldspar deformed by dynamic recrystallisation whereas phyllosilicates are able to deform by dislocation glide at all depths in the crust (Wintsch et al., 1995). Fluid-assisted DMT was also operative in the Early Ductile phase whilst the Gander Zone resided at depths of 15km and more in the crust. Through the operation of these deformation mechanisms, a well-defined gneissose fabric and foliation were developed in the HBG, which generated an early mechanical weakness in the Gander Zone fault rocks. The alignment of micas in continuous and discrete foliations in the HBG may have allowed the deformation of the bulk rock to be controlled by frictional slip on the mica cleavage planes. Muscovite and biotite are known to be frictionally weak with values of $\mu = 0.35\text{-}0.43$ for muscovite and $\mu = 0.25\text{-}0.40$ for biotite (Scruggs and Tullis, 1998; Ikari et al., 2011). When the weak basal slip planes of mica grains are aligned, the bulk rock strength can be significantly reduced even at low ($\leq$10%) proportions (e.g. Niemeijer and Spiers, 2005). The samples of HBG and Silurian granites contain moderate proportions of micas at 10-

30%, although the interconnectivity of the mica-rich domains is relatively low so that the effects of frictional slip in micas is unlikely to have caused significant weakening.

Of more importance to the Gander Zone region is the partial melting in the HBG and the intrusion of syn-tectonic granites during the Early Ductile phase. In situ partial melting is known to cause a significant decrease in crustal strength even for small melt volumes (Beaumont et al., 2001; Rosenberg and Handy, 2005; Lee et al., 2018). The introduction of melt into a system is so significant because it has been shown that, for a partially molten granite, there is a strength and viscosity contrast of up to 14 orders of magnitude between the solid and liquid state (Beaumont et al., 2001; Rosenberg and Handy, 2005). The volume of melt proportion is the major control on crustal strength: below the critical melt fraction of $\Phi = 0.07$, aggregate strength drops rapidly with increasing melt interconnectivity whereas above $\Phi = 0.07$, the dependence of aggregate strength on melt fraction decreases (Rosenberg and Handy, 2005). Partial melting of the HBG and magma intrusion into the Early Ductile shear zone would therefore have significantly reduced the aggregate strength of the Gander Zone fault rocks. Furthermore, the intrusion of large volumes of granitic melts into the eastern Gander Zone is thought to have produced a long-lived thermal perturbation in the continental lithosphere of the region (D'Lemos et al., 1997). High temperatures in lower crustal shear zones enhance strain localisation and weakening because the process of viscous creep is thermally activated so that higher strains can be more easily accommodated (Sibson, 1977; Knipe, 1989; Hirth and Tullis, 1992; Burgmann and Dresen, 2008).

A study of lower crustal rocks from Norway by Lee et al. (2018) proposed a mechanism of syn-melt strain localisation through stress-driven melt organisation in partially molten volumes – such as the mobilised gneisses and migmatites in the HBG. High melt connectivity in the modelled system leads to organisation of the melt into layers, which results in a reduction in viscosity and higher accommodated strains for lower shear stresses (Lee et al., 2018). Subsequently, strain is localised in to the melt zones and so results in a stress-driven organisation of melt (Lee et al., 2018) The modelled process produces strongly layered, mylonite-like rocks that contain a strong mechanical heterogeneity (Lee et al., 2018). The migmatites and intrusions that record syn-melt shear in the Gander Zone may have undergone similar syn-melt strain localisation as evidenced by

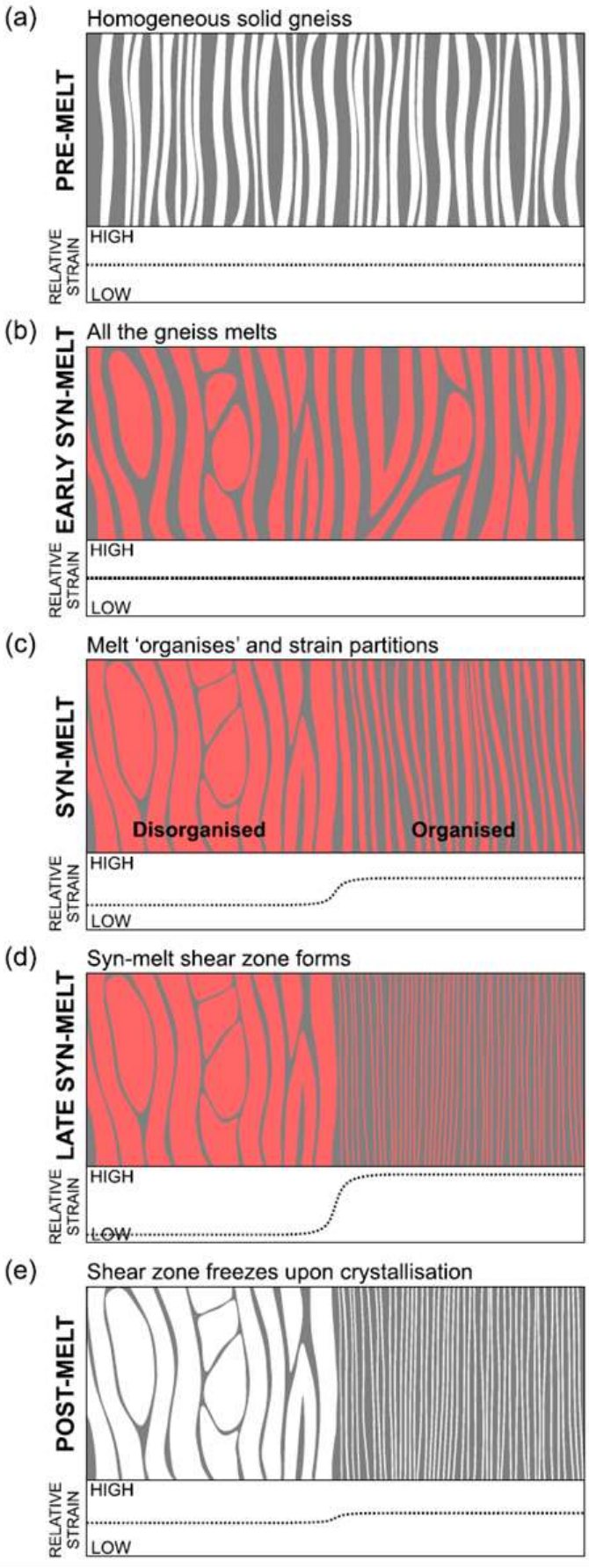

Figure 7.5: Schematic diagrams to show how strain localisation can vary during syn-melt shearing of a migmatized gneiss through a) homogeneous solid gneiss, b) pervasive melting, c) onset of organisation, d) runaway organisation and e) crystallisation (Lee et al., 2018). A relative strain profile is shown under each stage of the model to indicate the areas of strain localisation.

the observed pre-full crystallisation deformation textures. This process would have generated mechanical heterogeneities in the HBG for later strain localisation.

At the close of Salinic orogenesis, the Gander Zone exhibited a well-developed regional fabric and a positive thermal anomaly so that reactivation and strain localisation in the shear zone was highly likely. A lack of pre-existing mechanical heterogeneity existed in the rocks of the Avalon Zone, which likely lead to limited strain localisation during the early stages of the Acadian orogeny in comparison with the Gander Zone.

The processes of deformation weakening that were operative during the Late Ductile deformation phases occur in the FVTZ of crustal-scale faults and have been proposed to be the most significant in terms of absolute fault weakening (Imber et al., 1997; Handy et al., 1999; Stewart et al., 2000; Holdsworth, 2004; Wallis et al., 2013). It is in the Late Ductile shear zones in both of the Gander and Avalon Zones that the importance of processes in the FVTZ and fluids in deformation weakening is most clear.

Studies of other exhumed FVTZ fault zones (Stewart et al., 2000; Jefferies et al., 2006; Wallis et al., 2013) observed a link between brittle structures and alteration of the fault rock assemblages. It has been proposed, therefore, that brittle fracture and cataclasis in the FVTZ can produce pathways for chemically active fluids into shear zones. In the DFSZ, the overprinting of ductile structures on brittle structures, such as mylonitised quartz veins, indicates that brittle deformation mechanisms were active at depth in the FVTZ during the Late Ductile phases. The presence of significant volumes of a chemically active fluid within a FVTZ shear zone leads to substantial weakening through several mechanisms.

Firstly, the mylonitised quartz veins are evidence that pore fluid pressures were sufficient, at least limited periods of time, to promote hydrofracturing in the FVTZ (as in Wallis et al., 2013). Raising the pore fluid pressure in a fault system reduces the effective normal stress so that failure of the fault zone can occur at lower stresses than in a dry rock (Sibson, 1994). However, this is a transient weakening effect and so does not produce permanent weakening of the fault zone. Permanent weakening of a shear zone instead arises from the interaction of the pore fluids with the constituent

mineral phases. The fault rocks of the sinistral Bay du Nord shear zone and the dextral DFSZ in both terranes show variable but often pervasive alteration of feldspars to very fine grained muscovite and sericite, as shown in Equation 1. In addition, hornblende and biotite show evidence of hydration reactions to produce chlorite, as shown in Equation 2.

$$K\ feldspar + plagioclase + H^{+} \rightarrow muscovite + quartz + K^{+} + Na^{+} + Ca^{2+}$$

Equation 1: Sericitisation of feldspar (Beach, 1980; Imber et al., 1997)

$$hornblende + Al^{3+} + (Mg, Fe)^{2+} + H^{+} \rightarrow chlorite + quartz + Na^{+} + Ca^{2+}$$

Equation 2: Hydration of hornblende (Beach, 1980; Imber et al., 1997)

The reactions detailed above take place at temperatures consistent with the conditions of the FVTZ at 250-350°C and 3-4 kbar (Wintsch et al., 1995). The chemical alteration of the inherently strong feldspar and hornblende phases to inherently weak phyllosilicate phases caused the breakdown of the load-bearing framework microstructure of the Gander-Avalon lithologies. The production of phyllosilicate-rich fault rocks caused several weakening processes to affect the DFSZ including grain size reduction, interconnected weak layer development (IWL) and the operation of frictional-viscous flow.

As a result of the breaking of grains by brittle fracture and the production of the alteration mineral phases, the fault rocks underwent a reduction in grain size in the altered phyllonitic shear zones. Fine fault rock grain sizes likely led to a switch in deformation mechanism from grain-size-insensitive to grain-size-sensitive mechanisms, which would have resulted in a reduction of the solid state viscosity of the fault rock (De Bresser et al., 2001). The volcanic protolith of the LCG phyllonites in the DFSZ generally had extremely fine grain sizes (<50μm) prior to the Late Ductile deformation phases so that the effect of grain size reduction was not as significant a weakening mechanism in the Avalon Zone as in the Gander Zone.

The operation of DMT in parallel with dynamic recrystallisation and metamorphic reactions aids the formation of phyllosilicate-rich foliation planes. Samples of Late Ductile fault rocks show strong partitioning of phyllosilicates into discrete foliation planes in an IWL fabric with quartz and feldspar grains in the intervening microlithons. Slip on an IWL fabric of aligned phyllosilicate

minerals occurs at very low frictional strengths (μ = 0.2-0.45) especially along well connected and anastomosing networks (Shea and Kronenberg, 1993; Collettini et al., 2009). The IWL fabrics in the Late Ductile samples suggest that that the strength of fault rocks was controlled by the frictional slip along the basal planes of weak phyllosilicates.

Frictional-viscous flow is able to accommodate high degrees of strain at relatively low (<20MPa) stresses due to the dissolution of asperities that would hinder frictional slip (Imber et al., 2008). The operation of frictional-viscous flow in the Late Ductile shear zones is supported by the prevalence of phyllosilicate-rich IWL fabrics and the evidence of the action of fluid-assisted DMT. Fibrous overgrowths on porphyroclasts, stylolites and the association of oxide phases with foliation planes are all evidence that dissolution and precipitation in the presence of a solute were active during deformation. Hence, it is likely that frictional-viscous flow was active in the phyllosilicate-rich shear zones in the DFSZ and that the operation of this multi-mechanism deformation process led to significant weakening. Models of crustal-scale faults predict up to 50-70% of weakening due to frictional-viscous flow when compared to traditional two-mechanism profiles (Sibson, 1977; Imber et al., 2008).

From the evidence preserved at the grain-scale, the influx of chemically active fluids into the DFSZ and other Late Ductile shear zones led to permanent absolute weakening of the tectonic boundary by instigating and enhancing multiple deformation weakening mechanisms. The localisation of strain into strongly phyllonitic, high strain shear zones indicates that the weakening at the grain-scale was effectively transferred to the regional scale along the Gander-Avalon boundary.

In the Later Brittle phase of deformation, reactivation and overprinting in faults focused at areas of strong rheological anisotropy, such as lithological contacts and pluton margins, and in phyllosilicate rich fault rocks. As the Late Brittle phase is inferred to have resulted from the far distant accretion of the Meguma terrane to Laurentia, the reactivation of the Gander-Avalon boundary ~30 million years after the Late Ductile phases is clear evidence of the absolute weakness of the tectonic boundary. The Late Brittle phase may have also contributed to deformation weakening at a late stage through brittle fracturing and cataclasis.

Frying Pan Island in north Bonavista Bay included exposures of the pervasive alteration that had affected the Newport Granite in close proximity to the brittle fault zones. The high degree of alteration of the feldspar grains to very fine sericite suggests that the fracture and fault networks again acted as pathways for chemically active fluids in the Late Brittle phase. This is supported by the multiple generations of late stage mineral veins that occur throughout the study area. Brittle fracturing and alteration reactions in the Late Brittle deformation led to further grain size reductions and increased the proportion of weak mineral phases in the fault rocks. A reduction in grain size would have enhanced the operation of dynamic weakening processes that reduce the frictional strength of a brittle fault, such as grain rolling (Mair and Marone, 1999), time-dependent creep of asperities, powder lubrication (Reches and Lockner, 2010) or nanoparticle lubrication (Han et al., 2011). In addition, the presence of pore fluids in the fault zones likely produced pore fluid pressures that reduced the effective normal stress.

The hypothesis that this study aimed to test was that mid-crustal processes lead to the development of weak fault zones and that the mid-crustal deformation weakening processes impact fault strength through the crust. It is apparent from the DFSZ that the deformation weakening processes in the mid-crustal FVTZ produced the most significant weakening in this crustal-scale fault. It is also apparent that the influx of chemically active fluids into a fault or shear zone can have a dramatic impact on the strength of faults throughout the continental crust.

7.3 Implications of Deformation Weakening on the Continental Lithosphere

Crustal-scale faults in intraplate and plate boundary settings are thought to substantially influence the rheological behaviour of the lithosphere over very long time periods. Zones of pre-existing weakness in the continental lithosphere are persistent over long time periods because the buoyancy of continental lithosphere means that it is not normally subducted. Hence, the presence of pre-existing mechanical anisotropies in the continental lithosphere leads to non-rigid behaviour and reactivation of structures. Furthermore, the presence of weak crustal-scale faults such as the DFSZ in the continental crust is thought to influence the location of structures such as fault controlled basins, orogenic belts and the siting of continental rifting in Wilson Cycles (Wilson, 1966; Storti et al., 2003). For example, the Mesozoic rifting of Pangaea in the early opening of the Atlantic has

been shown to have reactivated the regional fabric in Newfoundland through the intrusion of basaltic dyke swarms (Peace et al., 2018).

There is some controversy as to whether the overall style of continental deformation is governed by the properties and activity of weakened shear zones or by the bulk rheology of the viscously deforming lower lithosphere (Burov and Watts, 2006; Burgmann and Dresen, 2008). In the Jelly Sandwich model of lithospheric rheology (Burov and Watts, 2006), a weak lower crust overlies a strong upper mantle thus suggesting that continental deformation would be strongly influenced by viscous flow in the upper crust. However, several geodetic studies (e.g. Pollitz et al., 2000; Freed et al., 2006) suggest that the upper mantle is weaker than the lower crust in tectonically active regions, which would cause lithospheric strength to be controlled by the upper crust in the crème brûlée model (Burov and Watts, 2006; Burgmann and Dresen, 2008). It is clear that pre-existing weakened structures such as the DFSZ do have an influence on continental deformation but it is uncertain at this stage as to the extent of that influence.

Deformation weakening also influences the behaviour of the individual fault so that it has been suggested that permanent weakening promotes failure by aseismic creep over seismic slip due to the presence of weak minerals, an IWL fabric and fluid overpressure (e.g. Sibson, 1994; Holdsworth, 2004; Collettini et al., 2009). As the DFSZ and the Gander-Avalon boundary are not active in modern times, it is not easily possible to determine the seismic potential of the fault system. Modern faults that record a history of deformation weakening do not show a straight forward relationship between weakening and seismicity. Examples of crustal-scale faults with potential for dynamic and permanent weakening can deform by both aseismic creep and large magnitude earthquakes (e.g. San Andreas Fault Zone, Lachenbruch and Sass, 1980; Holdsworth et al., 2011). As the deformation along active brittle faults is influenced by temperature, pore fluid pressure and dynamic weakening mechanisms, it is not guaranteed that weakening will lead to aseismic behaviour.

Another consequence of a reduced frictional strength across a fault is the reduced generation of frictional heat during slip. In addition, the presence of fluids in the fault zone would inhibit excess heat being generated from shearing through the advection of heat away from the fault. The fault

rocks of the DFSZ contain no evidence of frictional melts (pseudotachylytes), which may be an indication that shear heating was limited by both fault weakening and the presence of fluids in the fault zone. In fact, the fluids that were able to use the DFSZ and other major Newfoundland faults as conduits for fluid flow produced economic mineral deposits through precipitation and alteration in the fault rocks. As both magmas and hydrothermal fluid systems were able to utilise the regional fault networks for fluid migration, Newfoundland has rich and varied mineral deposits (e.g. Fe, Zn, Pb, Ur, Ni) that support a strong mining industry in the area (Government of Newfoundland and Labrador, 2018).

7.4 Further Research

Due to time and budget constraints, this research utilised methods primarily focused on the use of optical microscopy and analysis of field observations. There are several lines of further research that could be followed, such as more advanced microscopy techniques using the already available resource of oriented hand specimens from the DFSZ. The conditions of deformation and the compositions of the minerals in the fault rock samples can be better constrained by the use of scanning electron microscopes (SEM) in techniques such as electron back scatter diffraction (EBSD). EBSD data can be used to orient lattice preferred orientations (e.g. Dempsey et al., 2011) and to constrain quartz c' axis data (e.g. Kellett et al., 2016) to provide quantitative values of the conditions during deformation in the DFSZ.

Another line of enquiry is the unconstrained timing of the Late Brittle phase in the DFSZ, which may be rectified by the dating of the calcite veins and infills. Dating of calcite using U-Pb systems is a recent technique and is still under development (Hansman et al., 2018; Roberts et al., 2018). Whilst low proportions of U (<10ppm) makes dating calcite technically challenging, it has been successfully used to date multiple overprinting brittle events (e.g. Hansman et al., 2018). As no dates currently exist for movement on the brittle Dover Fault, this technique could shed light on the timing of the Late Brittle phase.

A final further avenue of research is to further test the hypothesis that fracturing in both the FVTZ and the upper brittle crust creates pathways for fluids to migrate into the cores of active fault zones. Techniques that could be used to test this hypothesis include the digital mapping of the fracture

patterns of the DFSZ either in the field using an unmanned aerial vehicle (UAV or drone) or though remote sensing (e.g. Hunt, 2010; Turner et al., 2012; Pavlis and Mason, 2017). Software packages such as FracPaQ (Healy et al., 2017) can be used to quantify fracture patterns, which would reveal the mechanical and transport properties of the rocks in the fault zone. This could then be compared to the spatial extent and degree of alteration in the fault rocks in order to better understand the processes of fault weakening that arise from fluid influx into a fault zone.

8 Conclusions

The aims of this study were to document the changes in mineralogy, fabric and intensity of overprinting in the DFSZ in order to form a detailed structural history of the area and to determine the distribution and nature of fluid-related changes in the DFSZ and the resultant effect on long-term fault strength. Through the study of microstructures, hand specimens and field observations, the DFSZ has been shown to comprise a retrogressive, down-temperature fault rock assemblage that records a history of multiple overprinting deformation phases during exhumation. The DFSZ structural history comprises:

- A sinistral, amphibolite grade Early Ductile phase is recorded only in the Gander Zone when the terrane was situated either at depths greater than 15km in the lower crust or in the mid-crust (10-15km) and syntectonically heated by magmatism. The Early Ductile phase formed during the later stages of the Silurian Salinic orogeny due to the accretion of the trailing edge of Ganderia to the Laurentian margin.
- The greenschist grade, Late Ductile phase that was first identified in both terranes by Holdsworth (1991, 1994) has been separated into an earlier sinistral phase and a later dextral phase. The Late Sinistral Ductile phase is correlated with the Acadian orogeny that resulted from the accretion of Avalonia in the end Silurian-early Devonian.
- The Late Dextral Ductile phase that formed the DFSZ is now correlated with the Neoacadian orogeny as a result of the accretion of the Meguma terrane southwest of Newfoundland. Fault rocks that developed during both Late Ductile phases are inferred to have formed at depths between 10-15km within the FVTZ.
- The final, dextral Late Brittle phase is inferred to have resulted from Carboniferous, upper crustal frictional slip along a regional network of NE-SW trending brittle faults in the latest stages of the Neoacadian orogeny.

From the case study of the DFSZ, the importance in terms of deformation weakening of the infiltration of fluids into fault zones within the FVTZ has been revealed. Field and microstructural evidence suggests that both frictional and viscous deformation mechanisms were operative during

the Late Ductile deformation phases and that brittle fractures likely acted as pathways for fluid migration in the mid-crust. The interaction of chemically active fluids with the DFSZ fault rocks led to the alteration of strong minerals including feldspars and amphiboles and the production of weak minerals including phyllosilicates. As a result of this alteration process, other deformation mechanisms were instigated or enhanced by both the presence of a chemically active fluid and the production of weak minerals. A switch in deformation mechanism from brittle fracture and dynamic recrystallisation to frictional-viscous flow occurred due to a reduction in grain size and the high proportions of phyllosilicates. An interconnected weak layer fabric was able to develop on all of the observed scales so that the fault strength was determined by the strength of the weak connected phyllosilicates. The permanent alteration in both mineralogy and fabric in the DFSZ led to long-term weakening along the Gander-Avalon boundary. This is evidenced by the history of exhumation and progressively lower temperature deformation events that reactivated and overprinted the higher temperature events in narrower and localised fault zones.

Bibliography

Beach, A., 1980. Retrogressive metamorphic processes in shear zones with special reference to the Lewisian complex. J. Struct. Geol. 2, 257–263.

Beaumont, C., Jamieson, R.A., Nguyen, M.H., Lee, B., 2001. Himalayan tectonics explained by extrusion of a low-viscosity crustal channel coupled to focused surface denudation. Nature 414, 738–742.

Burgmann, R., Dresen, G., 2008. Rheology of the Lower Crust and Upper Mantle: Evidence from Rock Mechanics, Geodesy, and Field Observations. Annu. Rev. Earth Planet. Sci. 36, 531–567.

Burov, E.., Watts, A.B., 2006. The long term strength of continental lithosphere: "jelly sandwich" or "creme brulee"? GSA Today 16, 4–10.

Collettini, C., Niemeijer, A.R., Viti, C., Marone, C., 2009. Fault zone fabric and fault weakness. Nature 462, 907–911.

Dallmeyer, R.D., Blackwood, R.F., Odom, A.L., 1981. Age and origin of the Dover Fault: tectonic boundary between the Gander and Avalon Zones of the northeastern Newfoundland Appalachians. Can. J. Earth Sci. 18, 1431–1442.

De Bresser, J.H.P., Ter Heege, J.H., Spiers, C.J., 2001. Grain size reduction by dynamic recrystallization: can it result in major rheological weakening? Int. J. Earth Sci. 90, 28–45.

Dempsey, E.D., Prior, D.J., Mariani, E., Toy, V.G., Tatham, D.J., 2011. Mica-controlled anisotropy within mid-to-upper crustal mylonites: an EBSD study of mica fabrics in the Alpine Fault Zone, New Zealand. Geol. Soc. Lond. Spec. Publ. 360, 33–47. https://doi.org/10.1144/SP360.3

D'Lemos, R.S., Schofield, D.I., Holdsworth, R.E., King, T.R., 1997. Deep crustal and local rheological controls on the siting and reactivation of fault and shear zones, northeastern Newfoundland. J. Geol. Soc. Lond. 154, 117–121.

Freed, A.M., Burgmann, R., Calais, E., Freymueller, J., 2006. Stress-dependent power-law flow in the upper mantle following the 2002 Denali, Alaska, earthquake. Earth Planet. Sci. Lett. 252, 481–489.

Government of Newfoundland and Labrador, 2018. Mines, Newfoundland and Canada, Natural Resources [WWW Document]. Nefoundland Can. Nat. Resour. URL http://www.nr.gov.nl.ca/nr/mines/index.html (accessed 9.14.18).

Han, R., Hirose, T., Shimamoto, T., Lee, Y., Ando, J.I., 2011. Granular nanoparticles lubricate faults during seismic slip. Geology 39, 599–602.

Handy, M.R., Wissing, S.B., Streit, L.E., 1999. Frictional-viscous flow in mylonite with varied bimineralic composition and its effect on lithospheric strength. Tectonophysics 303, 175–191.

Hansman, R.J., Albert, R., Gerdes, A., Ring, U., 2018. Absolute ages of multiple generations of brittle structures by U-Pb dating of calcite. Geology 46, 207–210.

Healy, D., Rizzo, R.E., Cornwell, D.G., Farrell, N.J.C., Watkins, H., Timms, N.E., Gomez-Rivas, E., Smith, M., 2017. FracPaQ: A MATLAB toolbox for the quantification of fracture patterns. J. Struct. Geol. 95, 1–16.

Hibbard, J., Waldron, J.W.F., 2009. Truncation and translation of Appalchian promontories: Mid-Paleozoic strike-slip tectonics and basin inversion. Geology 37, 487–490.

Hirth, G., Tullis, J., 1992. Dislocation creep regimes in quartz aggregates. J. Struct. Geol. 14, 145–159.

Holdsworth, R.E., 2004. Weak Faults - Rotten Cores. Science 303, 181–182.

Holdsworth, R.E., 1994. Structural evolution of the Gander-Avalon terrane boundary: a reactivated transpression zone in the NE Newfoundland Appalachians. J. Geol. Soc. Lond. 151, 629–646.

Holdsworth, R.E., 1991. The Geology and Structure of the Gander-Avalon Boundary Zone in Northeastern Newfoundland. Nfld. Dep. Mines Energy Geol. Surv. Branch 91–1, 109–126.

Holdsworth, R.E., D'Lemos, R.S., McErlean, M.A., O'Brien, S.J., 1993. Deformation of the Cape Freels Granite related to dextral displacements along the Dover Fault, Northeast Newfoundland (No. 93–1), Current Research. Department of Mines and Energy, Geological Survey Branch, Newfoundland.

Holdsworth, R.E., van Diggelen, E.W.E., Spiers, C.J., de Bresser, J.H.P., Walker, R.J., Bowen, L., 2011. Fault rocks from the SAFOD core samples: Implications for weakening at shallow depths along the San Andreas Fault, California. J. Struct. Geol. 33, 132–144.

Hunt, D.W., 2010. Development and Testing of New Automated Methods for the Capture of Quantitative Fracture Data from Outcrop Analogues.

Ikari, M.J., Niemeijer, A.R., Marone, C., 2011. The role of fault zone fabric and lithification state on frictional strength, constitutive behavior, and deformation microstructure. J. Geophys. Res. 116. https://doi.org/10.1029/2011JB008264

Imber, J., Holdsworth, R.E., Butler, C.A., Lloyd, G.E., 1997. Fault-zone weakening processes along the reactivated Outer Hebrides Fault Zone, Scotland. J. Geol. Soc. Lond. 154, 105–109.

Imber, J., Holdsworth, R.E., Smith, S.A.F., Jefferies, S.P., 2008. Frictional-viscous flow, seismicity and the geology of weak faults: a review and future directions. Geol. Soc. Lond. Spec. Publ., The Internal Structure of Fault Zones: Implications for Mechanical and Fluid Flow Properties 299, 151–173.

Jefferies, S.P., Holdsworth, R.E., Wibberley, C.A.J., Shimamoto, T., Spiers, C.J., Niemeijer, A.R., Lloyd, G.E., 2006. The nature and importance of phyllonite development in crustal-scale fault cores: an example from the Median Tectonic Line, Japan. J. Struct. Geol. 28, 220–235.

Jones, R.R., Holdsworth, R.E., Hand, M., Goscombe, B., 2006. Ductile extrusion in continental collision zones: ambiguities in the definition of channel flow and its identification in ancient orogens. Geol. Soc. Lond., Special Publications 268, 201–219.

Kellett, D.A., Rogers, N., McNicoll, V., Kerr, A., van Staal, C.R., 2014. New age data refine extent and duration of Paleozoic and Neoproterozoic plutonism at Ganderia-Avalonia boundary, Newfoundland. Can. J. Earth Sci. 51, 943–972.

Kellett, D.A., Warren, C., Larson, K.P., Zwingmann, H., van Staal, C.R., Rogers, N., 2016. Influence of deformation and fluids on Ar retention in white mica: Dating the Dover Fault, Newfoundland Appalachians. Lithos 254–255, 1–17.

King, T.R., 1997. P-T-t-d evolution paths within the Gander Zone, NE Newfoundland (PhD). Oxford Brookes University.

Knipe, R.J., 1989. Deformation mechanisms - recognition from natural tectonites. J. Struct. Geol. 11, 127–146.

Lachenbruch, A.H., Sass, J.H., 1980. Heat flow and energetics of the San Andreas Fault Zone. J. Geophys. Res. 85, 6185–6222.

Langille, A.E., 2012. A detailed petrographic, geochemical and geochronological study of the Hare Bay Gneiss, northeastern Newfoundland (MSc). Memorial University of Newfoundland.

Lee, A.M., Torvela, T., Lloyd, G.E., Walker, A.M., 2018. Melt organisation and strain partitioning in the lower crust. J. Struct. Geol. 113, 188–199.

Mair, K., Marone, C., 1999. Friction of simulated fault gouge for a wide range of velocities and normal stresses. J. Geophys. Res. 104, 28899–28914.

Niemeijer, A.R., Spiers, C.J., 2005. Influence of phyllosilicates on fault strength in the brittle-ductile transition: insights from rock analogue experiments. Geol. Soc. Lond. Spec. Publ. 245, 303–327.

O'Brien, S.J., 1987. Geology of the Eastport (West Half) Map Area: Bonavista Bay, Newfoundland. Mineral Development Division, Department of Mines, Government of Newfoundland and Labrador.

Pavlis, T.L., Mason, K.A., 2017. The New World of 3D Geologic Mapping. GSA Today 27. https://doi.org/10.1130/GSATG313A.1

Peace, A.L., Welford, J.K., Geng, M., Sandeman, H., Gaetz, B.D., Ryan, S.S., 2018. Rift-related magmatism on magma-poor margins: Structural and potential-field analyses of the Mesozoic Notre Dame Bay intrusions, Newfoundland, Canada and their link to North Atlantic Opening. Tectonophysics 745, 24–45.

Pollitz, F.F., Peltzer, G., Burgmann, R., 2000. Mobility of continental mantle: Evidence from postseismic geodetic observations following the 1992 Landers earthquake. J. Geophys. Res. Solid Earth 105, 8035–8054.

Pollock, J.C., Hibbard, J., van Staal, C.R., 2012. A Paleogeographical review of the peri-Gondwanan realm of the Appalachian orogeny. Can. J. Earth Sci. 49, 259–288.

Reches, Z., Lockner, D.A., 2010. Fault weakening and earthquake instability by powder lubrication. Nature 467, 452–455.

Roberts, N., Walker, R., Imber, J., Haslam, R., Drake, H., 2018. How to date faults, fractures and fluids with U-Pb calcite geochronology. EGU Gen. Assem. Conf. Abstr. 20, 10560.

Rosenberg, C.L., Handy, M.R., 2005. Experimental deformation of partially melted granite revisited: implications for the continental crust. J. Metamorph. Geol. 23, 19–28.

Schofield, D.I., D'Lemos, R.S., 2000. Granite petrogenesis in the Gander Zone, NE Newfoundland: mixing of melts from multiple sources and the role of lithospheric delamination. Can. J. Earth Sci. 37, 535–547.

Schofield, D.I., D'Lemos, R.S., 1998. Relationships between syn-tectonic granite fabrics and regional PTtd paths: an example from the Gander-Avalon boundary of NE Newfoundland. J. Struct. Geol. 20, 459–471.

Scruggs, V.J., Tullis, T.E., 1998. Correlation between velocity dependence of friction and strain localization in large displacement experiments on feldspar, muscovite and biotite gouge. Tectonophysics 295, 15–40.

Shea, J.W.T., Kronenberg, A.K., 1993. Strength and anisotropy of foliated rocks with varied mica contents. J. Struct. Geol. 15, 1097–1121.

Sibson, R.H., 1994. Crustal stress, faulting and fluid flow. Geol. Soc. Lond. Spec. Publ., Geofluids: Origin, Migration and Evolution of Fluids in Sedimentary Basins 78, 69–84.

Sibson, R.H., 1977. Fault rocks and fault mechanisms. J. Geol. Soc. 133, 191–213.

Stewart, M., Holdsworth, R.E., Strachan, R.A., 2000. Deformation processes and weakening mechanisms within the frictional-viscous transition zone of major crustal-scale faults: insights from the Great Glen Fault Zone, Scotland. J. Struct. Geol. 22, 543–560.

Storti, F., Holdsworth, R.E., Salvini, F., 2003. Intraplate strike-slip deformation belts. Geol. Soc. Lond. Spec. Publ. 210, 1–14.

Turner, D., Lucieer, A., Watson, C., 2012. An Automated Technique for Generating Georectified Mosaics from Ultra-High Resolution Unmanned Aerial Vehicle (UAV) Imagery, Based on Structure from Motion (SfM) Point Clouds. Remote Sens. 4, 1392–1410. https://doi.org/10.3390/rs4051392

Valverde-Vaquero, P., van Staal, C.R., McNicoll, G.R., 2006. Mid-Late Ordovician magmatism and metamorphism along the Gander margin in central Newfoundland. J. Geol. Soc. Lond. 163, 347–362.

van Staal, C.R., Whalen, J.B., Valverde-Vaquero, P., Zagorevski, A., Rogers, N., 2009. Pre-Carboniferous episodic accretion-related, orogenesis along the Laurentian margin of the northern Appalachians. Geol. Soc. Lond. Spec. Publ., Ancient Orogens and Modern Analogues 327, 271–316.

Waldron, J.W.F., Barr, S.M., Park, A.F., White, C.E., Hibbard, J., 2015. Late Paleozoic strike-slip faults in Maritime Canada and their role in the reconfiguration of the northern Appalachian orogen. Tectonics 34, 1661–1684.

Wallis, D., Phillips, R.J., Lloyd, G.E., 2013. Fault weakening across the frictional-viscous transition zone, Karakoram Fault Zone, NW Himalaya. Tectonics 32, 1227–1246.

Whalen, J.B., McNicoll, V., van Staal, C.R., Lissenberg, C.J., Longstaffe, F.J., Jenner, G.A., van Breeman, O., 2006. Spatial, temporal and geochemical characteristics of Silurian collision-zone magmatism, Newfoundland Appalachians: An example of a rapidly evolving magmatic systems to slab break-off. Lithos 89, 377–404.

Wilson, J.T., 1966. Did the Atlantic close and then re-open? Nature 211, 676–681.

Wintsch, R.P., Christoffersen, R., Kronenberg, A.K., 1995. Fluid-rock reaction weakening of fault zones. J. Geophys. Res. 100, 13021–13032.